Selected Chapters of Electronics

Lectures

Assosiate Professor of the Department
of Electric Drives and Equipment
Petrovich V.P.

INTRODUCTION

Power electronic devices advantages:

- Absense of rotating parts;
- Absense of sliding contacts;
- Sufficiently high efficiency;
- Acceptable weight and size figures;
- Ease of maintenance.

Classification of power converters

1. Rectifiers, which convert the energy of alternative current into the energy of direct current.

2. Inverters, which convert the energy of direct current into the energy of alternative current.

3. Alternative current converters, which convert the energy of alternative current of certain parameters into the energy of alternative current of another parameters.

4. Converters of direct current energy of one voltage into direct current voltage of another voltage.

ELEMENT BASE OF POWER CONVERTERS

Basic elements of power converters of electric energy are:

- Power semiconductor switches;
- Electrical capacitors;
- Resistors;
- Induction coils.

Classification scheme of power switches

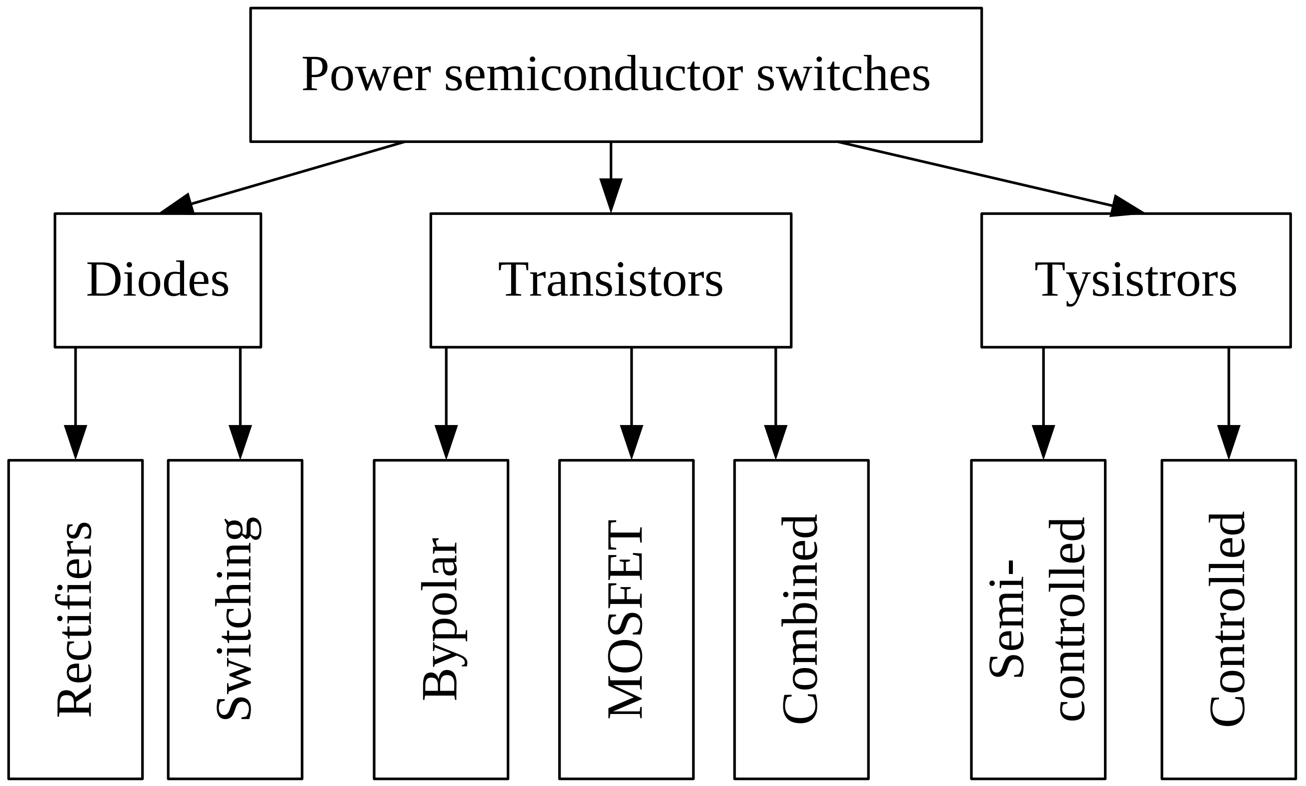

Fig. 1.1. Classification scheme of power switches

Semiconductor diodes

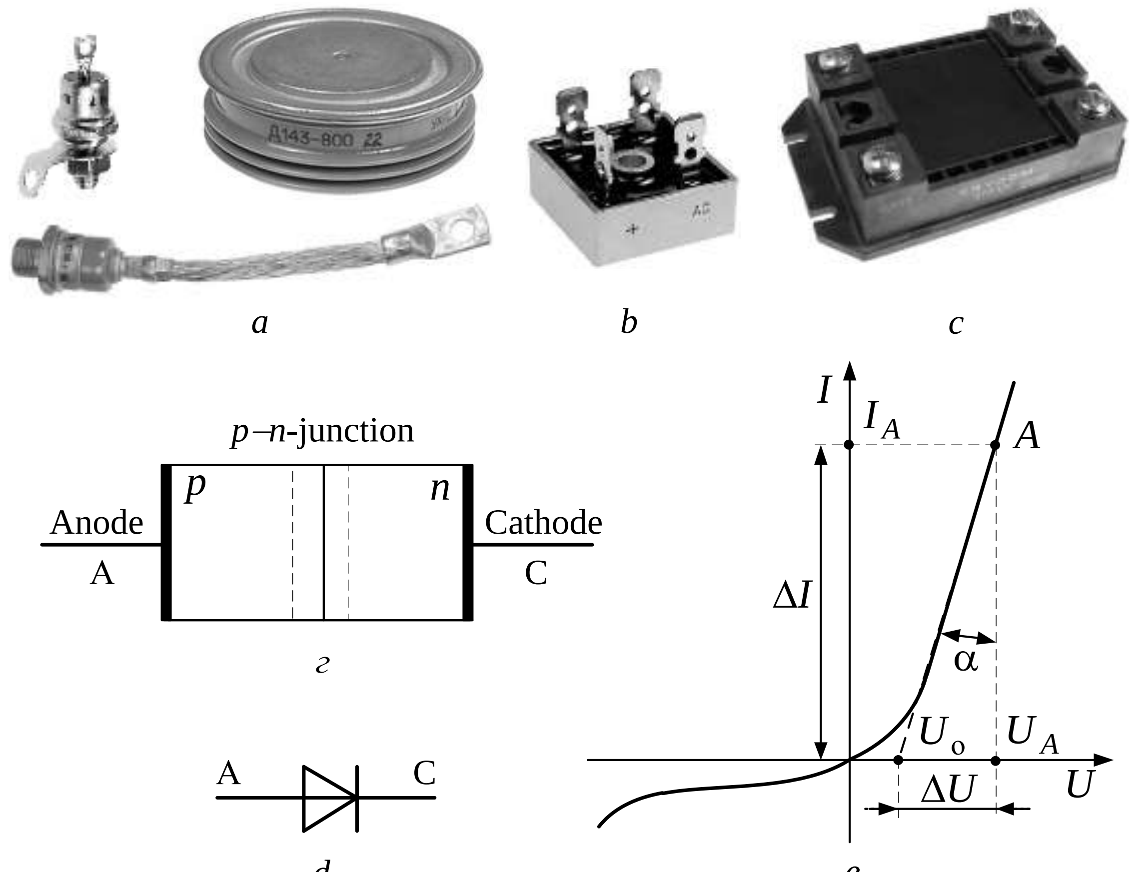

Fig. 1.2. Semiconductor diodes: discrete performance (a), diode bridge (b), power diode module (c), internal structure of diode (d), conventional graphical representation of diode (e), I-V curve of diode (f).

Dynamical resistance of diode

$$R_{\mathrm{dyn}} = \frac{\Delta U}{\Delta I} = \mathrm{tg}\,\alpha \qquad (1.1)$$

The equation of direct branch of diode I-V curve

$$U(I) = U_0 + R_{\mathrm{dyn}} \cdot I \qquad (1.2)$$

Parameters of diodes

Static parameters are:

- static resistance of diode $R_{st} = \frac{U_A}{I_A}$;
- nominal value of forward current I_{nf};
- nominal value of inverse current I_{nin};
- nominal value of inverse voltage U_{nin};
- nominal value of forward voltage drop U_{nf};
- cutoff voltage U_0.

Parameters of diodes

Dynamic parameters are:

- dynamic resistance R_{dyn};
- rate of rise of forward current $\dfrac{di}{dt}$;
- rate of rise of inverse voltage $\dfrac{dU}{dt}$;
- inverse voltage recovery time t_{rec};
- limiting frequency $f_{\max}$.

At present power diodes are being produced on currents up to 2000 A and voltages up to 4000 V. In order to increase this values it is necessary to use parallel, series or series-parallel diodes connections.

Parallel connection of the diodes

- The quantity of the diodes connected in parallel:

$$n = \frac{I}{I_{\text{a.max}}} \qquad (1.3)$$

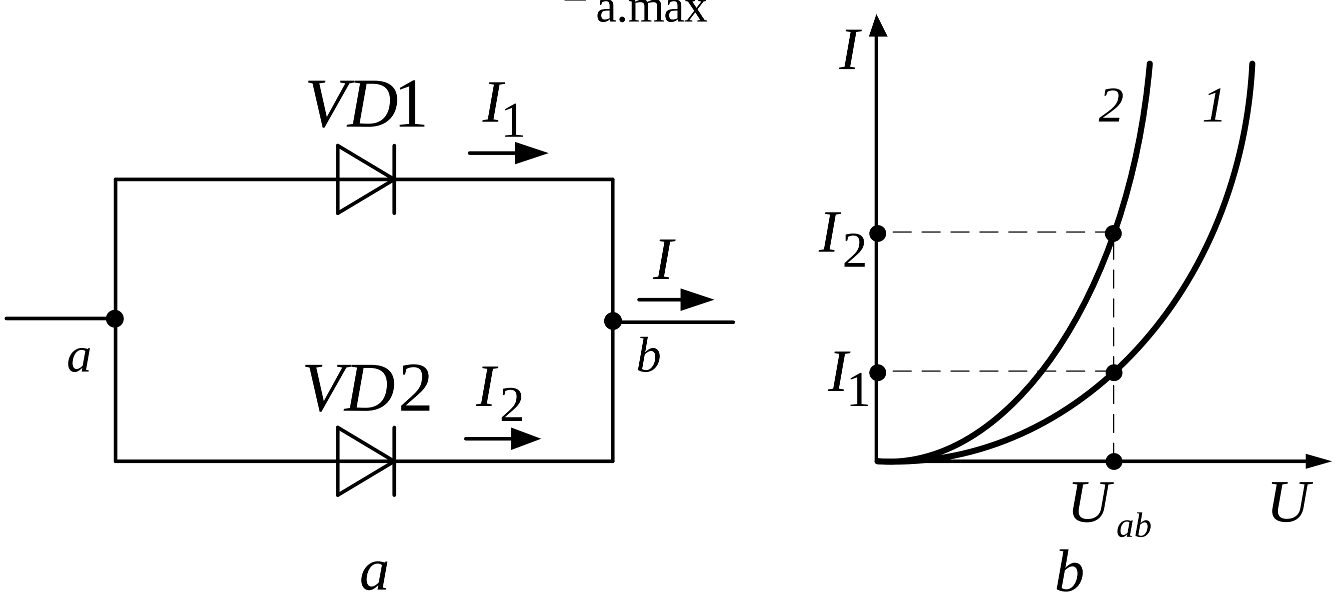

Fig. 1.3. Electric circuit of diodes, connected in parallel and their I-V-curves.

Because of unidentical straight sections of I-V curves of the diodes, connected in parallel, unacceptable distribution of direct current is possible (fig. 1.3, b).

Inequality between I_1 and I_2 can be so significant that maximum current value (e.g. I_2) can exceed the limit value of current for this type of diode: $I_2 > I_{\max}$.

To eliminate such the inequality special balancing resistors are used (fig. 1.4). The resistance should be greater than the resistance of diodes in the straight direction.

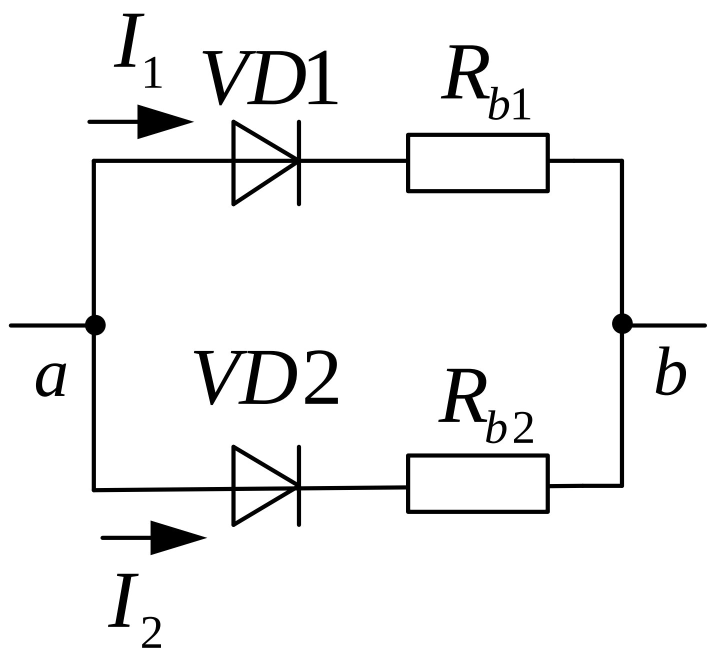

Fig. 1.4. Balancing of currents via using balance resistors

- Power loss on resistors R_{b1} and R_{b2} can be quite significant
- Thus resistances are replaced by inductances (fig. 1.5)

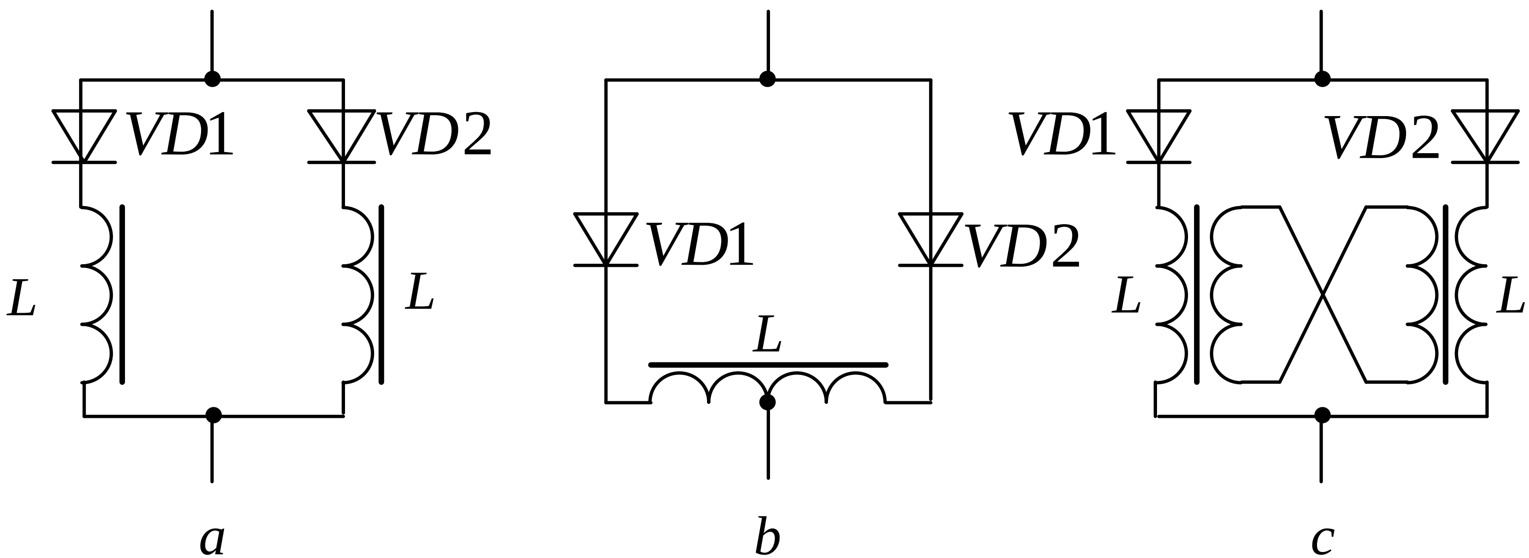

Fig. 1.5. Balancing of currents via inductive current dividers

- If the reverse voltage applied to diode is higher than maximum value then series connection of several diodes is used.
- The quantity of diodes is defined by the expression:

$$n = \frac{U_{\mathrm{rev}}}{U_{\mathrm{rev.max}}} \quad (1.4)$$

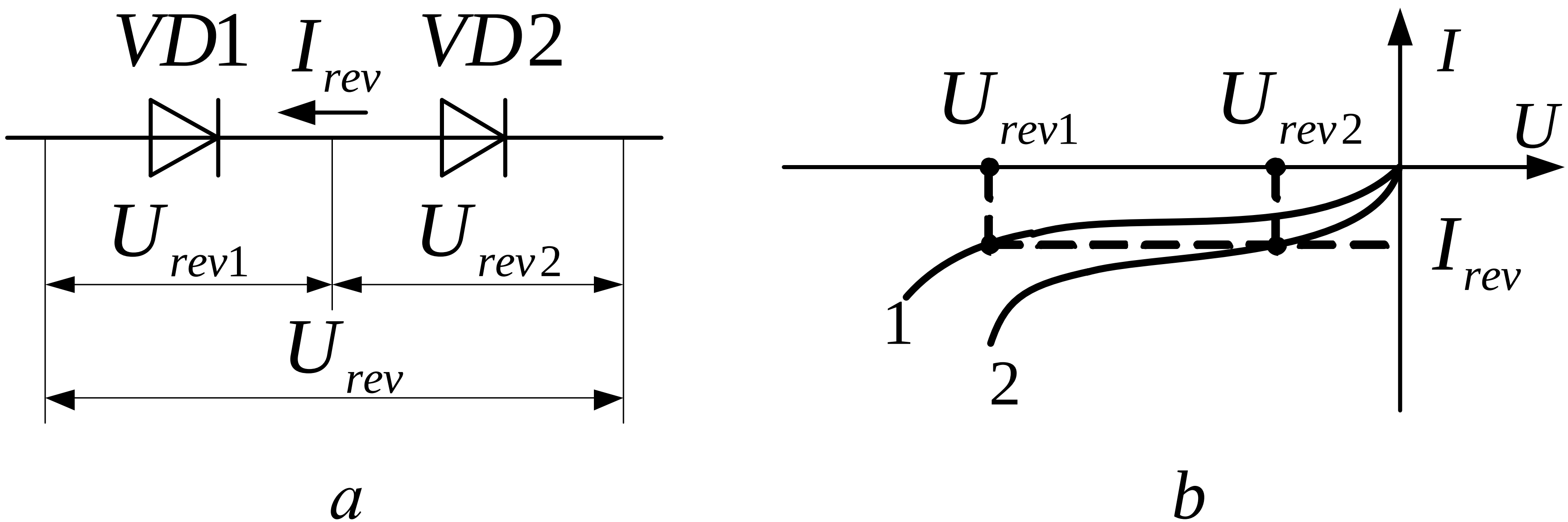

Fig. 1.6. Electric circuit of diodes connected in series and their I-V-curves

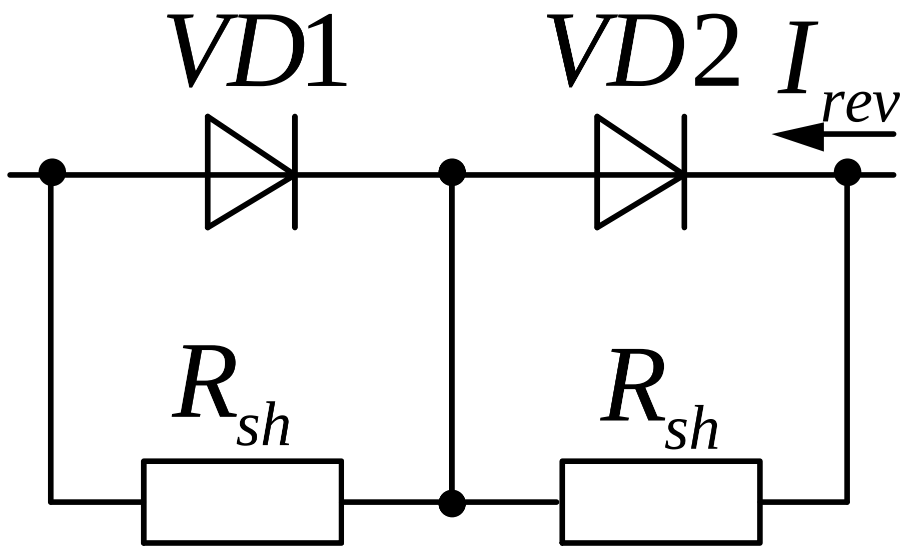

Fig. 1.7. Alignment of reverse voltages by shunt resistors

The resistance of aligning resistors is defined by the formula:

$$R_{\mathrm{sh}} < \frac{nU_{\mathrm{rev.max}} - U_{\mathrm{rev}}}{(n-1)I_{\mathrm{rev.max}}} \qquad (1.5)$$

n – number of diodes connected in series;

$U_{\mathrm{rev.max}}$ – maximum reverse voltge for a particular type of diode;

U_{rev} – total maximum reverse votage applied to diodes;

$I_{\mathrm{rev.max}}$ – maximum reverse curret of diodes.

Transistors

Bipolar transistors

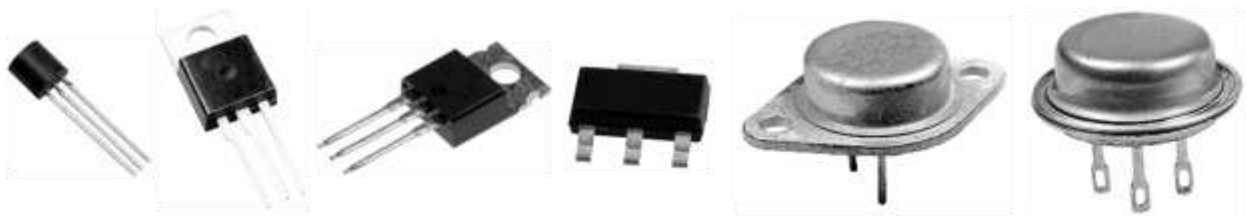

a

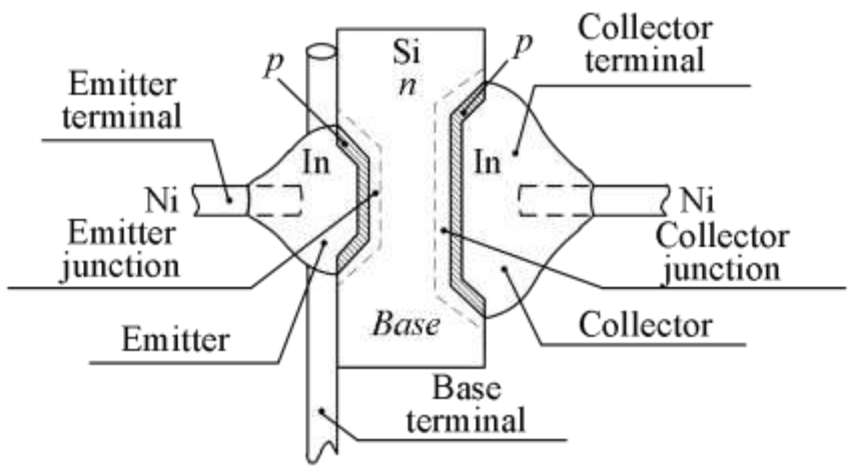

b

Fig. 1.8. Bipolar transistor: constructions (a), inner transistor structure (b)

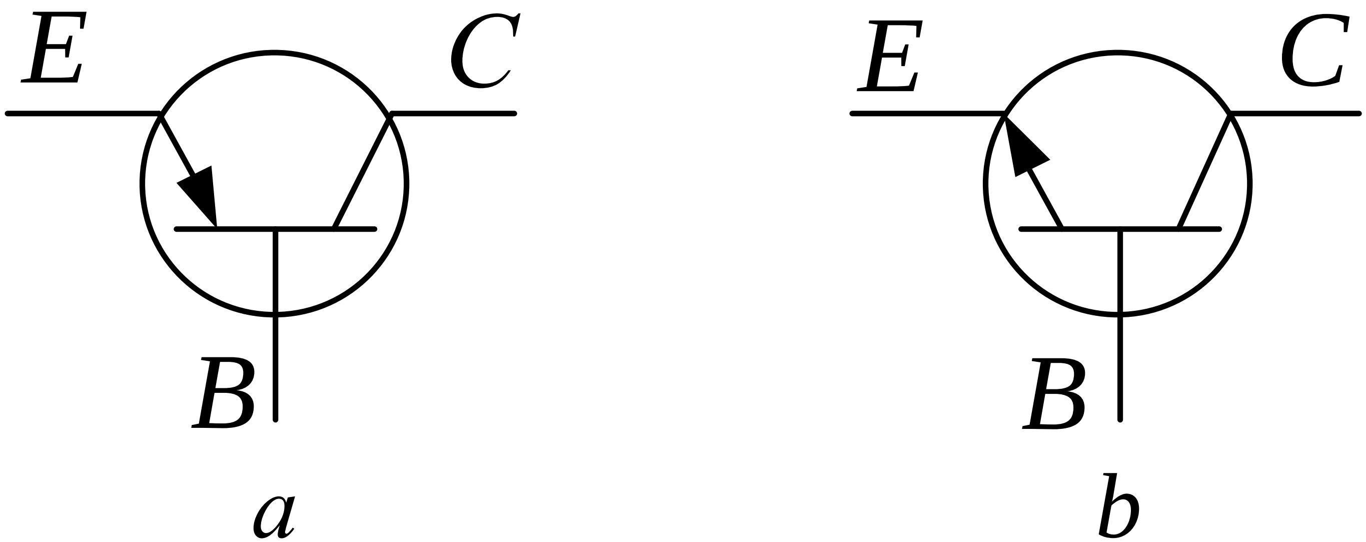

Fig. 1.9. Pictorial symbols of bipolar transistors: transistor of p-n-p-type (a); transistor of n-p-n-type (b)

Both transistors' types have almost the same physical processes, they differ from each other only by type of injected and extracted carriers and have equal wide field of application.

During transistor operation three modes are possible:

- linear (amplifying) mode;
- saturation mode;
- cutoff mode.

Modes of transistor

- In **linear mode** the emitter junction is forward biased and collector junction is reverse biased.
- In **saturation mode** both junctions are forward biased.
- In the **cutoff mode** both junctions a reverse biased.

Three ways of transistor connection are distinguished according to ways of connection of the two voltage sources which bias emitter and collector junctions:

- Transistor circuit with a common base;
- Transistor circuit with a common emitter;
- Transistor circuit with a common collector.

In power electronics, where energy indicators are supposed to be the most important, circuits with a common base and common collector are not applicable, but the circuits with a common emitter are widespread.

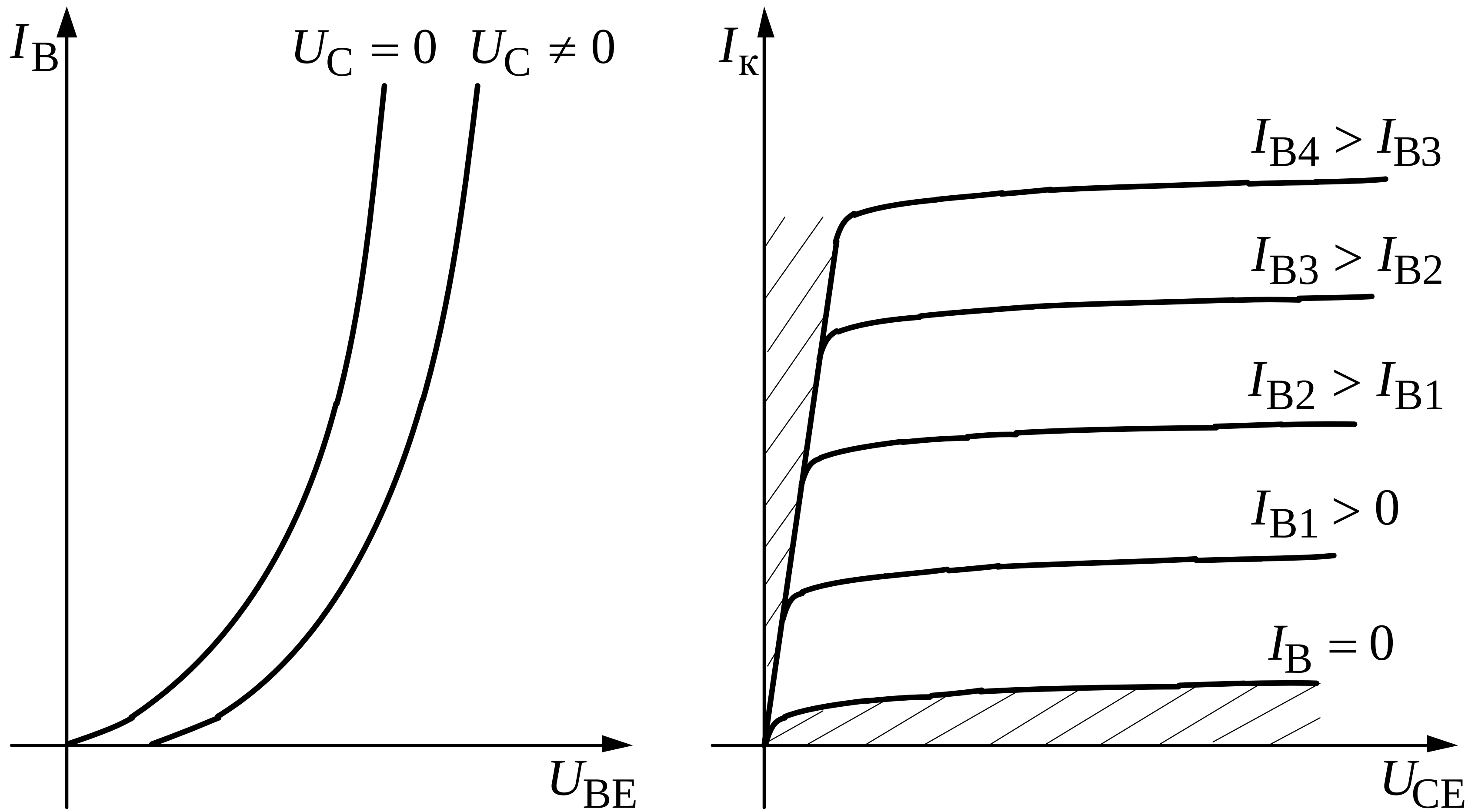

a *b*

Fig. 1.10. Families of input (a) and output (b) characteristics of a bipolar transistor

The main features of the transistor operated in the active zone are:

- Collector current is being changed directly proportional to the base current;
- Collector current under condition $I_{\mathrm{b}} = \mathrm{const}$ weakly depends on the voltage applied to collector;
- Voltage applied to the base is weakly depended on the voltage applied to collector;
- Voltage applied to the base is weakly depended on the base current I_{b}.

- The condition of transistor saturation is equality of voltages between collector and base, which is equal to zero:

$$U_{cb} = U_{ce} - U_{be} = 0 \quad (1.9)$$

- Expression (1.10) defines the relative value of transistor’s saturation, which called the degree of saturation:

$$N = \frac{I_{b} - I_{b.sat}}{I_{b.sat}} \quad (1.10)$$

Processes of transistors' switching

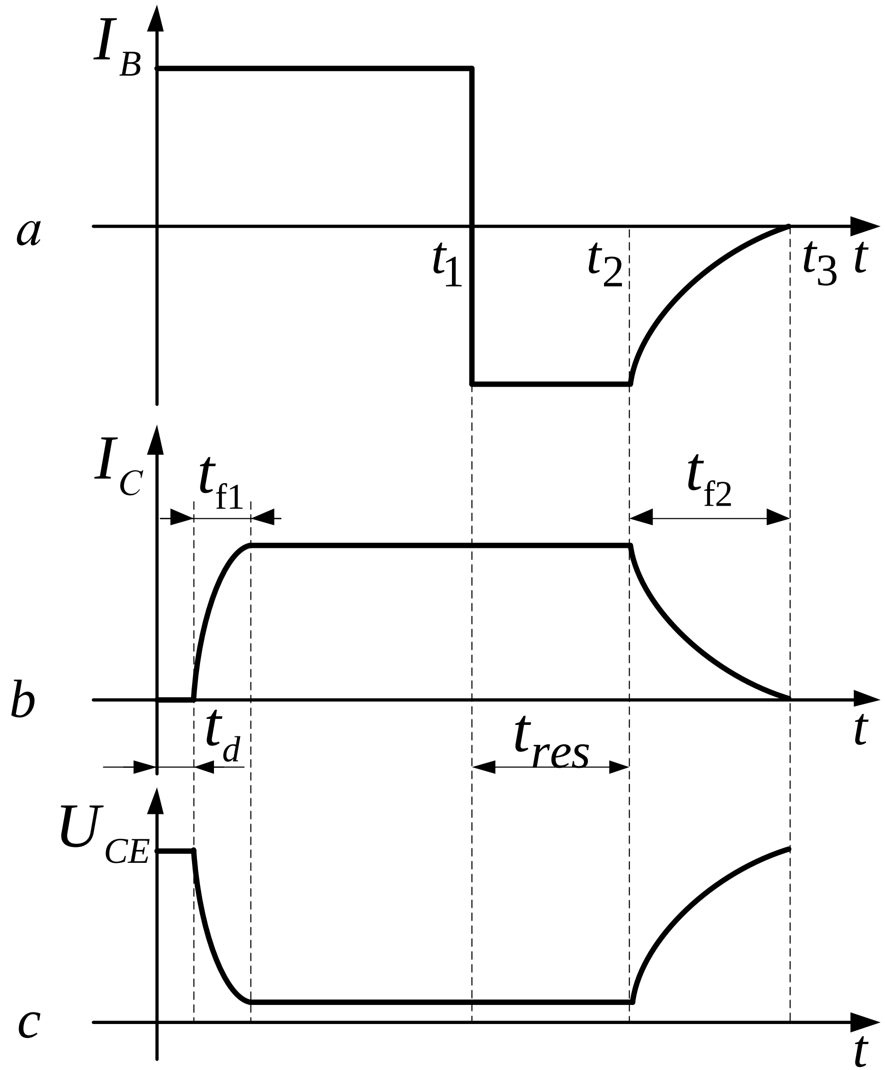

Fig. 1.11. Processes of bipolar transistors switching

t_{f1}, t_{f2} – front times;

t_d – delay time;

t_{res} – resorption time;

Power switches based on the bipolar transistors, have a number of serious disadvantages:

- low response in comparison with the switches of another type;
- low current transducer gain in the field of high electric loads and, in consequence, complexity of control systems and their high costs;
- low resistance to overload mode.

Field effect transistors (FET)

Field effect transistors are divided into two groups:

- p-n-junction controlled;
- insulated gate.

Insulated gate bipolar transistors are the most wide-spread in power electronics.

- The design of FETs is practically the same as the design of bipolar transistors.

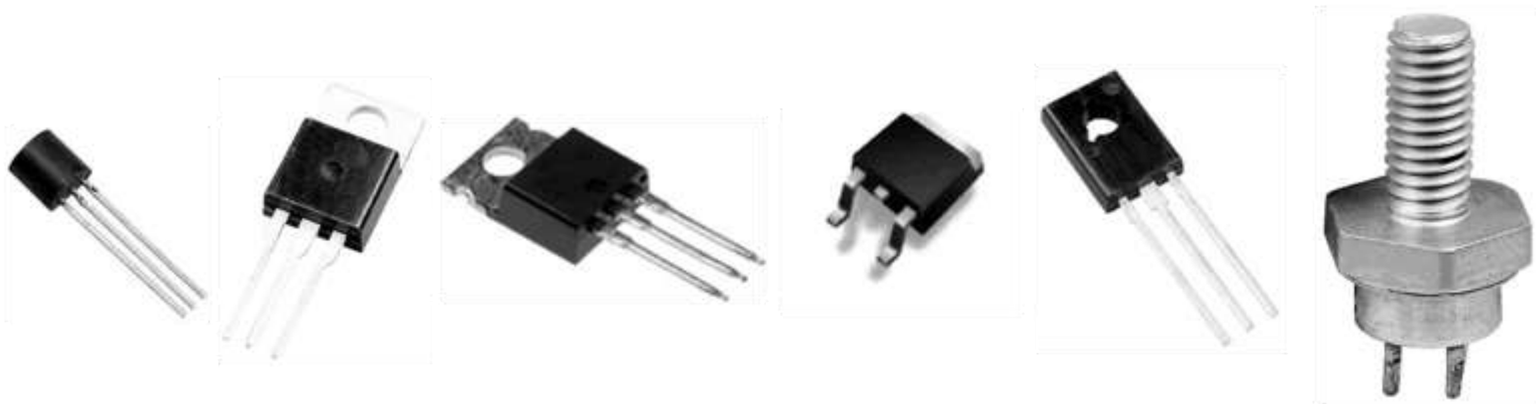

Fig. 1.12. Field Effect Transistors

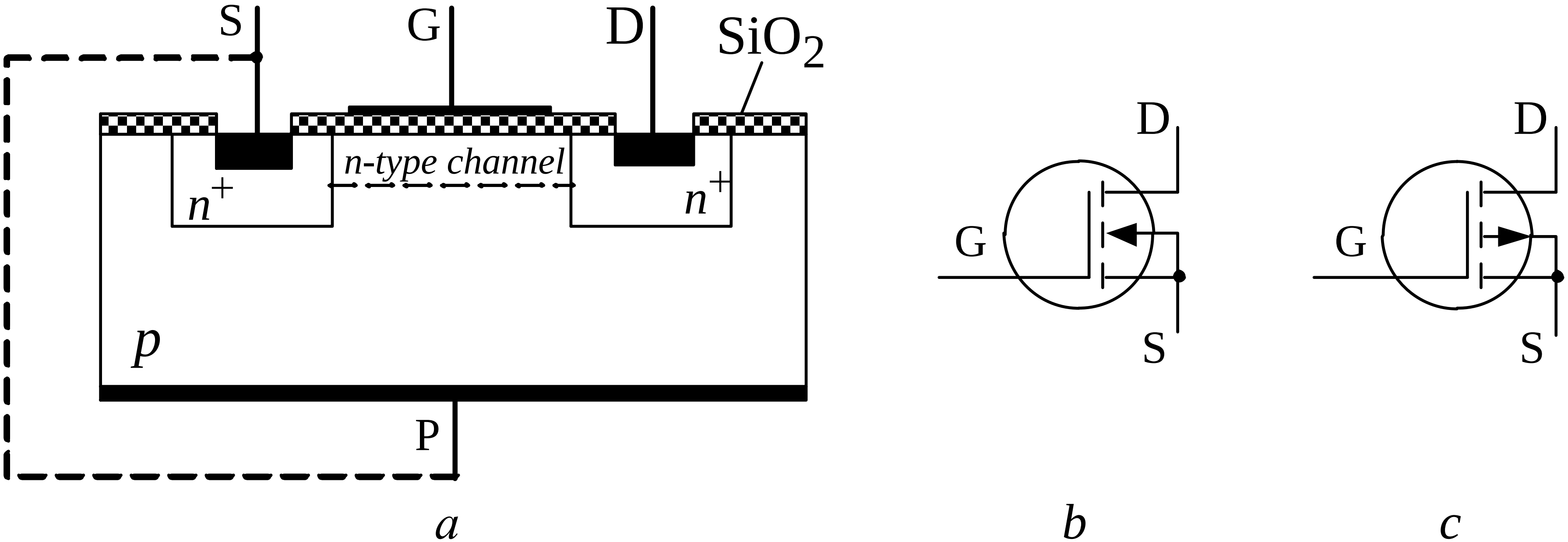

Fig. 1.13. Insulated gate field effect transistor: structure with n-type inducted channel (a); designation of the transistor with channel of n-type (b), p-type (c).

- The terminals are source (S), drain (D) and gate (G).

If now between source and drain control voltage is applied (+ – to the drain, - – to the source), between gate and initial semiconductor electric field is induced, which will pull out the holes from the near-surface region, but attract there the electrons and n-type conductivity channel is induced which connects the regions of source and drain.

- In the Russian technical literature insulated gate field effect transistors have got the notion MOS-transistors (Metal-Oxide-Semiconductor) or MDS-transistors (Metal-Dielectric-Semiconductor). Recently they are frequently noted by the abbreviation taken from the foreign literature MOSFET (Metal Oxide Semiconductor Field Effect Transistor).

- Analogous to bipolar transistor, field effect transistor has two operating regions: the region of linear mode and the region of saturation (region of small resistance between drain and source). In these modes its behaves like the bipolar transistor.

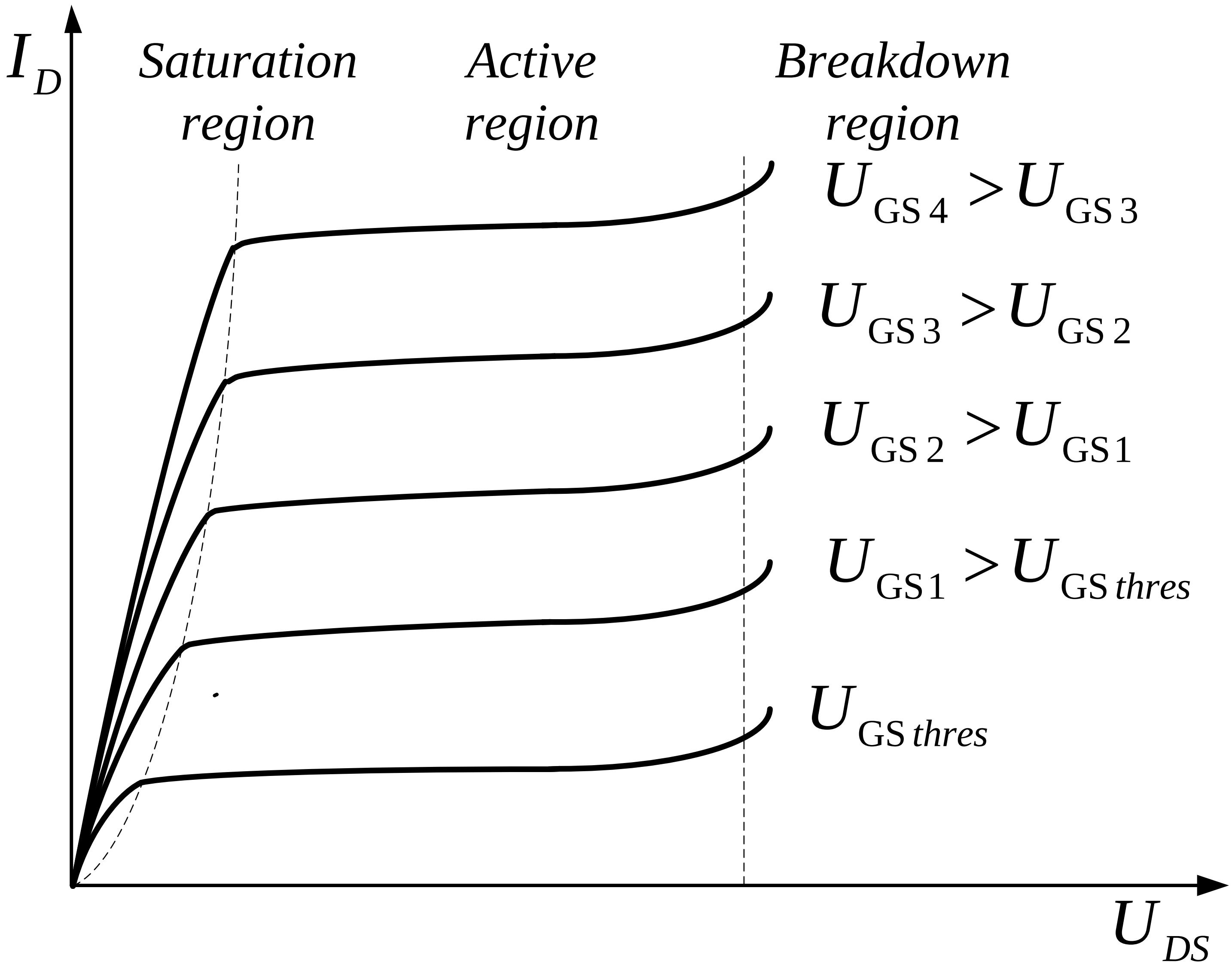

Fig. 1.14. Family of output (drain) characteristics of MOSFET

MOSFETs are used as controlled power switches and have the following advantages:

- simple control circuits and low control power;
- no injection of minority carriers and hence the lack of their accumulation in the form of the space charge, and thus the absence of so-called resorption time, which greatly improves the dynamic properties of the transistor;
- lack of self-heating of the MOSFET which is inherent for bipolar transistors, and therefore, good thermal stability which makes it easy to solve the problem of connecting multiple transistors in parallel;
- the complete absence of a secondary breakdown, allowing more effective use of MOSFET transistor according to the transmitted power.

- The main drawback of MOSFET is presence of a number of “parasitic” elements that occur in the structure of the transistor at the stage of its manufacture.

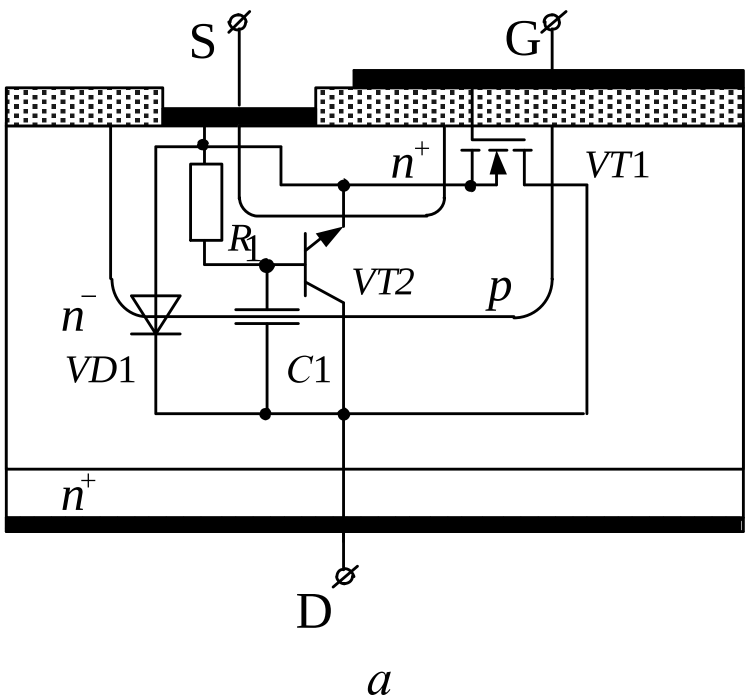

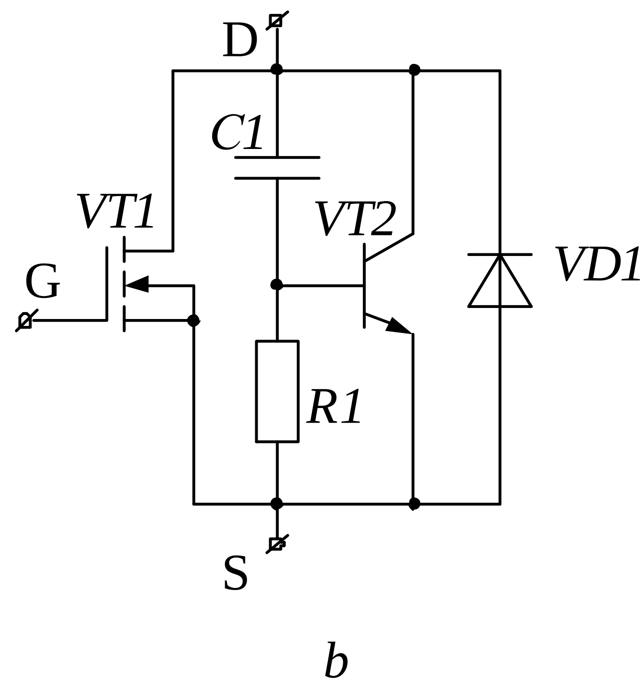

Fig. 1.15. MOSFET transistor: *a* – parasitic elements of the structure, b – the equivalent circuit of the base cell

Combined transistors

- Harm from the parasitic bipolar transistor in the structure of MOSFET can be transformed into benefit, adding one more bipolar transistor of the opposite type of conductivity to the parasitic one.
- The structure obtained is called insulated gate bipolar transistor (IGBT).

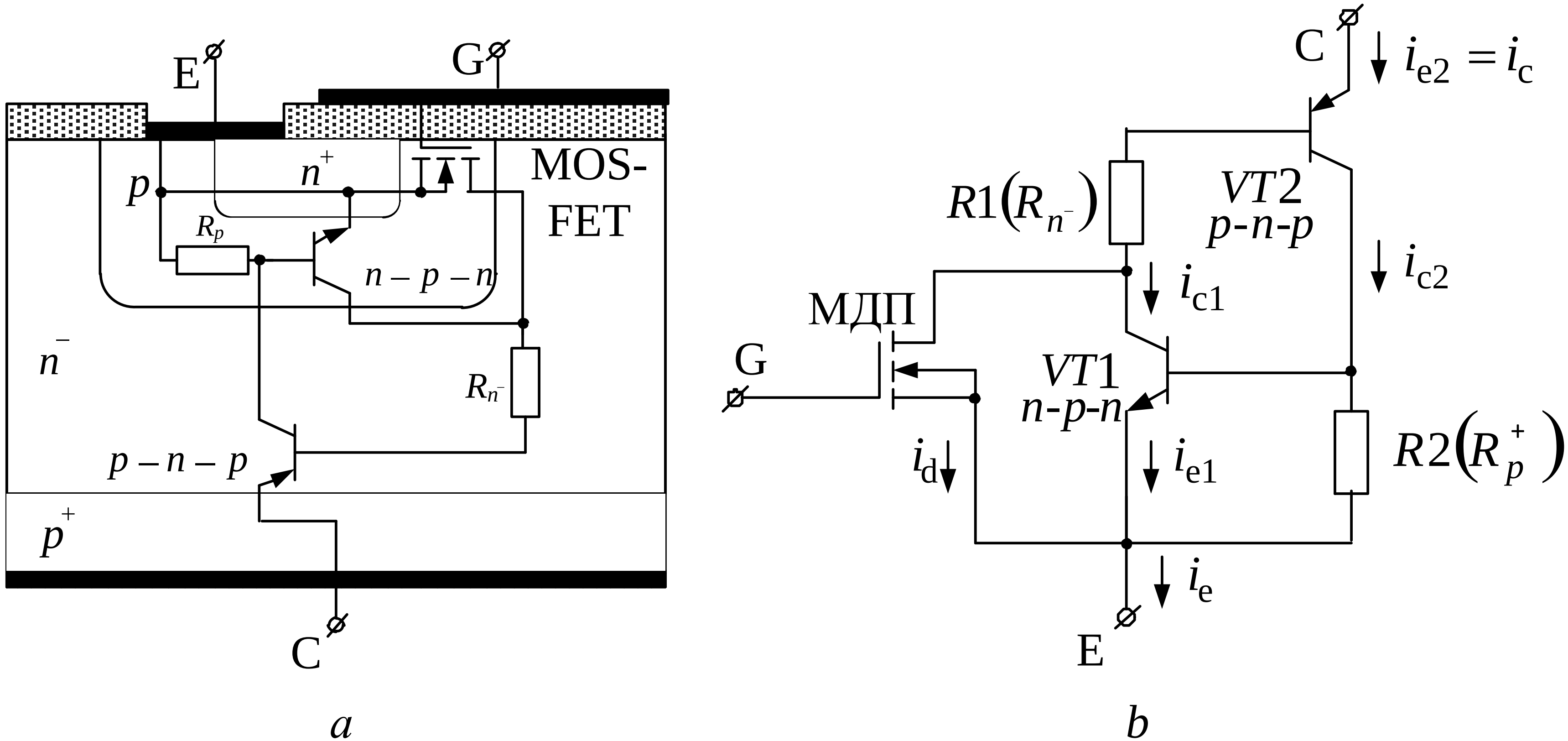

Fig. 1.16. Structure of IGBT (a) and its equivalent circuit (b)

- Collector and emitter currents of IGBT are defined by the expressions:

$$i_{\mathrm{c2}} = i_{\mathrm{e2}}\alpha_2 \qquad (1.9)$$

$$i_{\mathrm{c1}} = i_{\mathrm{e1}}\alpha_1 \qquad (1.10)$$

$$i_{\mathrm{e}} = i_{\mathrm{e1}} + i_{\mathrm{e2}} + i_{\mathrm{c}} \qquad (1.11)$$

Drain current of field effect transistor is defined by the formula:

$$i_{\mathrm{c}} = i_{\mathrm{e}}\left(1 - \alpha_1 - \alpha_2\right) \qquad (1.12)$$

- On the other hand, drain current can be expressed through the slope of the drain-gate characteristic:

$$i_{\mathrm{c}} = SU_{\mathrm{GE}}$$

Power current of the whole circuit is defined as follows:

$$i_{\mathrm{c}} = i_{\mathrm{e}} \frac{SU_{\mathrm{GE}}}{1-\left(\alpha_1 + \alpha_2\right)} = S_{\mathrm{eq}} U_{\mathrm{GE}} \quad (1.13)$$

- Equivalent slope of the whole circuit characteristic:

$$S_{\text{eq}} = \frac{S}{1-\left(\alpha_1+\alpha_2\right)}$$

It is obvious that at $\alpha_1+\alpha_2 \approx 1$ equivalent slope is substantially greater than the slope of field effect transistor included in this circuit.

- Varying the coefficients α_1 and α_2 we control the values of resistances R_1 and R_2

Constructively IGBT are performed as discrete elements (fig. 1.17, a), power modules (fig. 1.17, b) , which have several IGBT in their structure in a single package. Conventional graphical notations of the transistors are performed in figure 1.17, c, d.

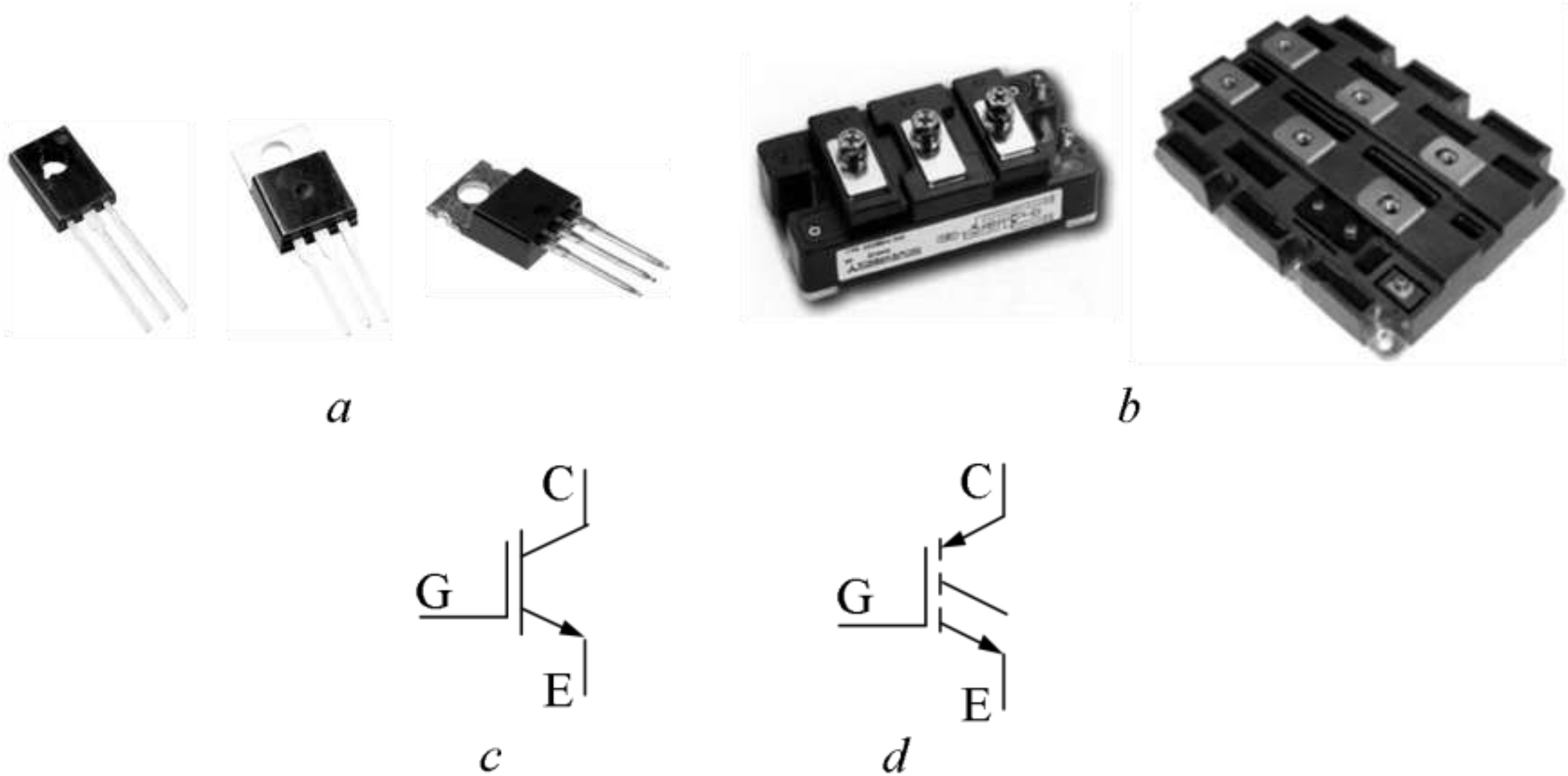

Fig. 1.17. Constructions of IGBT: discrete (a) and module (b) performance; conventional graphical notations: domestic (c); foreign (d)

• Typical output collector characteristics are performed in fig. 1.18.

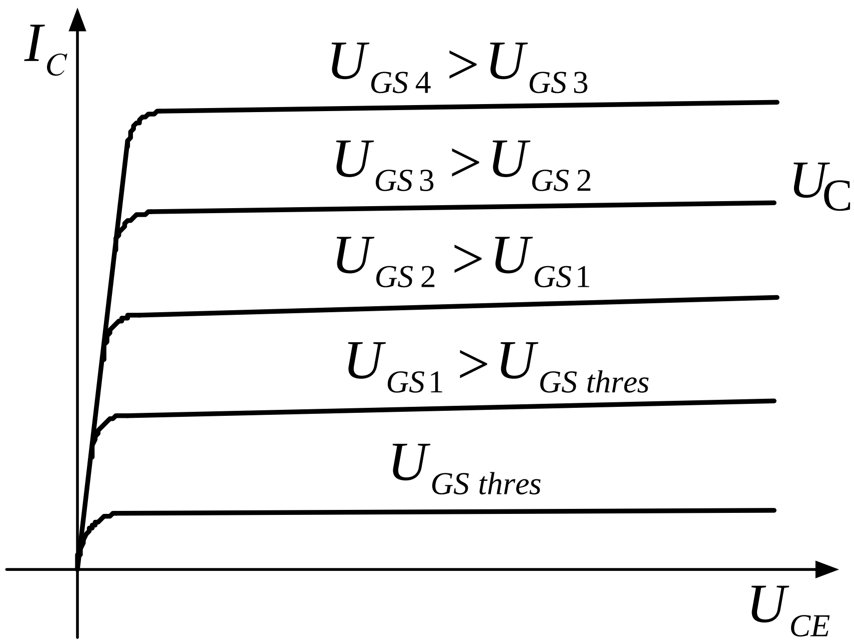

Fig. 1.18. Output characteristics of IGBT

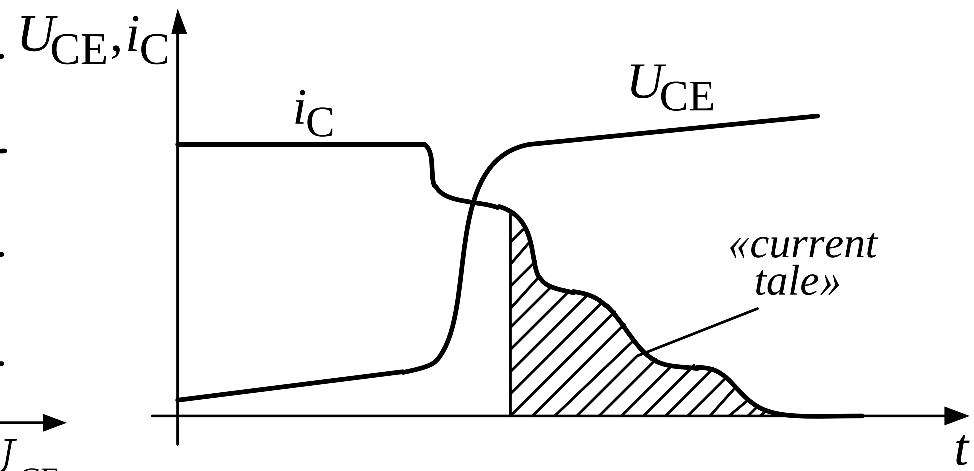

Fig. 1.19. Turning-off process of IGBT

Tyristors

a

b

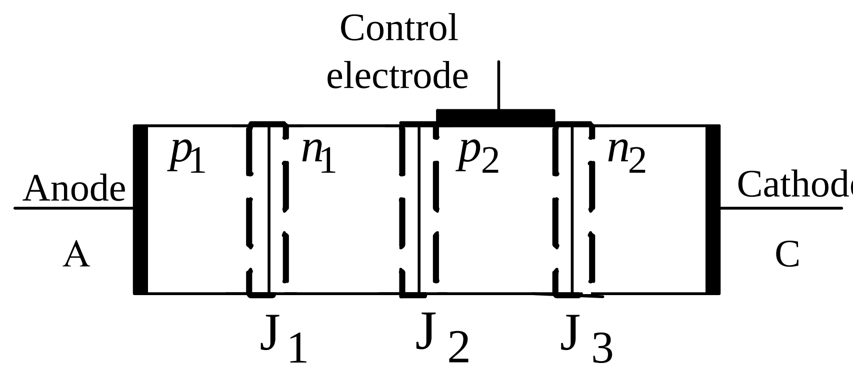

c

Fig. 1.20. Tyristors: discrete (a) and module (b) performance; structure of tyristors (c)

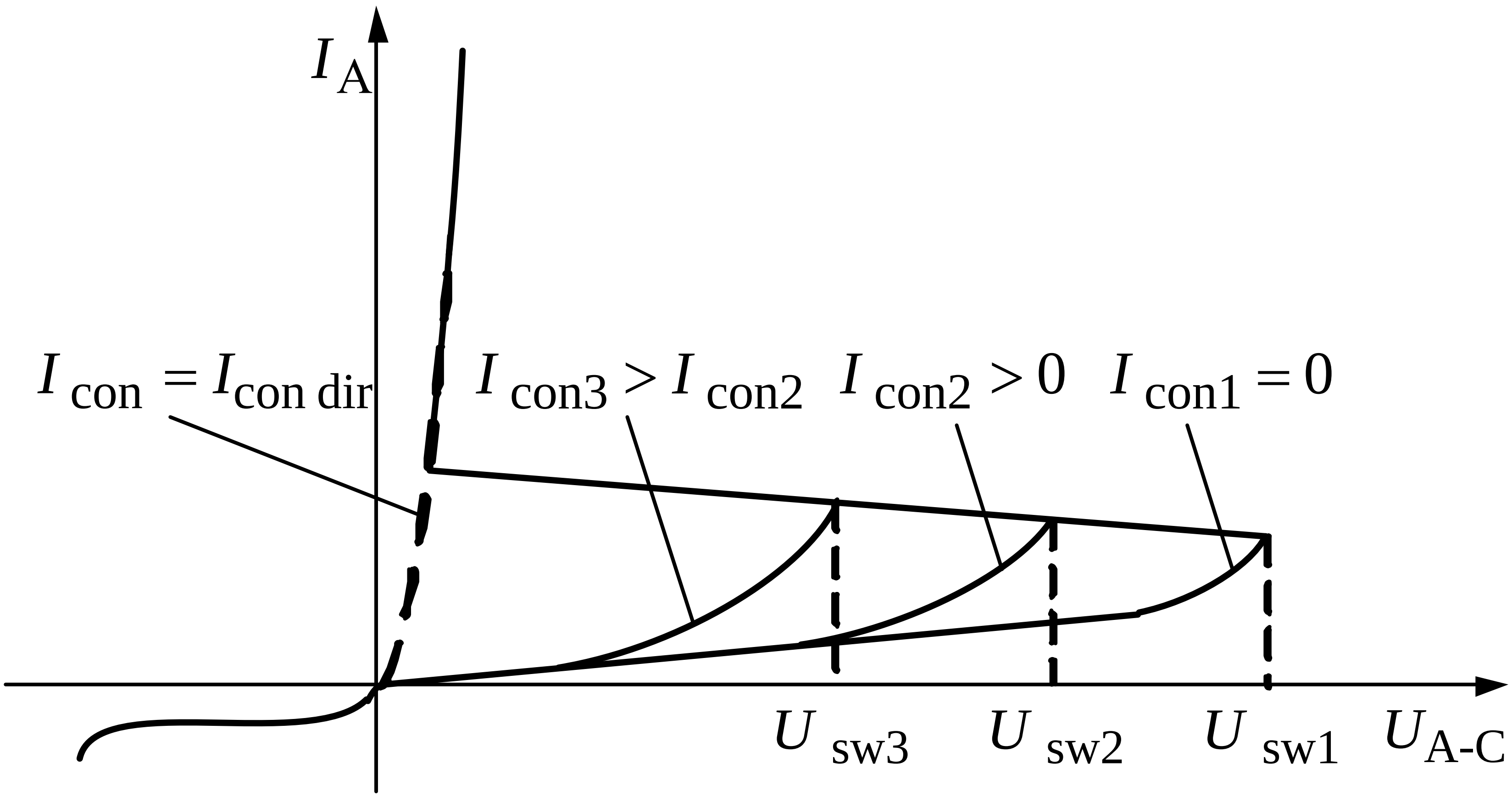

Fig. 1.21. I-V-curve of tyristor

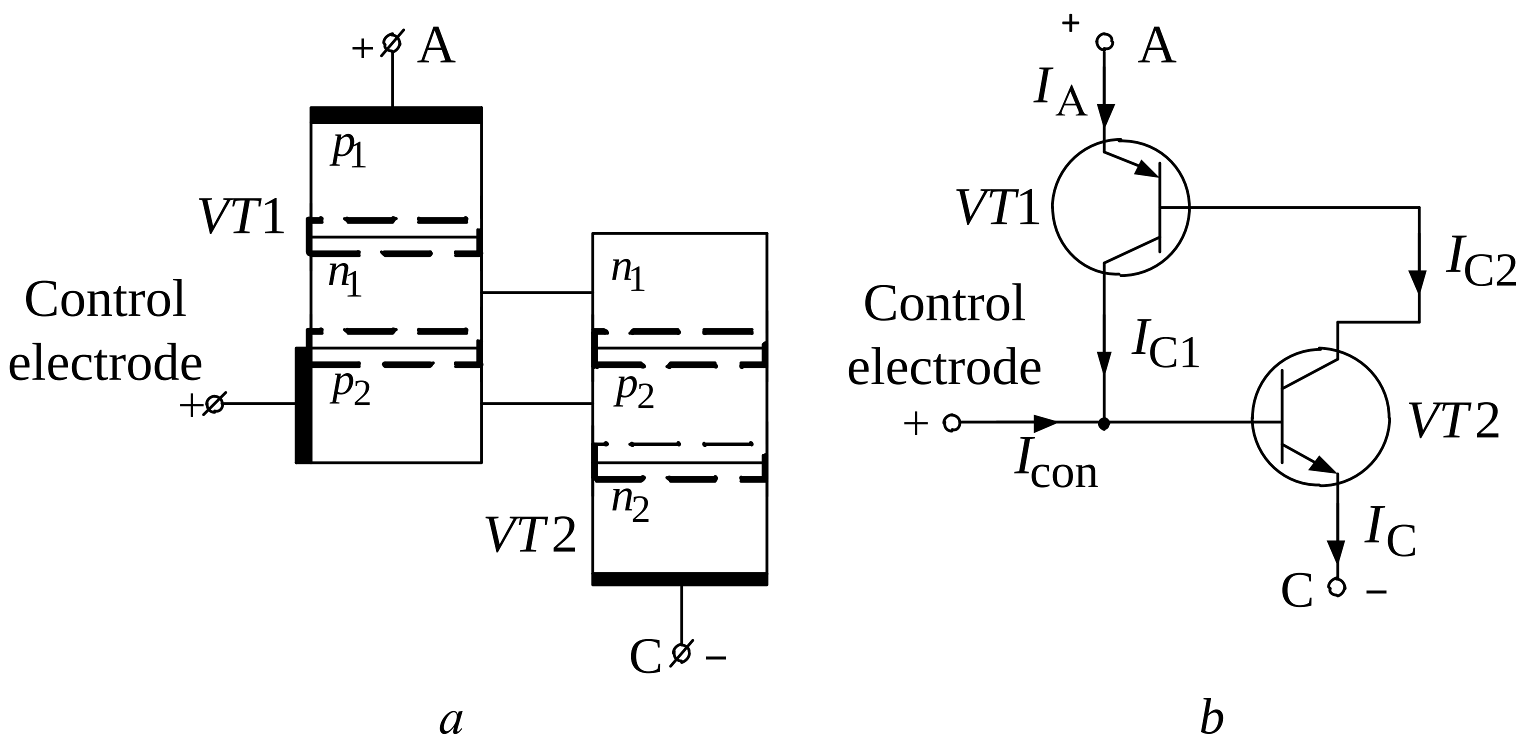

Fig. 1.22. Two-transistor model of tyristor

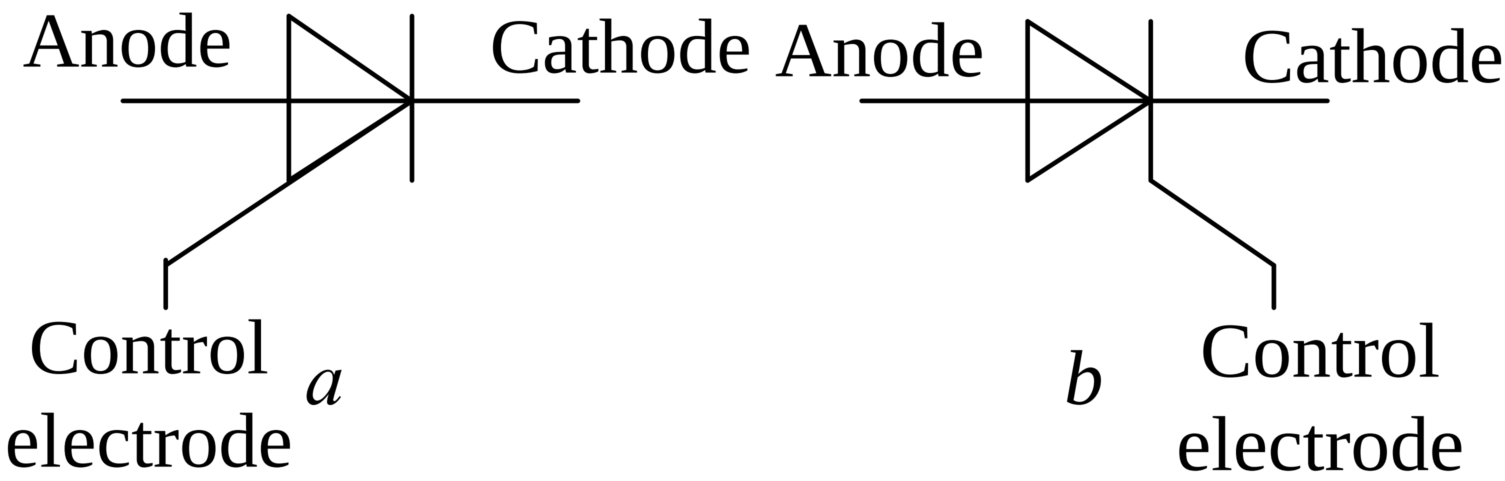

Fig. 1.23. Conventional graphical notation of tyristors

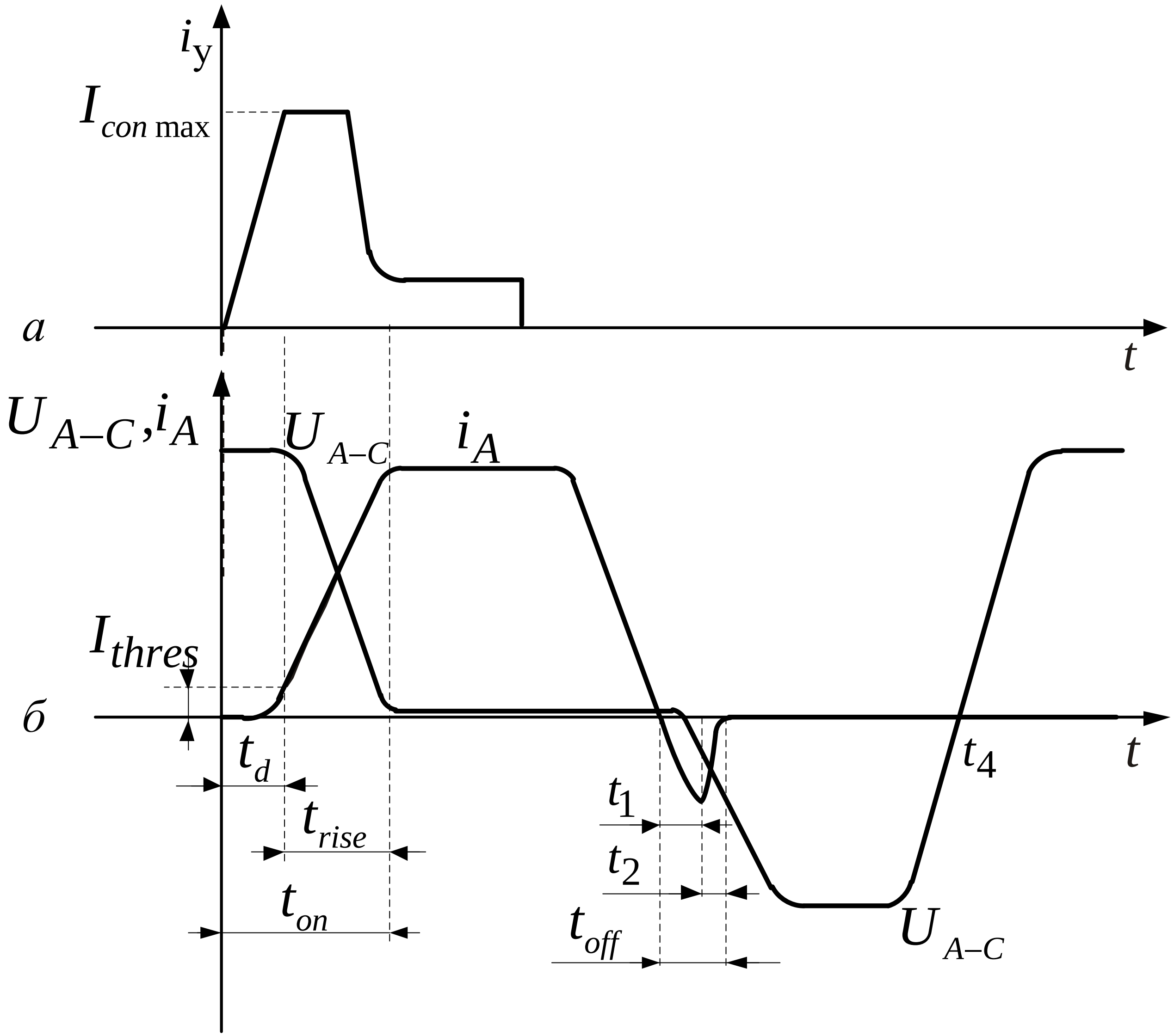

Fig. 1.24. Switching processes in thyristor

- For reliable switching-on of the tyristor it is necessary for the control current impulse on the initial interval – magnitude $I_{\text{con.max}}$, duration and rate of rise $\frac{di_{\text{con}}}{dt}$ to meet the definite requirements that guarantee fast and reliable switching-on of the tyristor.

During the time delay the tyristor current is rising until it achieves the holding current – minimum forward tyristor current at which the tyristor maintains its opened state.

- Usually the holding current is accepted to be

$$I_{\mathrm{h}} = 0.1 I_{\mathrm{n}}$$

Depending on control current time delay can might be from 0.1 μs to 1…2 μs. Then the current is rising up to the value, defined by the load resistance and by the load resistance. This process occurs during the time t_{rise} .

Switching-on time of the tyristor:

$$t_{\mathrm{on}} = t_{\mathrm{d}} + t_{\mathrm{rise}} \quad (1.14)$$

The switching-off process includes two stages (fig. 1.24, b):

- reverse current rising through the tyristor (time interval t_1);
- reverse current decreases to zero (time interval t_2);

And only after time interval, not less than t_{off}, equals to $t_{\text{off}} = t_1 + t_2$ forward voltage can be applied to the tyristor again.

- Among tyristors’ dynamic parameters the most important are: rate of voltage rise $\dfrac{dU}{dt}$, rate of current rise $\dfrac{di}{dt}$.

One-operational tyristors are usually used in self-switching converters when tyristors are switching-on as a result of mains supply voltage polarity change, as they possess inherent serious disadvantage of impossibility of switching-off process via control electrode.

- In contrast to considered one-operational tyristors, two-operational (GTO) tyristors can be both switched-on and switched-off via control electrode.

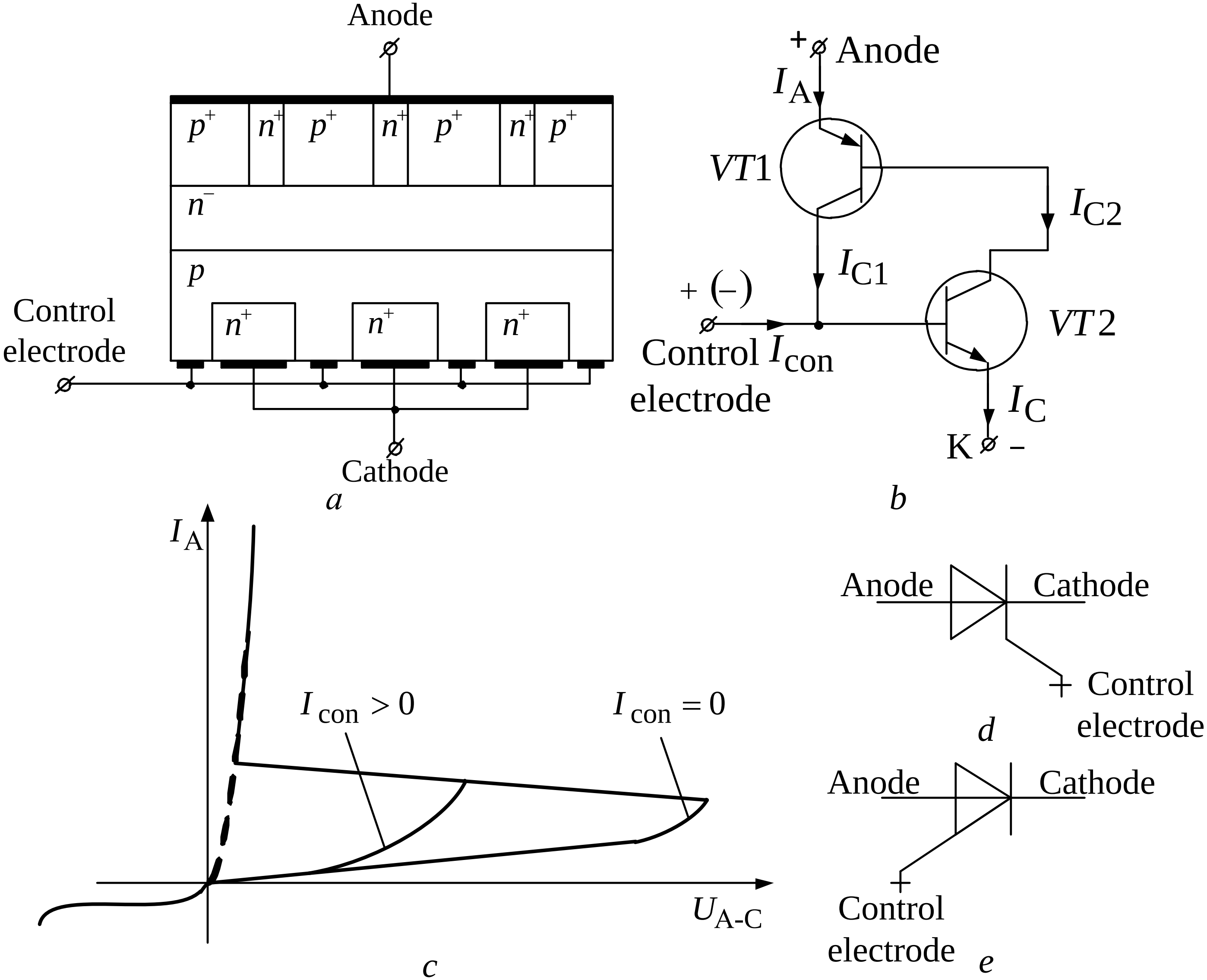

Fig. 1.25. GTO-tyristor: structure of tyristor (a); two-transistor model (b); I-V-curve (c); symbolic notations of tyristor controlled via cathode (d); tyristor controlled via anode (e)

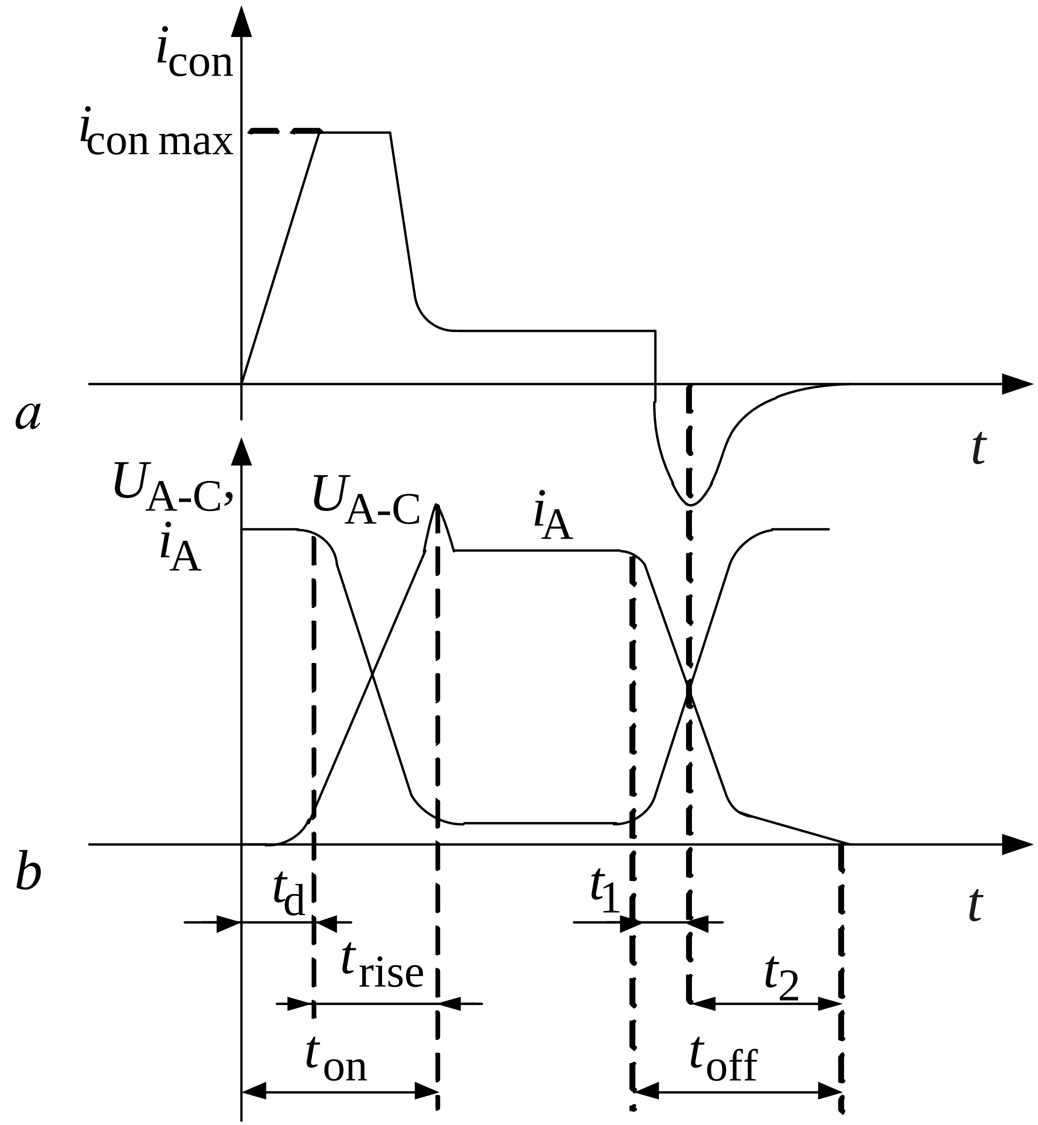

Fig. 1.26. Switching-on and switching-off processes of GTO-tyristor

Maximum characteristics of semiconductor switches

- voltage and current boundary values for input and output circuits;
- maximum permissible junction and housing temperatures;
- maximum possible power dissipation.

Safe modes band

- Safe modes band (SMB) is a system of electric parameters, which must be followed if reliable semiconductor switch operation is needed without significant decrease of its characteristics.
- Safe modes band is defined by the maximum permissible values of current, voltage, maximum power dissipated and permissible temperature of semiconductor structure.

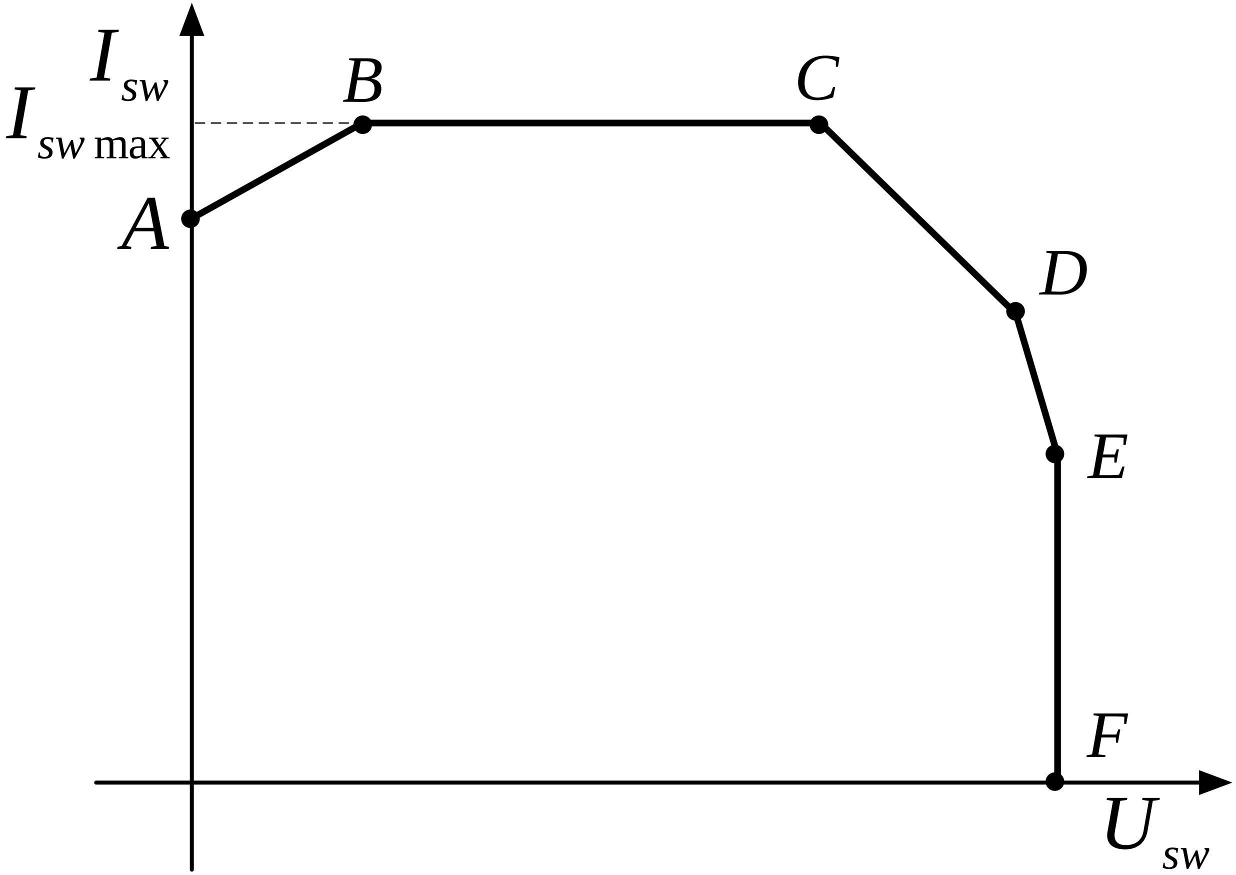

Fig. 1.27. Typical SMB diagram

U_{sw} – switch voltage, I_{sw} – switch current

- In pulse mode permissible switch current depends on current flow pulse durability. Consequently when the pulse durability decreases safe modes band enlarges with equal slope of temperature boundary and constant maximum voltage (fig. 1.28).

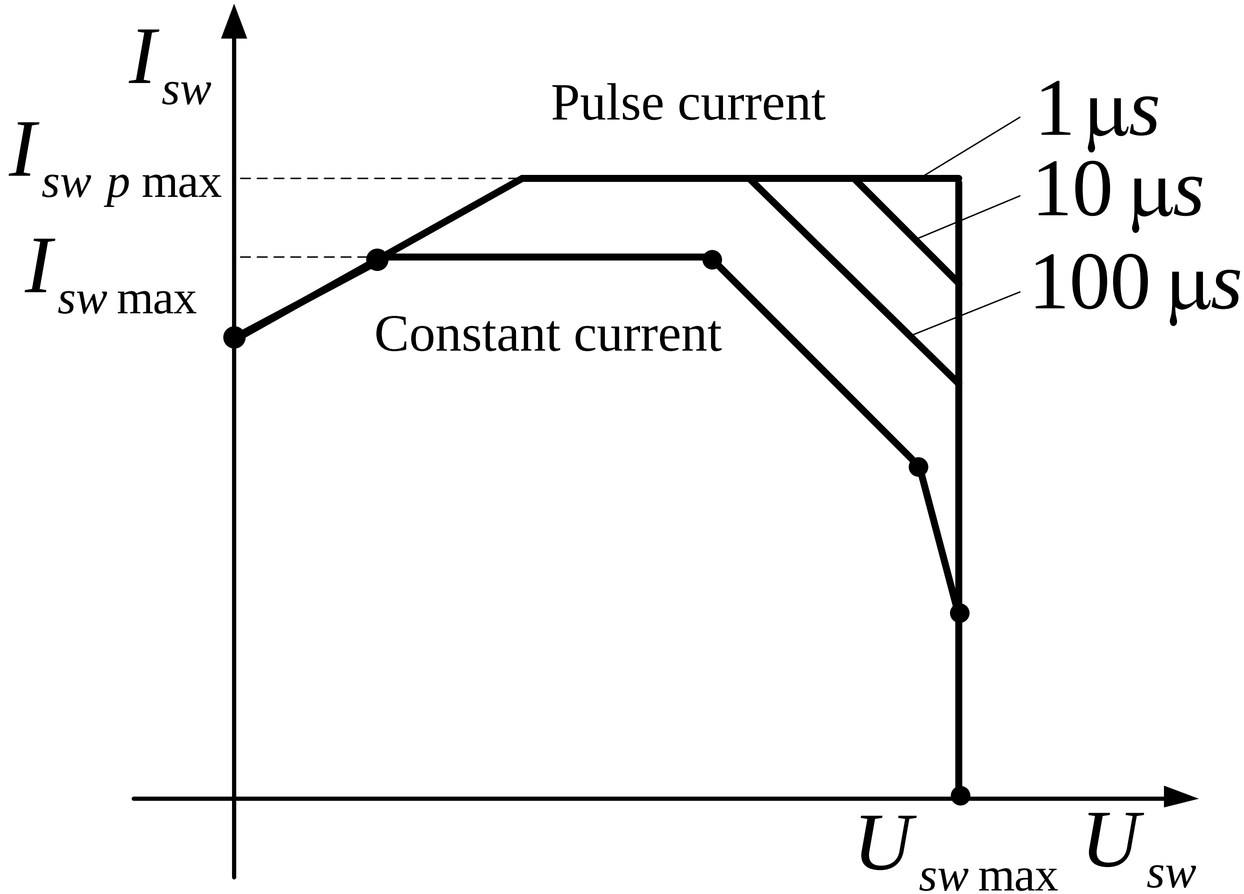

Fig. 1.28. Typical SMB diagram in the pulse mode

Semiconductor switch breakdown protection

Converter circuit and its elements protection have in general two ways:

- 1. Elimination of causes and sources of electrical overloads;
- 2. Control of natural overloads.

Basic kinds of voltage overloads are:

- 1. Voltage spikes in mains;
- 2. Voltage spikes connected with commutation process in converter circuit and conditioned by limited time of power switches commutation;
- 3. Overvoltages connected with load character.

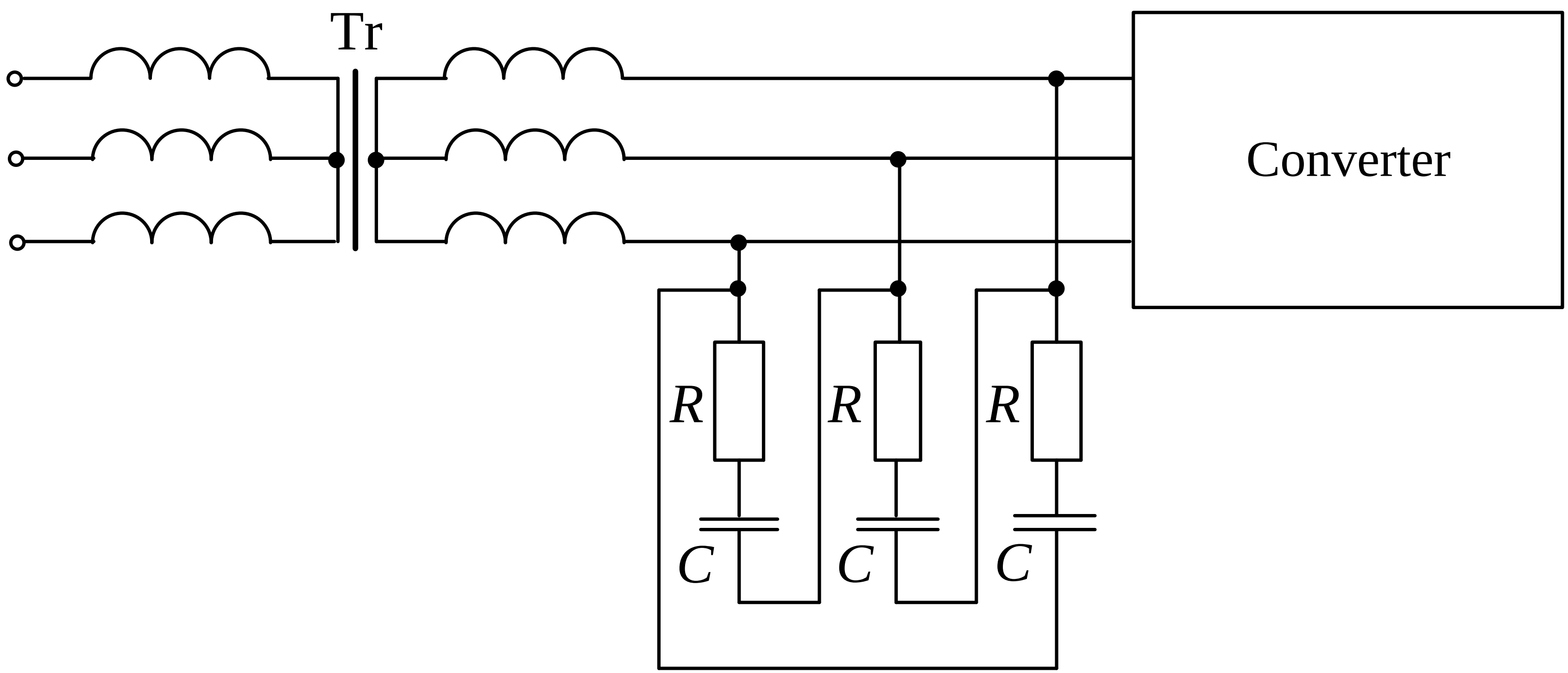

Fig. 1.29. External circuit protection device

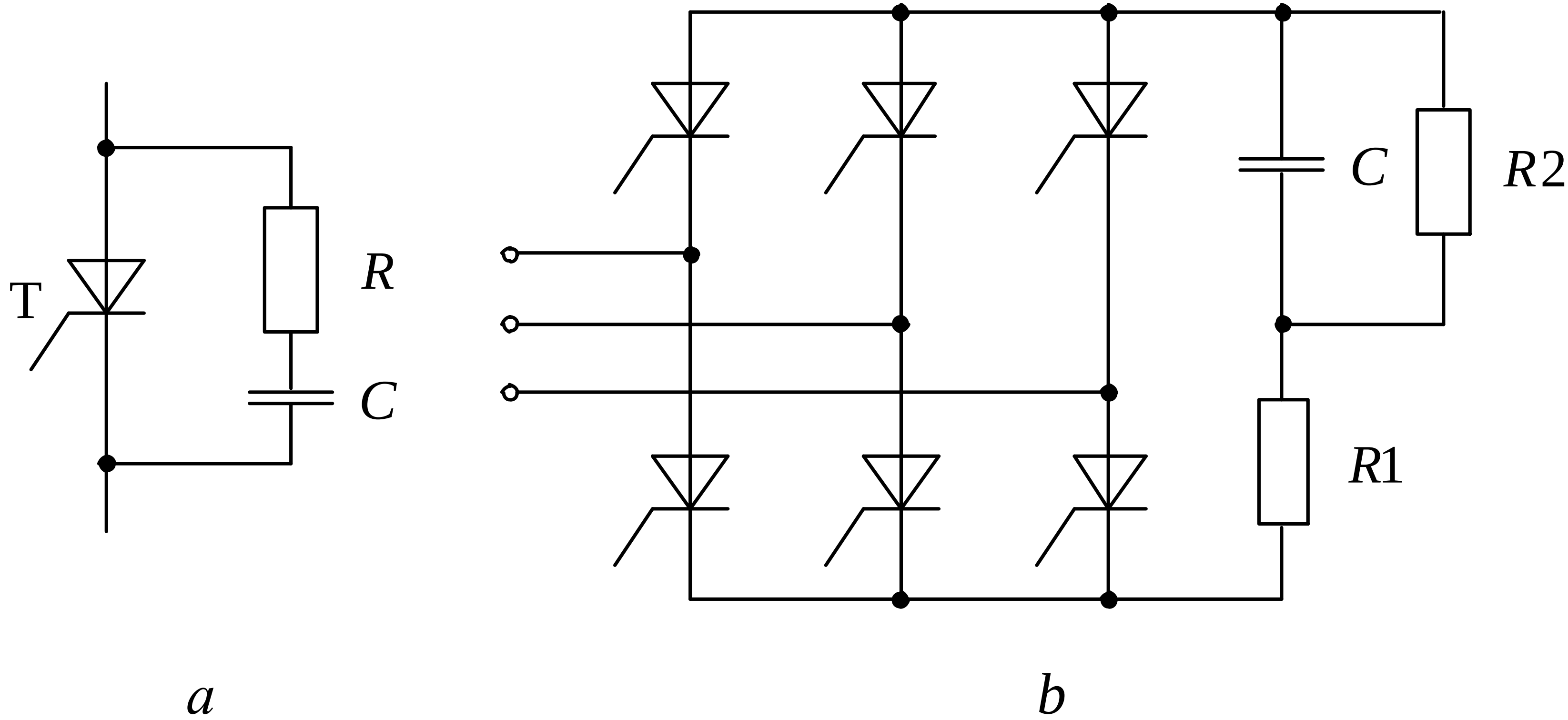

Fig. 1.30. Protection device circuit

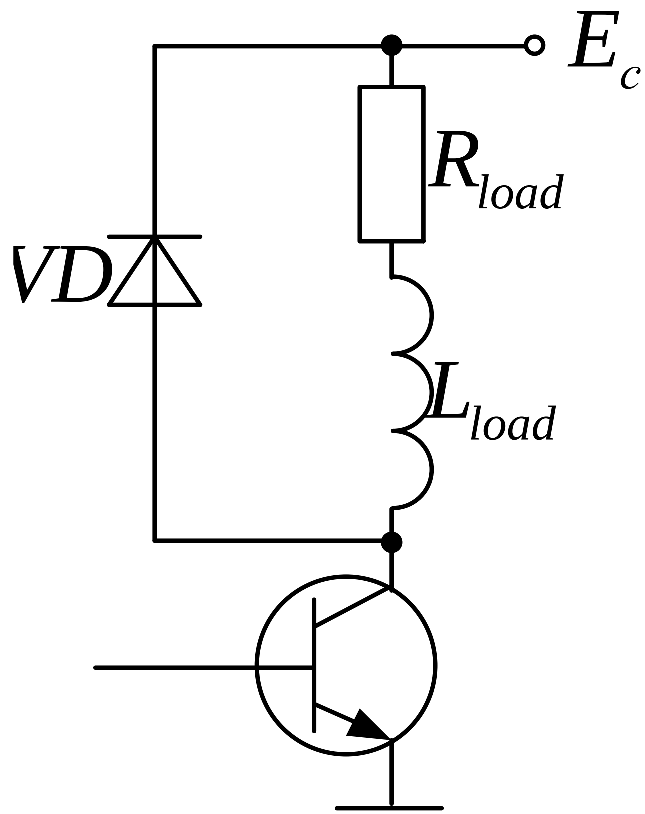

Fig. 1.31. Protection device circuit

Basic types of current overloads are:

- 1. Short-circuit of load circuit;
- 2. Short-circuit of output terminals of converter;
- 3. Short-circuit because of the power switches failure;
- 4. Overcurrents, connected with violation of power switches operation algorithm (inverter triggering, self-starting of turning-off switch, etc.);
- 5. Overcurrents, connected with operation peculiarities of power circuit and non-ideality of switches (through currents in bridge circuits, etc.);
- 6. Overcurrents, stipulated by transients and load character (starting mode, motor reverse, motor overload, etc.)

For overcurrent protection the most important actions are:

- 1. Increase of noise immunity of control system and the switch itself, which eliminates self-starting spontaneous turning-on process;
- 2. External protection devices use, which limits the overcurrent influence on power switches and other circuit components (current-limiting circuits and reactors);
- 3. Use of fast-acting protection systems.

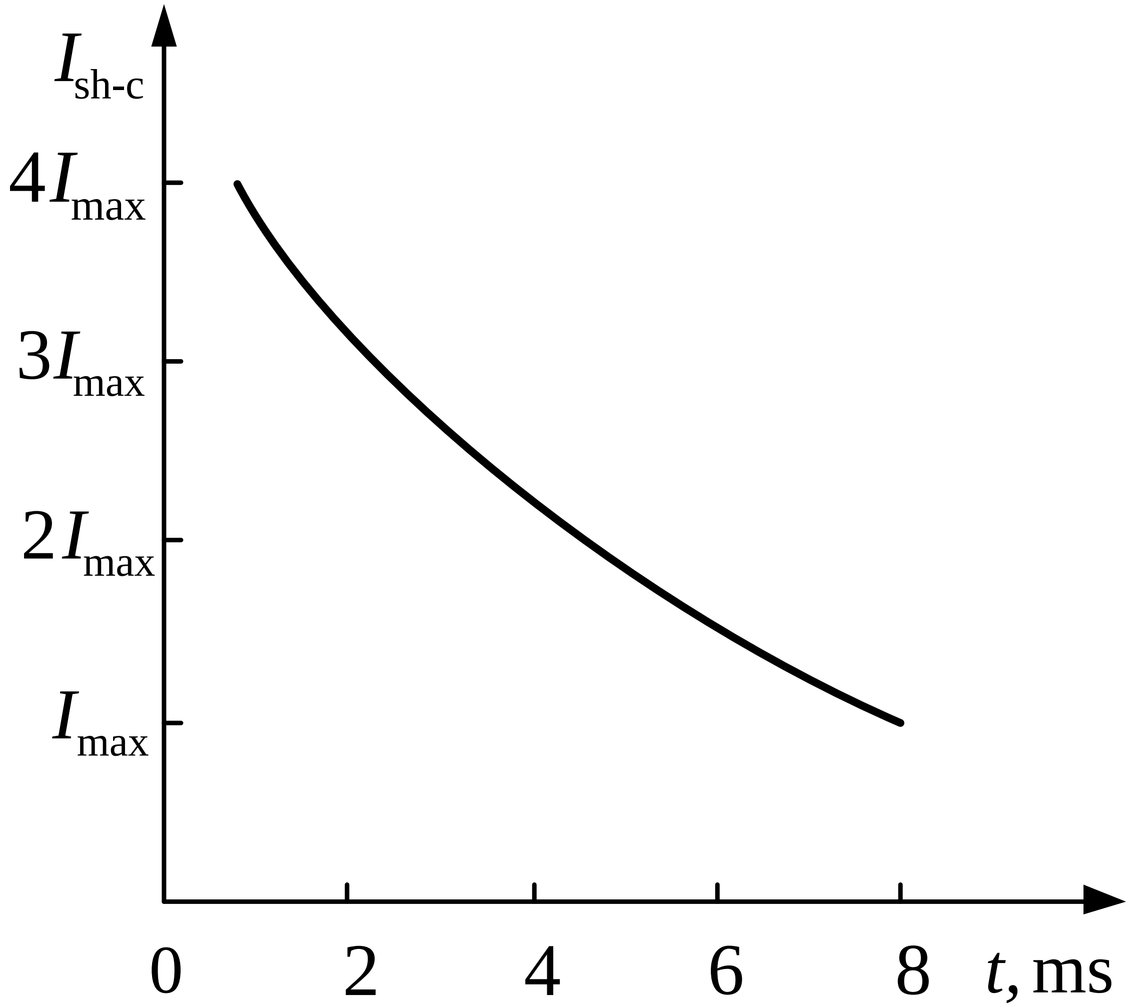

Fig. 1.32. Typical overload characteristic

Electrical capacitors

Electrical capacitors are widely used in power converters of electric energy:

- as AC and DC filters components;
- as energy storages;
- as reinforced switching blocks;
- as protection components of semiconductor devices and for other problems solving.

Fig. 1.33. Capacitors

- Voltage and frequency define dielectric loss power:

$$P_c = 2\pi \cdot U_c^2 \cdot f \cdot C \cdot \mathrm{tg}\,\delta \qquad (1.15)$$

where U_c – RMS value of capacitor voltage; f – operating frequency; C – capacitance; tg δ – dielectric loss tangent (outlined in capacitor’s nameplate).

- Capacitors operation in AC circuits with non-sinusoidal voltage usually occur in power electronics. In this case it is necessary to take into account the capacitor losses from each of the harmonic components, which present in non-sinusoidal function decomposition on harmonic series:

$$P_c = \sum_{n=1}^{\infty} P_{cn} \qquad (1.16)$$

where n – serial number of harmonic component.

Inductors

Fig. 1.34. Inductive elements: a – transformers, b – inductors (reactors, chokes)

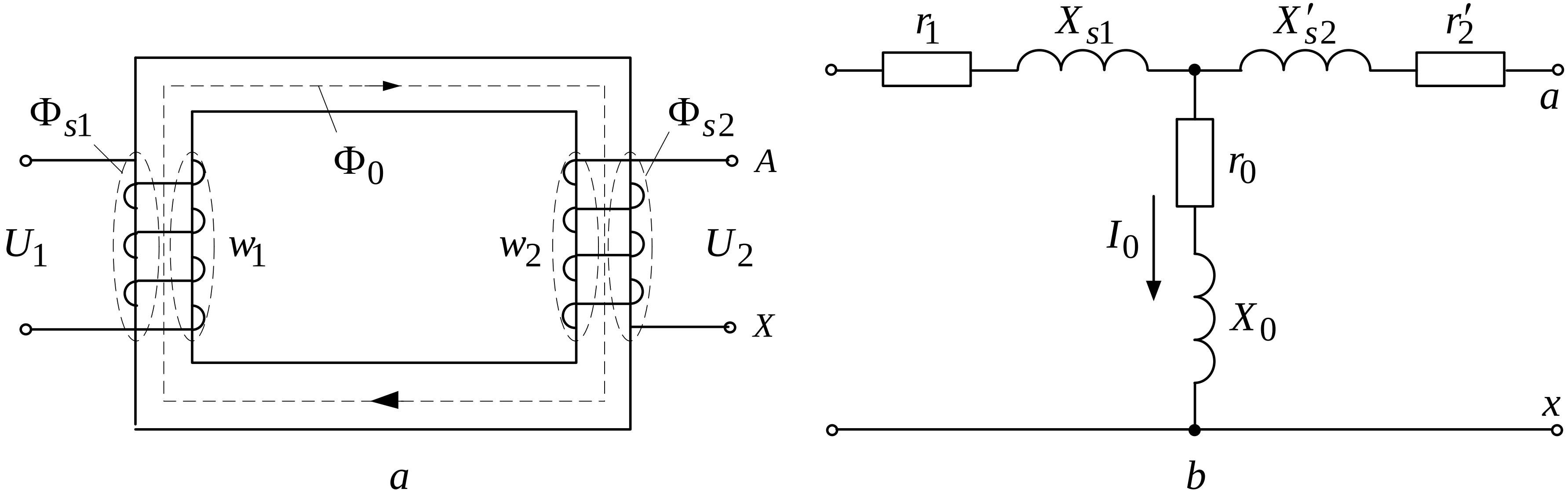

Fig. 1.35. Magnetic fluxes in transformer (a) and its equivalent circuit (b)

- Besides main flux Φ_0, connecting primary w_1 and secondary w_2 windings (fig. 1.35, a), leakage fluxes exist, connected only with the turns of their own winding: primary winding leakage flux Φ_{s1} and secondary winding leakage flux Φ_{s2}.

Leakage inductive reactances:

$$X_{s1} = w \cdot L_{s1}$$

$$X_{s2} = w \cdot L_{s2}$$

at cyclic frequency $w = 2 \cdot \pi \cdot f$

- Inductive magnetization reactance

$$X_0 = w \cdot L_0$$

- Transformation ratio

$$k_{tr} = \frac{w_1}{w_2}$$

$$X'_{s2} = k_{tr} \cdot X_{s2} \qquad r'_2 = k_{tr} \cdot r_2 \qquad (1.17)$$

- From the no-load test the parameters of magnetization circuit are defined as follows:

$$r_0 = \frac{P_{nl}}{I_0^2} \qquad \cos\varphi_{nl} = \frac{P_{nl}}{S_{nl}} \qquad X_0 = r_0 \cdot \mathrm{tg}\,\varphi_{nl} \quad (1.18)$$

where P_{nl} – no-load loss power,

I_0 – magnetizing current,

S_{nl} – gross capability.

$S_{nl} = U_{1r} \cdot I_0$,

where U_{1r} – primary winding rated voltage in the no-load mode.

- From the short-circuit test the windings' active resistances r_1 and r_2', leakage inductive reactances X_{s1}, X_{s2} are defined as follows:

$$r_1 + r_2' = \frac{P_{sc}}{I_{1r}^2} \quad \cos\varphi_{sc} = \frac{P_{sc}}{S_{sc}} \qquad (1.28)$$

$$X_{s1} + X_{s2}' = \left(r_1 + r_2'\right) \cdot tg\,\varphi_{sc}$$

where I_{1r} – rated primary winding current,

P_{sc} – loss power in the short-circuit mode,

S_{sc} – gross capability in the short-circuit mode

$S_{sc} = U_{sc} \cdot I_{1r}$

where U_{sc} – short-circuit voltage.

- Electric steel magnetic core losses are summarized from hysteresis losses and eddy currents losses. Both loss components depend on the frequency and magnitude of magnetic flux density in steel. Hysteresis losses depend on frequency to a lesser degree than eddy currents losses. For eddy currents losses reduction the transformers and chokes magnetic cores are made of thin sheet steel.

- EMF induced in transformer windings

$$E = k_{sh} \cdot w \cdot f \cdot B_m \cdot S \quad (1.29)$$

where k_{sh} – voltage shape factor (for sine wave $k_{sh} = 1{,}11$), w – the number f winding turns, f – frequency of conversion, B_m – the magnitude of magnetic flux density in core, S – core cross-section.

- For transformer overheating exception it is necessary to decrease magnetic flux density as frequency increases approximately by the next expression:

$$B = \frac{1}{f^{0,65}}$$

Typical specific transformer weight $\left(\frac{kg}{kW} \right)$ dependence is shown in fig. 1.42.

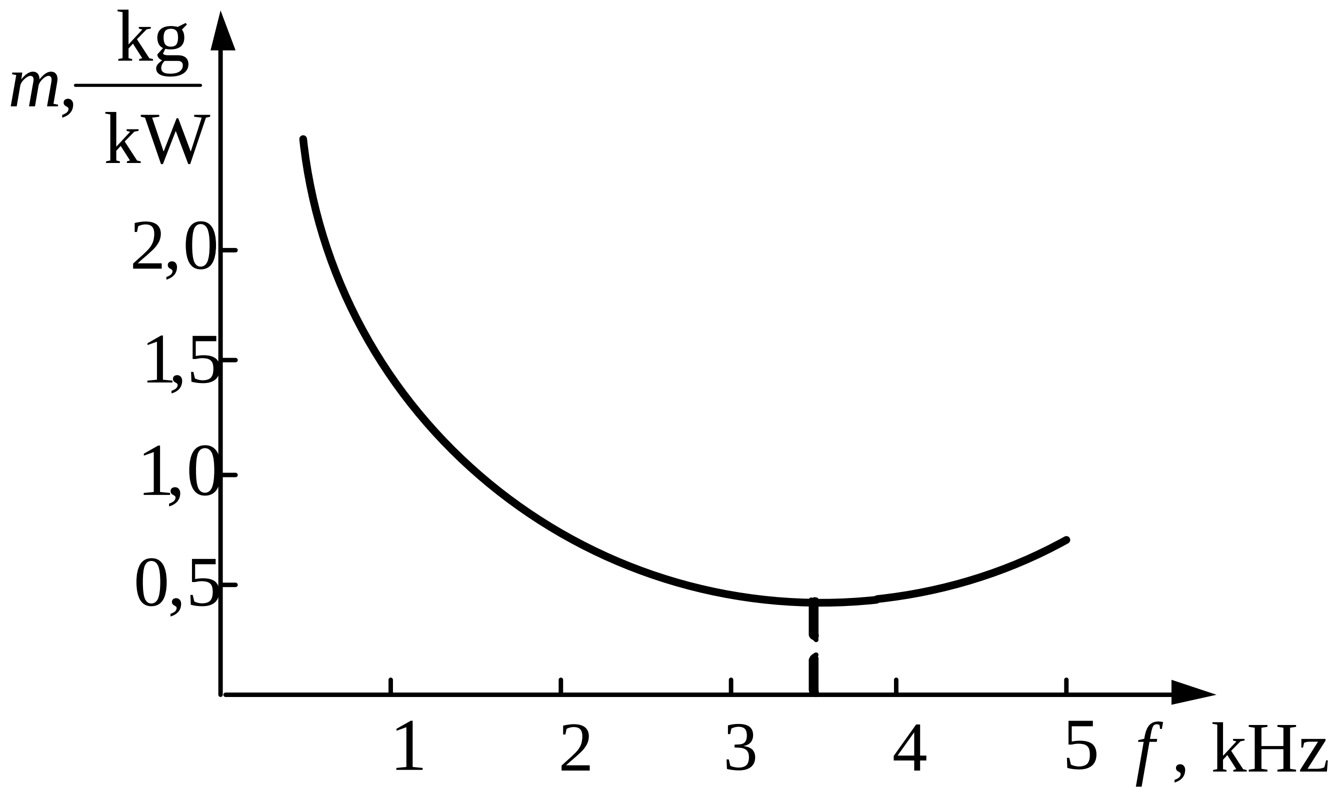

Fig. 1.42 Transformer specific weight dependence on frequency

From the dependence shown it follows that rated frequency value for electric steel is within the range 3…5 kHz. At higher frequency (5…15 kHz) iron-nickel alloys (permalloys) find wide application. At more higher frequency (15…40 kHz) ferrite materials are used.

Transformer winding losses are composed by the main losses – losses in active resistances of windings, and additional losses –losses produced by the current displacement in wire (skin effect) at frequency greater than 1 kHz.

RECTIFIERS

Rectifiers are the devices which convert electric energy of alternating current into electric energy of direct current.

For non-controlled rectifiers:

$$E_d = k_{cir} \cdot E_2$$

where E_d – output DC voltage,

E_2 – RMS value of input AC voltage,

k_{cir} – circuit coefficient.

Non-controlled rectifiers

Single-phase half-wave rectifier circuit

Assume that:

1. Active resistance and inductive reactance of transformer’s windings are neglected.
2. Load is active.
3. Diode VD is ideal.
4. Magnetizing current is neglected.
5. Transformer’s winding EMF is sinusoidal

$$e_2 = \sqrt{2} \cdot E_2 \cdot \sin \theta$$

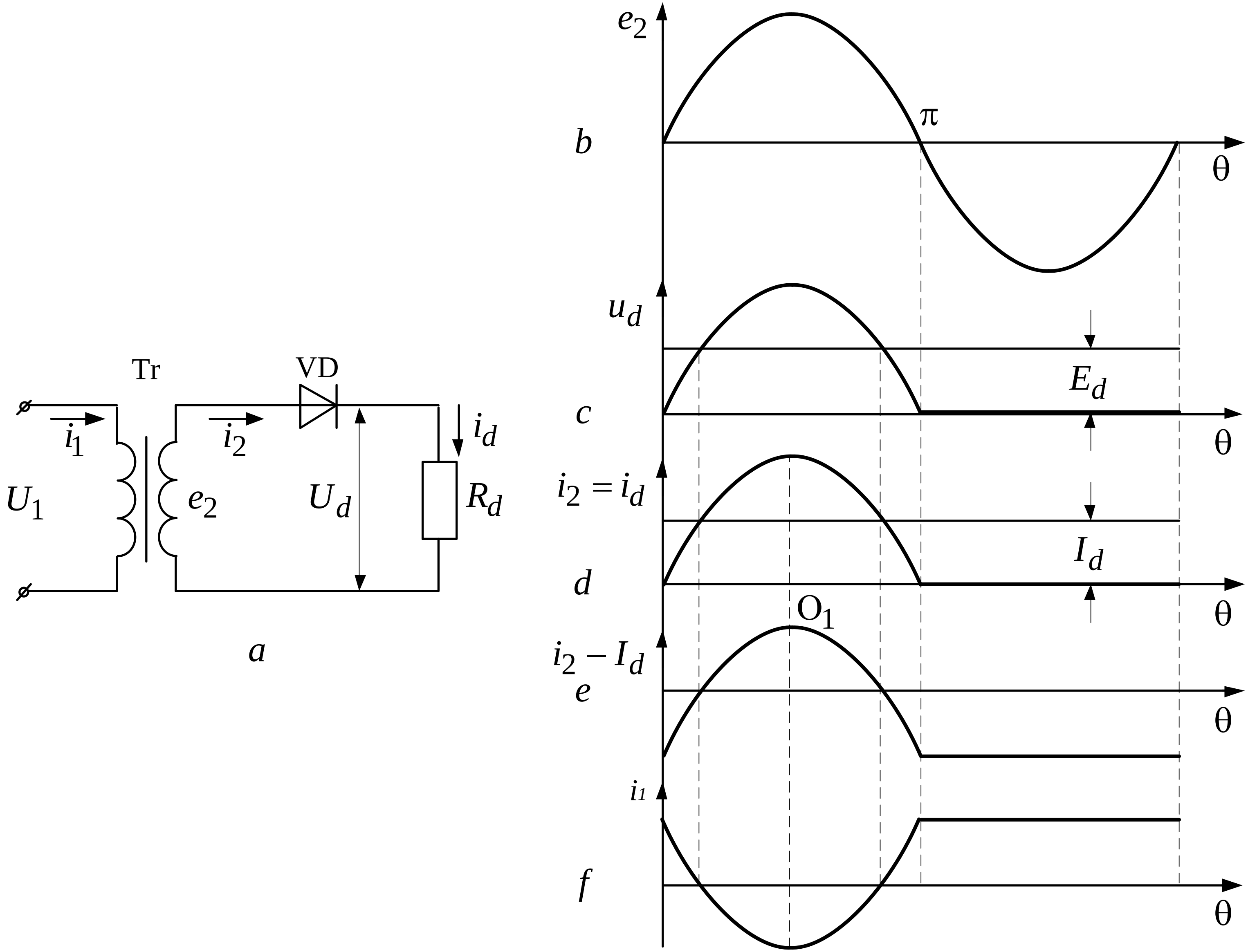

Fig. 2.1 Single-phase half-wave rectifier circuit and diagram explaining its operation

Instantaneous value of rectified voltage, (fig. 2.1, c)

$$U_d\big|_{0\ldots\pi} = \sqrt{2}\cdot E_2 \cdot \sin\theta, U_d\big|_{\pi\ldots 2\pi} = 0$$

Constant component of rectified voltage

$$E_d = \frac{1}{2\pi}\int_0^{2\pi} U_d \, d\theta = \frac{1}{2\pi}\int_0^{2\pi} \sqrt{2}\cdot E_2 \cdot \sin\theta \, d\theta = \\ = \frac{\sqrt{2}\cdot E_2}{\pi} = 0,45\cdot E_2 \qquad (2.1)$$

Instantaneous value of rectified current (fig. 2.1, d):

$$i_d = i_2 = \frac{U_d}{R_d}$$

Constant component of rectified current

$$I_d = \frac{E_d}{R_d}$$

Average anode current

$$I_{a.av} = I_d$$

Maximum anode current

$$i_{a.\max} = \frac{\sqrt{2} \cdot E_2}{R_d} = I_d \cdot \pi \quad (2.2)$$

Maximum value of reverse voltage on the diode

$$U_{rev.\max} = \sqrt{2} \cdot E_2 = E_d \cdot \pi$$

Calculated power of transformer Tr:

$$P_{calc} = \frac{P_1 + P_2}{2} \quad (2.3)$$

where P_1 and P_2 – calculated powers of primary and secondary windings accordingly.

Effective value of secondary winding current

$$I_2 = \sqrt{\frac{1}{2\pi}\int_0^{2\pi} i_2^2 \, d\theta} = I_d \cdot \frac{\pi}{2} \quad (2.4)$$

Secondary winding power

$$P_2 = \frac{E_d \cdot \pi}{\sqrt{2}} \cdot \frac{\pi}{2} \cdot I_d = 3,49 \cdot P_d \quad (2.5)$$

where $P_d = E_d \cdot I_d$ – load power.

Transformer's primary winding power

$$P_1 = E_1 \cdot I_1$$

where E_1 and I_1 are effective values of EMF and current of transformer's primary winding accordingly.

EMF E_1 is defined by the next expression

$$E_1 = E_2 \cdot k_{tr}$$

where $k_{tr} = \frac{w_1}{w_2}$ is transformation coefficient,

w_1 and w_2 are numbers of turns of primary and secondary windings accordingly.

The primary current I_1 is defined as

$$I_1 = \sqrt{\frac{1}{2\pi}\int_0^{2\pi} i_1^2 \, d\theta} \quad (2.6)$$

where i_1 is instantaneous value of the primary current.

From the condition of equality of primary and secondary transformer's windings magnetizing forces it is implied that

$$i_1 \cdot w_1 + \left(i_2 - I_d\right) \cdot w_2 = 0 \quad (2.7)$$

From the equation (2.7) we find i_1

$$i_1 = -\frac{w_2}{w_1} \cdot \left(i_2 - I_d\right) = -\frac{1}{k_{tr}} \cdot \left(i_2 - I_d\right) \quad (2.8)$$

Since current i_2 flows through secondary transformer's winding only in the range 0…π and in the range π…2π the current equals to zero, then

$$\begin{cases} i_1\big|_{0\ldots\pi} = \dfrac{I_d}{k_{tr}} \cdot \left(1 - \pi \cdot \sin\theta\right) \\ i_1\big|_{\pi\ldots 2\pi} = \dfrac{I_d}{k_{tr}}. \end{cases} \qquad (2.9)$$

Effective value of primary current

$$I_1 = 1,21 \cdot \frac{I_d}{k_{tr}} \quad (2.10)$$

Transformer's primary winding power

$$P_1 = E_1 \cdot I_1 = 2,69 \cdot P_d \quad (2.11)$$

Substituting in the formula (2.3) equations (2.11) and (2.5), we get the calculated power of the transformer

$$P_{calc} = \frac{P_1 + P_2}{2} = 3,06 \cdot P_d \quad (2.12)$$

Higher order harmonic components

$$B_k = \frac{1}{\pi} \int_{-\pi/2}^{\pi/2} i_2 \cdot \cos k\theta \, d\theta \quad (2.13)$$

Function i_2 expansion in a Fourier series can be expressed as

$$i_d = \frac{2 \cdot I_m}{\pi} \left(\frac{1}{2} + \frac{\pi}{4} \cdot \cos\theta + \right.$$

$$\left. + \frac{1}{3 \cdot 1} \cdot \cos 2\theta - \frac{1}{3 \cdot 5} \cdot \cos 4\theta + \ldots \right) \quad (2.14)$$

where I_m – magnitude of current i_2

Instantaneous power value transferred by the first harmonic component of that current equals to

$$P_2^{'} = \sqrt{2} \cdot E_2 \cdot \left(\cos\theta\right) \cdot \frac{I_m}{2} \cdot \left(\cos\theta\right) = \qquad (2.15)$$

$$= \frac{\sqrt{2} \cdot E_2 \cdot I_m}{2} \cdot \cos^2\theta$$

Since the losses are neglected then the same power is transferred by the first harmonic component of primary current:

$$P_1^{'} = P_2^{'}$$

Power transferred by the second current harmonic component

$$P_2^{''} = P_1^{''} = \sqrt{2} \cdot E_2 \cdot \left(\cos\theta\right) \cdot \frac{2 \cdot I_m}{3 \cdot \pi} \cdot \left(\cos 2\theta\right) \quad (2.16)$$

But in the secondary winding constant component of the current I_d transfers the power:

$$\Delta P = \sqrt{2} \cdot E_2 \cdot I_d \cdot \cos \theta \quad (2.17)$$

More frequently the rectifier’s load has active-inductive character, particularly in rectifiers of medium and high power.

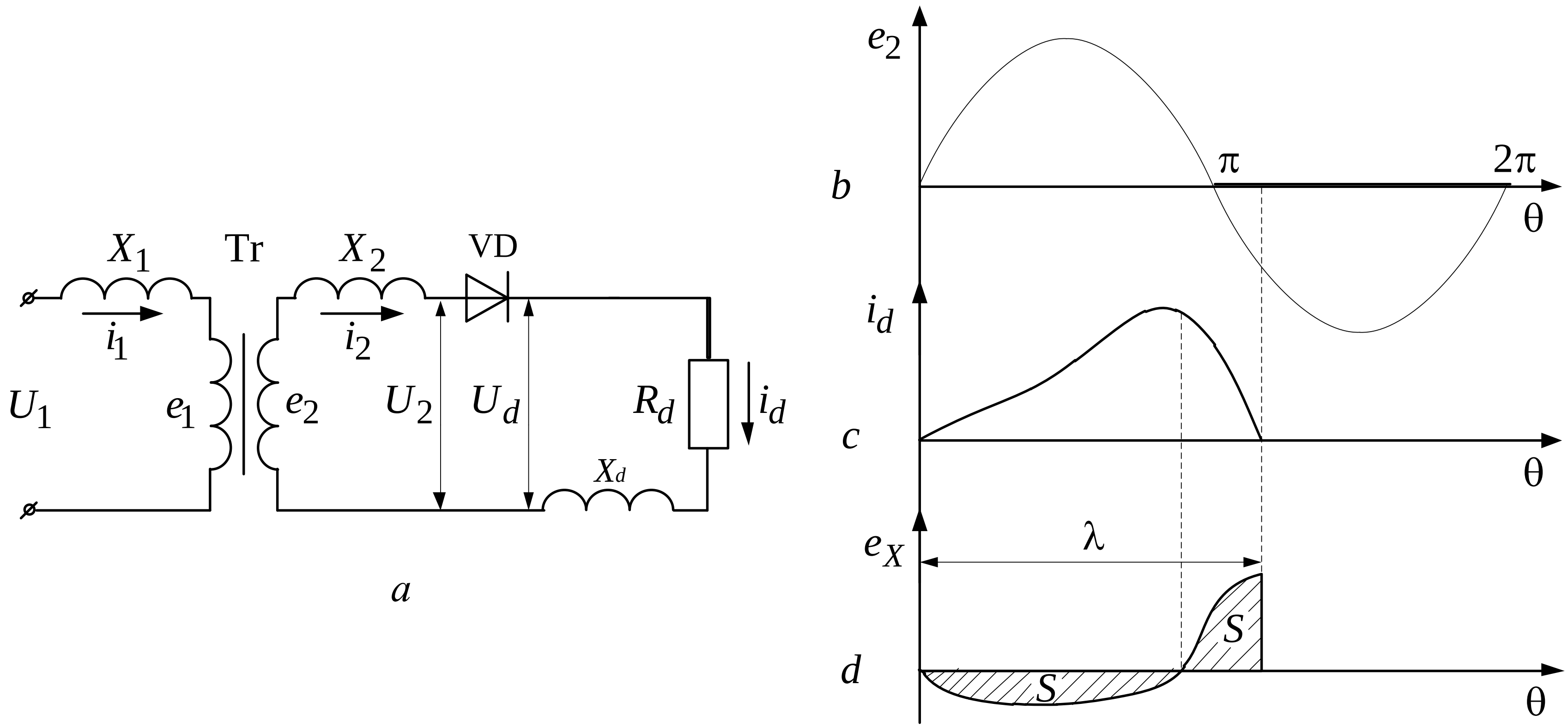

Fig. 2.2. Single-phase half-wave rectifier operation on active-inductive load

Equation for the primary winding circuit:

$$e_1 - X_1 \frac{di_1}{d\theta} + U_1 = 0 \quad (2.18)$$

Expressing e_1 from (2.18) we get:

$$e_1 = -U_1 + X_1 \frac{di_1}{d\theta} \quad (2.20)$$

where the primary current i_1 is expressed

is expressed in compliance with (2.19):

$$i_1 = -\frac{1}{k_{tr}} \cdot \left(i_2 - I_d \right)$$

For the secondary winding of transformer the equality is true:

$$U_2 = e_2 + X_2 \frac{di_2}{d\theta} \quad (2.20)$$

where $e_2 = \dfrac{e_1}{k_{tr}}$

This expression conversion gives:

$$U_2 = -\frac{U_1}{k_{tr}} \cdot \left(\frac{X_1}{k_{tr}^2} + X_2 \right) \cdot \frac{di_2}{d\theta} = -\frac{U_1}{k_{tr}} - X_{leak} \frac{di_2}{d\theta} \quad (2.21)$$

where X_{leak} – total leakage inductive reactance of transformer’s windings reduced to the secondary winding circuit.

For the load circuit it can be written:

$$U_d = i_d \cdot R_d = \sqrt{2} \cdot E_2 \cdot \sin\theta$$

Designating $-\dfrac{U_1}{k_{tr}} = E_2,\ X_d + X_{leak} = X$

and substituting U_2 from the equation (2.21),

we get:

$$X \cdot \frac{di_d}{d\theta} + i_d \cdot R_d = \sqrt{2} \cdot E_2 \cdot \sin\theta \quad (2.22)$$

Solution of this equation relative to the current i_d subject to zero initial conditions gives the expression:

$$i_d = \frac{\sqrt{2} \cdot E_2}{\sqrt{X^2 + R_d^2}} \left[\left(\sin \varphi \right) \cdot e^{-\mathrm{ctg}\,(\varphi\theta)} + \sin\,(\theta - \varphi) \right] \quad (2.23)$$

where $\varphi = \mathrm{arctg}\,\dfrac{X}{R_d}$

Constant component of rectified voltage:

$$E_d = \frac{1}{2\pi}\int_0^{\lambda} U_d \, d\theta = \frac{1}{2\pi}\int_0^{\lambda}\left(e_2 - e_x\right) d\theta = \qquad (2.24)$$
$$= \frac{\sqrt{2}\cdot E_2}{2\pi}\cdot\left(1-\cos\lambda\right)$$

where λ is the duration of conducting state interval of the diode VD.

In relative units the expression (2.24) will get the next form:

$$E_d^* = \frac{E_d}{E_{\max}} = \frac{1-\cos\lambda}{2} \qquad (2.25)$$

For finding λ assume the next condition:

$i_d\big|_{\theta-\lambda}=0$ or $(\sin\varphi)\cdot e^{-\mathrm{ctg}(\varphi\lambda)}+\sin(\lambda-\varphi)=0$ (2.26)

The dependence $\lambda=f(\varphi)$ has the form depicted. in fig. 2.3.

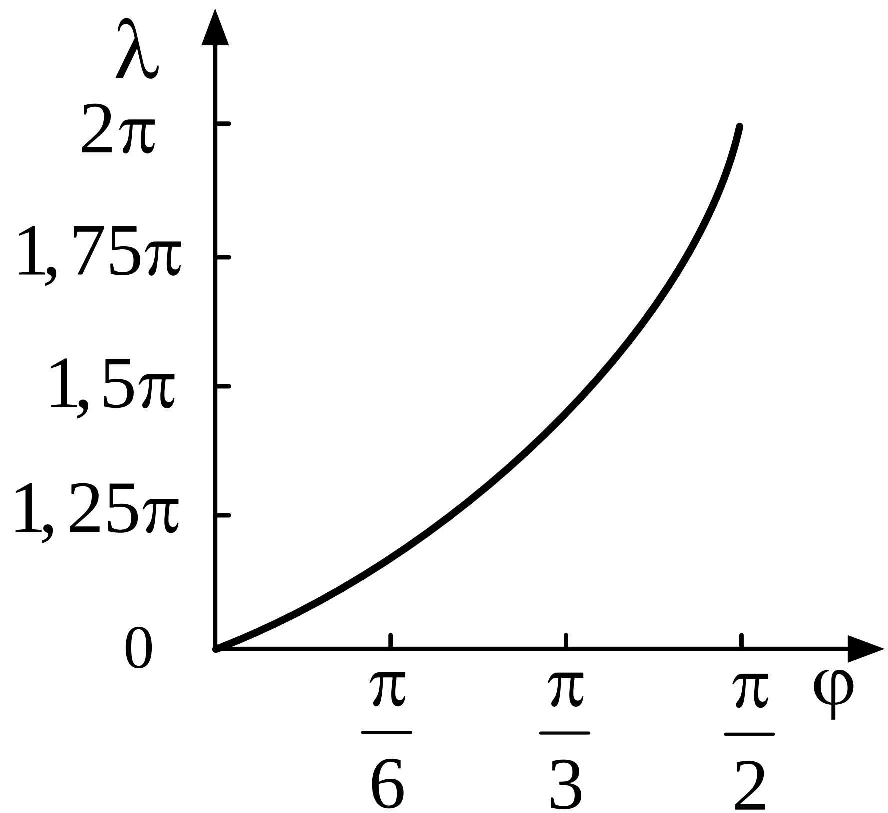

Fig. 2.3. Dependence of conducting state duration of diode VD from load parameters

Constant component of rectified current

$$i_d = \frac{E_d}{R_d} = \frac{\sqrt{2} \cdot E_2}{2\pi \cdot R_d}\left(1 - \cos\lambda\right) \quad (2.27)$$

or in relative units:

$$I_d^* = \frac{I_d}{I_{d.\max}} = \frac{1 - \cos\lambda}{2\pi} \cdot \operatorname{tg}\varphi = \frac{E_d^*}{\pi} \cdot \operatorname{tg}\varphi \quad (2.28)$$

where $I_{d.\max} = i_d\Big|_{R_d = 0} = \dfrac{\sqrt{2} \cdot E_2}{X}$

Thus expression (2.28) is the equation of rectifier's external characteristic $E_d^* = f\left(I_d^*\right)$, depicted in Fig. 2.4.

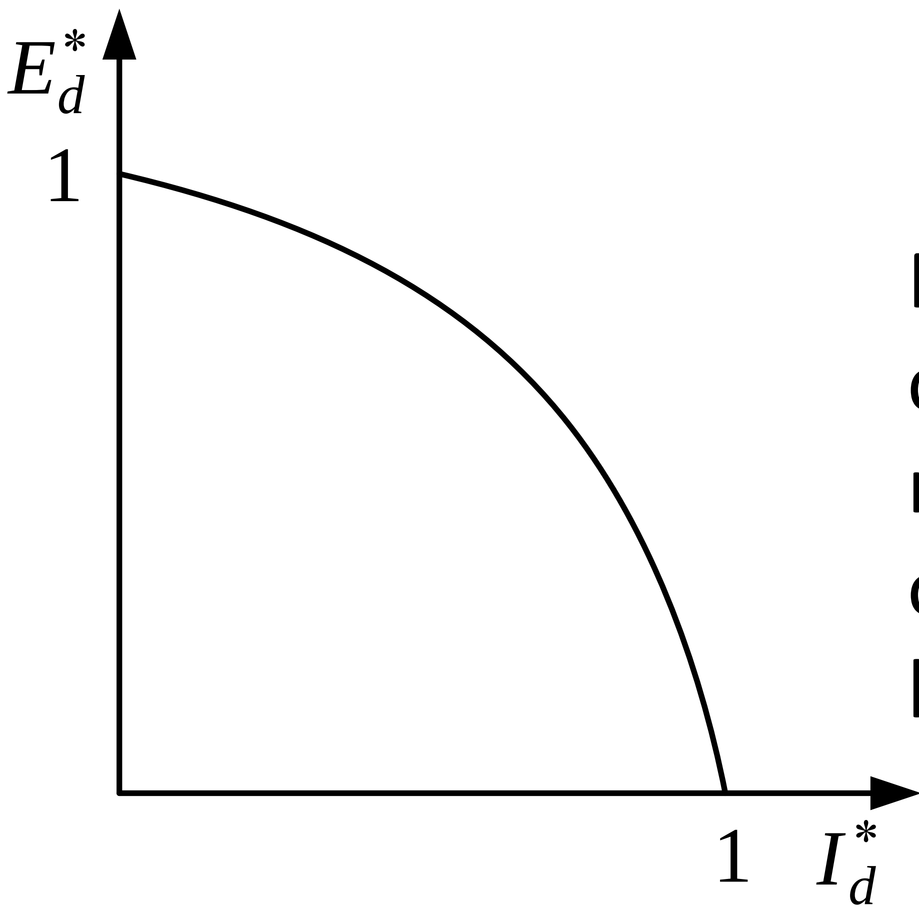

Fig. 2.4. External characteristic of rectifier operating on active-inductive load

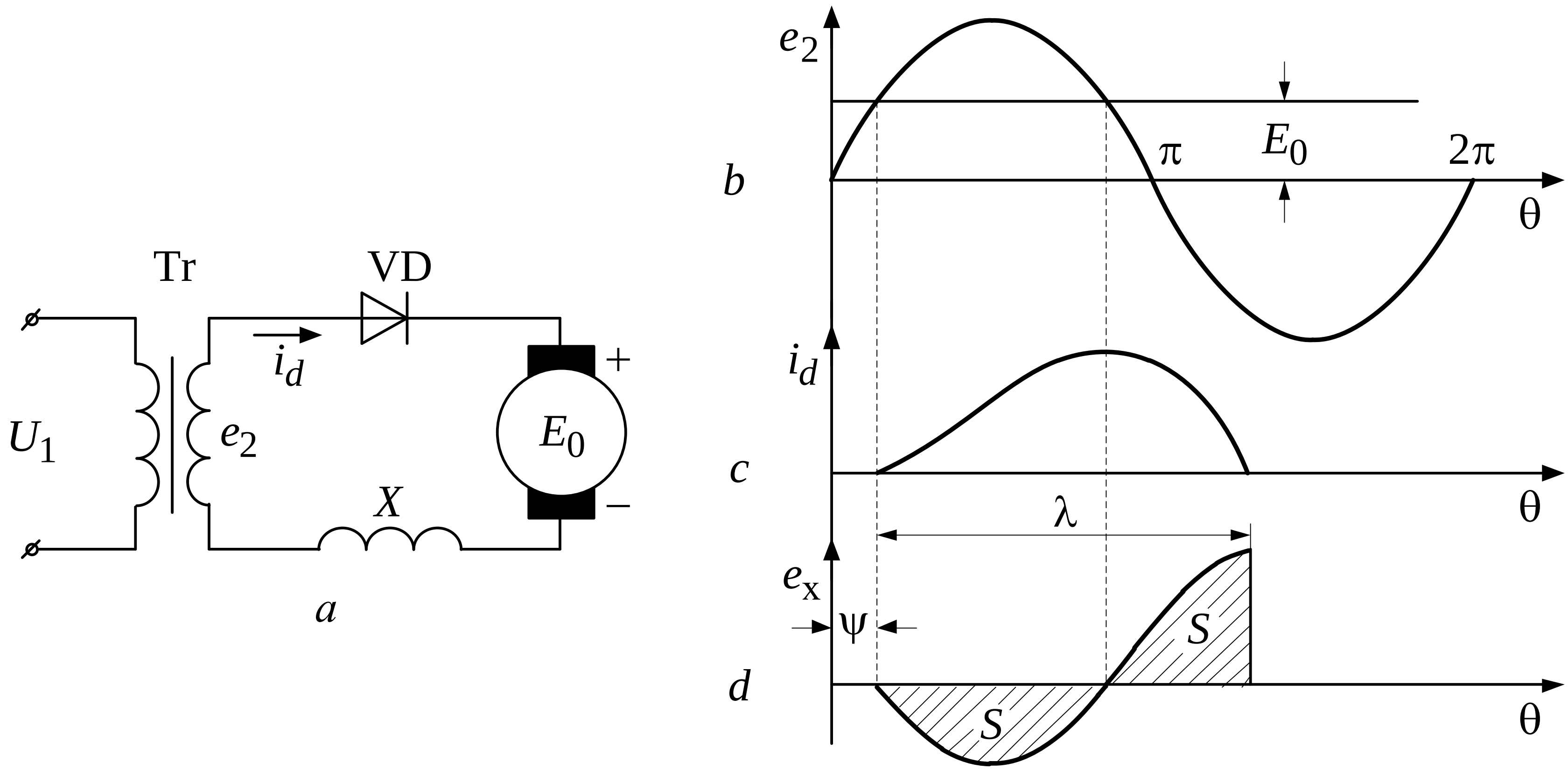

Fig. 2.5. Single-phase half-wave rectifier operation on DC motor load

For the load circuit the equation is as follows:

$$e_2 - X\,\frac{di_d}{d\theta} = E_0 \text{ or}$$

$$\sqrt{2}\cdot E_2\cdot \sin\left(\theta+\psi\right) - X\,\frac{di_d}{d\theta} = E_0 \qquad (2.29)$$

Solving this equation for i_d we get

$$i_d = \frac{\sqrt{2}\cdot E_2}{X}\left[\cos\psi - \cos\left(\theta+\psi\right)\right] - \frac{E_0}{X}\cdot\theta \quad (2.30)$$

Constant component of load current:

$$I_d = \frac{1}{2\pi}\int_0^{\lambda} i_d \, d\theta =$$

$$= \frac{\sqrt{2}\cdot E_2}{2\pi\cdot X}\left[\lambda\cdot\cos\psi - \sin\left(\lambda+\psi\right)+\sin\psi\right] - \frac{E_0\cdot\delta^2\cdot\pi}{X} \qquad (2.31)$$

where $\delta = \dfrac{\lambda}{2\pi}$

In relative values:

$$I_d^* = \frac{I_d}{I_{d\,\max}} =$$

$$= \frac{1}{2\pi} \cdot \left[\lambda \cdot \cos\psi - \sin\left(\lambda + \psi\right) + \sin\psi\right] - E_d \cdot \delta^2$$

where $I_{d\,\max}\Big|_{E_0=0} = \dfrac{\sqrt{2} \cdot E_0}{X}$; $E_d^* = \dfrac{E_0}{E_{d\,\max}}$;

$$E_{d\,\max} = \frac{\sqrt{2} \cdot E_2}{\pi}$$

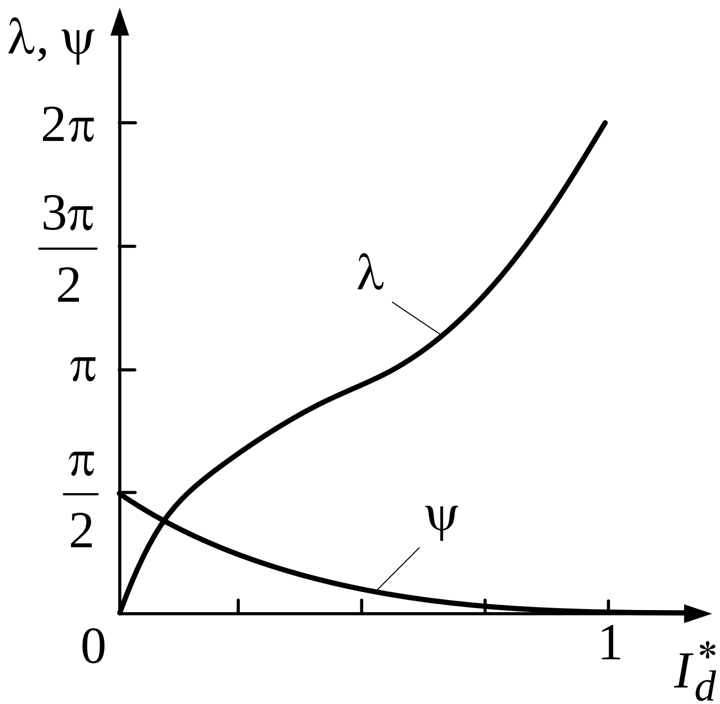

Fig. 2.6. Dependence the diode conducting state duration and the delay angle from the load current

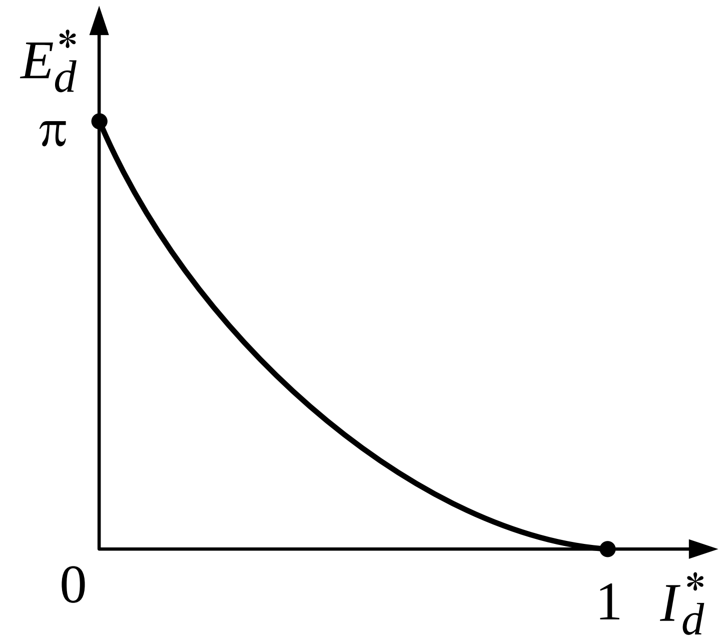

Fig 2.7. External characteristic of the rectifier with DC motor load

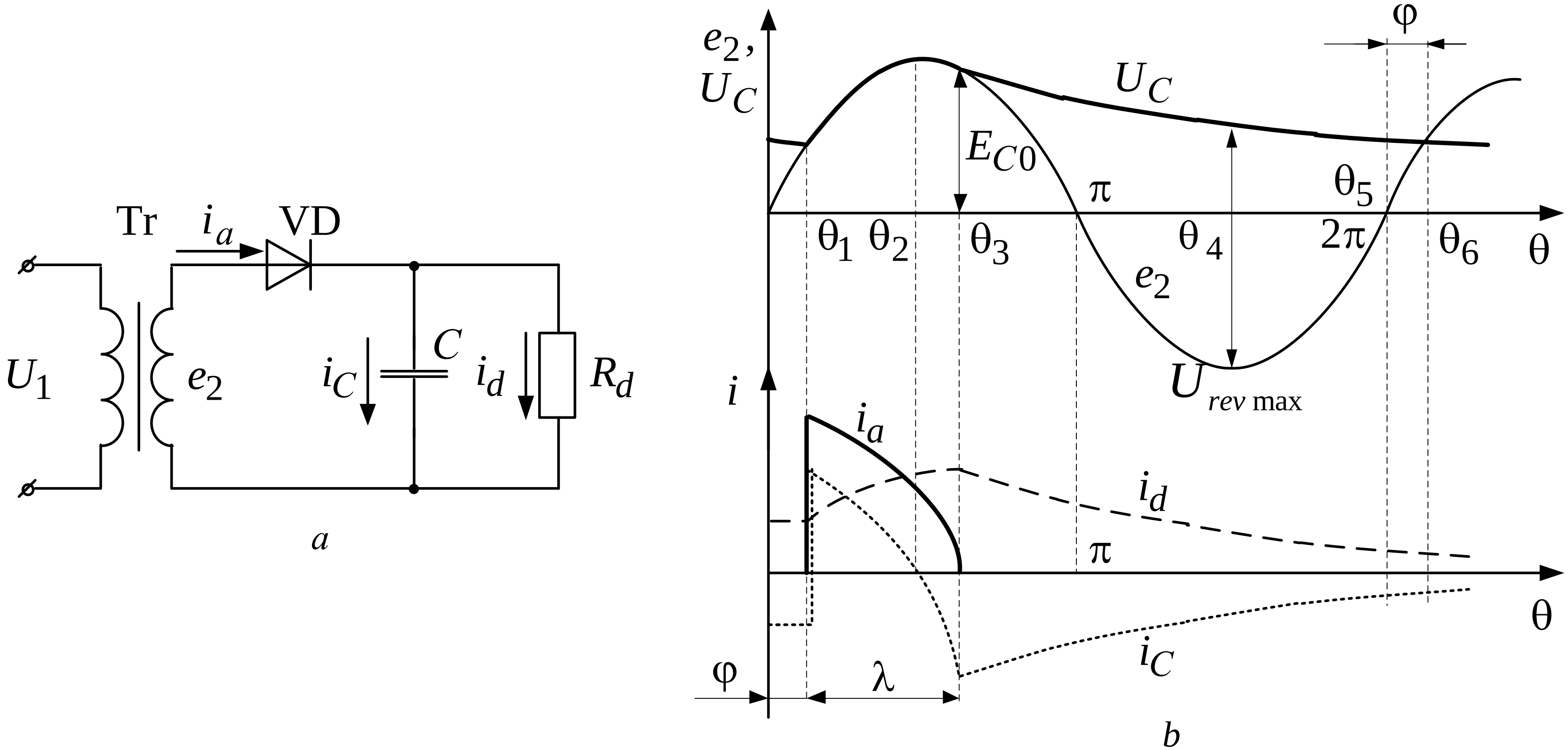

Fig. 2.8. Single-phase half-wave rectifier operation with active-capacitive load

In the range $O_1 \ldots O_2$ current flowing through diode VD charges the capacitor C.

The next expressions are equitable:

$$i_a = i_C + i_d = \frac{e_2}{R_d} = \frac{\sqrt{2} \cdot E_2 \cdot \sin\left(\theta + \phi\right)}{R_d} \qquad (2.32)$$

$$i_C = \omega \cdot C \cdot \frac{dU_C}{d\theta} = \sqrt{2} \cdot E_2 \cdot \omega \cdot C \cdot \cos\left(\theta + \phi\right).$$

Within the range $O_2 \dots O_3$ the equality is right

$$i_d = i_C + i_a$$

In the range $O_3 \dots O_6$ load current flows through only due to capacitor C discharge. In this case the next expression reasonable:

$$U_d = U_C = E_{C0} \cdot e^{-\frac{\theta - \lambda - \phi}{\omega \cdot C \cdot R_d}} \quad (2.33)$$

At a point O_6 $U_d = U_{C\min} = E_{C0} \cdot e^{-\frac{2\pi - \lambda}{\omega \cdot C \cdot R_d}}$

$$U_{rev\max} = \sqrt{2} \cdot E_2 + E_{C0} \cdot e^{-\frac{\frac{3}{2}\pi - \lambda - \phi}{\omega \cdot C \cdot R_d}} \quad (2.34)$$

Simplified expressions given the diode VD is ideal:

$$\lambda = \frac{\pi}{2} - \phi$$

$$E_{C0} = \sqrt{2} \cdot E_2$$

$$U_d = U_C = E_{C0} \cdot e^{-\frac{\theta + \frac{\pi}{2}}{\omega \cdot C \cdot R_d}}$$

$$U_{C\min} = \sqrt{2} \cdot E_2 \cdot e^{-\frac{\frac{3}{2}\pi+\phi}{\omega \cdot C \cdot R_d}}$$

$$\phi = \arcsin\left(e^{-\frac{\frac{3}{2}\pi+\phi}{\omega \cdot C \cdot R_d}} \right)$$

One of rectified voltage quality criterion is the ratio:

$$\frac{U_{C\max}}{U_{C\min}} = k = \frac{\sqrt{2} \cdot E_2}{\sqrt{2} \cdot E_2 \cdot e^{-\frac{\frac{3}{2}\pi+\phi}{\omega \cdot C \cdot R_d}}}$$

$$k = e^{\frac{\frac{3}{2}\pi + \phi}{\omega \cdot C \cdot R_d}}$$

$$\ln k = \frac{\frac{3}{2}\pi + \phi}{\omega \cdot C \cdot R_d} \qquad (2.35)$$

$$C = \frac{\frac{3}{2}\pi + \phi}{\omega \cdot R_d \cdot \ln k}$$

Full-wave midpoint rectifier circuit

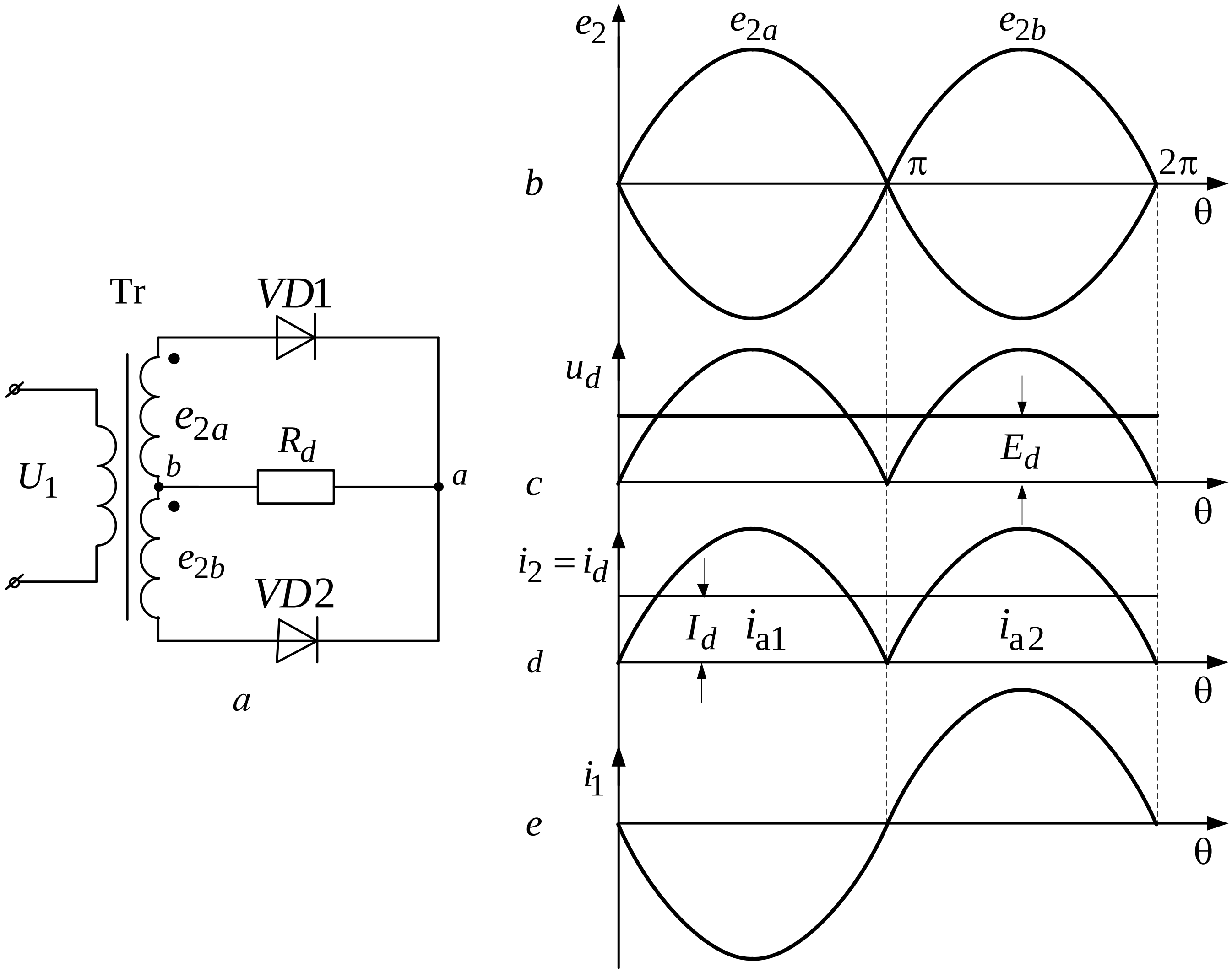

Fig. 2.9. Full-wave midpoint rectifier circuit

Basic relations for the circuit

$$E_d = \frac{1}{\pi}\int_0^{\pi} \sqrt{2} \cdot E_2 \cdot \sin\theta \, d\theta = \frac{2\sqrt{2} \cdot E_2}{\pi}$$

$$I_d = \frac{E_d}{R_d}$$

$$i_{a\,\max} = \frac{\sqrt{2} \cdot E_2}{R_d} \qquad I_{a\,mean} = \frac{I_d}{2}$$

$$U_{rev\,\max} = 2 \cdot \sqrt{2} \cdot E_2 \quad (2.36)$$

Instantaneous value of the primary current

$$i_1 = \frac{1}{k_{tr}} \cdot \left(i_{a2} - i_{a1} \right)$$

$$I_1 = \frac{k_f}{k_{tr}} \cdot I_d$$

where $k_f = 1{,}11$ – form factor for sine-wave curve

$$P_2 = 2 \cdot E_2 \cdot I_2 = 1{,}74 \cdot P_d$$

$$P_1 = E_1 \cdot I_1 = 1{,}23 \cdot P_d$$

$$P_{calc} = \frac{P_1 + P_2}{2} = 1{,}48 \cdot P_d$$

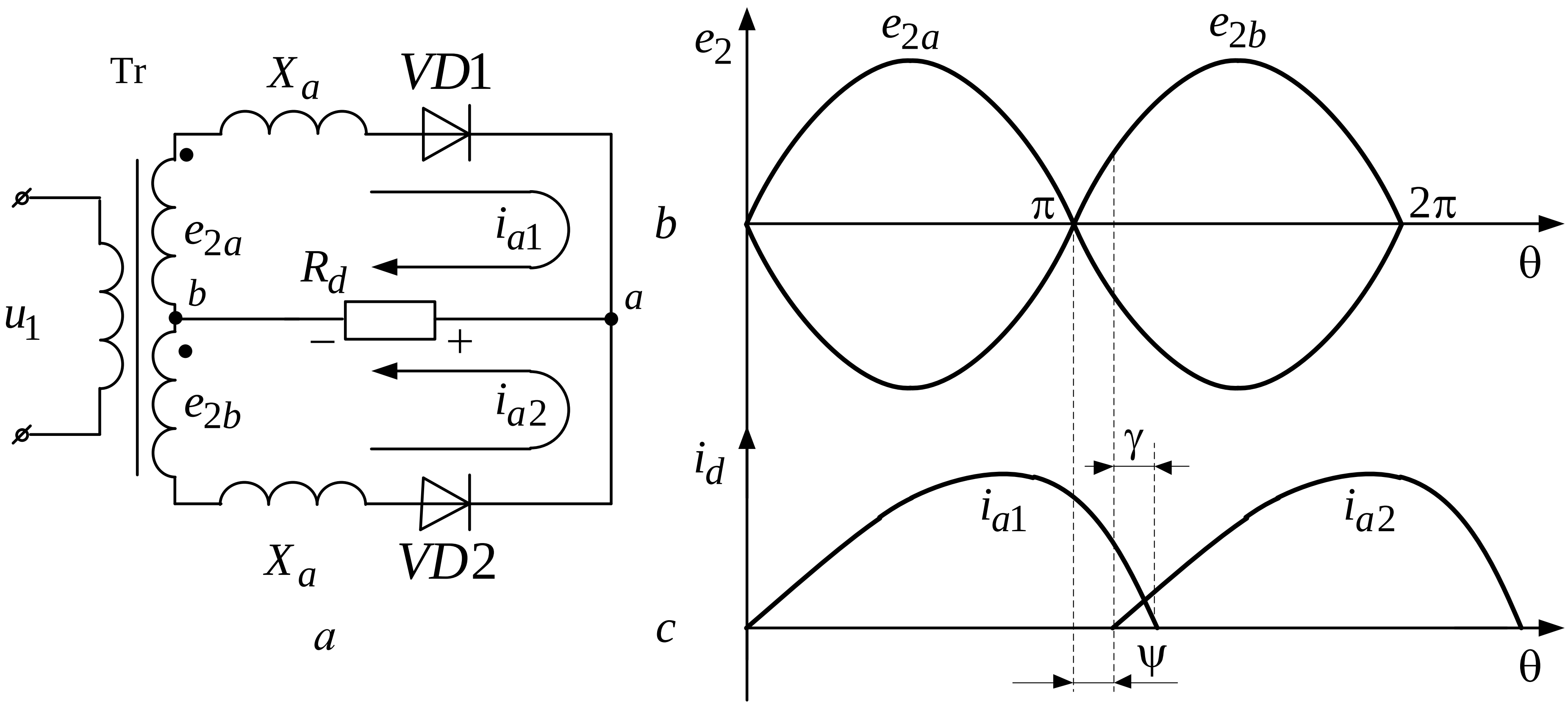

Fig. 2.10. Full-wave midpoint rectifier subject to leakage reactances of the transformer

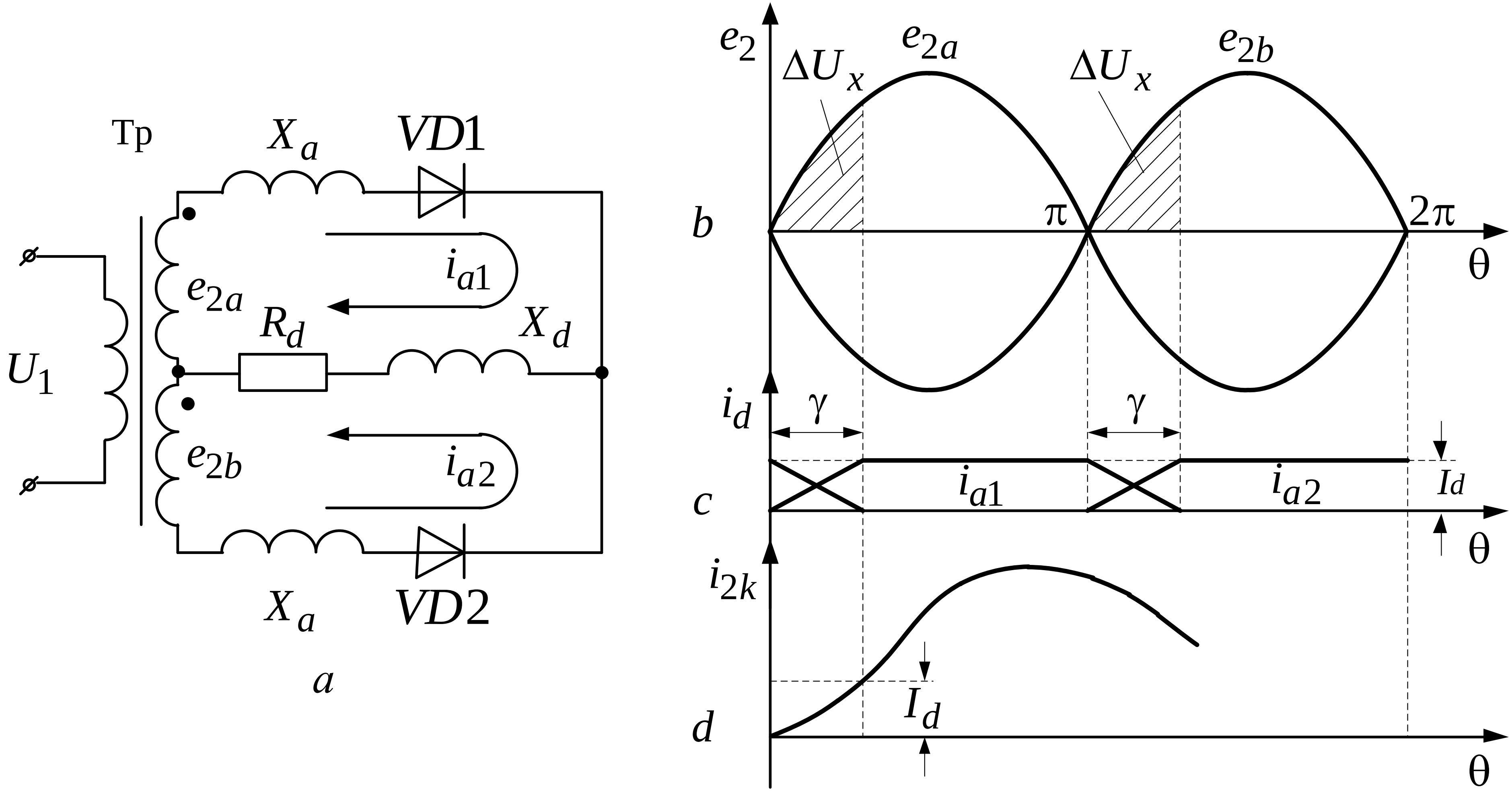

Fig. 2.11. Switching processes in full-wave midpoint rectifier at $X_d = \infty$

When the diodes VD1 and VD2 are opened at the same time the switching loop occurs (fig. 2.12). For it the equation is valid:

$$e_{2a} - X_a \frac{di_{2k}}{d\theta} - X_a \frac{di_{2k}}{d\theta} + e_{2b} = 0 \quad (2.37)$$

where i_{2k} subject to zero initial conditions gives:

This equation solution with respect to i_{2k} subject to zero initial conditions gives:

$$i_{2k} = \frac{\sqrt{2} \cdot E_2}{X_a} \cdot (1 - \cos\theta) \quad (2.38)$$

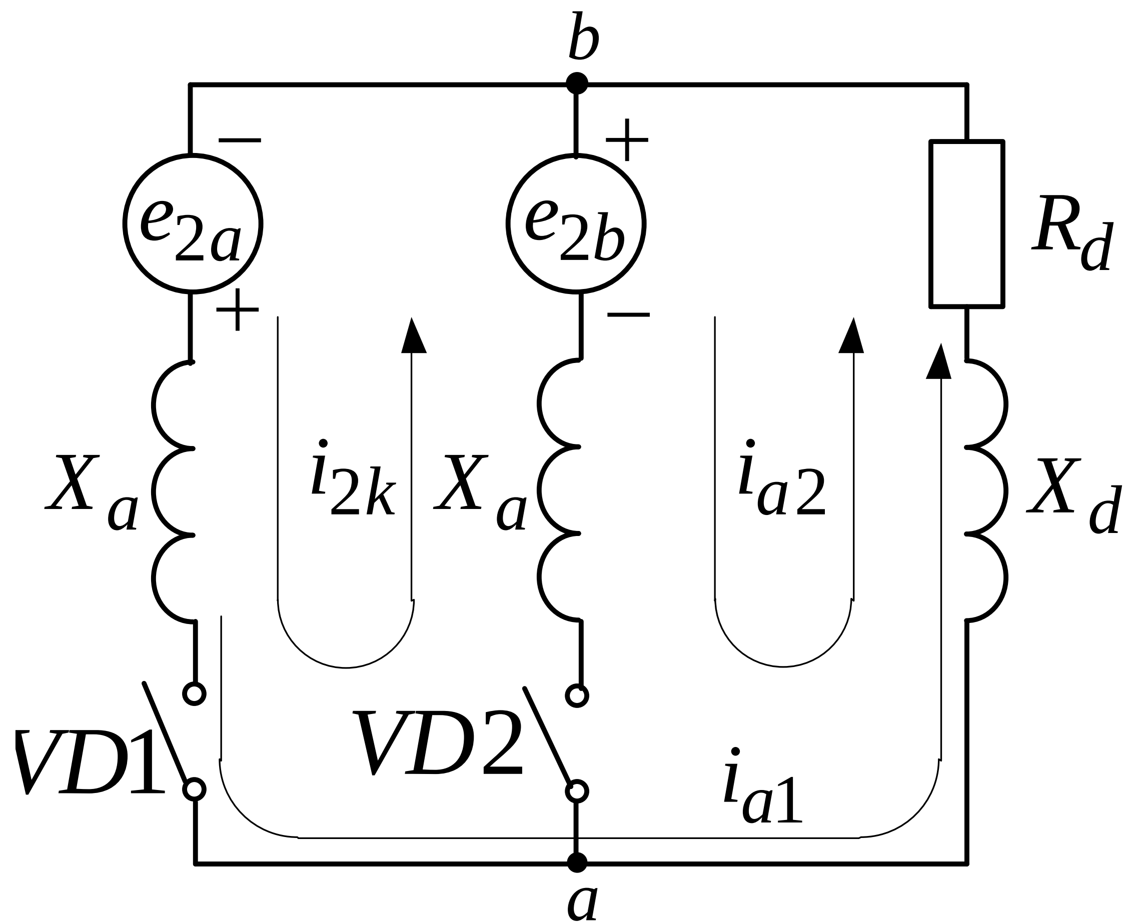

Fig. 2.12. Switching loop in the full-wave midpoint rectifier circuit

The current i_{2k} exists only within the switching range and is the current of the diode VD1:

$$i_{2k}\Big|_{0\ldots\gamma} = i_{a1}\Big|_{0\ldots\gamma}$$

Diode VD2 current:

$$i_{a2}\Big|_{0\ldots\gamma} = I_d - i_{a1}\Big|_{0\ldots\gamma}$$

The switching interval duration:

$$\gamma = \arccos\left(1 - \frac{I_d \cdot X_a}{\sqrt{2} \cdot E_2}\right) \quad (2.39)$$

Since during the switching interval γ

both diodes $VD1$ and $VD2$ are opened,

it is obvious that rectified voltage

$$U_d = \frac{e_{2a} + e_{2b}}{2} = 0$$

Constant rectified voltage component decreases by the value:

$$\Delta U_x = \frac{1}{\pi}\int_0^{\gamma} \sqrt{2} \cdot E_2 \cdot \sin\theta \, d\theta = \frac{I_d \cdot X_a}{\pi} \quad (2.40)$$

$$E_d = E_{d\max} - \Delta U_x = \frac{2\sqrt{2} \cdot E_2}{\pi} - \frac{I_d \cdot X_a}{\pi} \quad (2.41)$$

$E_{d\max}$ – rectified voltage constant component in the absence of switching processes.

Expression (2.41) is the equation of rectifier external characteristic (Fig. 2.13)

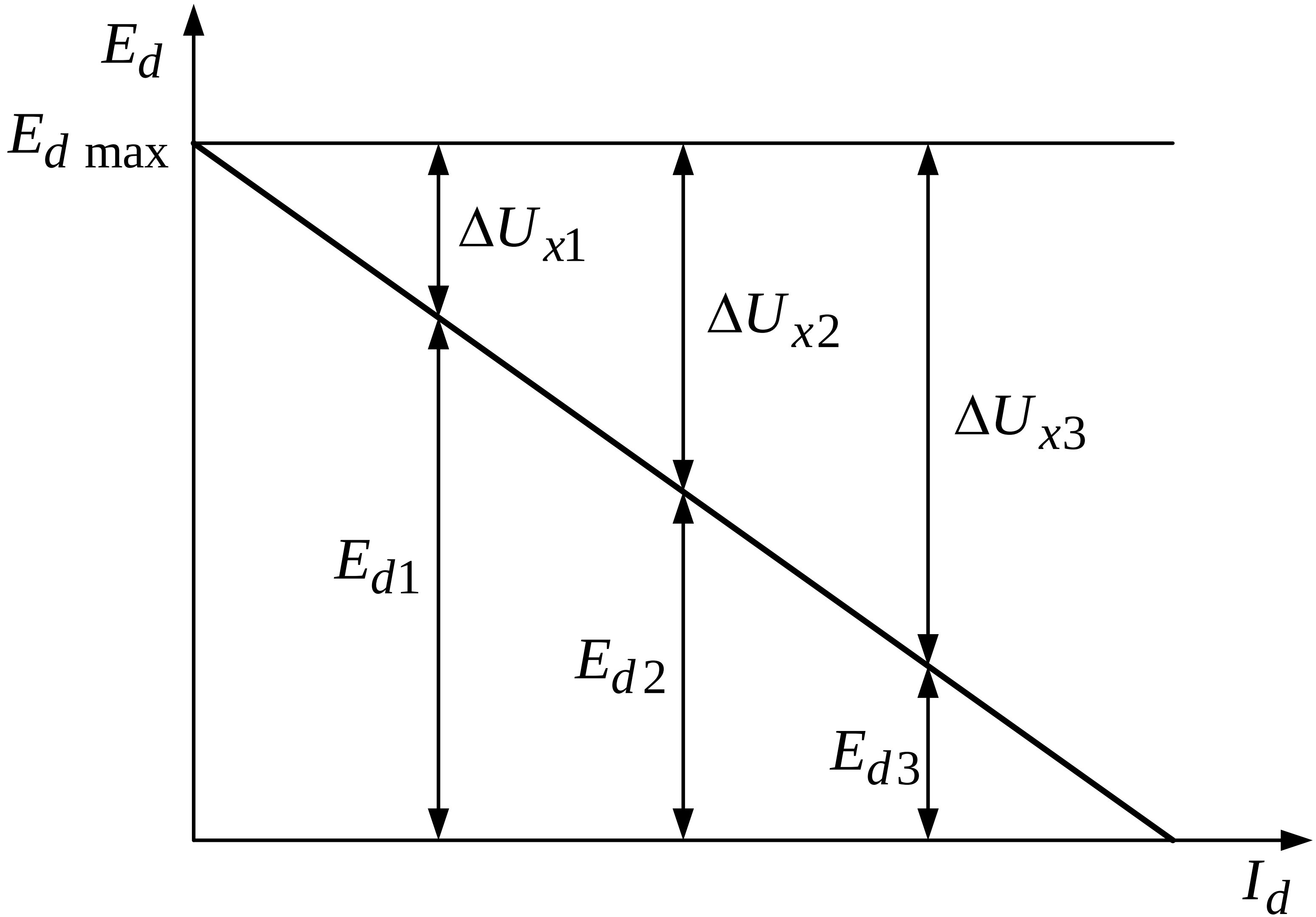

Fig. 2.13. External characteristic of full-wave center-point rectifier

Relative to X_d and $E_{d\max}$ three modes are possible:

- Discontinuous current mode (fig. 2.14, c), when $\lambda < \pi$;
- Boundary-continuous mode (fig. 2.14, d), when $\lambda = \pi$;
- Continuous current mode (fig. 2.14, e).

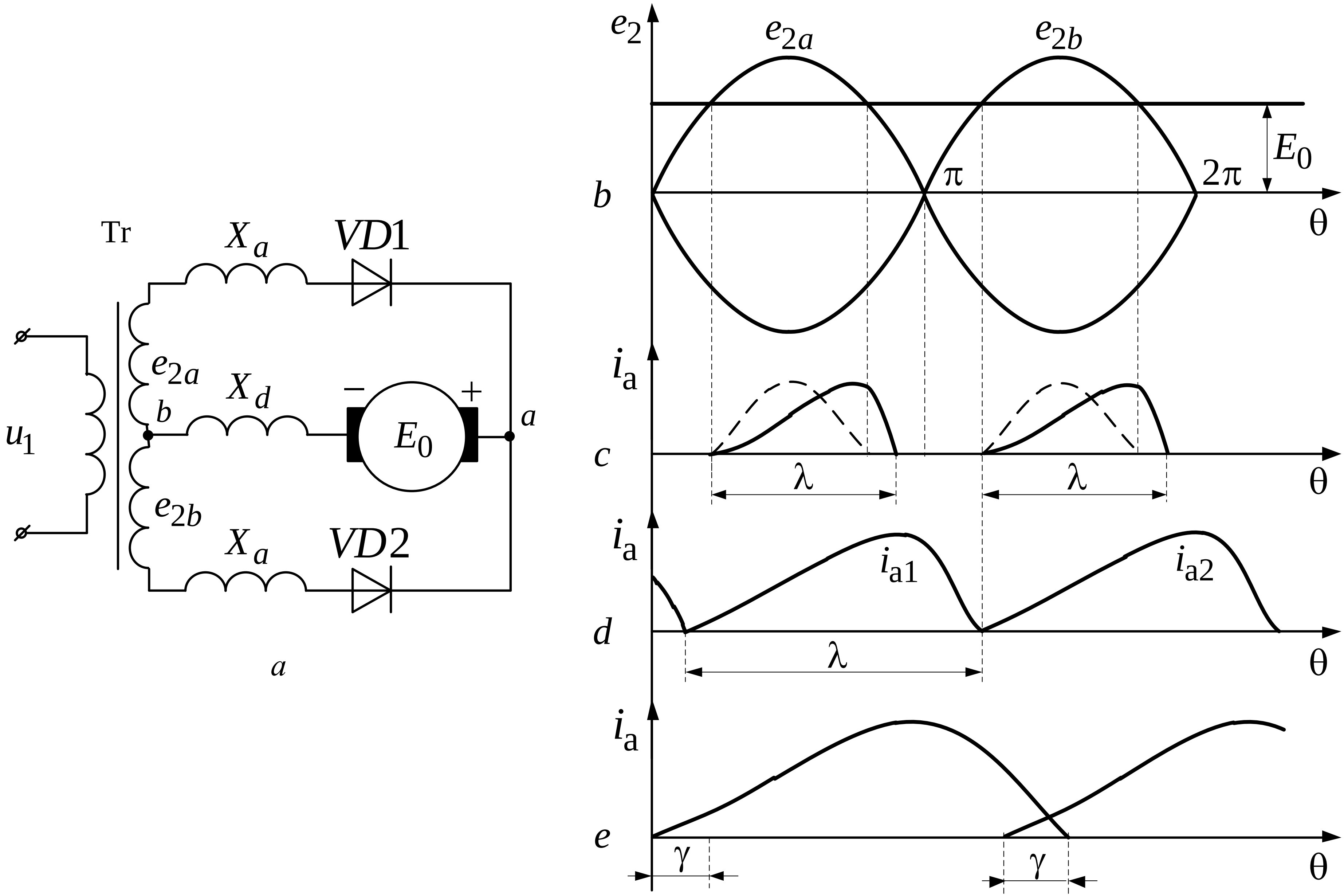

Fig. 2.14. Full-wave center-point rectifier operation on the motor load

Single-phase bridge rectifier circuit

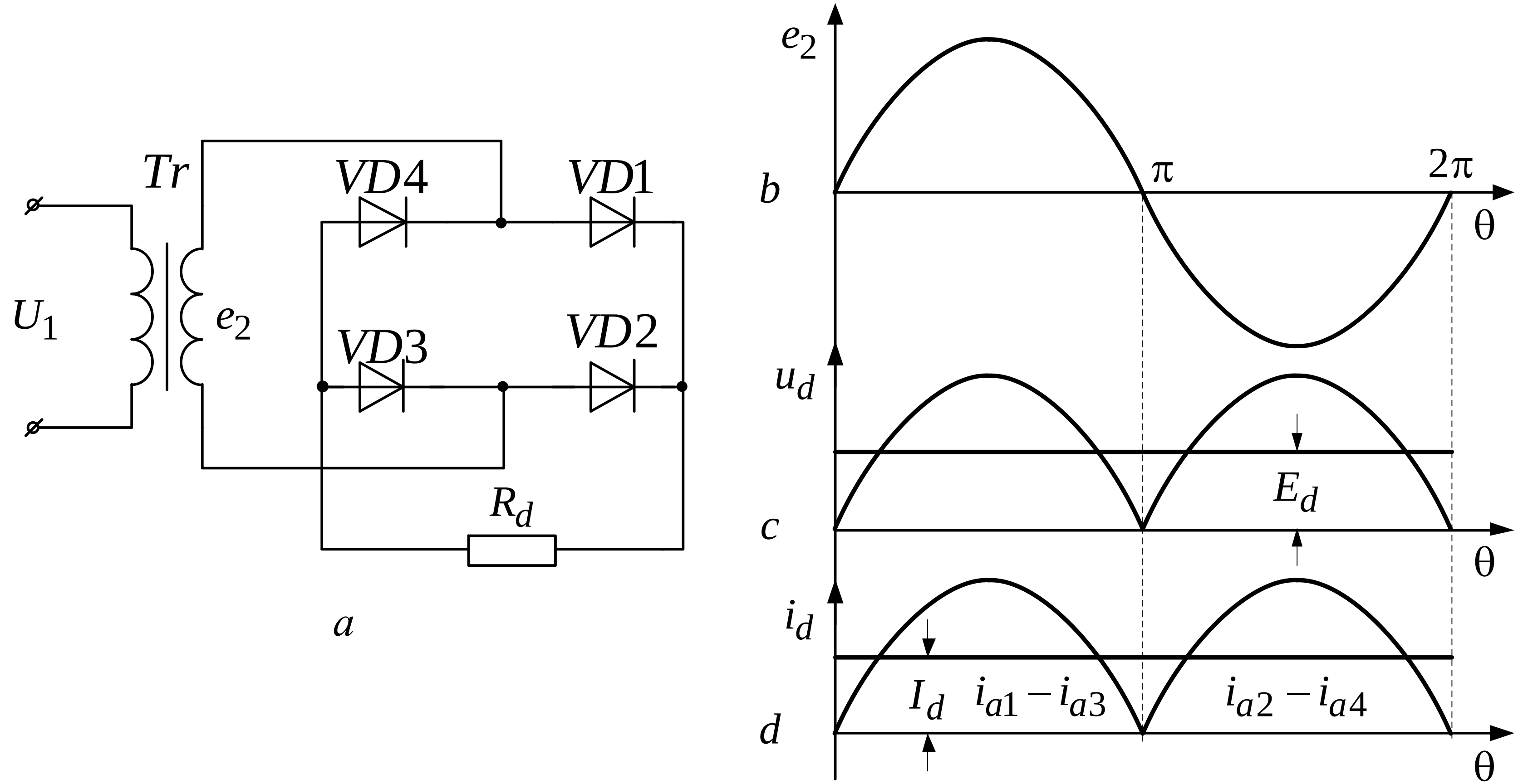

Fig. 2.15. Single-phase bridge rectifier

For the circuit the following expressions are valid:

$$E_d = \frac{1}{\pi}\int_0^{\pi} \sqrt{2} \cdot E_2 \cdot \sin\theta \, d\theta = \frac{2\sqrt{2} \cdot E_2}{\pi} = 0{,}9 \cdot E_2 \quad (2.42)$$

$$I_d = \frac{E_d}{R_d} \quad (2.43)$$

$$i_{a\,\max} = \frac{\sqrt{2} \cdot E_2}{R_d} \quad (2.44)$$

$$i_{a\,mean} = \frac{I_d}{2} \quad (2.45)$$

$$U_{rev\,\max} = \sqrt{2} \cdot E_2 \tag{2.46}$$

$$i_2 = \frac{\sqrt{2} \cdot E_2}{R_d} \cdot \sin\theta \tag{2.47}$$

$$i_1 = \frac{1}{k_{tr}} \cdot i_2 \tag{2.48}$$

$$P_1 = E_1 \cdot I_1 = 1{,}23 \cdot P_d \tag{2.49}$$

$$P_2 = E_2 \cdot I_2 = 1{,}23 \cdot P_d \tag{2.50}$$

$$P_{calc} = \frac{P_1 + P_2}{2} = 1{,}23 \cdot P_d \tag{2.51}$$

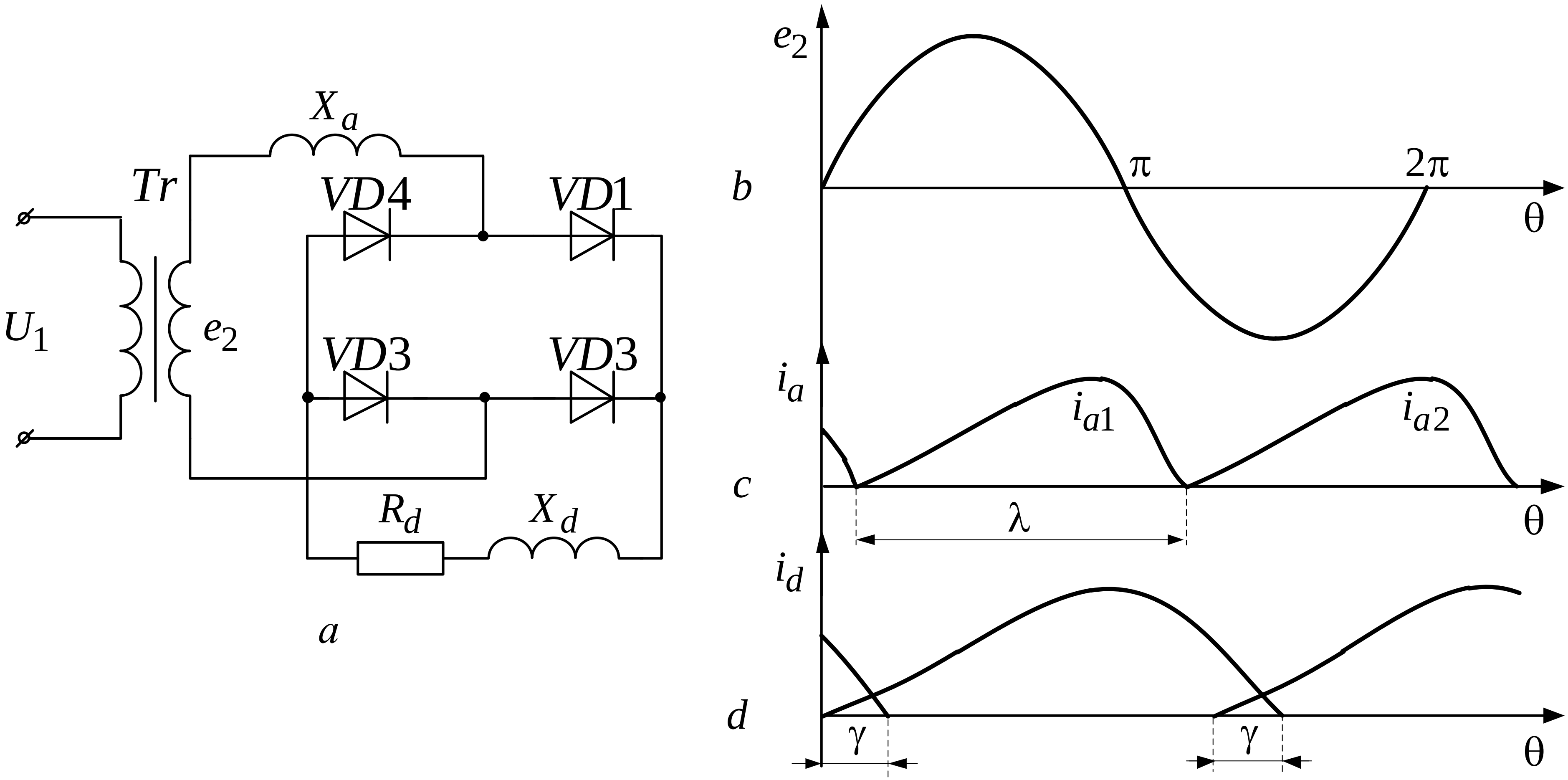

Fig. 2.16. Switching transients in the single-phase bridge rectifier

For the switching loop the next expression is valid:

$$E_2 - X_a \cdot \frac{di_{2k}}{dt} = 0 \quad (2.52)$$

All the conclusions made for switching processes in full-wave midpoint rectifier circuit are also valid for single-phase bridge circuit.

Three-phase zero-point rectifier

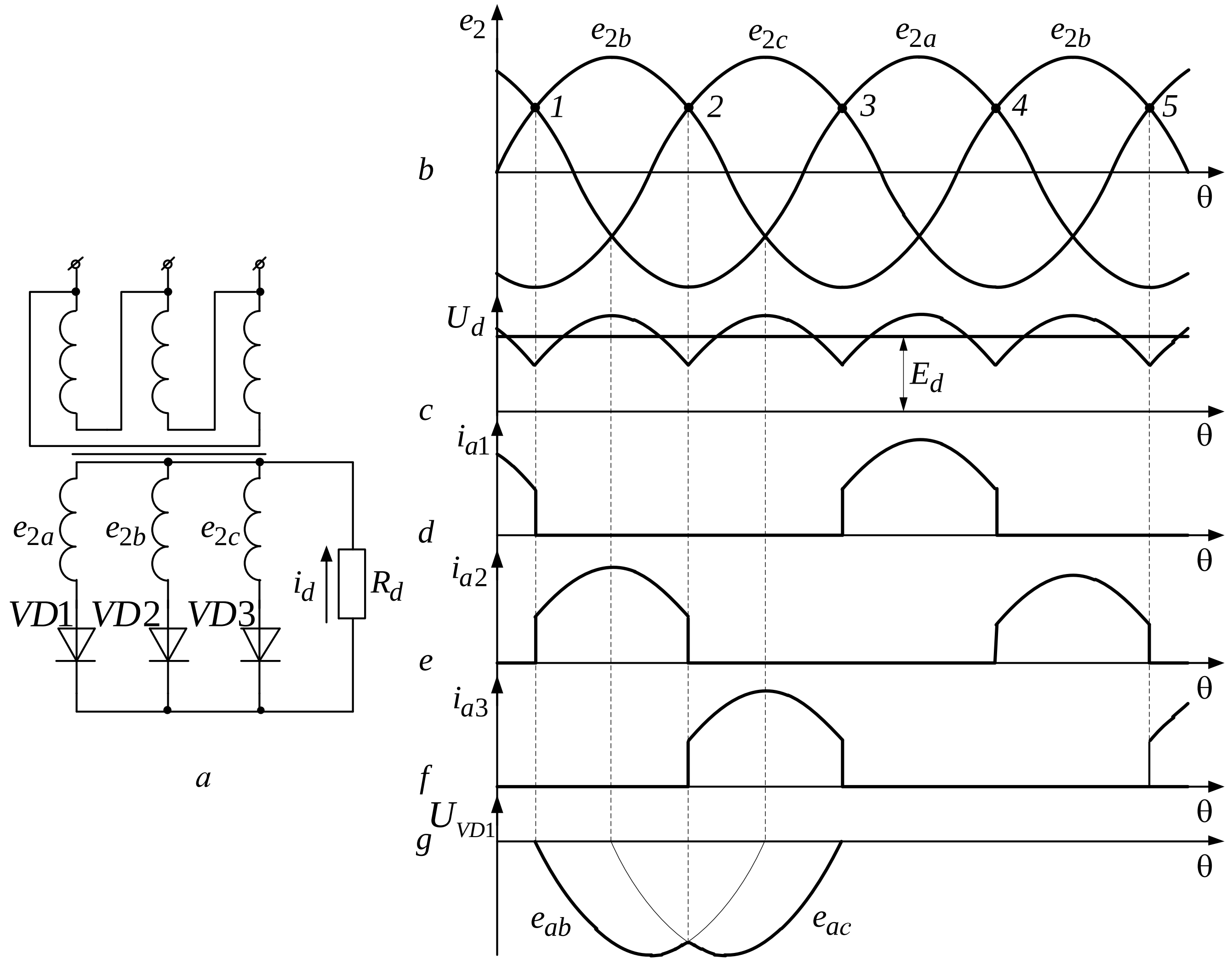

Fig. 2.17. Three-phase zero-point rectifier and diagrams which explain its operation

Basic ratios for the circuit are:

$$E_d = \frac{1}{\frac{2\pi}{3}} \int_{\frac{\pi}{6}}^{\pi-\frac{\pi}{6}} \sqrt{2} \cdot E_2 \cdot \sin\theta \, d\theta = 1{,}17 \cdot E_2 \quad (2.53)$$

$$I_d = \frac{E_d}{R_d} \quad (2.54)$$

$$i_{a\,mean} = \frac{I_d}{3} \quad (2.55)$$

$$i_{a\,\max} = \frac{\sqrt{2} \cdot E_2}{R_d} \quad (2.56)$$

$$U_{rev\,\max} = \sqrt{6} \cdot E_2 \qquad (2.57)$$

$$I_2 = \sqrt{\frac{1}{2\pi} \cdot \int_{\frac{\pi}{6}}^{\frac{5\pi}{6}} \frac{2 \cdot E_2^2}{R_d^2} \cdot \sin^2 \theta \, d\theta} = 0{,}577 \cdot I_d \qquad (2.58)$$

$$I_1 = \frac{\sqrt{2}}{3} \cdot \frac{I_d}{k_{tr}} \qquad (2.59)$$

$$P_2 = E_2 \cdot I_2 = 1{,}48 \cdot P_d \qquad (2.60)$$

$$P_1 = E_1 \cdot I_1 = 1{,}21 \cdot P_d \qquad (2.61)$$

$$P_{calc} = \frac{P_1 + P_2}{2} = 1{,}34 \cdot P_d \qquad (2.62)$$

Zigzag circuit

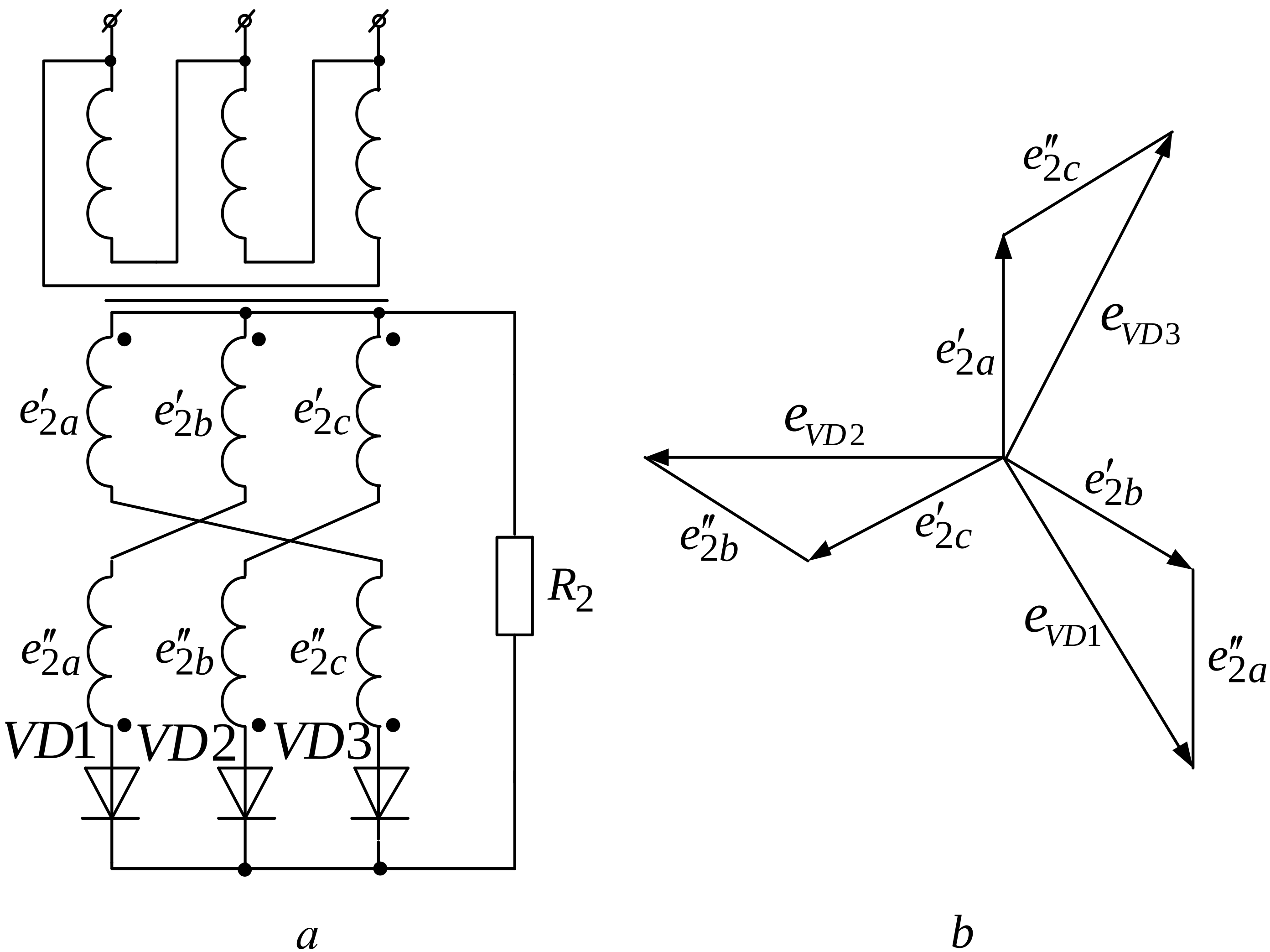

Fig. 2.18. Three-phase zero-point rectifier with zigzag connection of secondary transformer windings

$$P_1 = E_1 \cdot I_1 = 1,21 \cdot P_d \qquad (2.63)$$

$$P_2 = E_2 \cdot I_2 = 1,71 \cdot P_d \qquad (2.64)$$

$$P_{calc} = \frac{P_1 + P_2}{2} = 1,46 \cdot P_d \qquad (2.65)$$

The magnetizing forces generated by constant components of anode currents in each phase are mutually compensated by upper and lower sections of secondary windings

Switching processes in three-phase zero-point rectifier

$$X_d = \infty \qquad X_a \neq 0$$

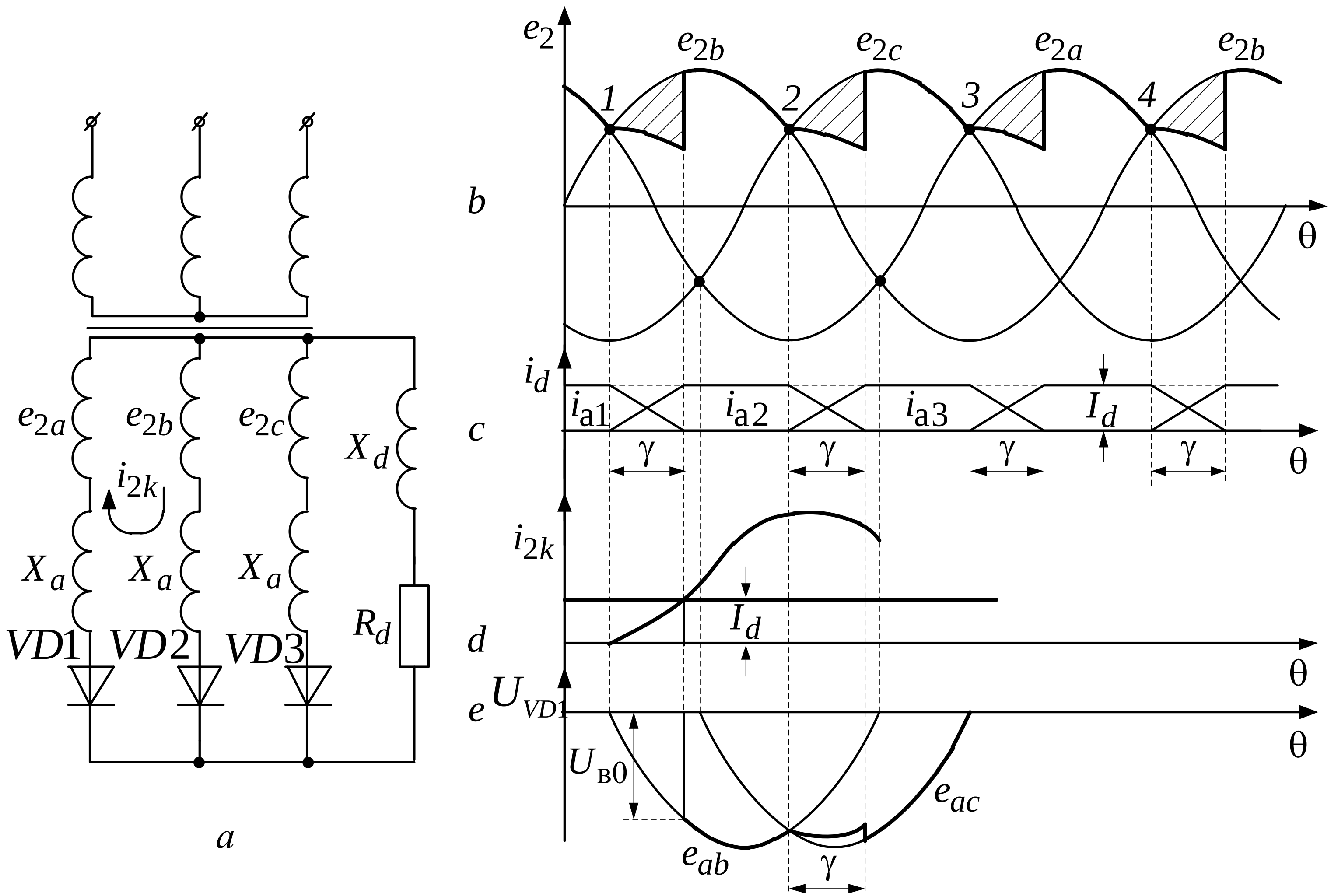

Fig. 2.19. Switching processes in three-phase zero-point rectifier

For the switching processes the next equation is valid:

$$e_{2b} - X_a \frac{di_{2k}}{d\theta} - X_a \frac{di_{2k}}{d\theta} - e_{2a} = 0 \quad (2.66)$$

where i_{2k} is current of the commutation loop.

$$i_{2k} = \frac{\sqrt{6} \cdot E_2}{X_a} \cdot \left(1 - \cos\theta\right) \quad (2.67)$$

$$\gamma = \arccos\left(1 - \frac{I_d \cdot X_a}{\sqrt{6} \cdot E_2}\right) \quad (2.68)$$

In the switching interval rectified voltage decreases by the value:

$$\Delta U_x = \frac{1}{\frac{2\pi}{3}} \int_0^{\gamma} \left(e_{2b} - \frac{e_{2b} + e_{2a}}{2} \right) d\theta = \frac{I_d \cdot X_a}{\frac{2\pi}{3}} \quad (2.69)$$

$$E_d = E_{d\max} - \Delta U_x = 1{,}17 \cdot E_2 - \frac{I_d \cdot X_a}{\frac{2\pi}{3}} \quad (2.70)$$

where $E_{d\max}$ – rectified voltage value in the absence of switching processes.

The latter expression is the equation of rectifier’s external characteristic $E_d = f\left(I_d\right)$ (Fig. 2.20).

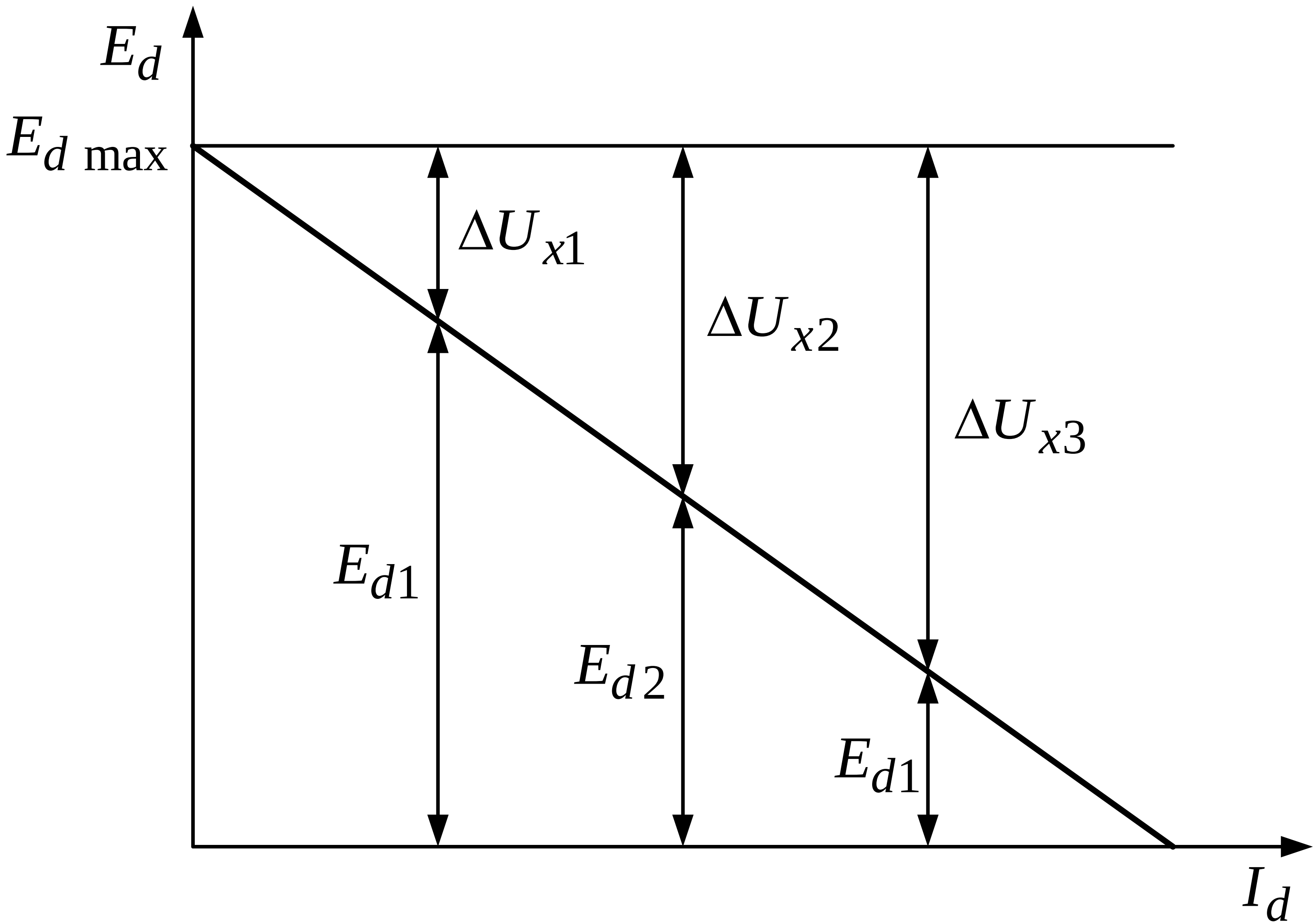

Fig. 2.20. External characteristic of three-phase zero point rectifier

Three-phase bridge rectifier circuit

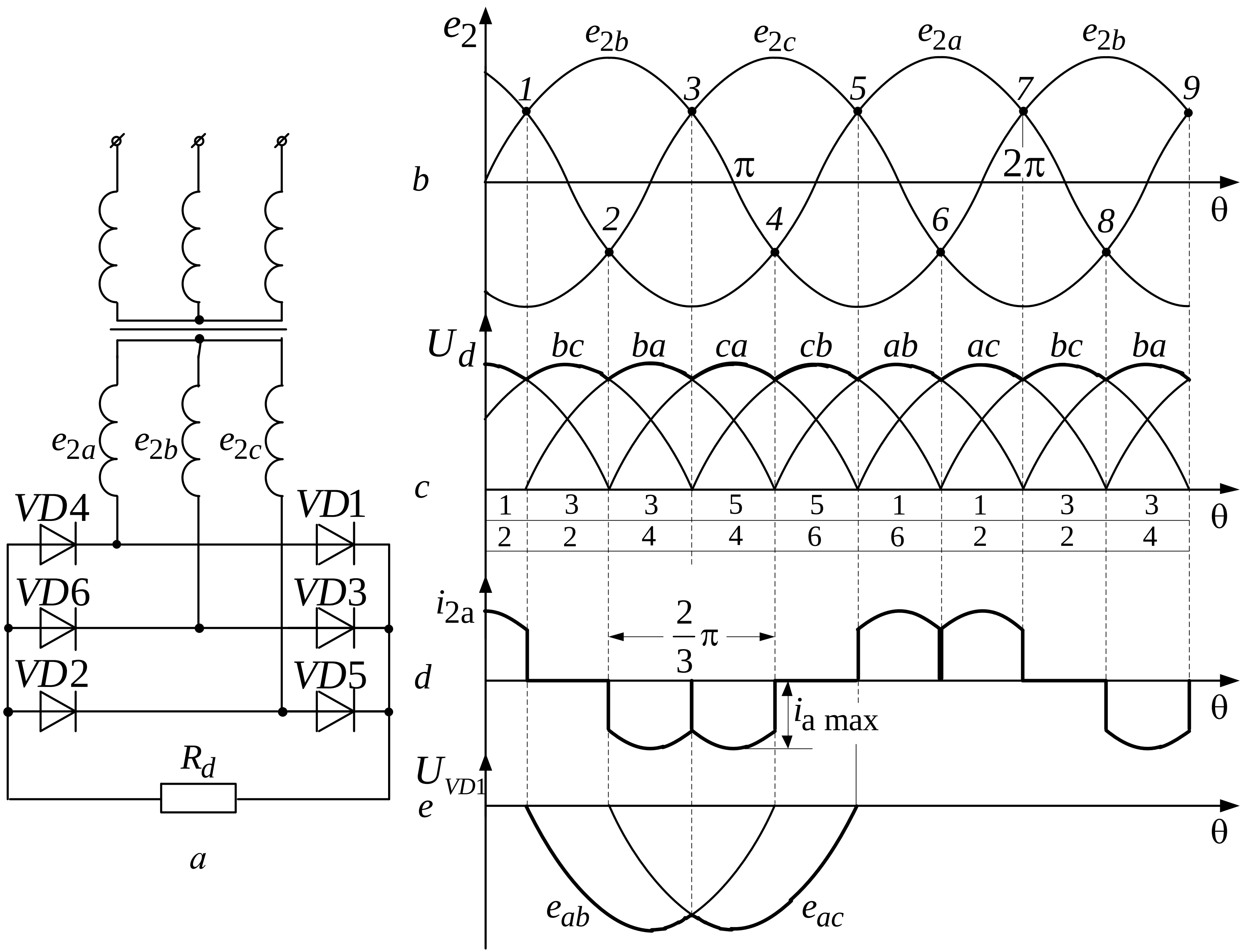

Fig. 2.21. Three-phase bridge rectifier and diagrams explaining its operation

The principle of operation of this circuit is similar to the principle of operation of the zero-point rectifier with the only difference being that the load current is flowing simultaneously through one of the diodes of the cathode group and one of the diodes of the anode group.

It flows due to the action of phase voltage, not linear one.

The following relations are valid:

$$E_d = \frac{1}{\frac{2\pi}{6}} \int_{\frac{\pi}{3}}^{\frac{2\pi}{3}} \sqrt{3} \cdot \sqrt{2} \cdot E_2 \cdot \sin\theta \, d\theta = 2{,}34 \cdot E_2 \quad (2.71)$$

$$I_d = \frac{E_d}{R_d} \quad (2.72)$$

$$i_{\mathrm{a\ max}} = \frac{\sqrt{6} \cdot E_2}{R_d} \quad (2.73)$$

$$i_{a\,mean} = \frac{I_d}{3} \tag{2.74}$$

$$U_{rev\,\max} = \sqrt{6} \cdot E_2 \tag{2.75}$$

$$I_2 = \sqrt{\frac{2}{3}} \cdot I_d \tag{2.76}$$

$$I_1 = \sqrt{\frac{2}{3}} \cdot \frac{I_d}{k_{tr}} \tag{2.77}$$

$$P_2 = P_1 = P_{calc} = 1{,}045 \cdot P_d \tag{2.78}$$

When considering the characteristics of switching processes in three-phase bridge circuit in comparison with three-phase zero-point circuit it should be noted that the switching processes will occur both in the anode and cathode groups, i.e. two times more often than in the zero-point circuit (fig. 2.22). The diagrams shown in fig. 2.22 correspond to the mode at $X_d = \infty$; $X_a \neq 0$.

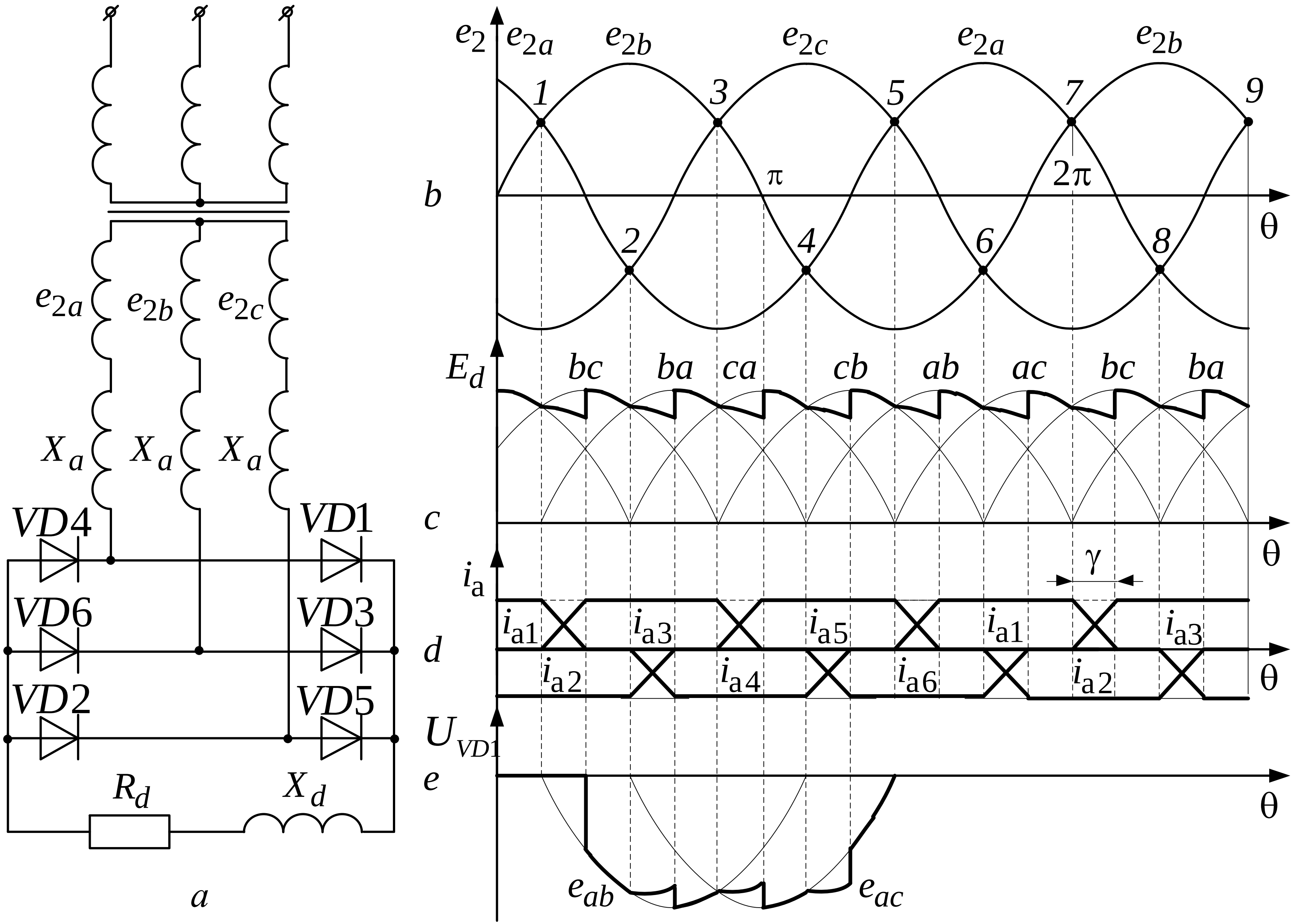

Fig. 2.22. Switching processes in three-phase bridge rectifier

Rectified voltage decrease due to switching processes in this circuit is defined by the next expression:

$$\Delta U_x = \frac{I_d \cdot X_a}{2\pi/6}$$

The external characteristic equation has the form:

$$E_d = E_{d\,\max} - \Delta U_x = 2{,}34 \cdot E_2 - \frac{I_d \cdot X_a}{2\pi/6} \quad (2.79)$$

Single-phase controlled rectifiers

Half-wave controlled rectifier

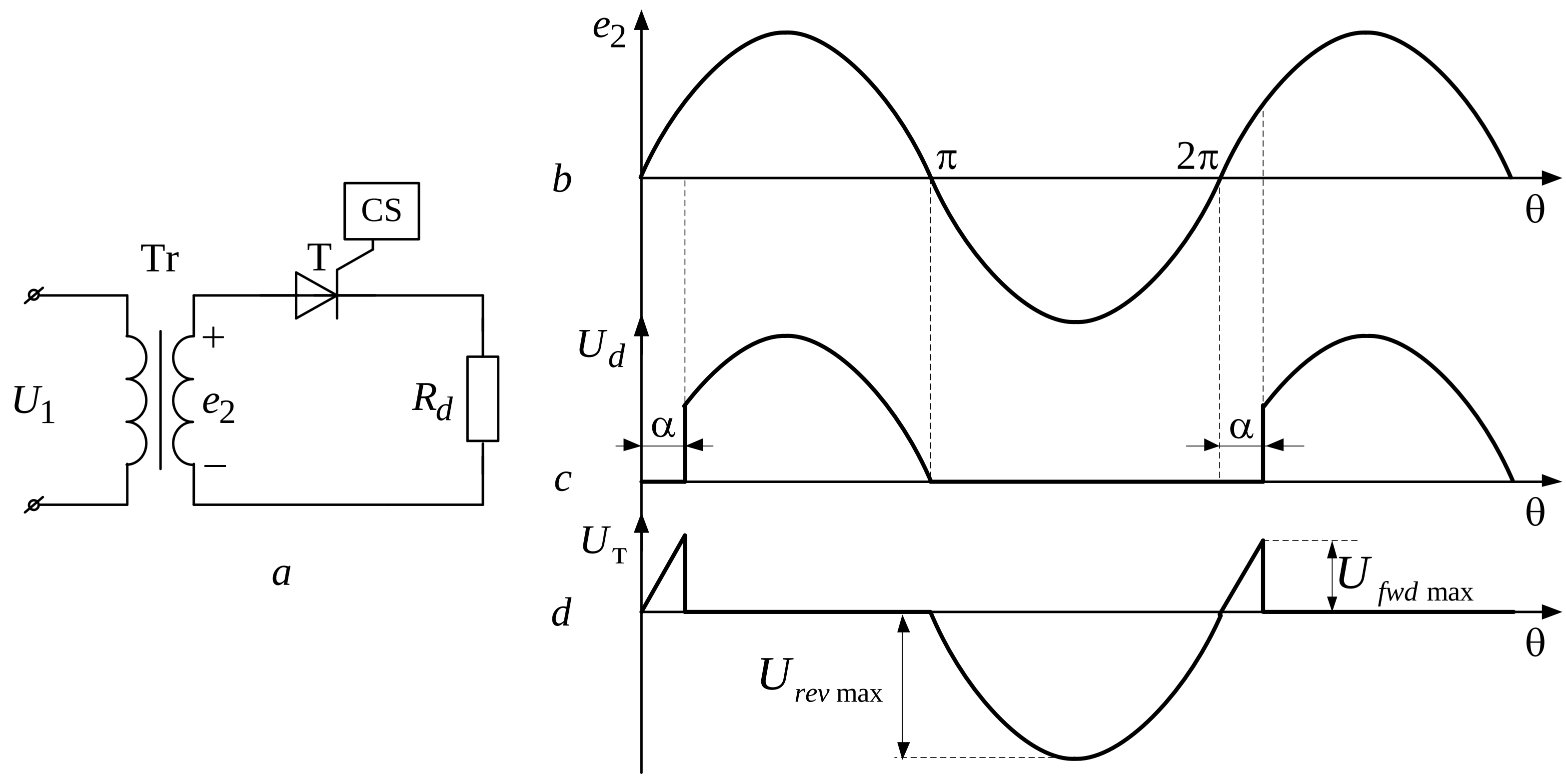

Fig. 2.23. Single-phase half-wave controlled rectifier

The constant component of the rectified voltage is defined by the next expression:

$$E_d = \frac{1}{2\pi}\int_0^{\pi}\sqrt{2}\cdot E_2 \cdot \sin\theta \, d\theta = \frac{\sqrt{2}\cdot E_2}{\pi}\cdot\frac{(1+\cos\alpha)}{2}. \quad (2.80)$$

Obviously that $E_{d\max}\big|_{\alpha=0} = \dfrac{\sqrt{2}\cdot E_2}{\pi}$,

$$E_{d\min}\big|_{\alpha=\pi} = 0.$$

In the interval $2\pi \ldots (2\pi + \alpha)$ besides the reverse (locking) voltage the forward voltage is also applied to the switch :

$$U_{f\ \max} = \sqrt{2} \cdot E_2 \cdot \sin\theta$$

When the active-inductive load is connected to the circuit (fig. 2.24) the next equation is valid

$$i_d R_d + \left(X_a + X_d \right) \frac{\mathrm{d}i_d}{\mathrm{d}\theta} = e_2. \quad (2.81)$$

Denoting $X_a + X_d = X$ and assuming that $e_2 = \sqrt{2} \cdot E_2 \cdot \sin\theta$, we solve this equation relative to i_d:

$$i_d = \frac{\sqrt{2} \cdot E_2}{\sqrt{R_d^2 + X^2}} \left[\sin(\theta - \varphi) - \sin(\alpha - \varphi) e^{-(\theta - \alpha) \cdot \mathrm{ctg}\varphi} \right] \quad (2.82)$$

where $\varphi = \mathrm{arctg}\left(\dfrac{X}{R_d} \right)$

Graphical representation of the function (2.82) is depicted in fig. 2.24, c.

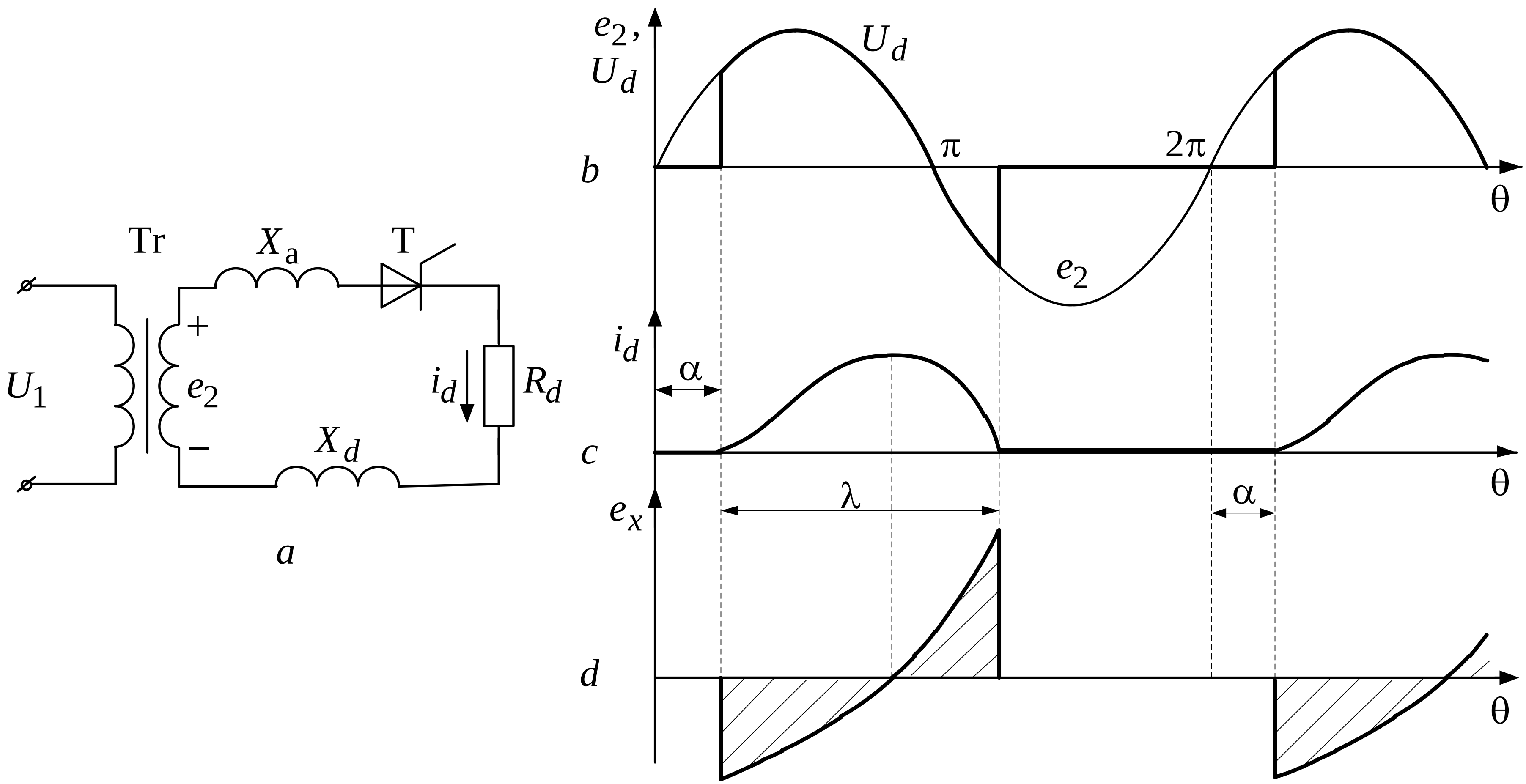

Fig. 2.24. Single-phase half-wave controlled rectifier with active-inductive load

From the condition $\left. i_d \right|_{\theta = \alpha + \lambda} = 0$ we find:

$$\sin(\alpha + \lambda - \varphi) = \sin(\alpha - \varphi) e^{-\mathrm{ctg}\varphi\lambda}.$$

The dependence between λ, α and φ is shown in fig. 2.25.

Knowing the dependence, it is possible to plot the regulating characteristics (fig. 2.26).

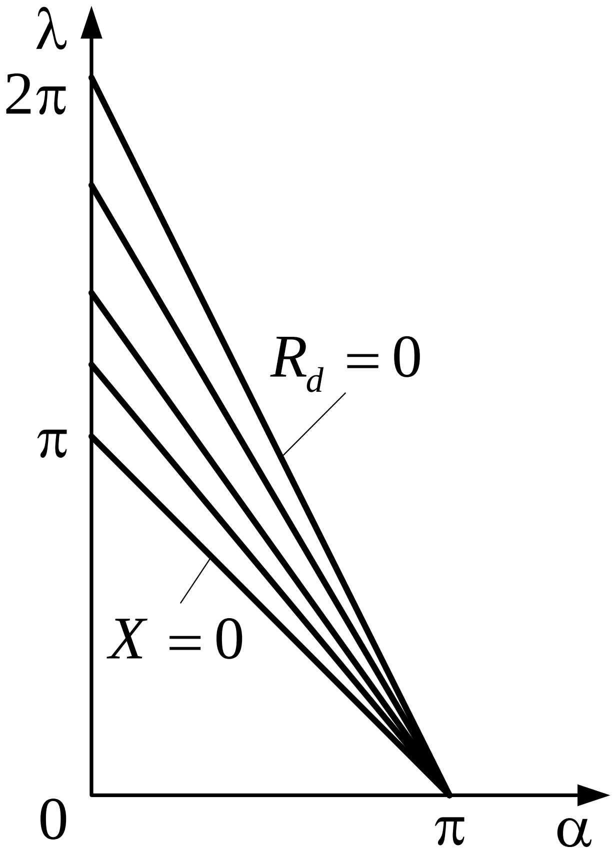

Fig. 2.25. Dependence of the duration of the conductive state of tyristor

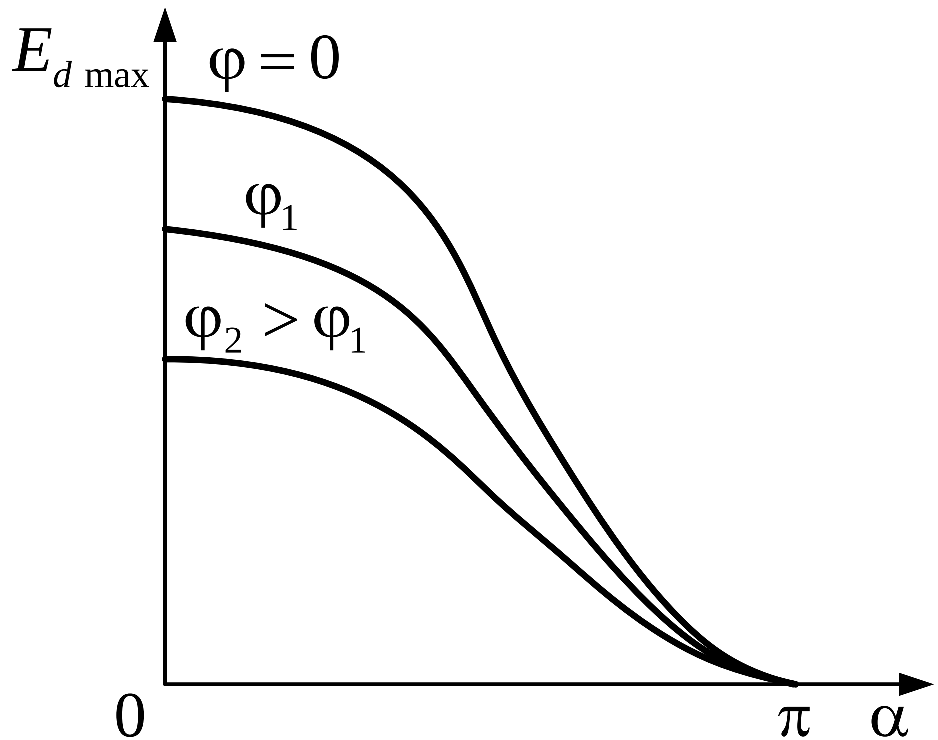

Fig. 2.26. A family of single-phase half-wave controlled rectifier control characteristics

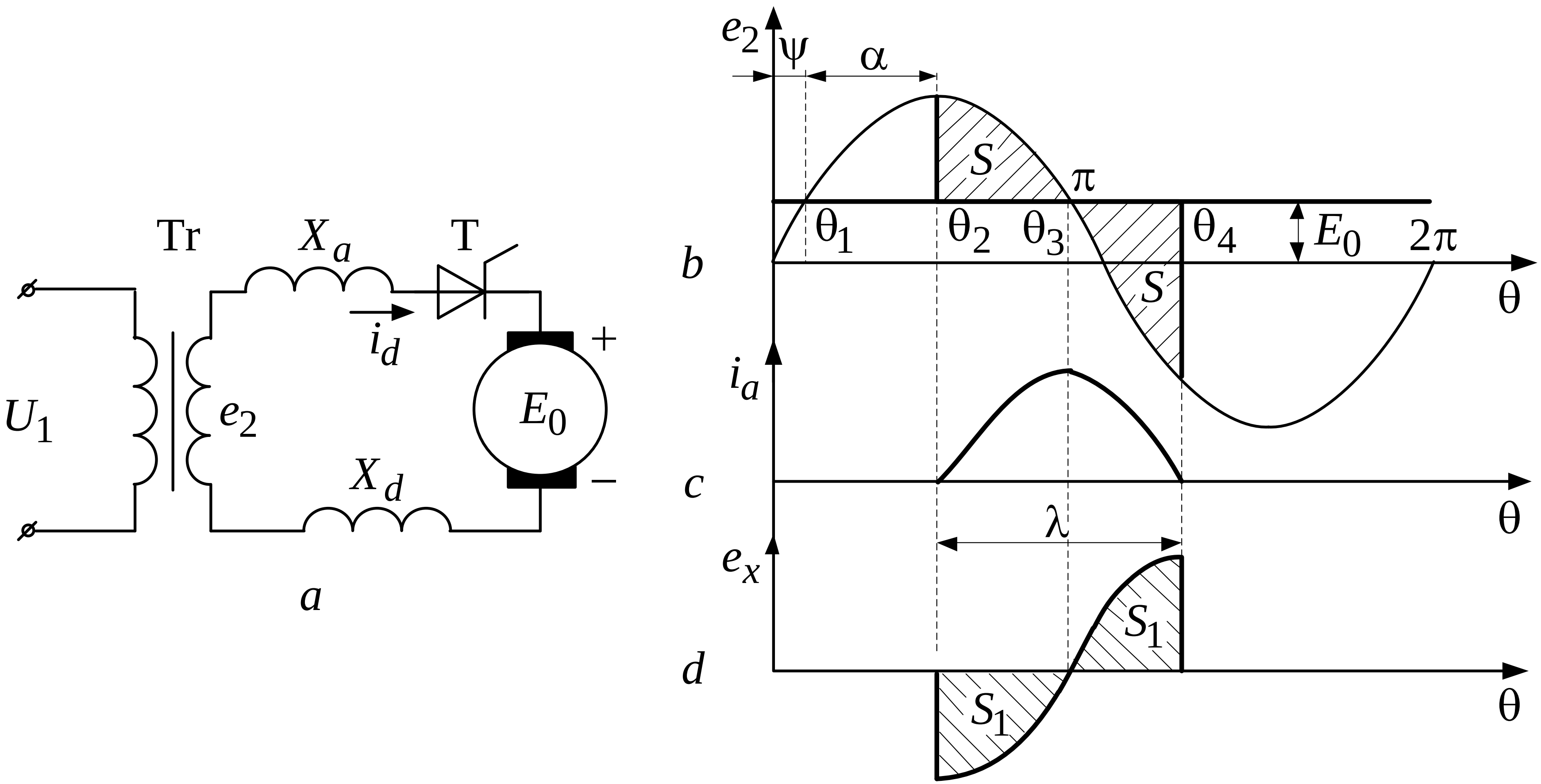

Fig. 2.27. Single-phase half-wave controlled rectifier operation with the motor load

The current i_d can be determined from the equation:

$$e_2 - \left(X_a + X_d\right)\frac{\mathrm{d}i_d}{\mathrm{d}\theta} = E_0 \qquad (2.83)$$

Solving the equation (2.83), we obtain

$$i_d = \frac{\sqrt{2}E_2}{\left(X_a + X_d\right)}\left[\cos\left(\alpha + \psi\right) - \cos\left(\theta + \psi\right)\right] + \frac{E_0}{X}\left(\alpha - \theta\right) \qquad (2.84)$$

Self-induced EMF curve which is defined by the equation:

$$e_X = -(X_a + X_d)\frac{\mathrm{d}i_d}{\mathrm{d}\theta},$$

is shown in fig. 2.27, d, and at the point $\theta = \psi + \alpha$ it is equal to: $-e_X = e_2 - E_0$.

Full-wave controlled rectifier with midpoint

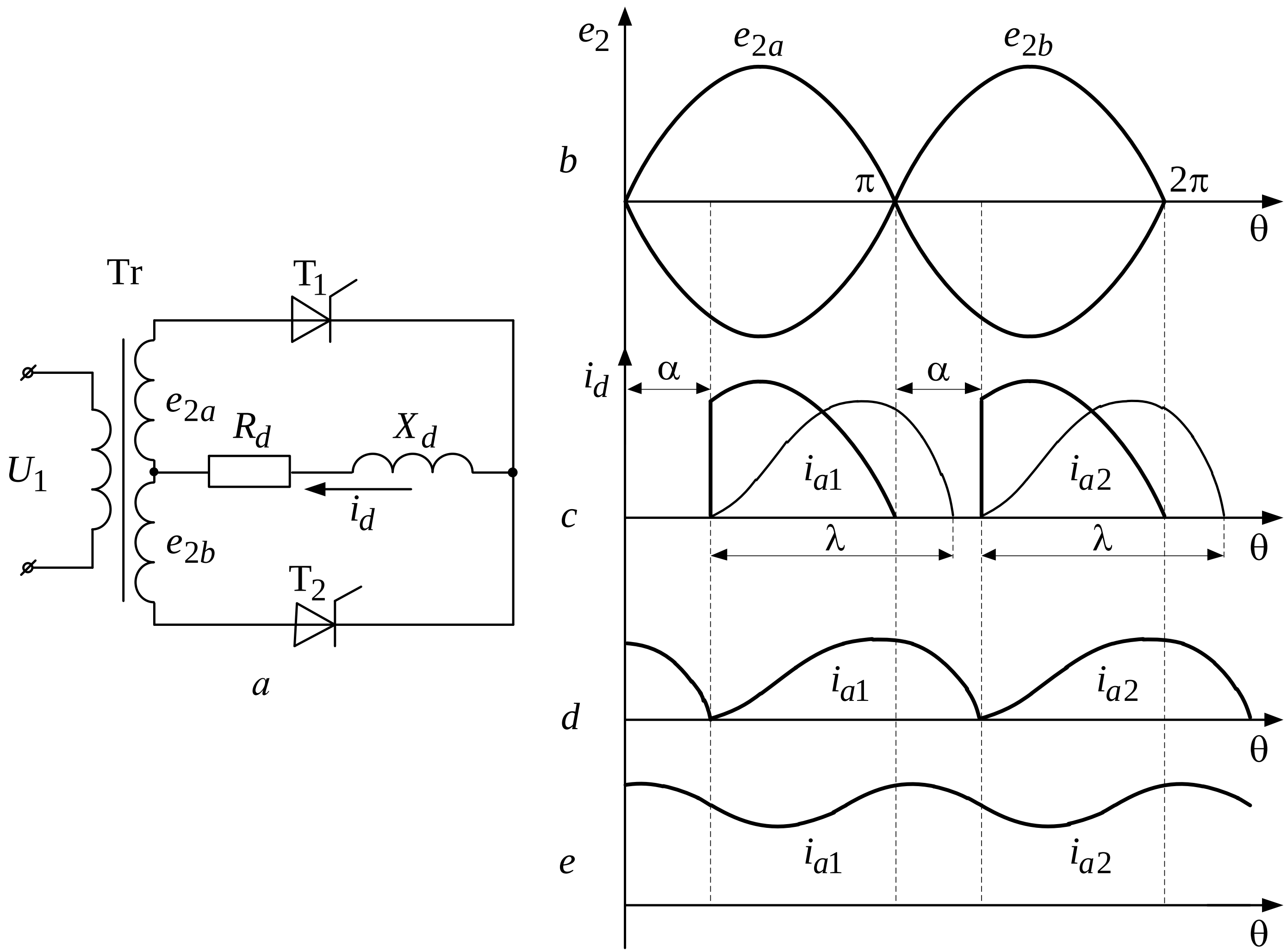

Fig. 2.28. The full-wave controlled rectifier with active-inductive load

The load current is determined from the expression

$$i_d = \frac{\sqrt{2} \cdot E_2}{\sqrt{R_d^2 + X^2}} \left[\frac{\sin(\alpha - \varphi)}{e^{-\mathrm{ctg}\,\varphi\pi} - 1} \cdot e^{-\mathrm{ctg}\varphi(\theta - \alpha)} + \sin(\theta - \varphi) \right] \quad (2.85)$$

In continuous current and boundary-continuous current modes the rectified voltage is determined by the expression:

$$E_d = \frac{1}{\pi} \int_{\alpha}^{\pi+\alpha} \sqrt{2} \cdot E_2 \cdot \sin\theta \, d\theta = \frac{2\sqrt{2} \cdot E_2}{\pi} \cdot \cos\alpha \quad (2.86)$$

In the discontinuous current mode rectified voltage is defined by the expression

$$E_d = \frac{1}{\pi}\int_0^{\lambda+\alpha} \sqrt{2}E_2 \sin\theta d\theta = \frac{\sqrt{2}E_2}{\pi}\left[\cos\alpha - \cos\left(\alpha+\lambda\right)\right] \quad (2.87)$$

When operating with a purely resistive load, the expression (2.87) takes the form:

$$E_d = \frac{1}{\pi}\int_\alpha^{\pi} \sqrt{2}\cdot E_2 \cdot \sin\theta \, d\theta = \frac{\sqrt{2}\cdot E_2}{\pi}\cdot\left[1+\cos\alpha\right]. \quad (2.88)$$

Regulating characteristics defined by the expressions (2.82) and (2.88), have the form shown in Fig. 2.29.

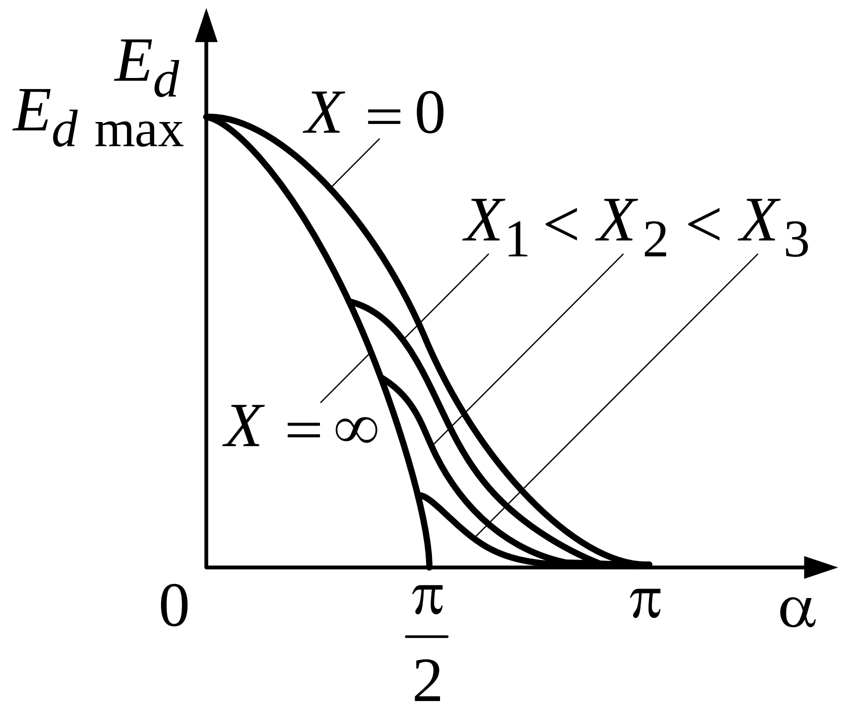

Fig. 2.29. The regulating characteristics family of full-wave controlled rectifier

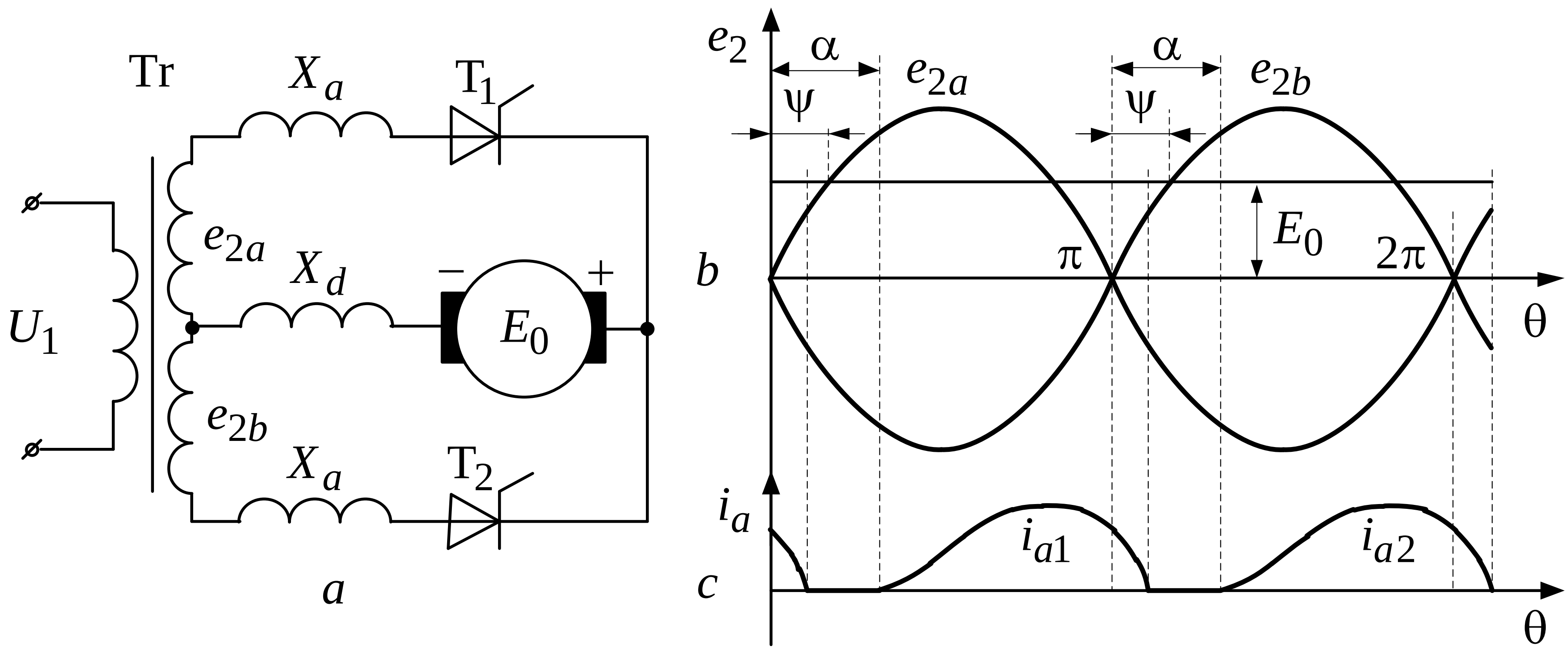

Fig. 2.30. Full-wave controlled rectifier operation with the motor load

Discontinuous current mode will be in the case when $E_0 > E_{d\alpha}$,

where $E_{d\alpha} = \dfrac{\sqrt{2}E_2}{\pi}\cos\alpha$ – average value of the rectified voltage at a given value of α.

Provided $E_0 \le E_{d\alpha} - \Delta U_x$, where

$\Delta U_x = \dfrac{I_d X_a}{\pi}$ – switching losses of rectified voltage, continuous current mode occurs.

The condition $E_0 \leq E_{d\alpha}$ corresponds to boundary-continuous mode (fig. 2.30).

In continuous current mode at $X_a = \infty$,

the overlapping of the anode valve currents will occur. That leads to the switching processes, with all inherent features.

Single-phase controlled bridge rectifier

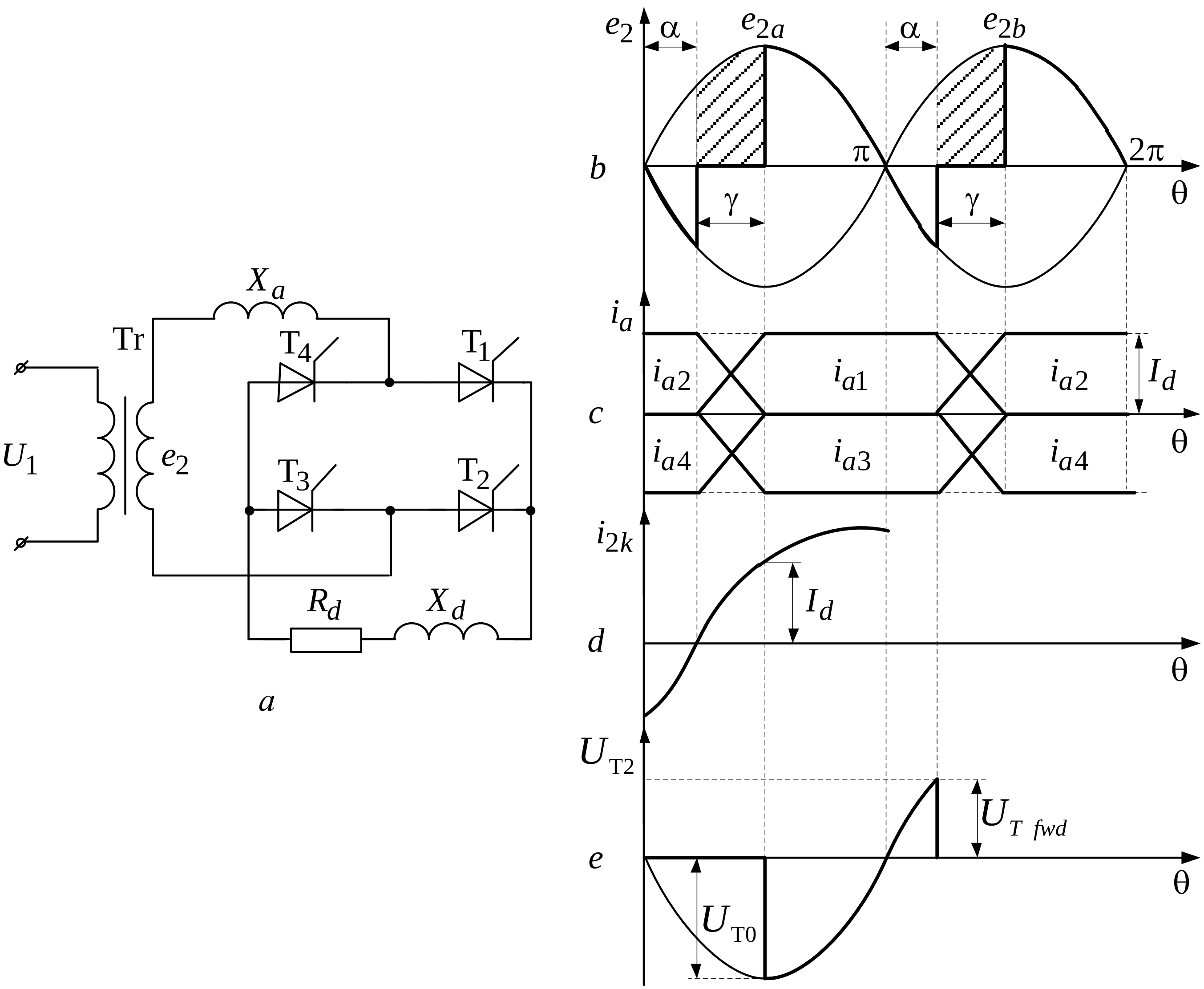

Fig. 2.31. Switching processes in single-phase controlled bridge rectifier

The equation for this switching loop is as follows:

$$e_2 - X_a \frac{\mathrm{d}i_{2k}}{\mathrm{d}\theta} = 0,$$

from here we find the current

$$i_{2k} = \frac{\sqrt{2}E_2}{X_a}\left(\cos\alpha - \cos\theta\right).$$

$$U_{d0} = \sqrt{2} \cdot E_2 \cdot \sin\left(\alpha + \gamma\right),$$

$$U_{d\ fwd} = \sqrt{2} \cdot E_2 \sin\alpha.$$

Three-phase controlled rectifiers

Three-phase zero-point rectifier

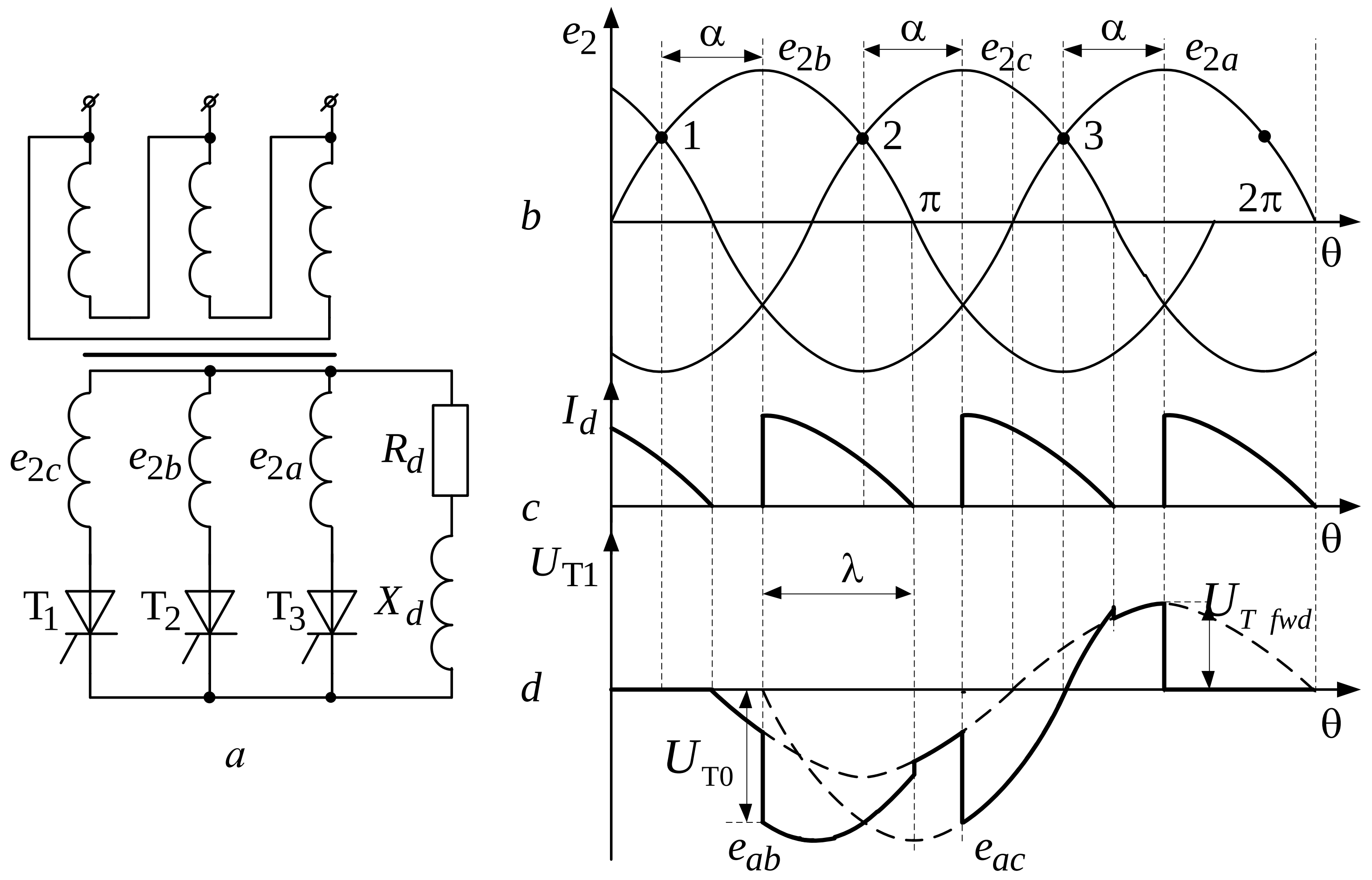

Fig. 2.32. Three-phase zero-point rectifier

In this case at $\alpha < 30^\circ$ the continuous current mode takes place; at $\alpha = 30^\circ$ – boundary-continuous current mode, at $\alpha > 30^\circ$ – discontinuous current mode

In the discontinuous current mode at $X_d = 0$ the rectified voltage is defined by the expression:

$$E_d = \frac{1}{\frac{2\pi}{3}} \int_{\pi/6+\alpha}^{\pi} \sqrt{2} \cdot E_2 \cdot \sin\theta \, d\theta = \frac{\sqrt{2} \cdot E_2}{2\pi/3} \cdot \left[1 - \sin\left(\alpha - \frac{\pi}{3} \right) \right] \quad (2.89)$$

In the same mode, but at $X_d > 0$

$$E_d = \frac{1}{2\pi/3} \int_{\pi/6+\alpha}^{\pi/6+\alpha+\lambda} \sqrt{2} E_2 \sin\theta d\theta =$$

$$= \frac{\sqrt{2}E_2}{2\pi/3}\left[\cos\left(\alpha+\frac{\pi}{6}\right)-\cos\left(\alpha+\frac{\pi}{6}+\lambda\right)\right]. \tag{2.90}$$

In continuous current mode:

$$E_d = \frac{1}{2\pi/3} \int_{\pi/6+\alpha}^{5\pi/6+\alpha} \sqrt{2} E_2 \sin\theta d\theta = \frac{\sqrt{6}E_2}{2\pi/3}\cos\alpha \tag{2.91}$$

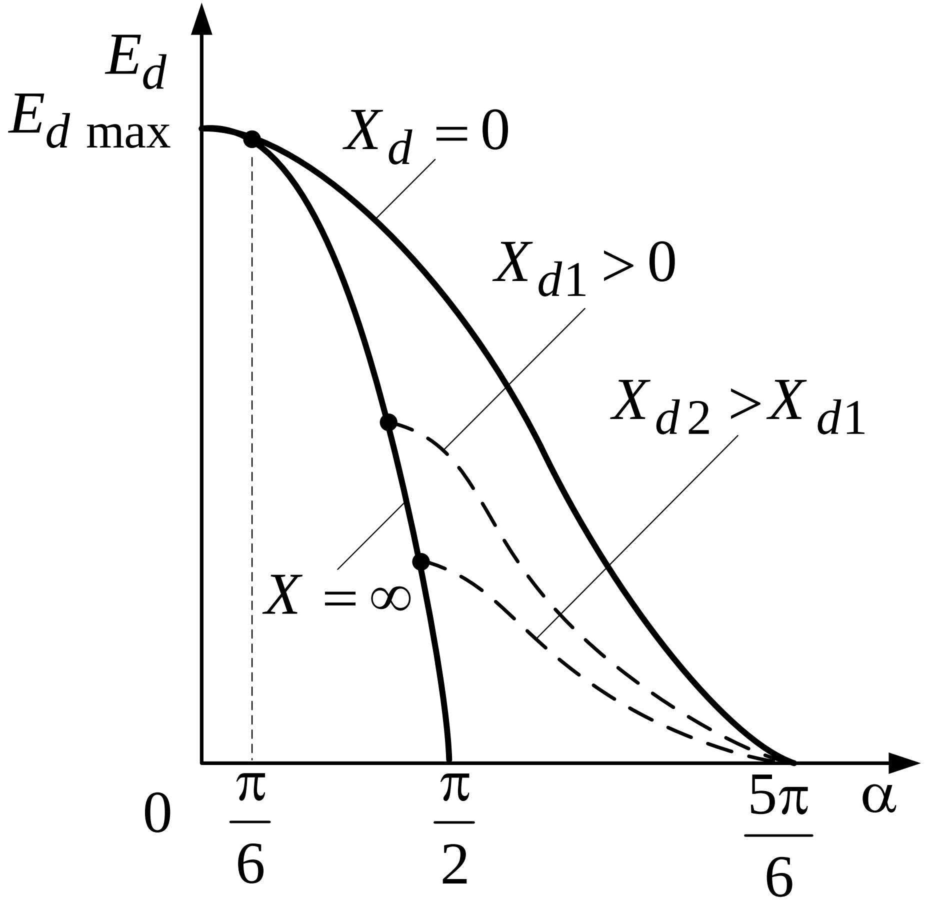

Fig. 2.33. The family of regulating characteristics of the three-phase zero-point controlled rectifier

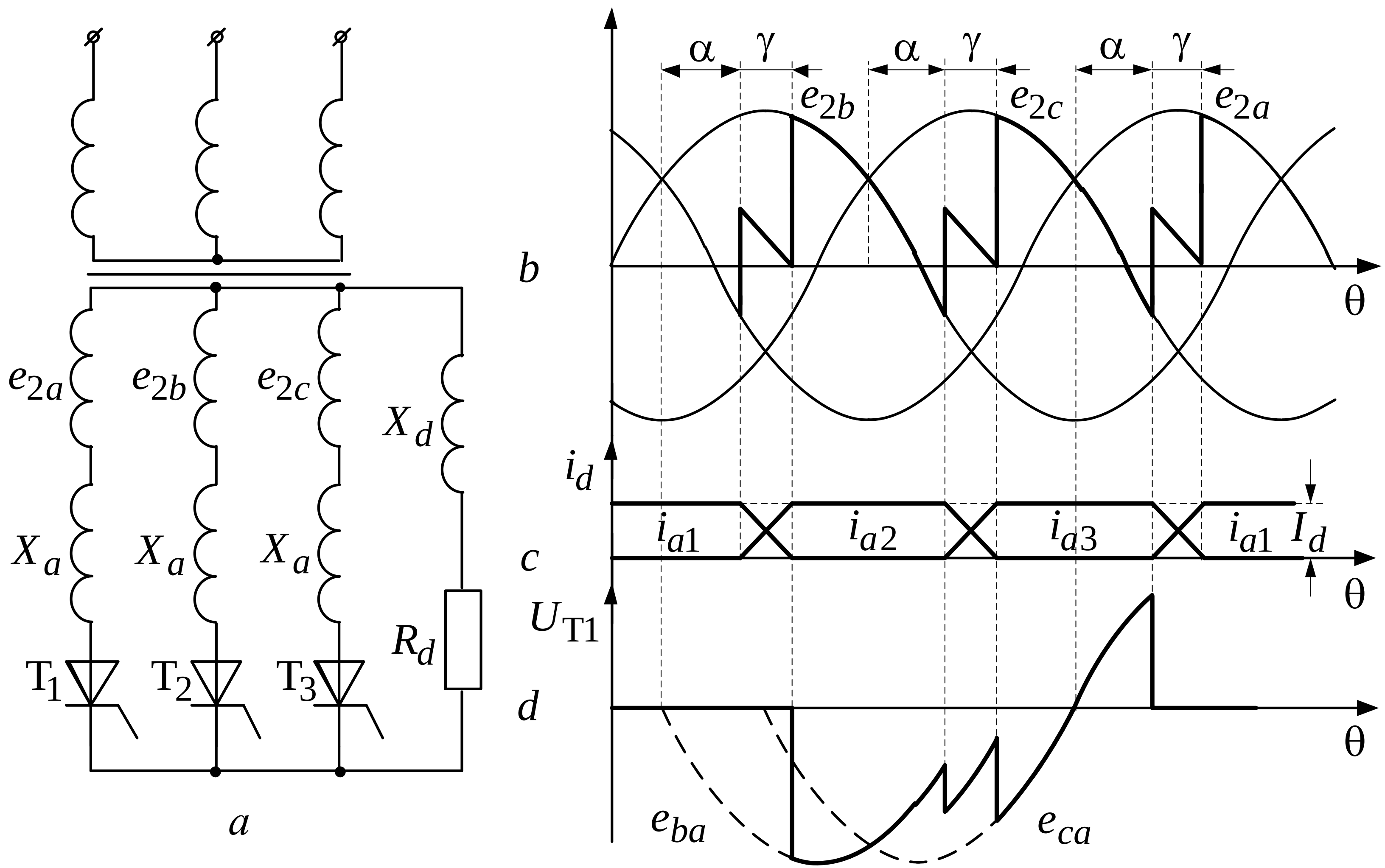

Fig. 2.34. Switching processes in a three-phase zero-point rectifier

$$\gamma = \arccos\left(\cos\alpha - \frac{I_d \cdot X_a}{\sqrt{2} \cdot E_2 \cdot \sin\left(\pi/3\right)} \right) - \alpha \quad (2.92)$$

$$E_d = E_{d\,\max} - \Delta U_x = 1{,}17 \cdot E_2 \cdot \cos\alpha - \frac{I_d \cdot X_a}{2\pi/3} \quad (2.93)$$

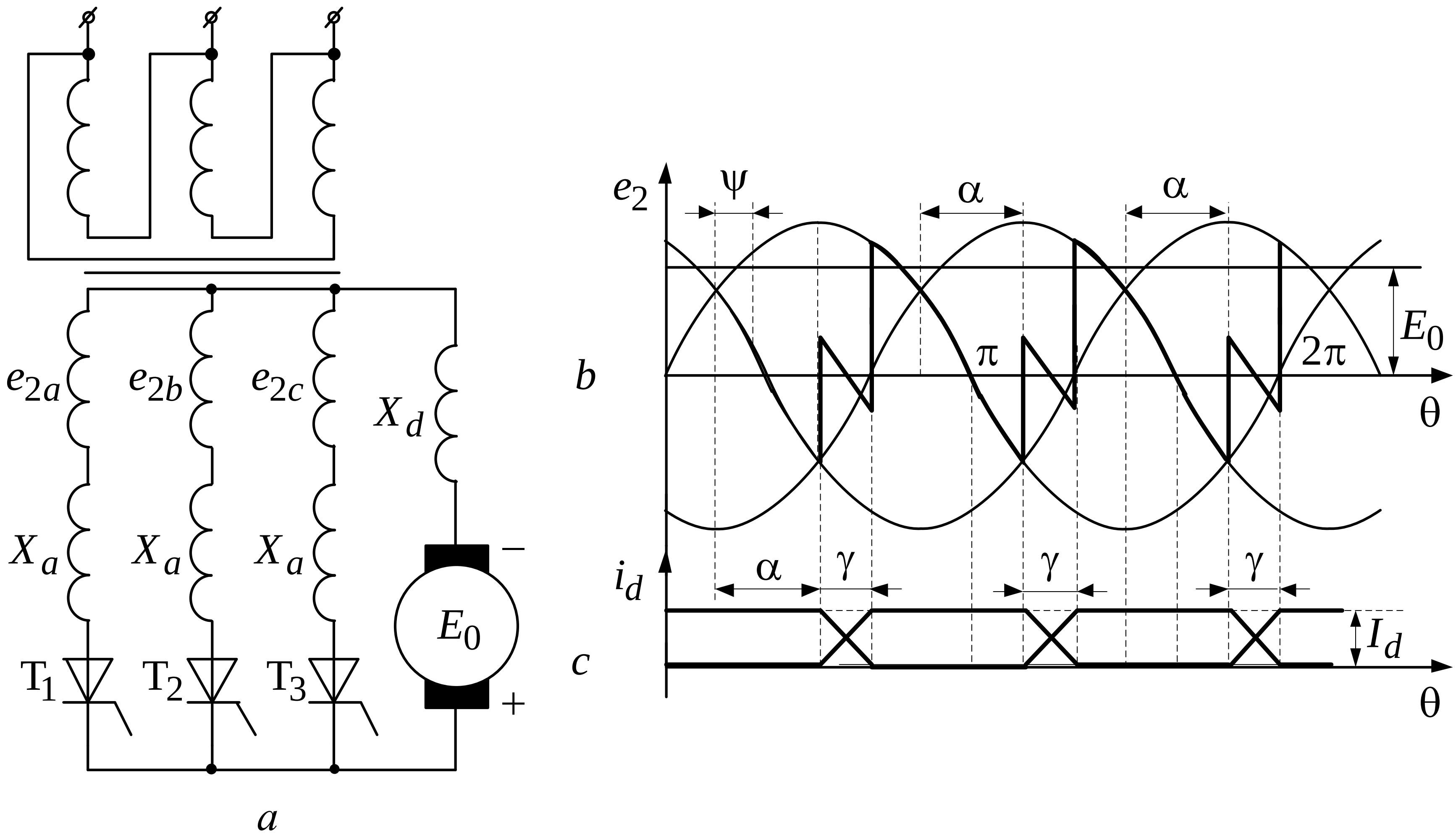

Fig. 2.35. Three-phase zero-point controlled rectifier operation with the motor load

The condition of discontinuous current mode is as follows: $E_0 > E_{d\alpha}$, where $E_{d\alpha} = 1{,}17 \cdot E_2 \cdot \cos\alpha$.

At $E_0 = E_{d\alpha}$ boundary-continuous mode occurs.

When $E_0 < \left(E_{d\alpha} - \Delta U_x\right)$, where $\Delta U_x = \dfrac{I_d X_a}{2\pi/3}$ – rectified voltage switching losses, continuous current mode occur.

Three-phase bridge controlled rectifier

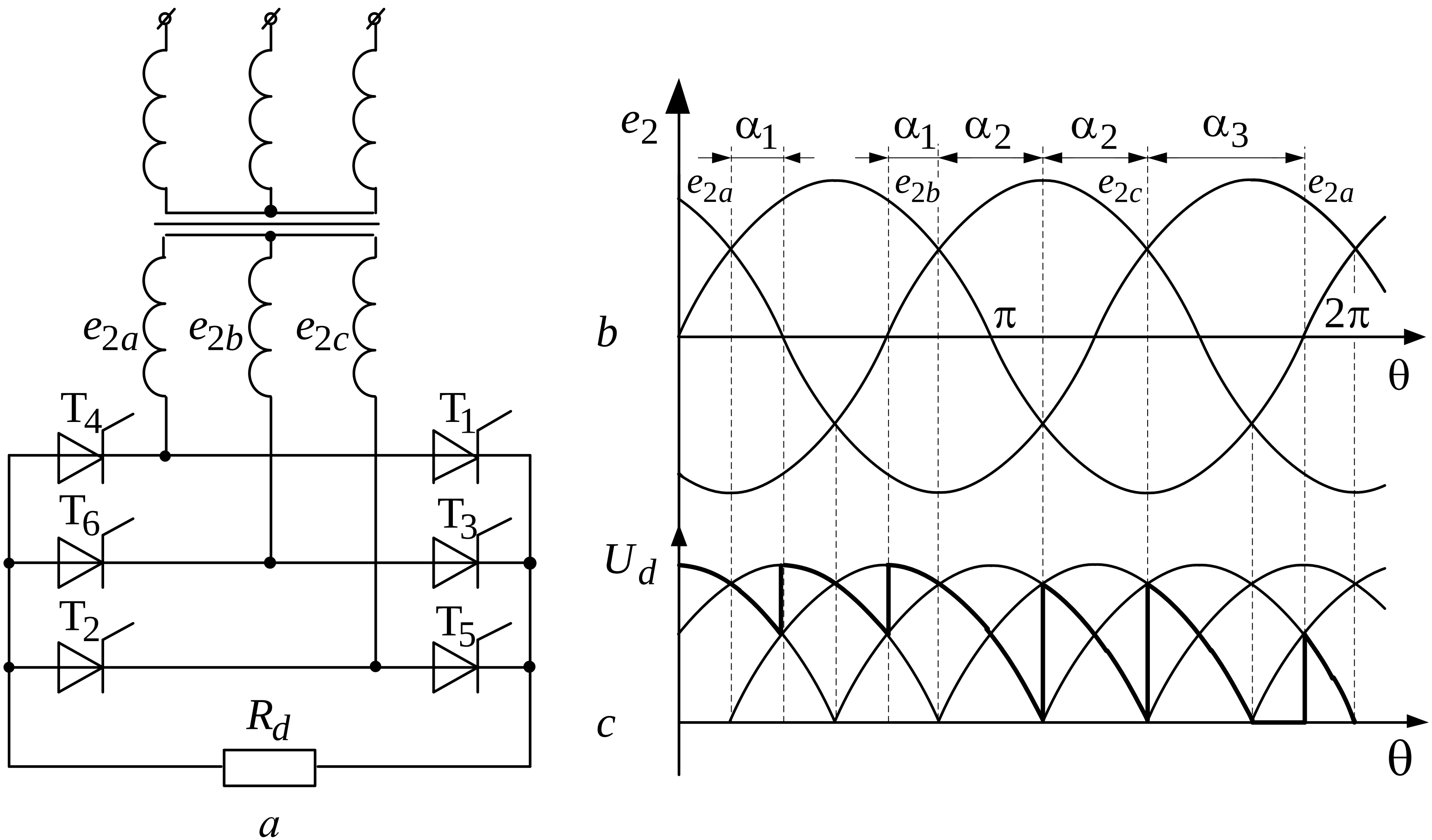

Fig. 2.36.Three-phase bridge controlled rectifier

At $\alpha < 60^{\circ}$ continuous current mode will occur, at $\alpha > 60^{\circ}$ – discontinuous current mode, and if $\alpha = 60^{\circ}$ – boundary-continuous current mode.

Rectified voltage in continuous and boundary-continuous current modes is defined by the expression:

$$E_{d\alpha} = \frac{1}{2\pi/6} \int_{\pi/3+\alpha}^{2/3\pi+\alpha} \sqrt{6} \cdot E_2 \cdot \sin\theta \, d\theta = 2{,}34 \cdot E_2 \cdot \cos\alpha \quad (2.94)$$

In the discontinuous current mode

$$E_{d\alpha} = \frac{1}{2\pi/6} \int_{\pi/3+\alpha}^{\pi} \sqrt{6} \cdot E_2 \cdot \sin\theta \, d\theta = \tag{2.95}$$

$$= 2{,}34 \cdot E_2 \cdot \left[1 + \cos\alpha \left(\frac{\pi}{3} + \alpha \right) \right]$$

At $X_d = \infty$ the continuous current mode will be at any value of control angle.

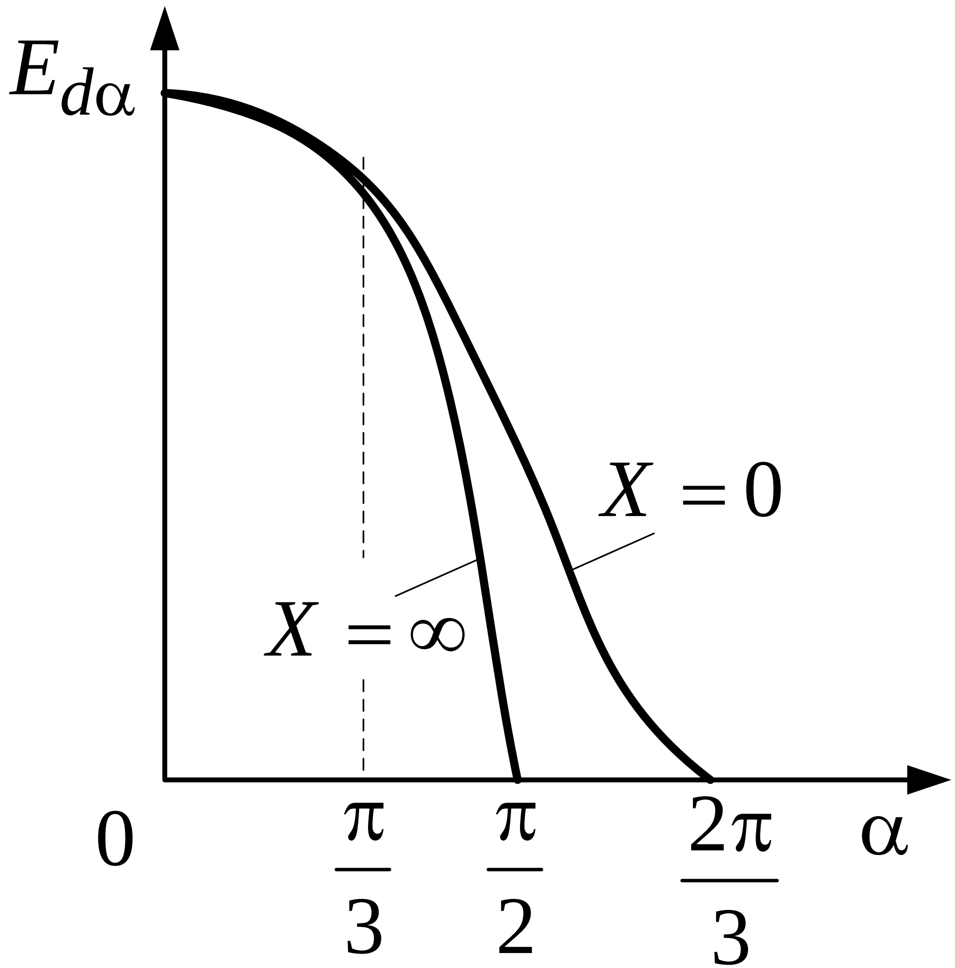

Fig. 2.37. Regulating characteristics family of three-phase bridge controlled rectifier

Switching processes occur during the interval

$$\gamma = \arccos\left(\cos\alpha - \frac{I_d \cdot X_a}{\sqrt{2} \cdot E_2 \cdot \sin\left(\pi/3\right)}\right) - \alpha \quad (2.96)$$

and lead to rectified voltage decrease by the value

$$\Delta U_x = \frac{I_d \cdot X_a}{2\pi/6}$$

Energy indicators of rectifiers

- Efficiency takes into account the losses in rectifier circuit and is defined as

$$\eta = \frac{P_d}{P_d + \Delta P_{tr} + \Delta P_v + \Delta P_{add}}, \quad (2.97)$$

where P_d – the active power released in the load;

ΔP_{tr} – losses in the power transformer which include the losses in magnetic core steel and losses in the windings;

ΔP_v – losses in valves of the rectifier;

ΔP_{add} – additional losses in the auxiliary devices.

The power factor χ determines the effect of the rectifier on the mains supply and is defined as

$$\chi = \frac{P}{S},$$

where P – the active power consumed by the rectifier from the mains,

S – total power.

Since the voltage of mains supply is assumed to be sinusoidal, and current consumed from the mains, is in most cases non-sinusoidal, then

$$P_1 = U_1 \cdot I_{1(1)} \cdot \cos\varphi_1 \qquad (2.98)$$

$$S = U_1 \cdot I_1 = U_1 \cdot \sqrt{I_{1(1)}^2 + \sum_{k \to \infty} I_k^2}, \qquad (2.99)$$

where $I_{1(1)}$ – the RMS value of the fundamental harmonic of the consumed current, φ_1 – the angle of the phase shift between the mains voltage and the first harmonic component of the consumed current; I_1 – the RMS value of current consumed from the mains; I_k – RMS value of the current harmonic component with the order number k.

$$\chi = \frac{U_1 \cdot I_{1(1)} \cdot \cos\varphi_1}{U_1 \cdot \sqrt{I_{1(1)}^2 + \sum\limits_{k \to \infty} I_k^2}} = \nu \cdot \cos\varphi_1, \quad (2.100)$$

$$\nu = \frac{I_{1(1)}}{\sqrt{I_{1(1)}^2 + \sum\limits_{k \to \infty} I_k^2}}, \quad (2.101)$$

where ν – the distortion factor.

As it has been shown above, the power of the higher harmonic components of the consumed current does not have a constant component and oscillates between power transformer and mains supply.

The component of the total power defined by the coefficient ν called the distortion power

$$\nu = \frac{\sqrt{P^2 + Q^2}}{\sqrt{P^2 + Q^2 + T^2}}, \qquad (2.102)$$

where Q – the reactive power consumed by the mains determined by $\cos\varphi_1$, called the shift factor:

$$\cos\varphi_1 = \frac{P}{\sqrt{P^2 + Q^2}}. \quad (2.103)$$

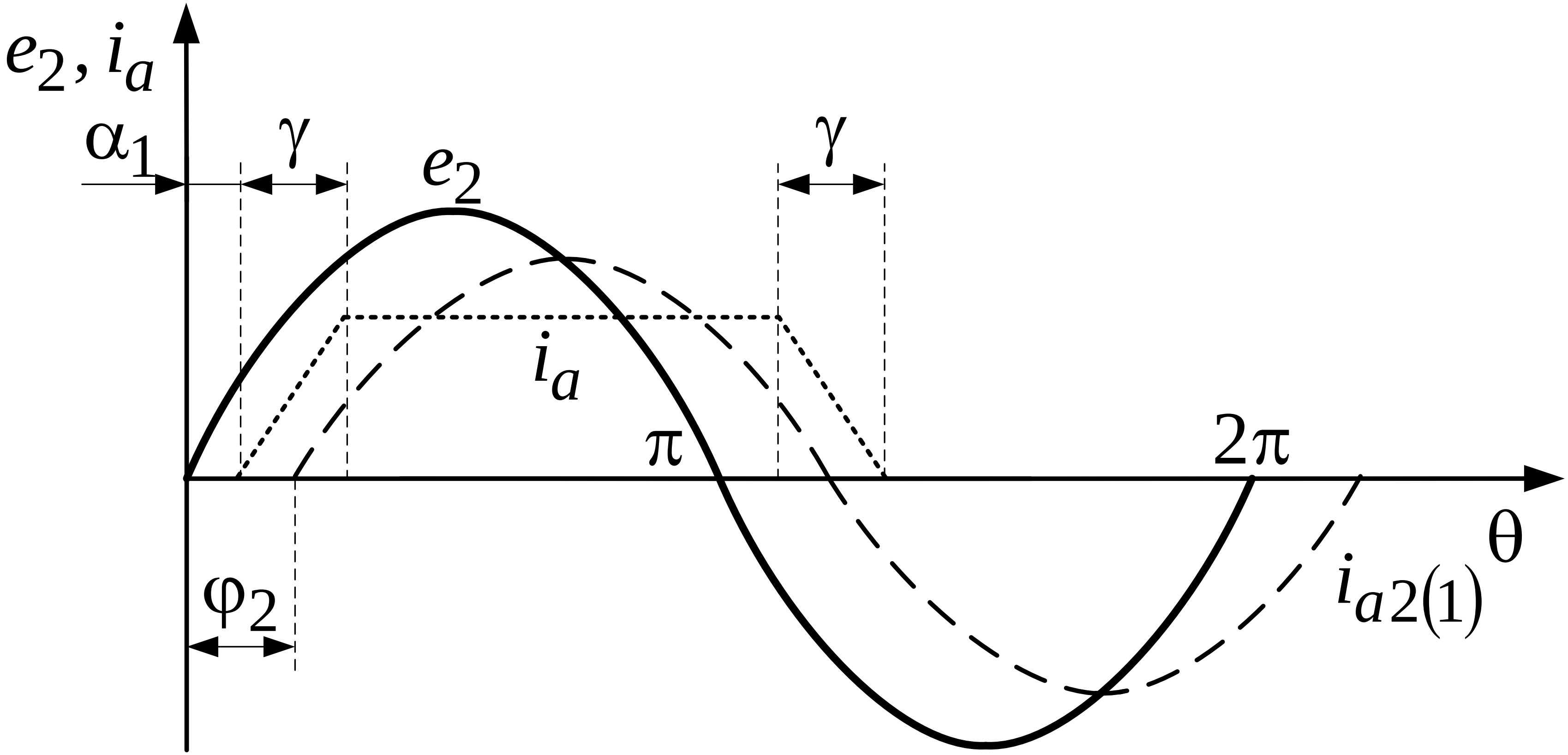

Fig. 2.38. The diagram for the secondary winding rectifier transformer circuit

In multi-phase rectifier with asymmetrical load in phases there is another component of the total power – the power of asymmetry

$$H = \sqrt{S^2 - (P^2 + Q^2 + T^2)},$$

determined by the asymmetry factor

$$k_a = \sqrt{\frac{P^2 + Q^2 + T^2}{S^2}}. \quad (2.104)$$

Total power factor

$$\chi = \nu \cdot k_{\text{н}} \cdot \cos \varphi_1 \quad (2.105)$$

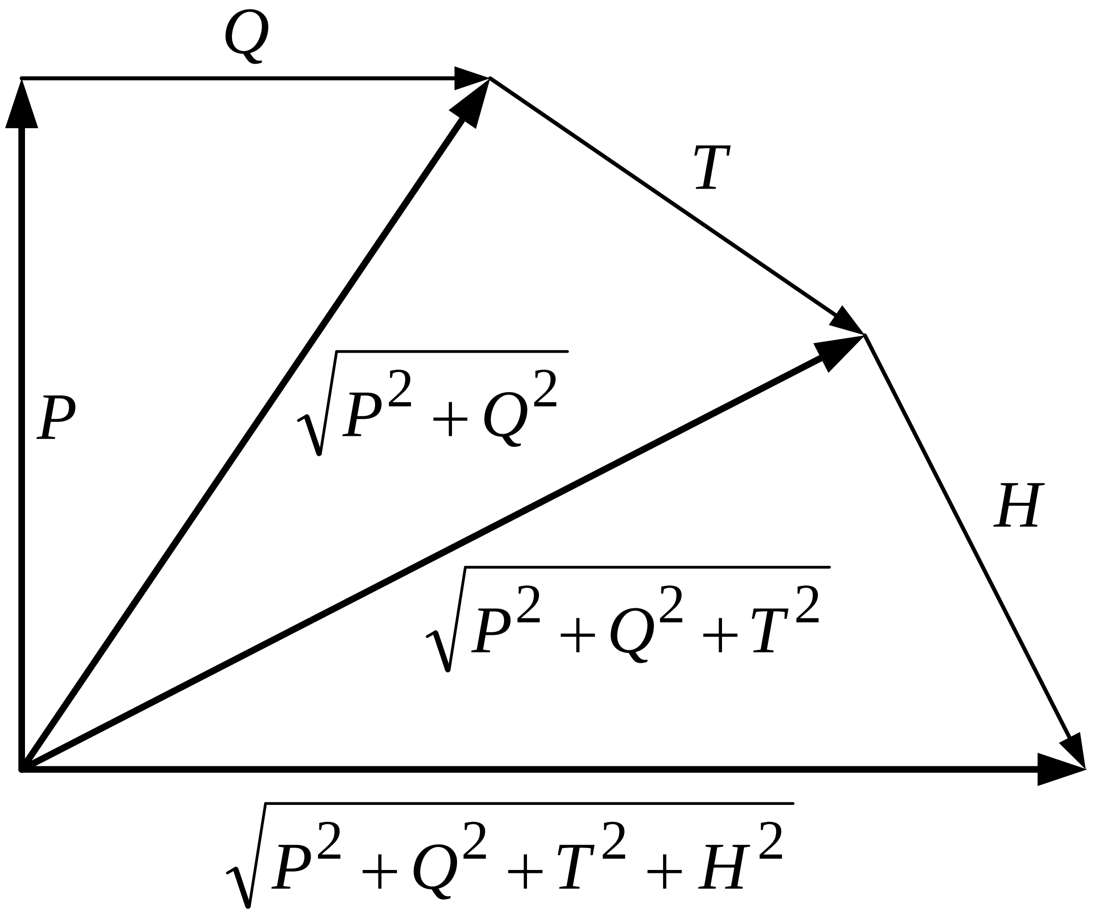

Fig. 2.39. Power chart of the controlled rectifier

Methods of improving the energy indicators of controlled rectifiers

As it can be seen from the expression (2.105), power factor increase improvement can be performed in two ways:

- improvement of the distortion factor ν;
- reduction of the angle φ.

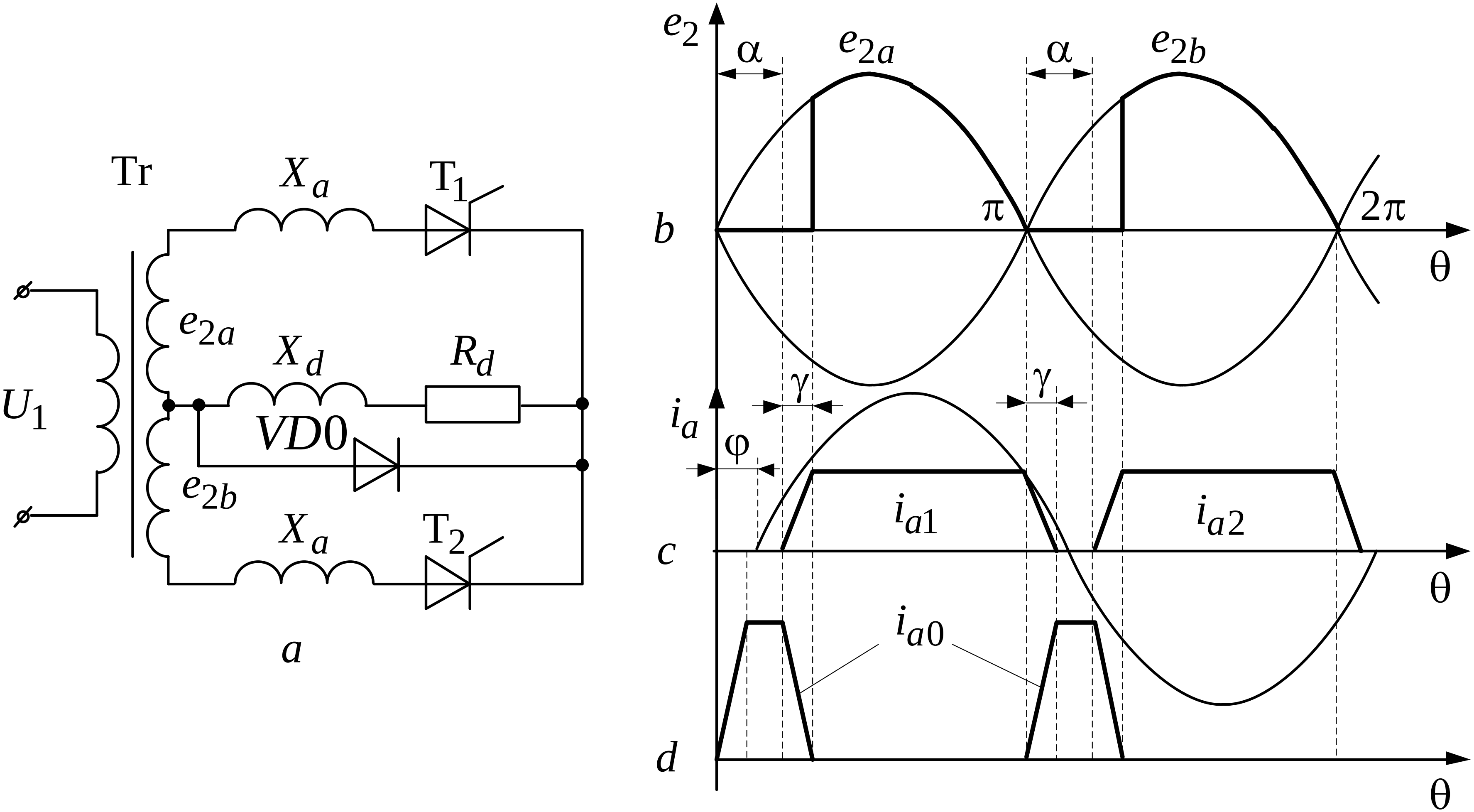

Fig. 2.40. Controlled rectifier with zero valve

The first harmonic component of the primary current will have the same phase shift relative to the supply voltage U_1:

$$\varphi_1 = \frac{\alpha}{2} + \frac{\gamma}{2}$$

That allow to increase significantly $\cos\varphi_1$ and the power factor of the rectifier and as a whole.

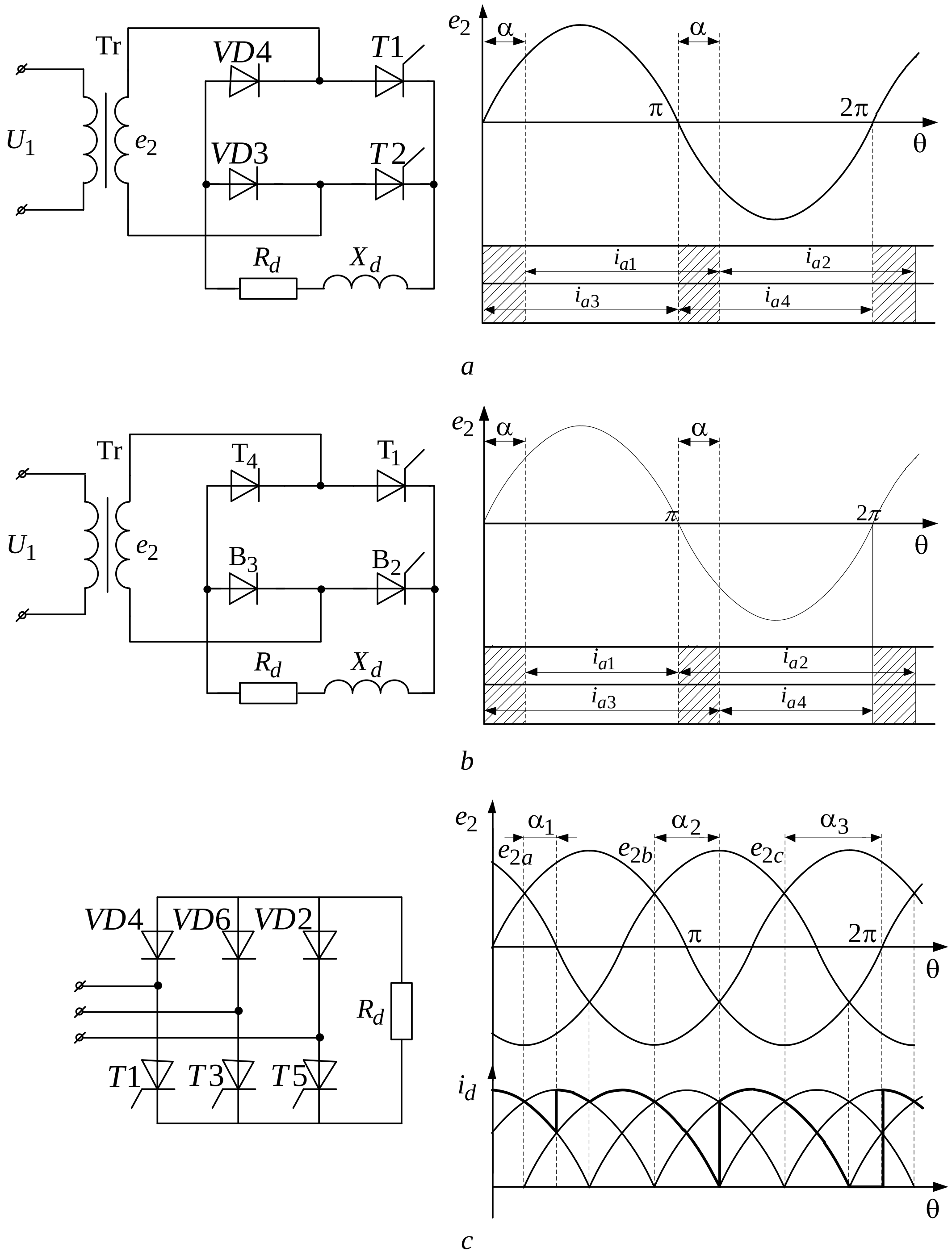

Fig. 2.41. Non-symmetric controlled rectifiers circuits

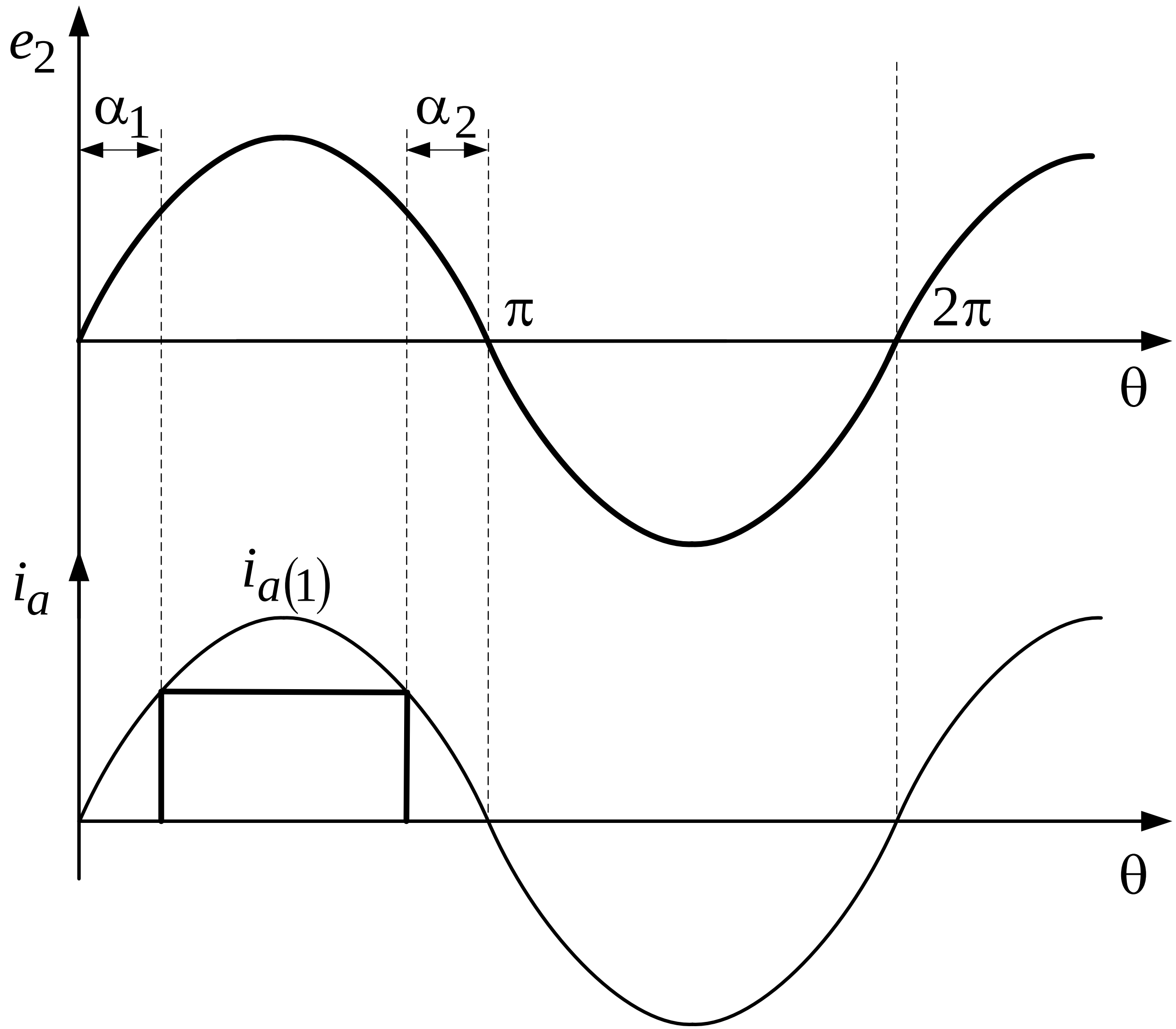

Fig. 2.42. Controlled rectifier operation with fully controlled valves

To maximize the value of the distortion coefficient

$$\nu = \frac{I_{1(1)}}{I_1}$$

it is necessary approximate the shape of the primary current i_1 consumed from the mains, to a sinusoid waveform, which is extremely difficult if $X_d >> R_d$.

To solve this problem it is necessary to increase the number of pulses per period.

However, it is connected to the complication of the power circuit.

This problem can be solved if, along with a fully controlled switches use in the power rectifier circuit, to implement the methods of pulse width modulation (PWM) for the regulation of rectified voltage (fig. 2.43).

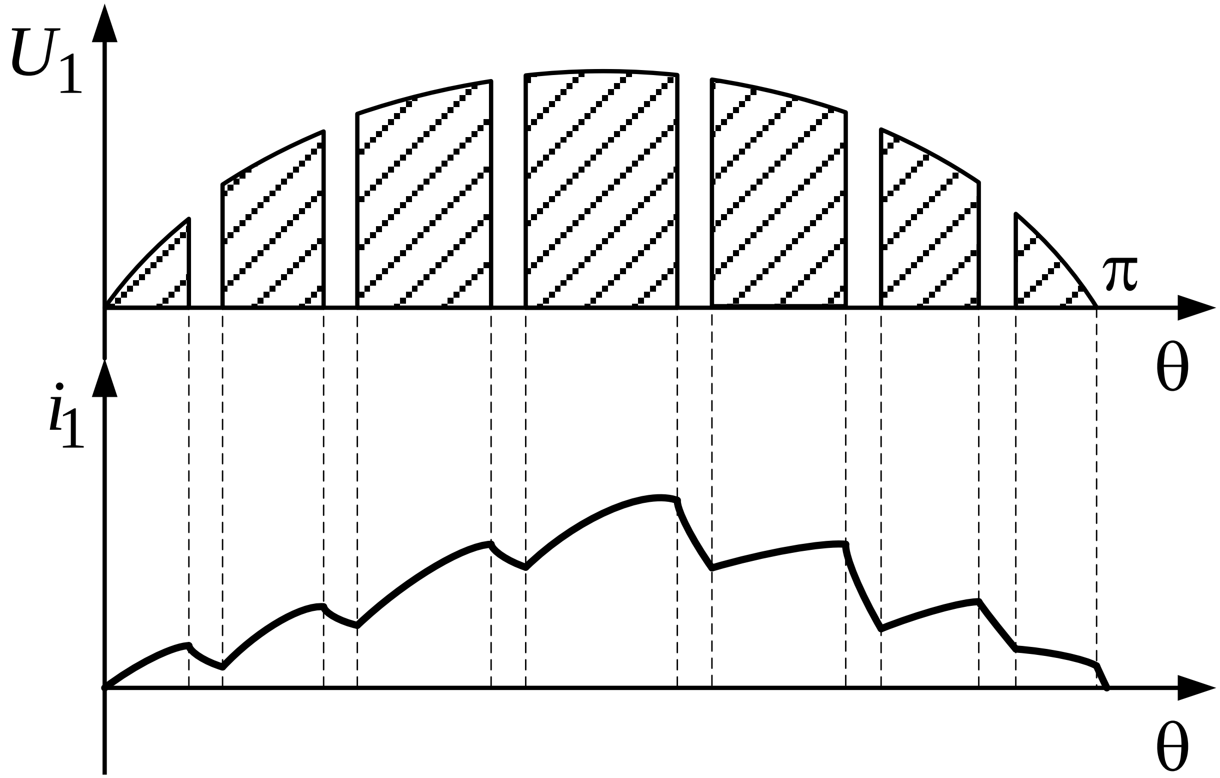

Fig. 2.43. Formation of the input current of active rectifier

POWER SMOOTHING FILTERS

One of the main criteria for assessing the quality of the rectified voltage and current is ripple factor:

$$k_r = \frac{U_r}{E_d},$$

where E_d – constant component,

U_r – the predominant harmonic magnitude of the variable component.

Inductive smoothing filter

Imagine a rectifier as a series connection of DC source of voltage E_d and AC component source of voltage U_r (Fig. 3.1).

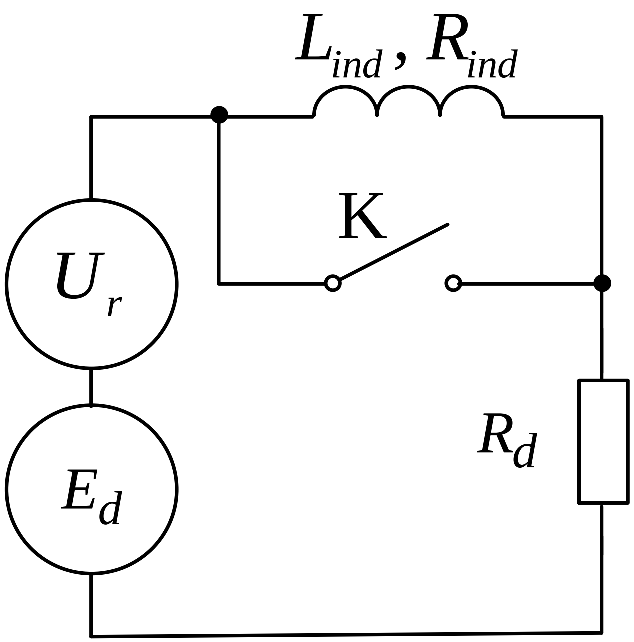

Fig. 3.1 The diagram explaining the operation of inductive smoothing filter

Constant component of the current:

$$I_d = \frac{E_d}{R_d}$$

Variable component: $I_r = \frac{U_r}{R_d}$

Ripple factor without a filter:

$$k_r = \frac{U_r}{E_d}$$

When the inductor is connected in series with the load (switch K it turned off) current and voltage components in the load are changed according to the next expressions:

$$I'_d = \frac{E_d}{R_d + R_{ind}}, \quad I'_r = \frac{U_r}{\sqrt{\left(R_d + R_{ind}\right)^2 + \left(m \cdot \omega \cdot L_{ind}\right)^2}}, \quad (3.2)$$

R_{ind} – the resistance of the inductance coil;

m – the number of pulses per period of the rectifier

$$E'_d = I'_d \cdot R_d = \frac{E_d \cdot R_d}{R_d + R_{ind}},$$

$$U'_r = \frac{U_r \cdot R_d}{\sqrt{\left(R_d + R_{ind}\right)^2 + \left(m \cdot \omega \cdot L_{ind}\right)^2}}, \quad (3.3)$$

$$k'_r = \frac{U'_r}{E'_d} = k_r \cdot \frac{R_d + R_{ind}}{\sqrt{(R_d + R_{ind})^2 + (m \cdot \omega \cdot L_{ind})^2}}. \quad (3.4)$$

Taking into consideration that $\frac{k_r}{k'_r} = q$ – smoothing factor of the filter, we find a value of inductance that provides given smoothing factor:

$$L_{ind} = \frac{R_{ind} + R_d}{m \cdot \omega}\sqrt{q^2 - 1} \quad (3.5)$$

Since $R_d >> R_{ind}$ and $q >> 1$ then

$$L_{ind} = \frac{R \cdot q}{m \cdot \omega} \quad (3.6)$$

Capacitive smoothing filter

Capacitive smoothing filter is a capacitor *C* connected in parallel to the rectifier load.

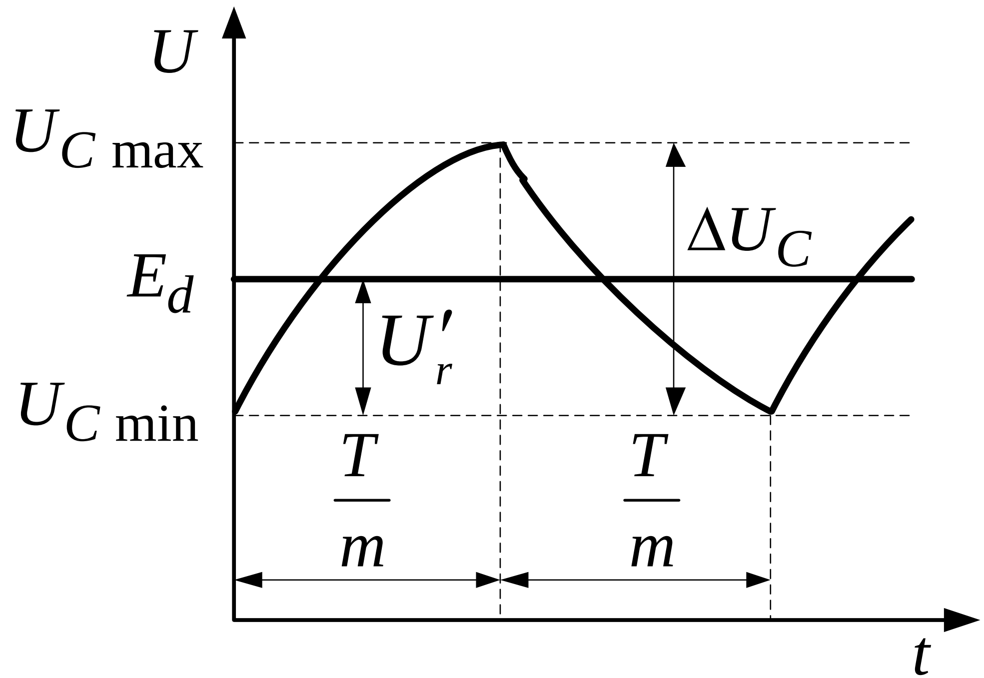

Fig. 3.2. Diagram of the capacitive smoothing filter operation

Assume that the capacitor current i_C in the discharge mode does not change: $i_C = I_C = I_d$ and the charge and discharge of the capacitor occur during the interval $\frac{T}{m}$, where *m* – the number of pulses per period of the rectifier, *T* – mains voltage period. Then

$$\Delta U_C = \frac{1}{C}\int_0^{T/m} i_d \mathrm{d}t = \frac{I_d T}{Cm} \quad (3.7)$$

Since

$$T = \frac{1}{f};\ \Delta U_C = 2U'_r = \frac{I_d}{Cfm};$$

$$k'_r = \frac{I_d}{2CfmE_d} = \frac{1_d}{2CfmR_d}, \qquad (3.8)$$

hence find the value of C providing the required ripple factor k_r' on the load:

$$C = \frac{1}{2R_d mfk_r'} \qquad (3.9)$$

INVERTERS

Inverters are devices that convert DC power into AC power.

Inverters are divided into commutated (or led by mains) and self-commutated (or autonomous). On the basis of a logical sequence, start with a consideration of the commutated inverters.

Commutated inverters

Single-phase led by mains inverters

Led by mains inverter is similar schematically to the controlled rectifier.

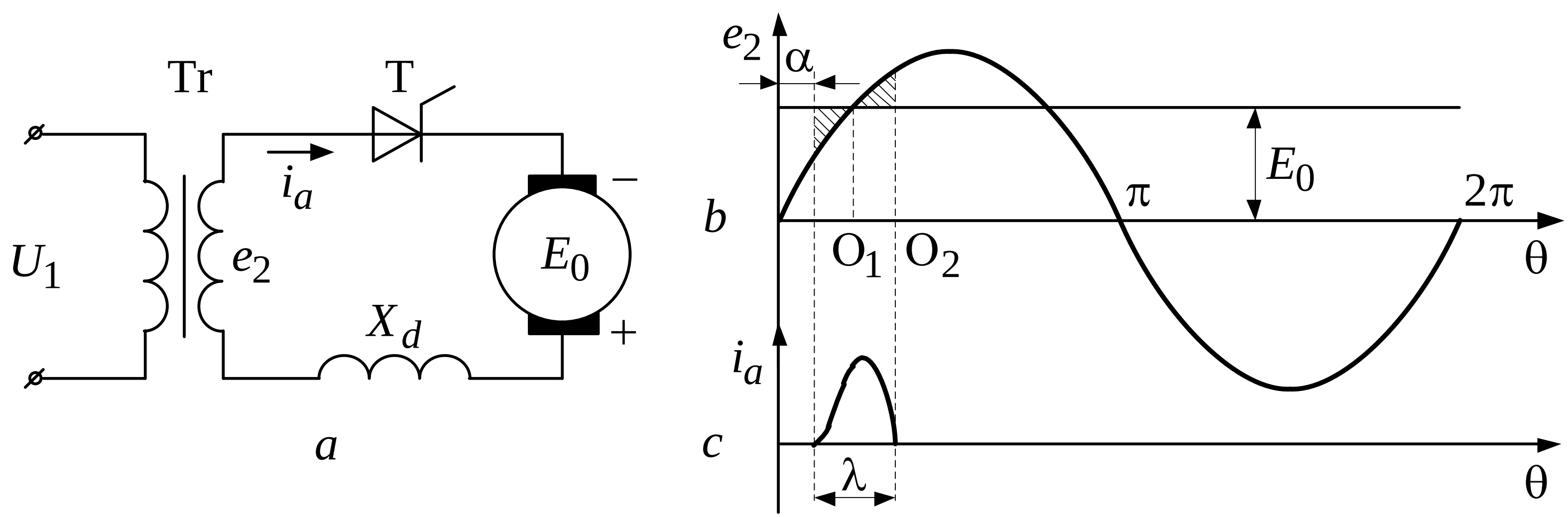

Fig. 4.1. Led by mains single-phase half-wave inverter

In order to send the energy flow to the mains, it is necessary that the same current i_a flows through the secondary winding of the transformer, overcoming back-EMF e_2.

The thyristor T switching on will lead to emergency mode which is called “inverter rollover” when the circuit of two sources e_2 and E_0 current i_a is limited only by the inductive reactance X_d:

$$i_a = \frac{e_2 + E_0}{X_d}$$

Led by mains full-wave inverter with midpoint

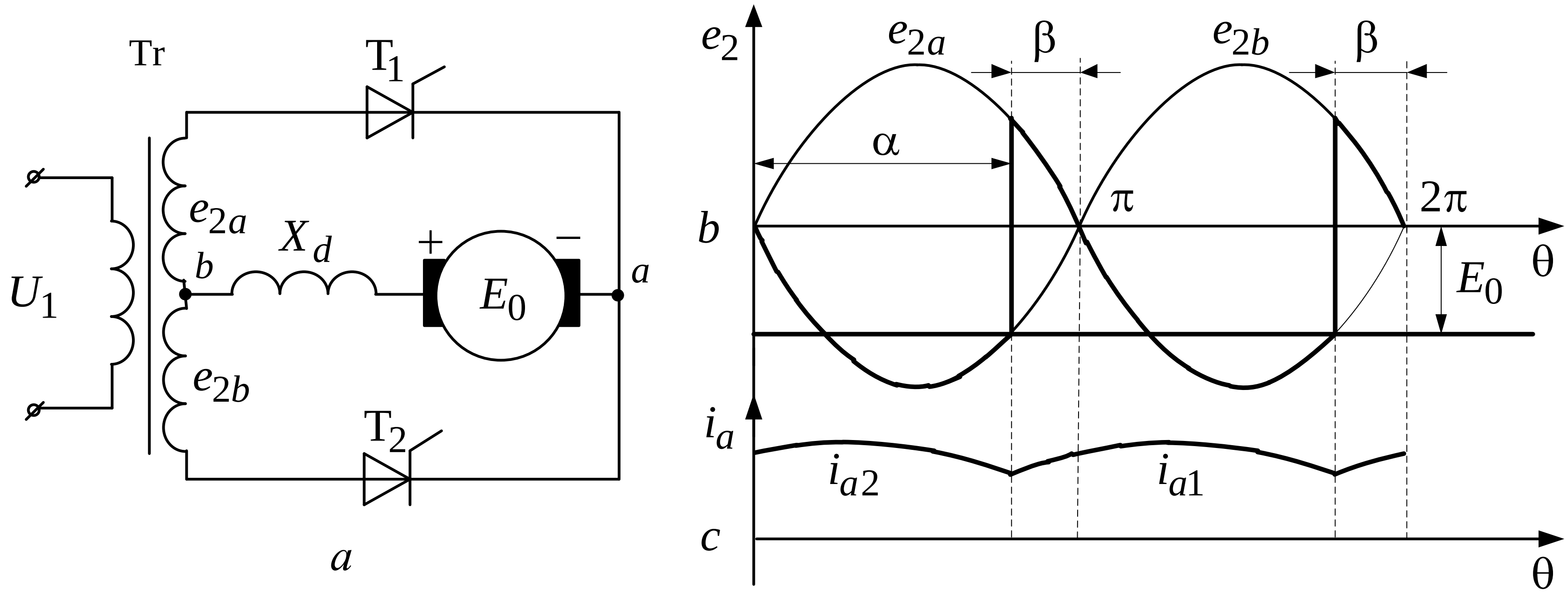

Fig. 4.2. Led by mains full-wave inverter with midpoint

Angle β is called the lead angle

The point $(\pi - \beta)$ can be defined as the angle α, known as the control angle.

The correlation between these two angles is defined by the expression:

$$\alpha + \beta = \pi$$

The mean value of back-EMF:

$$E_{d\beta} = \frac{1}{\pi} \int\limits_{\pi-\beta}^{2\pi-\beta} \sqrt{2} \cdot E_2 \cdot \sin\theta d\theta = -\frac{2\sqrt{2} \cdot E_2}{\pi} \cdot \cos\beta \quad (4.1)$$

Features of switching processes in the led by mains inverters

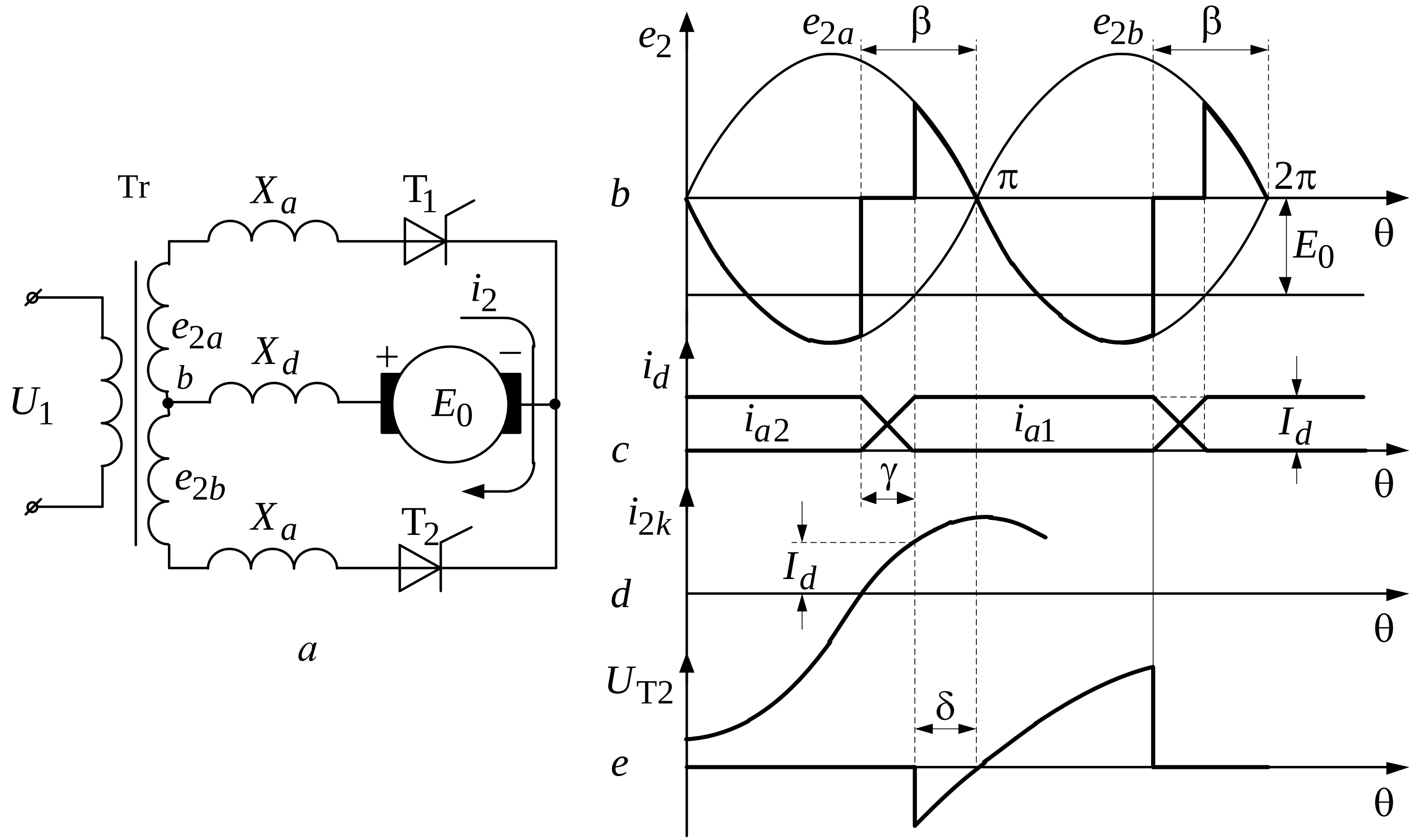

Fig. 4.3. Switching processes in a full-wave led by mains inverter

Within the interval $(\pi-\beta)\ldots(\pi-\beta+\gamma)$ the next equation is valid:

$$e_{2a} - X_a \frac{\mathrm{d}i_{2k}}{\mathrm{d}\theta} - \frac{X_a \mathrm{d}i_{2k}}{\mathrm{d}\theta} + e_{2b} = 0. \quad (4.2)$$

Solving equation (4.2) with respect to current i_{2k}, taking into account zero initial conditions, we obtain:

$$i_{2k} = \frac{\sqrt{2}E_2}{X_a}\left[\cos(\pi-\beta) - \cos\theta\right] \quad (4.3)$$

In the considered interval current i_{2k}

is the current i_{a1} of the valve T_1, incoming into operation. When this current reaches the value I_d, switching process ends.

Therefore

$$i_{2k}\Big|_{\theta=\pi-\beta+\gamma} = I_d$$

Hence we find the commutation angle γ:

$$\gamma = \beta - \arccos\left(\frac{I_d X_a}{\sqrt{2}E_2} + \cos\beta\right) \quad (4.4)$$

The current of the valve which is switching off in the commutation interval:

$$i_{a2} = I_d - i_{a1} = I_d - i_{2k}$$

During the interval γ the secondary winding of the transformer is short-circuited, so the instantaneous value of back-EMF:

$$e_{d\beta} = \frac{e_{2a} + e_{2b}}{2} = 0$$

The average inverter back-EMF

$$E_{d\beta} = \frac{1}{\pi} \int_{\pi-\beta+\gamma}^{2\pi-\beta} \sqrt{2} E_2 \sin\theta d\theta$$

differs from (4.1) by the value

$$\left|\Delta U_x\right| = \frac{1}{\pi} \int_{\pi-\beta}^{\pi-\beta+\gamma} \sqrt{2} E_2 \sin\theta d\theta = \frac{I_d X_a}{\pi} \quad (4.5)$$

Inverter input characteristic equation:

$$E_{d\beta}(I_d) = E_{d\beta 0} - \Delta U_x = -\frac{2\sqrt{2}E_2}{\pi}\cos\beta - \frac{I_d X_a}{\pi} \quad (4.6)$$

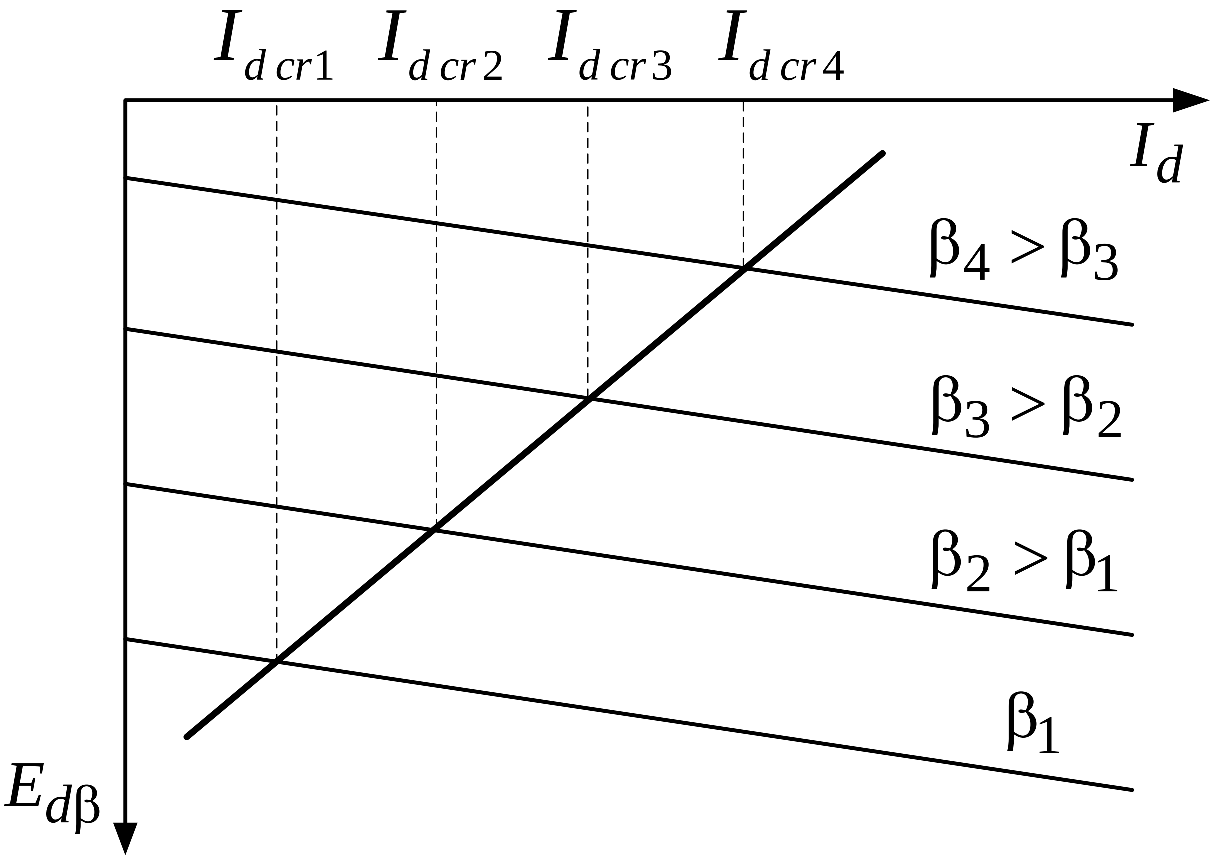

Fig. 4.4. The family of input characteristics of led by mains inverter and limiting characteristic

The input characteristics of the inverter $E_{d\beta} = f\left(I_d\right)$ is convenient to combine in one diagram (Fig. 4.5).

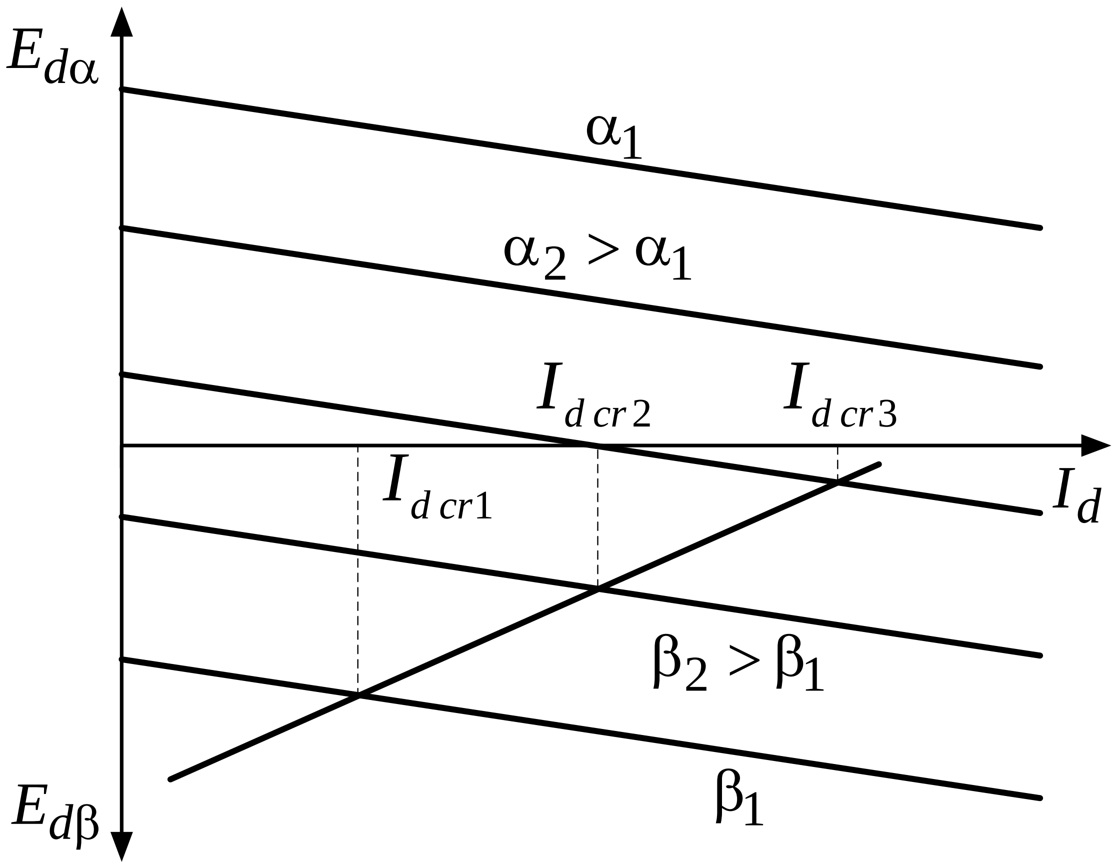

Fig. 4.5. Diagram explaining the converter transition from the rectifier mode into inverter one

The angle $\delta = \beta - \gamma$ is called stock angle, and its minimum value is determined by time of the thyristor switching off:

$$\delta_{\min} = \omega \cdot t_{\text{off}}$$

This implies that the commutation angle increase is limited by a certain critical value

$$\gamma_{\min} = \beta - \delta_{\min}$$

Exceeding the value $I_{d\,\text{cr}}$ leads to inverter "rollover".

Connecting all points $E_{d\beta}$ which correspond to critical values of the current $I_{d\ \mathrm{cr}}$, we get the limiting characteristic of dependent inverter that separates the working area of the output characteristics from the non-working one.

Taking into account that $\delta = \beta - \gamma$ from (4.4) we get

$$I_{d\ \mathrm{cr}} = \frac{\sqrt{2}E_2}{X_a}\left(\cos\delta_{\min} - \cos\beta\right) \quad (4.7)$$

and then from (4.6):

$$E_{d\beta\,cr} = -\frac{2\sqrt{2}E_2}{\pi}\frac{\cos\delta_{min} + \cos\beta}{2} \quad (4.8)$$

It is sufficient for limiting characteristic plotting.

Three-phase dependent inverters

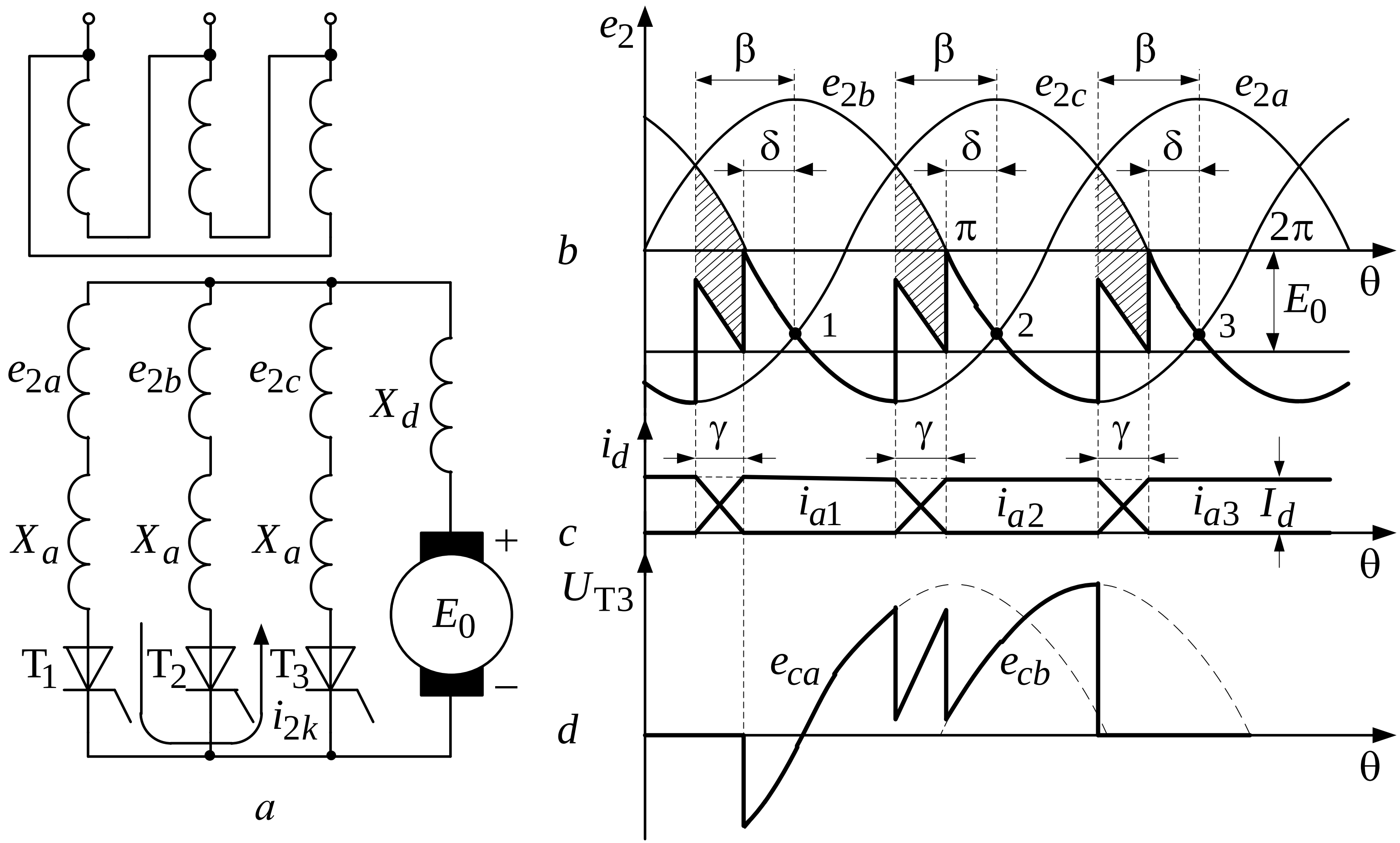

Fig. 4.6. Three-phase zero-point dependent inverter, provided $X_d = \infty, X_a \neq 0$

Electromagnetic processes in switching circuit between phases a and c are described by the equation:

$$e_{2a} - X_a \frac{\mathrm{d}i_{ak}}{\mathrm{d}\theta} - X_a \frac{\mathrm{d}i_{ak}}{\mathrm{d}\theta} - e_{2c} = 0 \quad (4.9)$$

Transferring the origin of coordinated to the point 1, we obtain:

$$e_{2a} - e_{2c} = -2\sqrt{2}E_2 \sin\frac{\pi}{m}\sin\theta \quad (4.10)$$

Solving equation (3.9) with respect to i_{2k} and taking into account the initial conditions, we obtain:

$$i_{2k}\Big|_{\theta=-\beta}=0,\quad i_{2k}=\frac{\sqrt{2}E_2\sin\left(\pi/3\right)}{X_a}\left(\cos\theta-\cos\beta\right) \quad (4.11)$$

On the switching interval this current is the current of the valve T_1 which is coming into operation: $i_{2k}=i_{a1}$

The switching process ends when $i_{a1}\Big|_{\theta = -\beta + \gamma} = I_d$

From this condition we find γ:

$$\gamma = \beta - \arccos\left(\frac{I_d X_a}{\sqrt{2} E_2 \sin\left(\pi / m \right)} + \cos\beta \right) \quad (4.12)$$

The average value of inverter back-EMF:

$$E_{d\beta} = E_{\alpha\beta_0} + \Delta U_x \quad (4.13)$$

where $E_{d\beta_0}$ – in the back-EMF in the absence of switching processes (no-load mode)

$$E_{d\beta 0} = \frac{1}{2\pi/3} \int_{\pi/2-\beta}^{7/6\,\pi-\beta} \sqrt{2} E_2 \sin\theta \, d\theta = \qquad (4.14)$$

$$= -\frac{\sqrt{2} E_2}{2\pi/3} \sin\frac{\pi}{m} \cos\beta = -1{,}17 E_2 \cos\beta.$$

The average value of inverter back-EMF increases by the value

$$\Delta U_x = \frac{1}{2\pi/3} \int_{-\beta}^{-\beta+\gamma} \left(\frac{e_{2c} + e_{2a}}{2} - e_{2a} \right) d\theta = -\frac{I_d X_a}{2\pi/3} \qquad (4.15)$$

Thus

$$E_{d\beta} = -1{,}17\cos\beta - \frac{I_d X_a}{2\pi/3} \quad (3.16)$$

is the equation of the input characteristic of the inverter (Fig. 4.7).

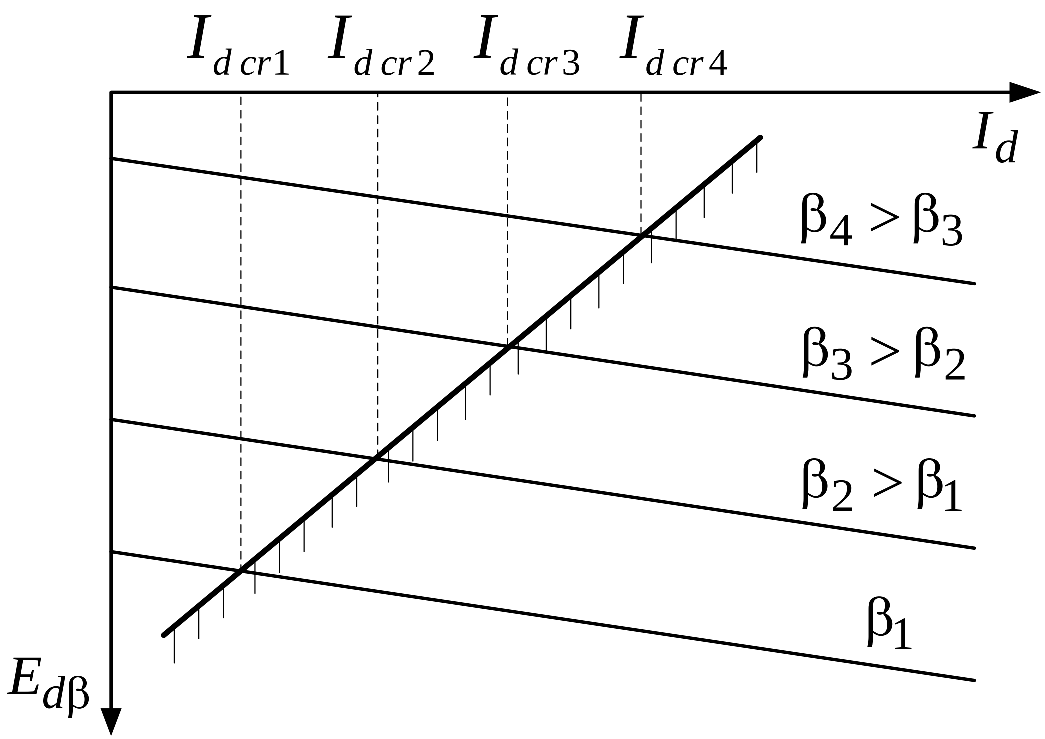

Fig. 4.7. Limiting characteristic of three-phase zero-point dependent inverter

The critical current value $I_{d\mathrm{cr}}$ corresponding to γ_{cr} is derived from (4.12):

$$I_{d\ \mathrm{cr}} = \frac{\sqrt{2}E_2}{X_a}\sin\frac{\pi}{3}(\cos\delta_{\min} - \cos\beta) \quad (4.17)$$

$$U_{d\beta\ cr} = -1{,}17E_2\left(\frac{\cos\delta_{\min} + \cos\beta}{2}\right). \quad (4.18)$$

The switching processes in three-phase bridge dependent inverter are quite similar to the considered ones, but in expressions (4.12) (4.14) (4.15) (4.16) (4.17) (4.18) it should be taken into account that number of pulses per period of the bridge circuit m=3, as opposed to zero-point circuit and the circuit coefficient $k_{cir} = 2{,}34$.

Energy indicators of dependent inverters

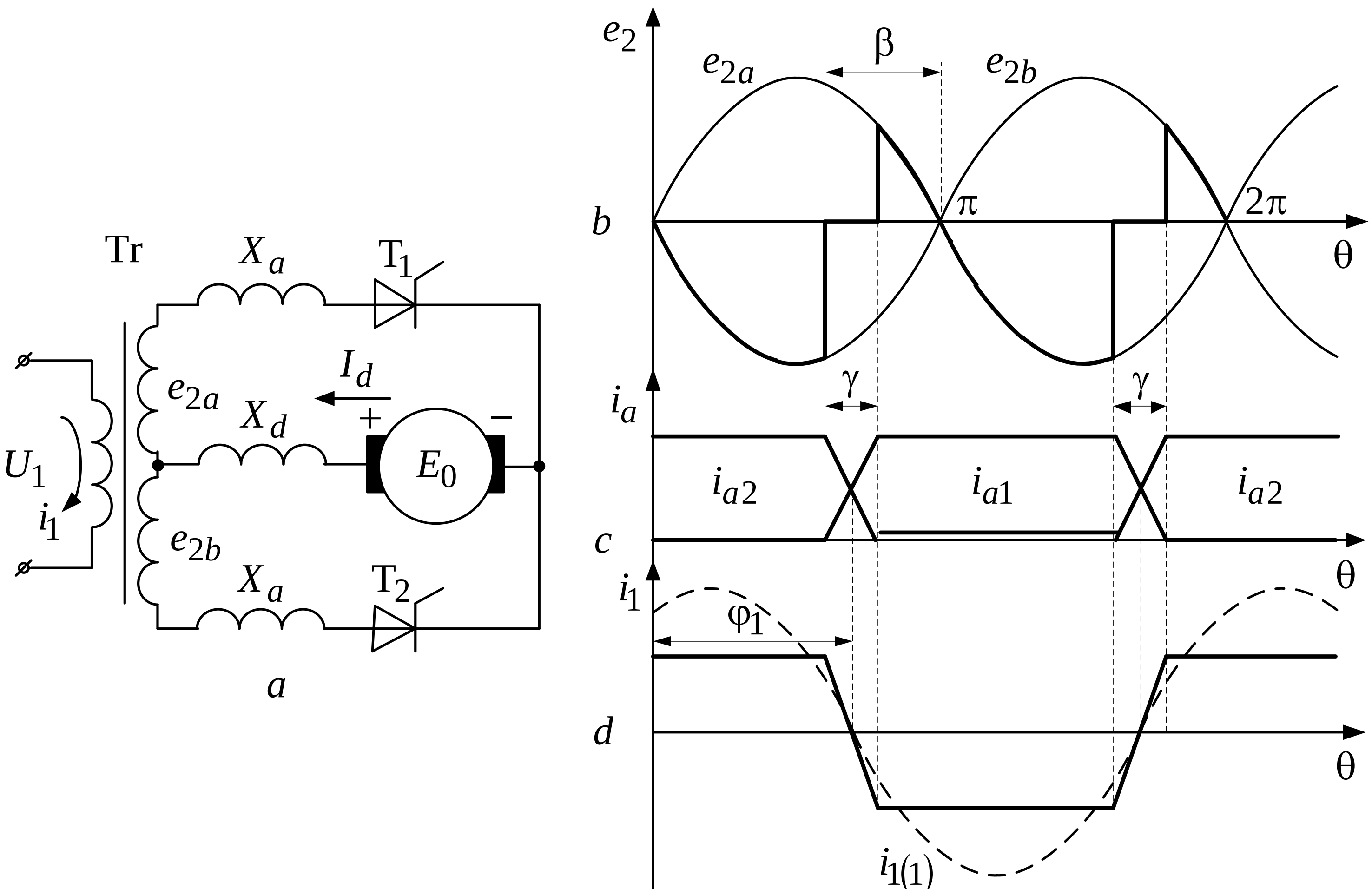

Fig. 4.8. Determination of the shear angle between the primary current and voltage of the mains supply of full-wave dependent inverter

The phase shift φ_1 between the current $i_{1(1)}$ and mains supply voltage U_1 equals to:

$$\varphi_1 = \pi - \beta + \frac{\gamma}{2}, \quad (4.19)$$

and therefore, the dependent inverter is the reactive power consumer:

$$Q_{inv} = U_1 I_{1(1)} \sin\phi_1 \quad (4.20)$$

Total power factor is defined as:

$$\chi = \frac{P_{\text{inv}}}{S} = \nu \cos \phi_1 \text{ (4.21)}$$

where $P_{\text{inv}} = U_1 I_{1(1)} \cos \phi_1$ – the active power of inverter, which is equal to the converted power of DC power source $P_d = E_0 I_d$.

Distortion factor $\nu = \dfrac{I_{1(1)}}{I_1}$ is defined the same way as in the rectifier circuits by the presence of higher harmonic components in the current of the primary winding of the transformer.

Autonomous inverters

Autonomous inverters, unlike dependent inverters do not need AC mains supply in the process of energy conversion.

By the character of the electromagnetic processes autonomous inverters are divided into current inverters, voltage inverters and resonant inverters, inverter voltage and the resonant inverter.

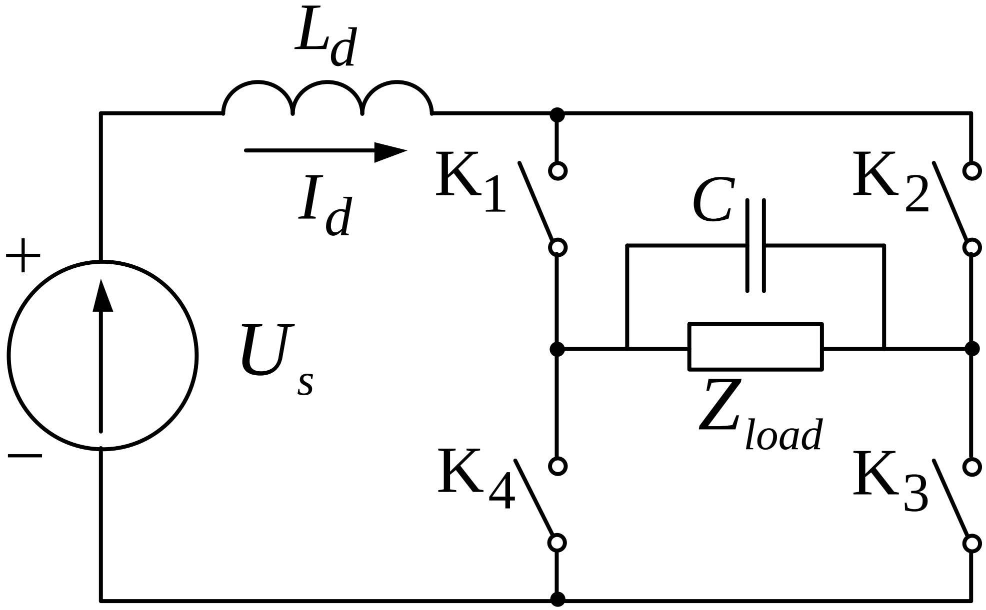

a

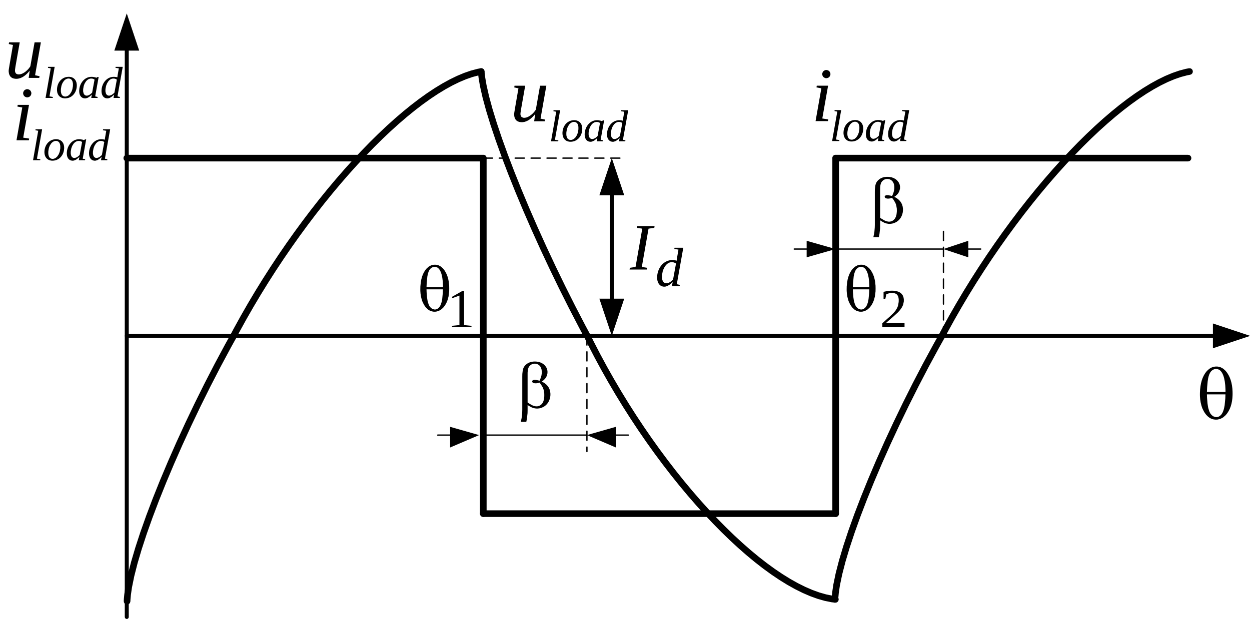

b

Fig. 4.9. Autonomous current inverter

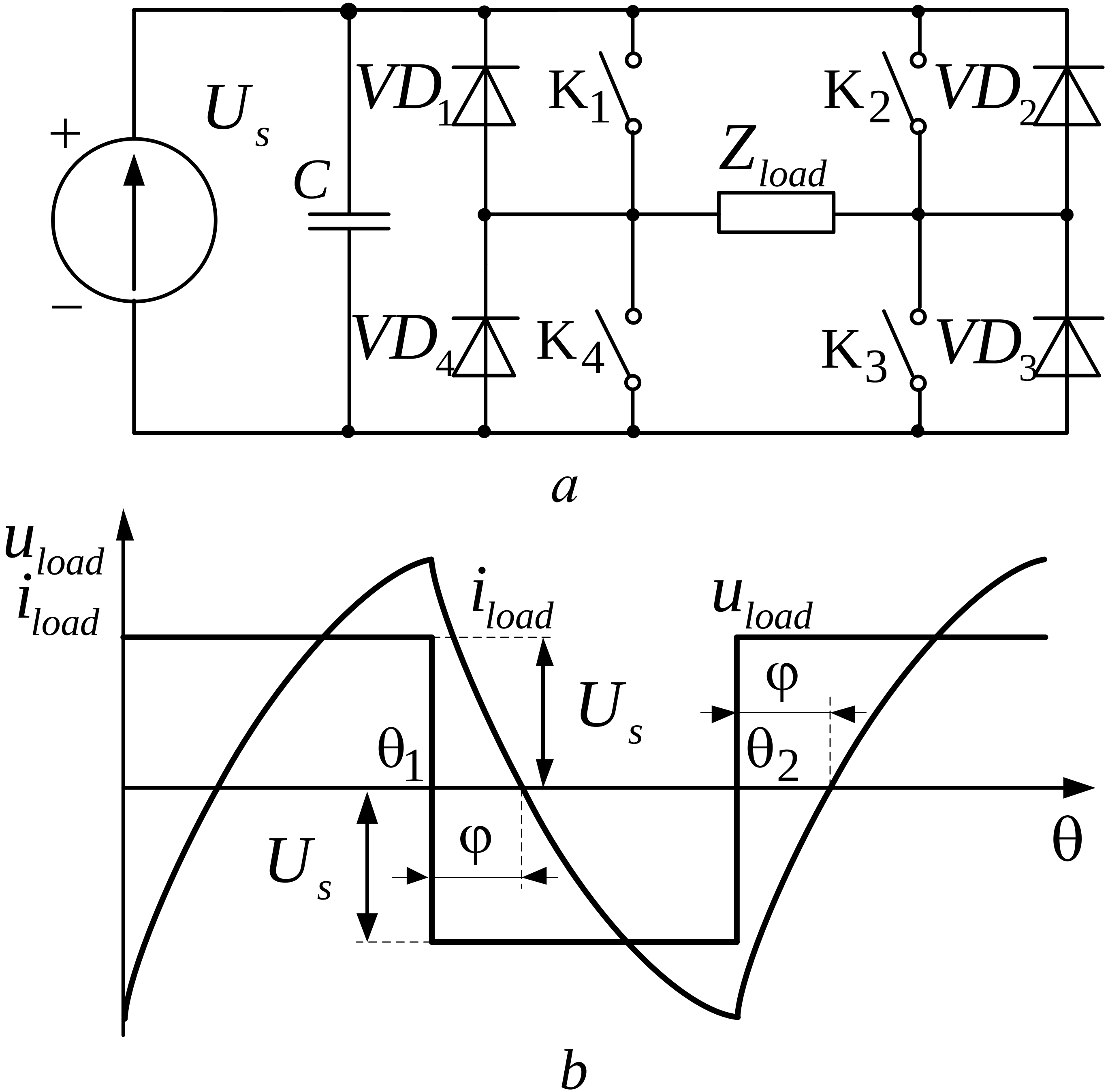

Fig. 4.10. Autonomous voltage inverter

In the resonant inverters the load is incorporated into the oscillating circuit tuned to a certain frequency, whereby the currents and voltages are close to sinusoidal. Sometimes, for oscillations of high frequency acquisition several inverters are combined into one circuit (multi-cell inverters).

In all types of autonomous inverters full-controlled switches are commonly used (transistors, GTO-thyristors). The valves with partial controllability may also be used (SCR-thyristors) is they are supplied by additional device – switching node capable to switch the thyristor off at any time.

Current inverters

The total character of the load circuit of the current inverter must be capacitive.

This fact often dictates the choice of power thyristors as the switches, since in this case the capacitor, as a part of the load circuit, is used to commutate them. Depending on the way of the capacitor connection in the load circuit parallel, serial and serial-parallel current inverters are distinguished.

Parallel current inverters

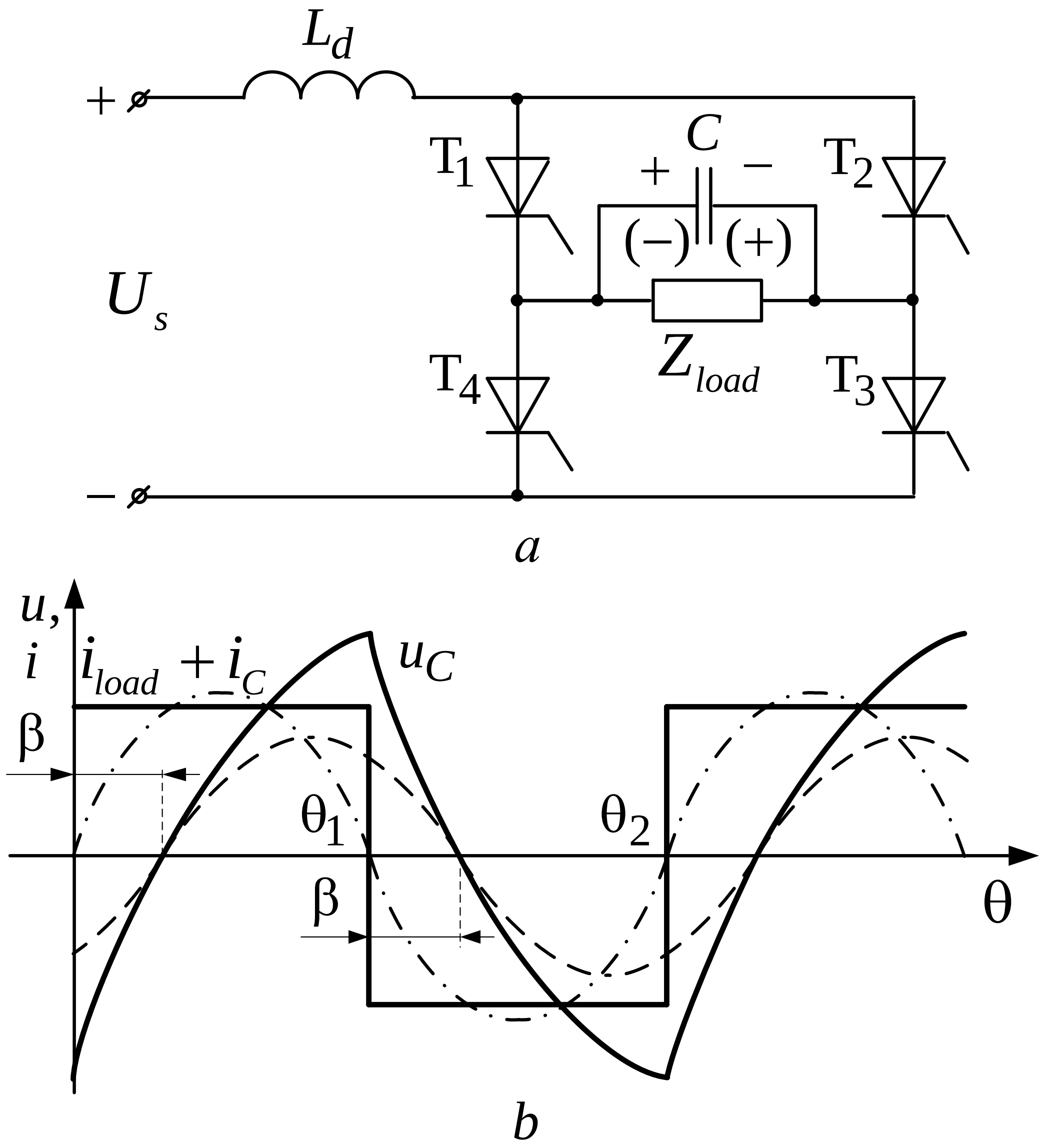

Fig. 4.11. Parallel current inverter

In order to restore the control properties of thyristors the next requirement must be met:

$$\beta \geq \beta_{\min} = \omega t_{off} \qquad (4.22)$$

where $\omega = 2 \cdot \pi \cdot f$,

$f = \dfrac{1}{T}$ – the output frequency

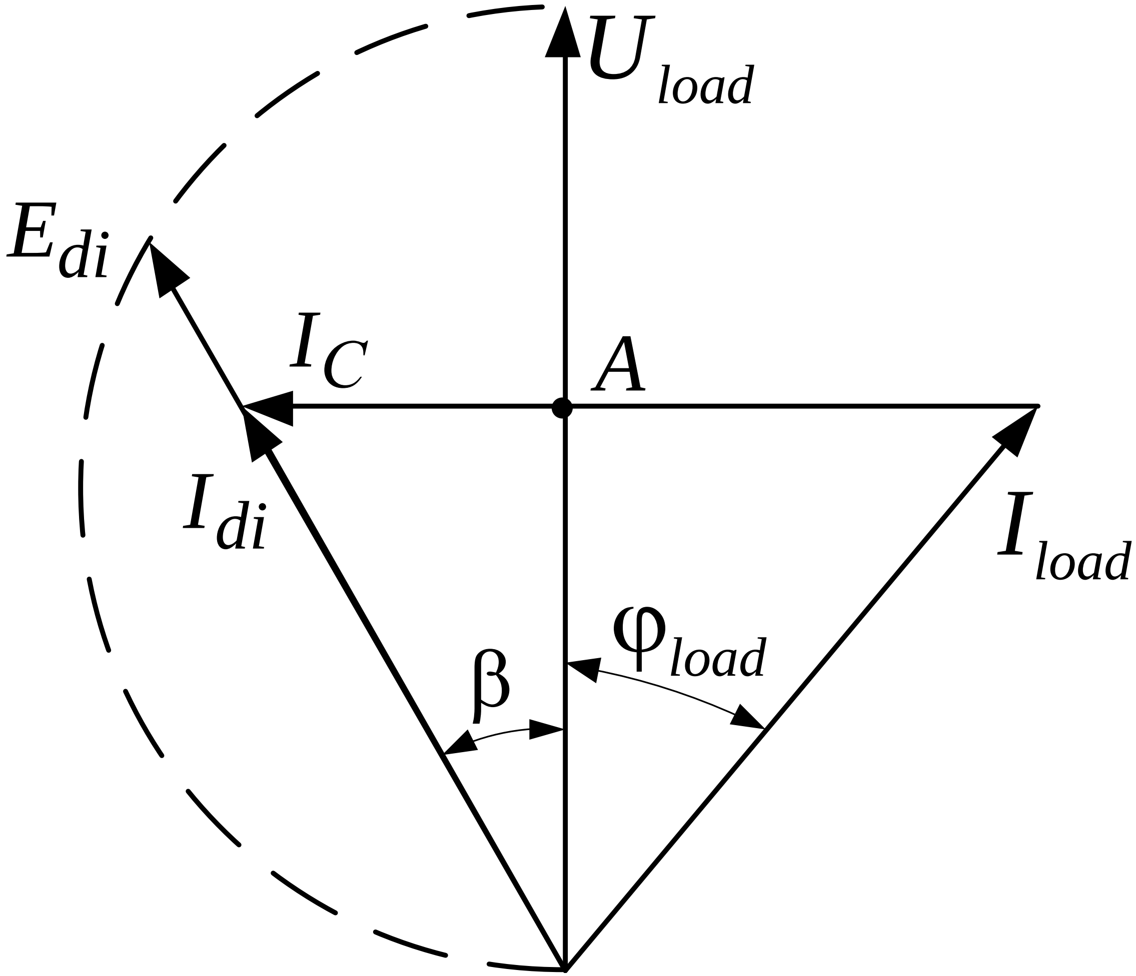

Fig. 4.12. Vector diagram of the parallel current inverter

The following considerations are accepted:

1. Equivalent AC power source generates only active power $P_{inv} = E_{di} I_{di} = U_d I_d$ as well as real power source. For this reason, these vectors coincide with each other in phase.

2. The dependence between the voltages E_{di} and U_s the real source is established on the basis of the theory of rectifiers $E_d = k_{cir} \cdot E_2$

In our case, E_2 is replaced by E_{di}, E_d – by U_s.

Hence $E_{di} = \dfrac{U_s}{k_{cir}}$ (4.23)

From Fig. 4.12 we find:

$$I_{load} \cdot \cos\varphi_{load} = I_{di} \cdot \cos\beta$$

$$E_{di} \cdot I_{di} = U_{load} \cdot I_{load} \cdot \cos\varphi_{load} = U_{load} \cdot I_{di} \cdot \cos\beta$$

$$E_{di} = U_{load} \cdot \cos\beta \quad (4.24)$$

$$\frac{Q_{inv}}{P_{inv}} = \mathrm{tg}\,\beta \qquad (4.25)$$

$$Q_{inv} = U_{load}^2 \cdot \omega \cdot C - U_{load} \cdot I_{load} \cdot \sin\varphi_{load};$$
$$P_{inv} = U_{load} \cdot I_{load} \cdot \cos\varphi_{load};$$

$$\operatorname{tg}\beta = \frac{U_{load}^2 \cdot \omega \cdot C - U_{load} \cdot I_{load} \cdot \sin\varphi_{load}}{U_{load} \cdot I_{load} \cdot \cos\varphi_{load}} = \qquad (4.26)$$
$$= \frac{Y_{load}^*}{Y_{load}^* \cdot \cos\varphi_{load}} - \operatorname{tg}\varphi_{load}$$

where $Y_{load}^* = \dfrac{Y_{load}}{\omega \cdot C}$, $Y_{load} = \dfrac{1}{Z_{load}}$

From (4.26) we obtain the dependence

$\beta = f\left(Y_{load}^*\right)$ in Fig. 4.13.

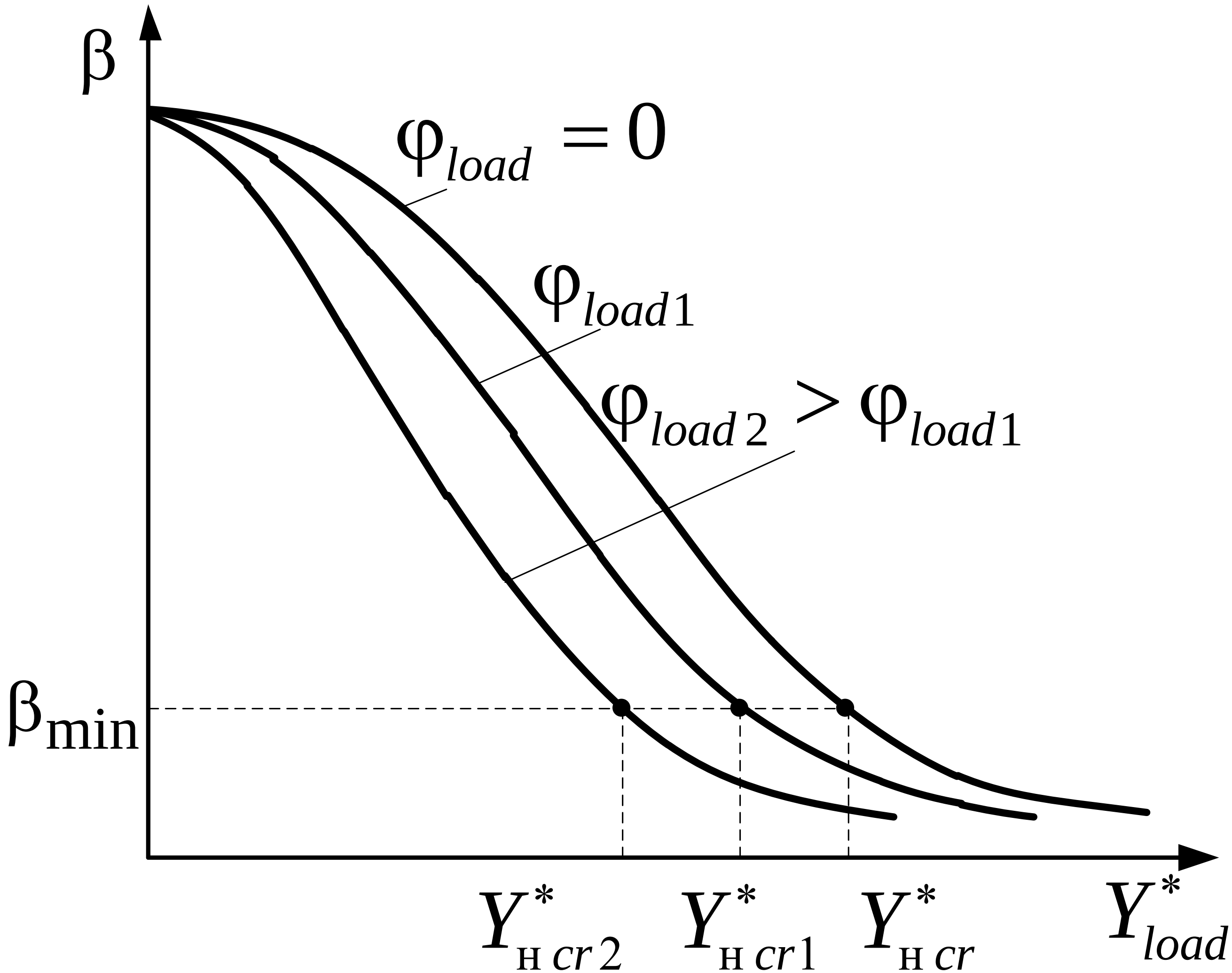

Fig. 4.13. Stability characteristic of parallel current inverter

From (4.24), the load voltage

$$U_{load} = \frac{E_{di}}{\cos\beta} = \frac{U_s}{k_{cir}\cos\beta}$$

Given that $\cos\beta = \dfrac{1}{\sqrt{1+\mathrm{tg}^2\beta}}$, then

$$\frac{U_{load}}{U_s} = \frac{1}{k_{cir}}\sqrt{1+\left(\frac{1}{Y^*_{load}\cdot\cos\varphi_{load}} - \mathrm{tg}\,\varphi_{load}\right)^2} \quad (4.27)$$

The expression (4.27) is the equation of the parallel inverter external characteristic (Fig. 4.14).

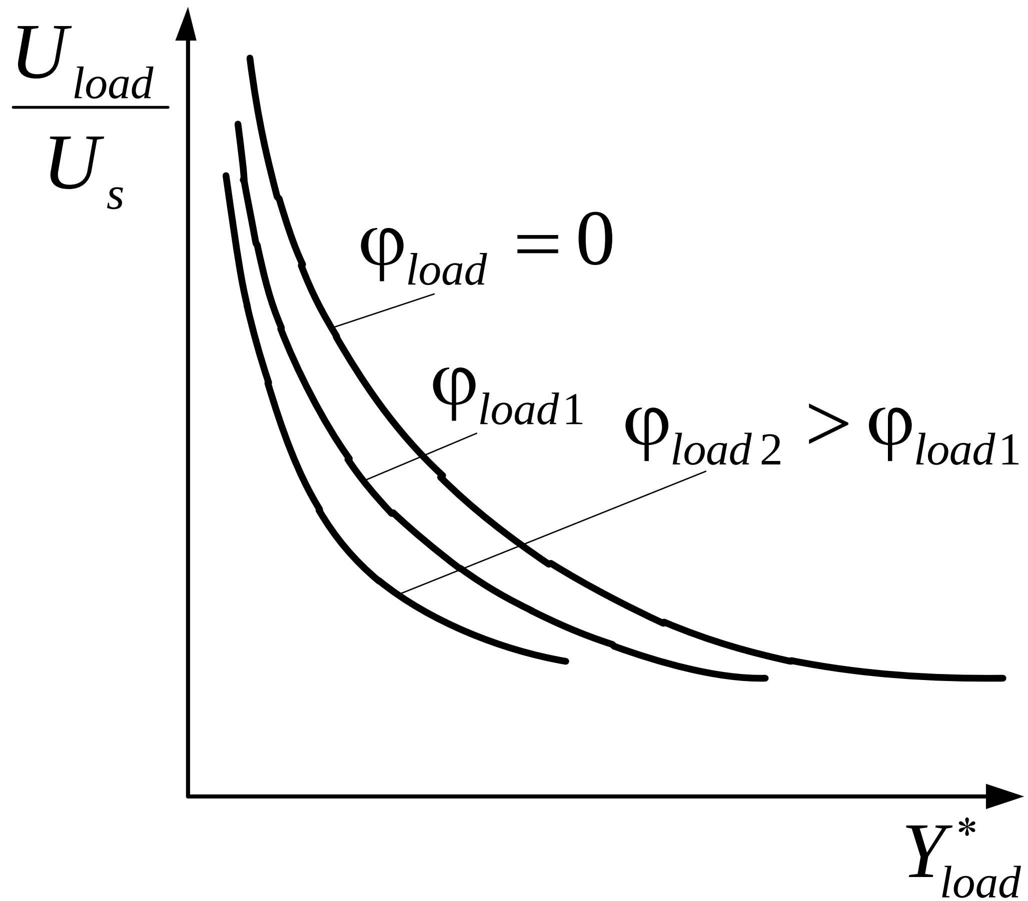

Fig. 4.14. External characteristic of parallel current inverter

The equation of the input characteristic of the inverter:

$$\frac{I_d}{\omega \cdot C \cdot U_s} = \frac{\pi^2}{8}\left[1+\left(\frac{1}{Y^*_{load} \cdot \cos\phi_{load}} - \text{tg}\,\varphi_{load}\right)^2\right] Y^*_{load}\cos\varphi_{load} \quad (4.28)$$

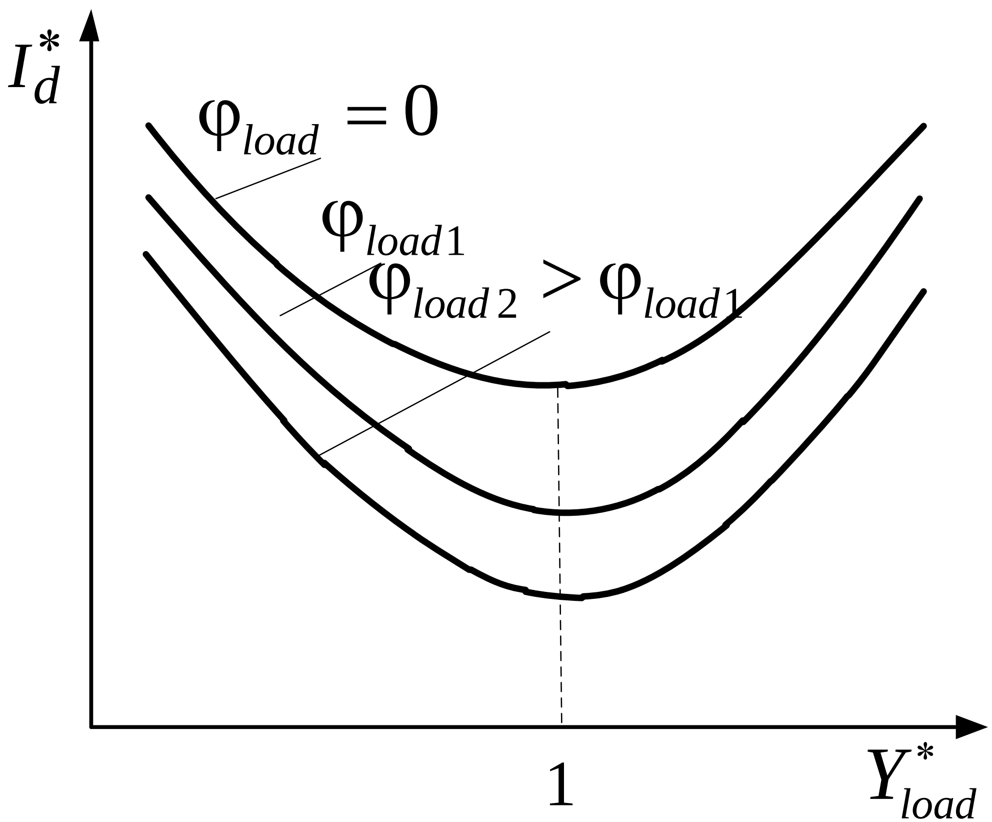

Fig. 4.15. Input characteristics of the parallel current inverter

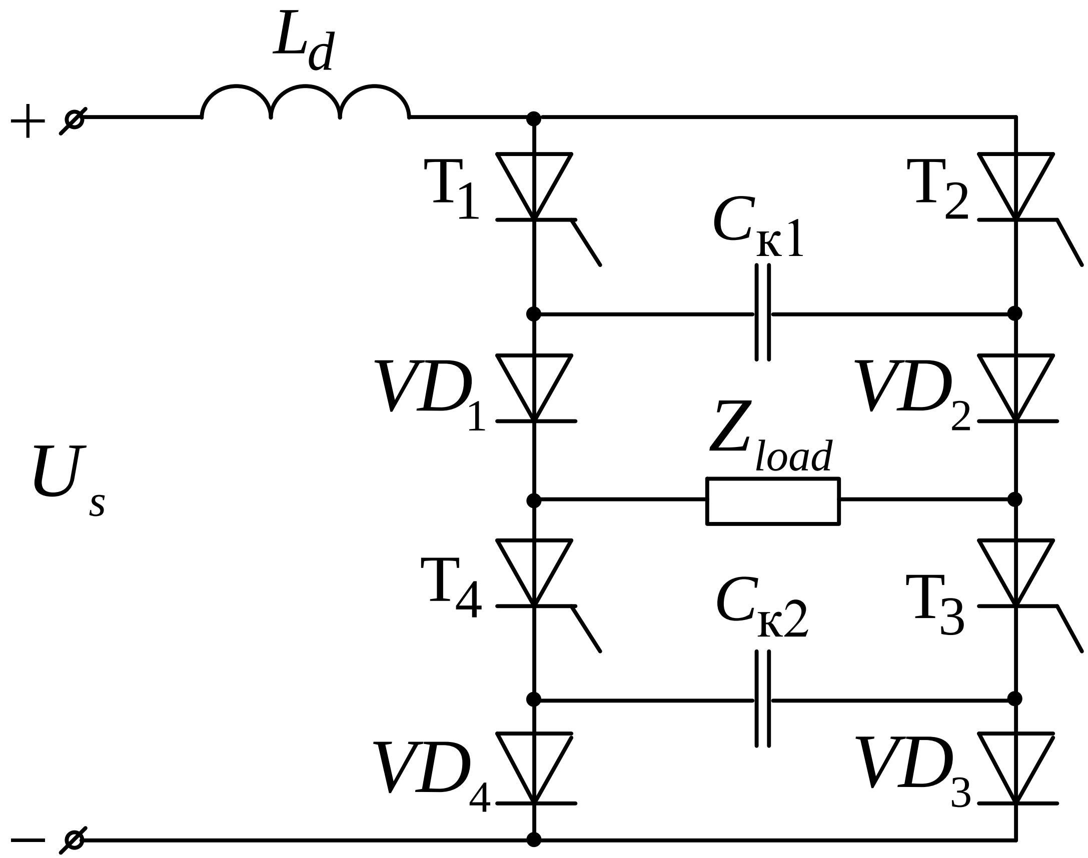

Fig. 4.16. Single-phase bridge inverter with pick-off valves

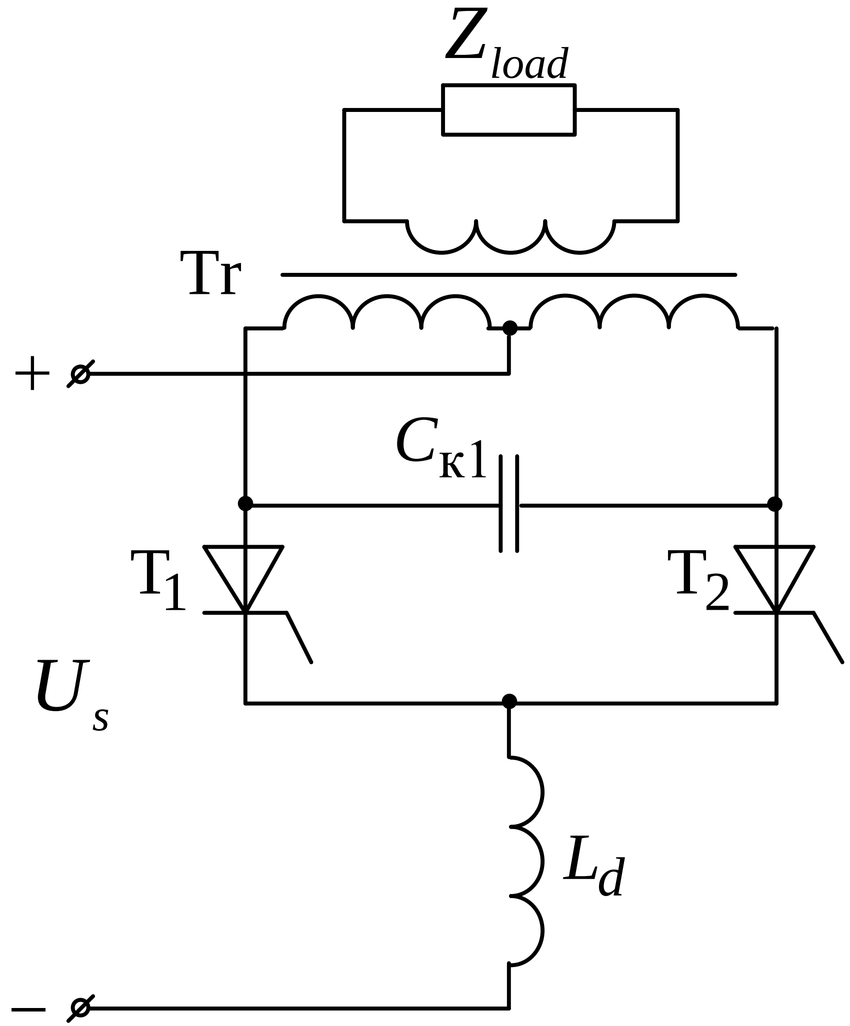

Fig. 4.17. Single-phase parallel current inverter with a midpoint

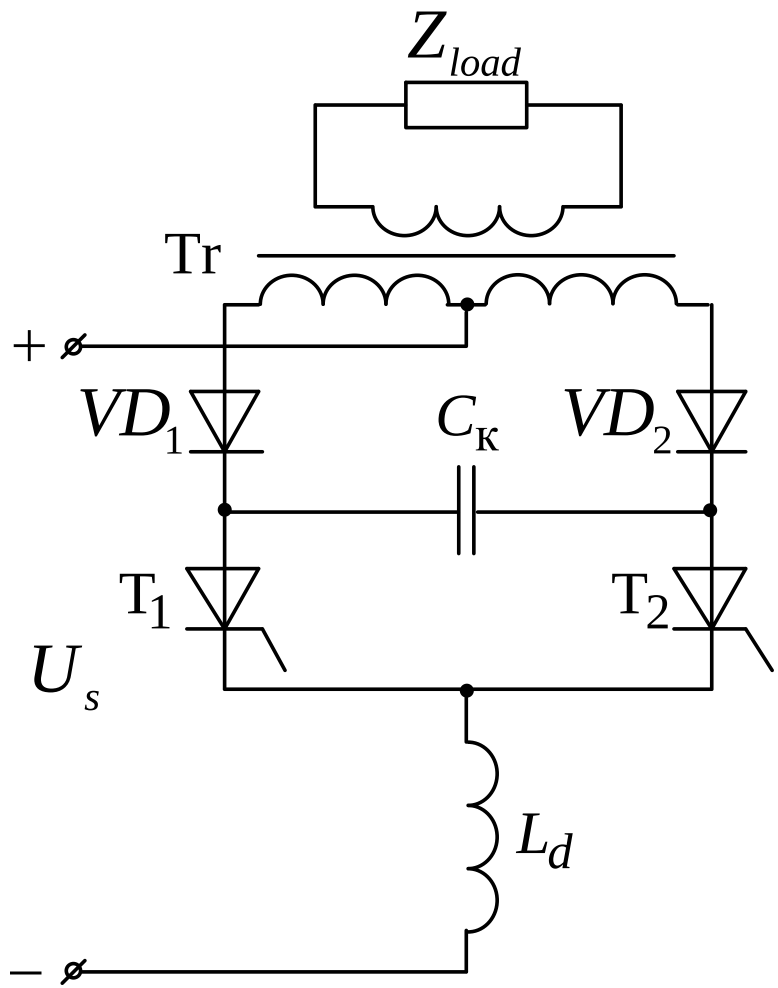

Fig. 4.18. Single-phase inverter with midpoint and pick-off valves

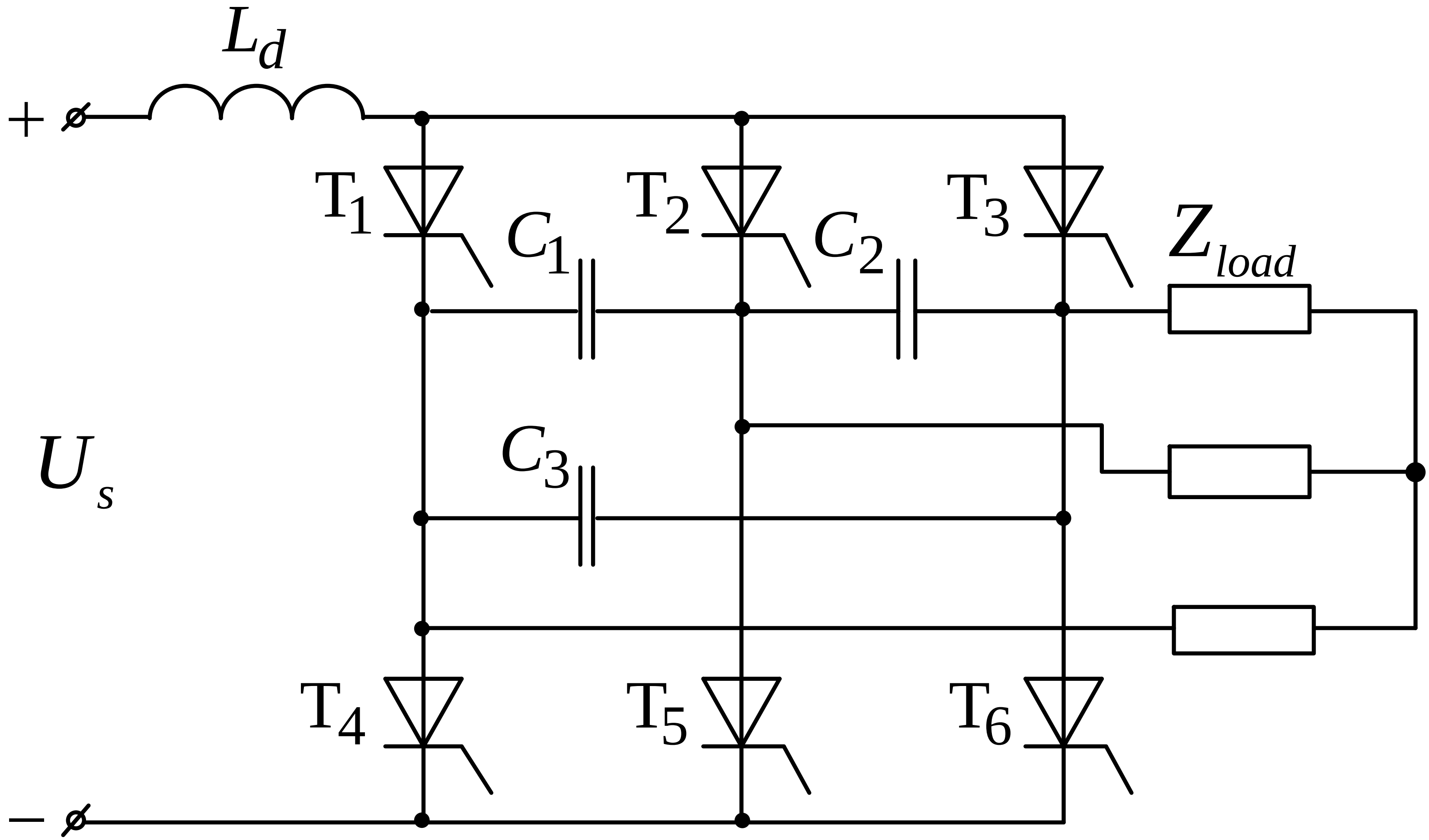

Fig. 4.19. Three-phase bridge current inverter

Series current inverters

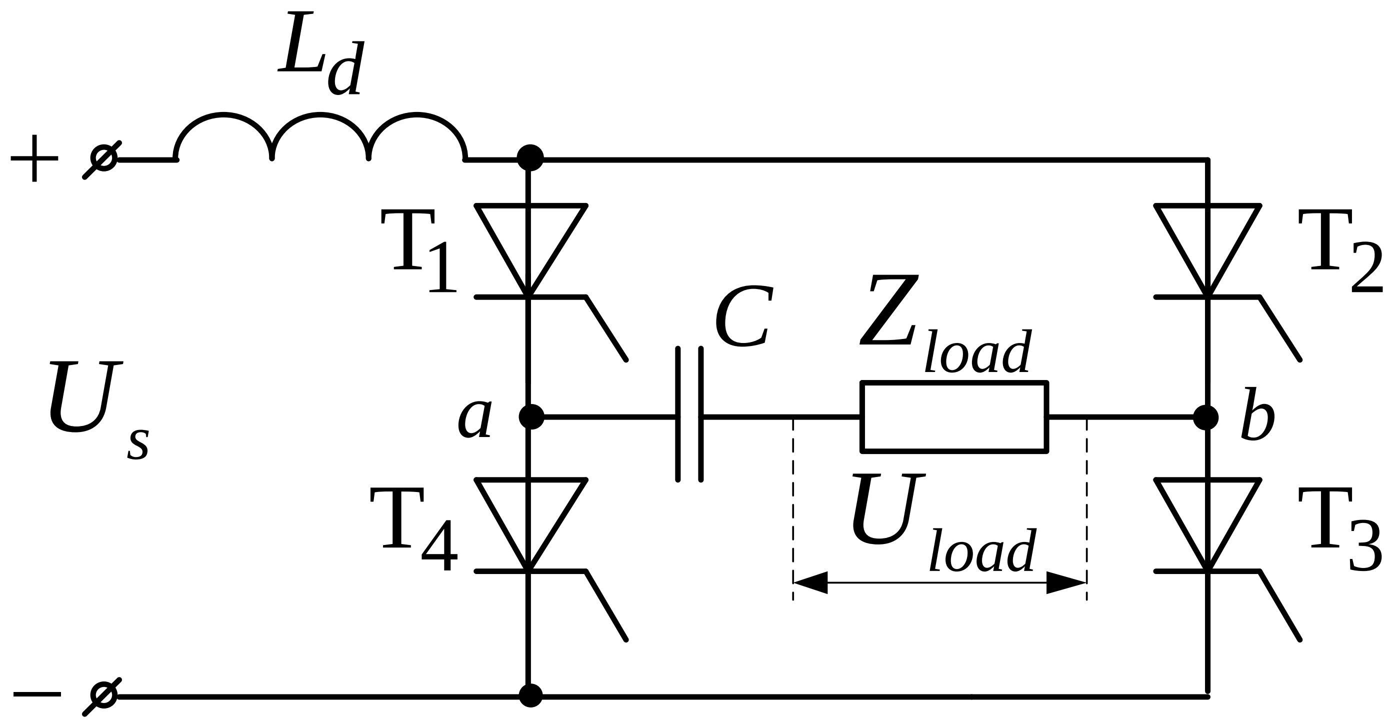

Fig. 4.20. Series current inverter

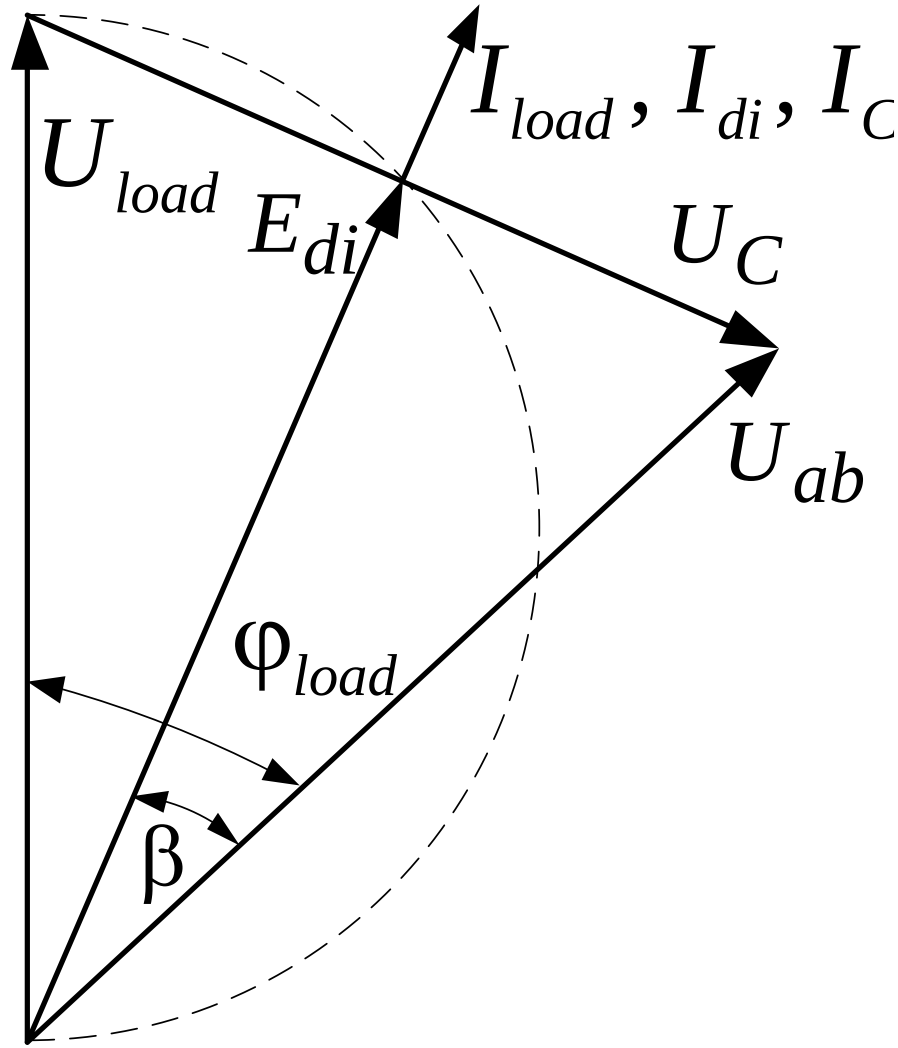

Fig. 4.21. Vector diagram of series current inverter

When replacing the real source of power by the equivalent AC power source the equality is valid:

$$E_{di} \cdot I_{di} = U_{load} \cdot I_{load} \cdot \cos\varphi_{load}$$

Since $I_{load} = I_{di}$ then $E_{di} = U_{load} \cdot \cos\varphi_{load}$ (4.29)

i.e. equivalent source EMF is equal to the voltage drop on the active resistance of the load.

From expression (4.29) it follows that

$$U_{н} = \frac{E_{di}}{\cos\varphi_{load}} = \frac{U_s}{k_{cir}\cos\varphi_{load}} \qquad (4.30)$$

The expression (4.25) for series inverter, taking into account that $I_{load} = I_C$, has the following form:

$$\mathrm{tg}\,\beta = \frac{Q_C}{P_{inv}} = \frac{I_C^2 \cdot \frac{1}{\omega \cdot C} - U_{load} \cdot I_{load} \cdot \sin\varphi_{load}}{U_{load} \cdot I_{load} \cdot \cos\varphi_{load}} = \qquad (4.31)$$

$$= \frac{I_{load}^2}{\omega \cdot C \cdot U_{load} \cdot I_{load} \cdot \cos\varphi_{load}} - \mathrm{tg}\,\varphi_{load} = \frac{Y_{load}^*}{\cos\varphi_{load}} - \mathrm{tg}\,\varphi_{load},$$

where $Y_{load}^* = \dfrac{Y_{load}}{\omega \cdot C}, Y_{load} = \dfrac{1}{Z_{load}} = \dfrac{I_{load}}{U_{load}}$

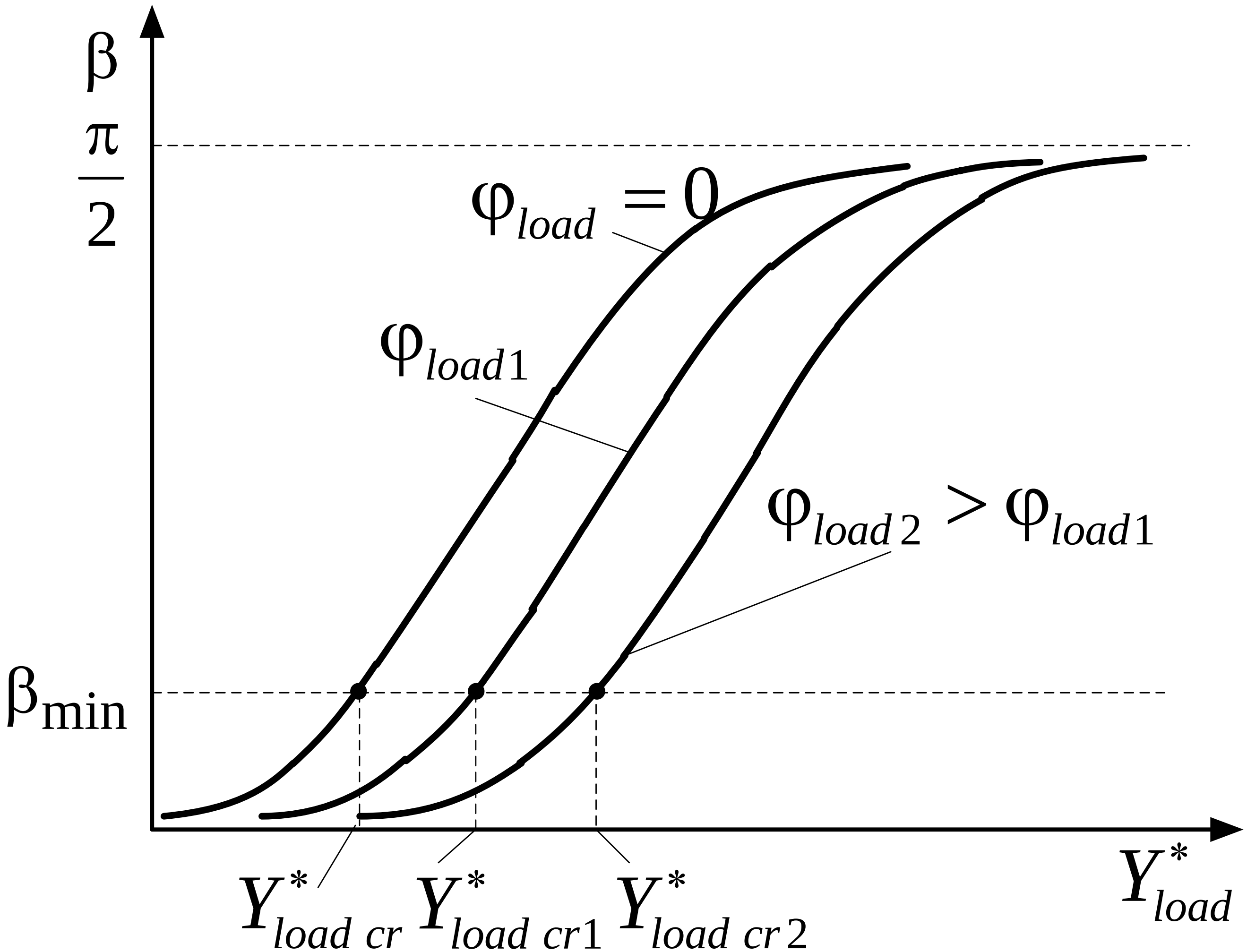

Fig. 4.22. Stability characteristic of the series current inverter

For single-phase or bridge inverter circuit

$$\frac{U_{load}}{U_s} = \frac{\pi}{2\sqrt{2} \cdot \cos\varphi_{load}} \qquad (4.32)$$

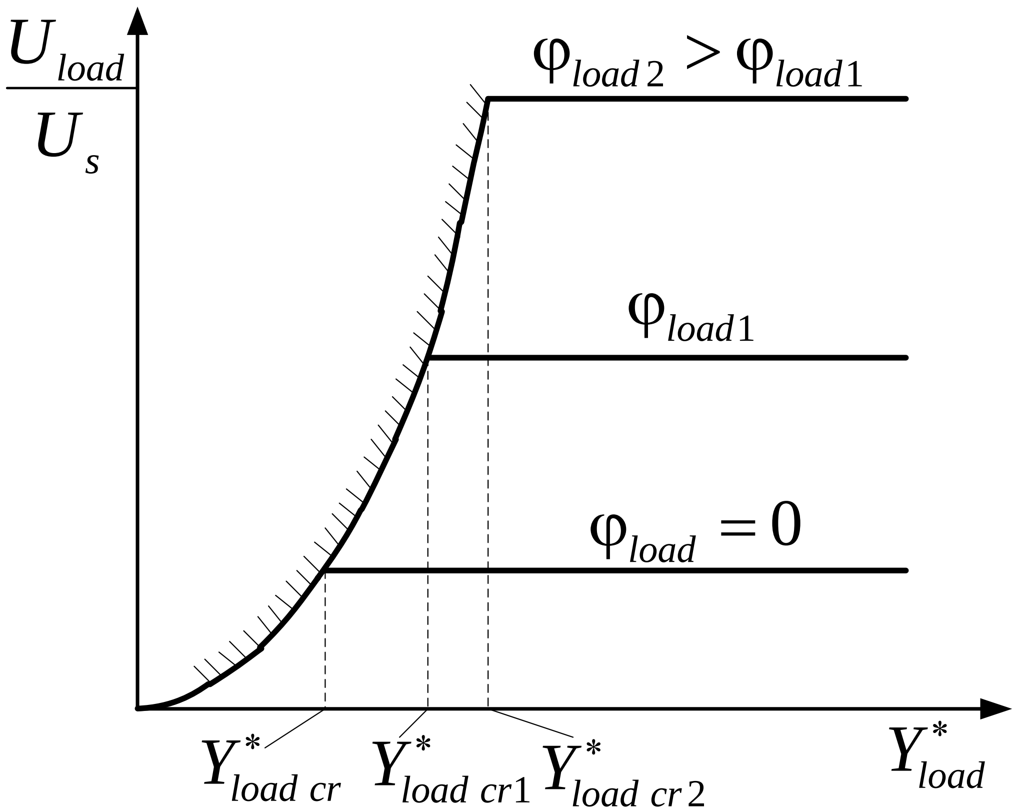

Fig. 4.23. External characteristic of the series current inverter

Series-parallel current inverters

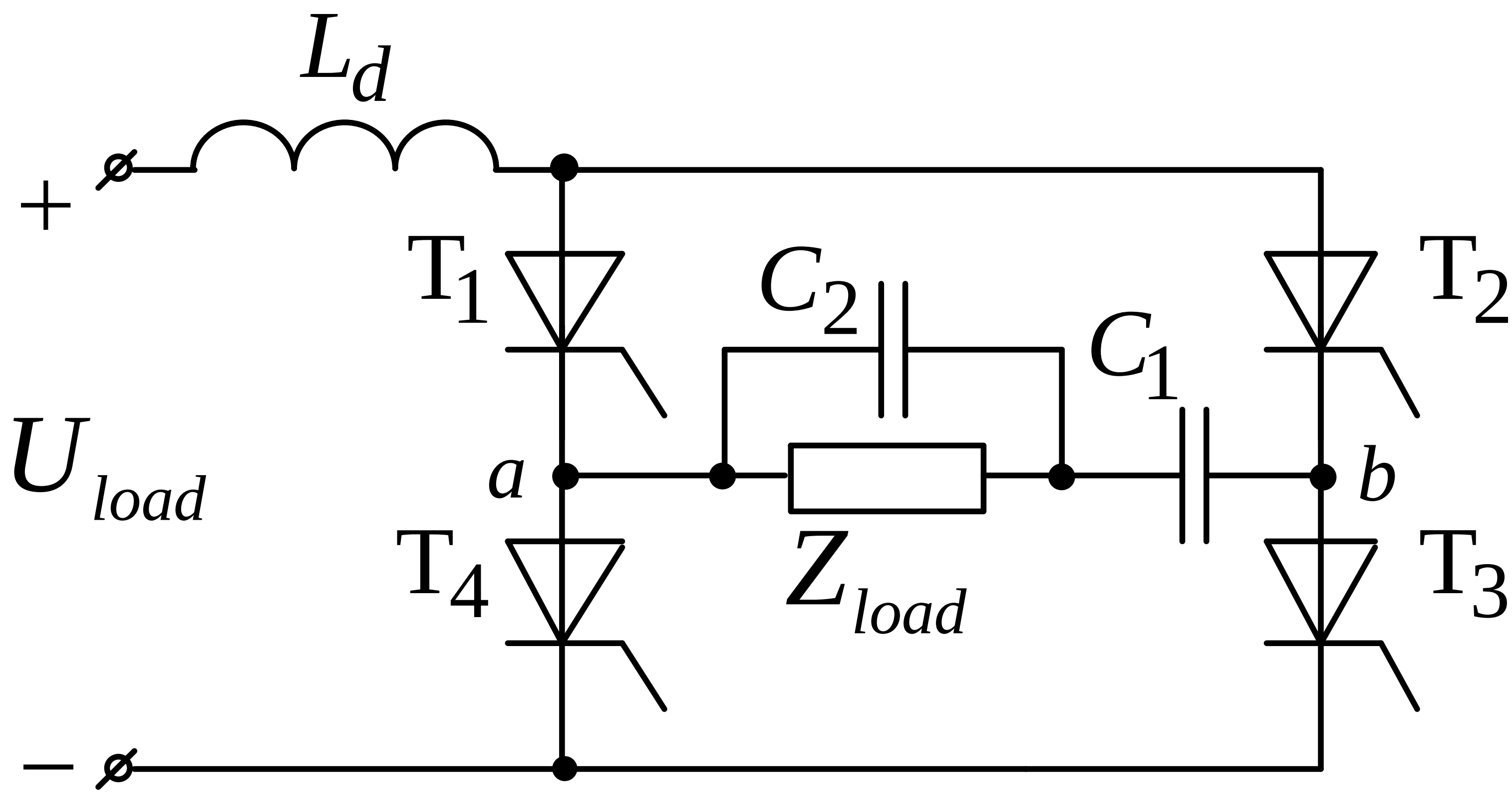

Fig. 4.24. Series-parallel current inverter

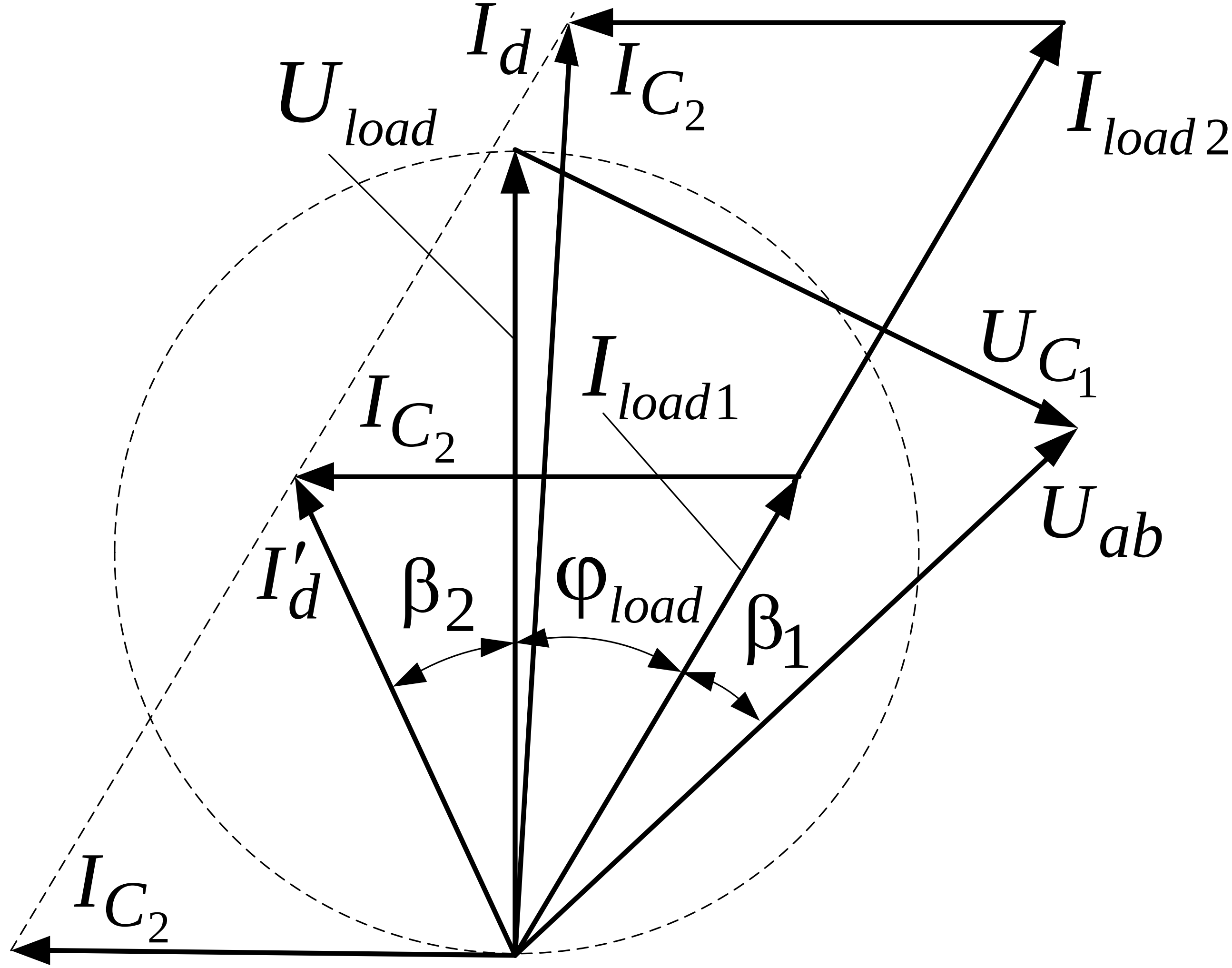

Fig. 4.25. Vector diagram of series-parallel current inverter

Power ratio in a series-parallel inverter is determined by the expression:

$$\operatorname{tg}\beta = \frac{Q_{inv}}{P_{inv}} = \frac{1}{\cos\varphi_{load}} \cdot \left[\frac{Y_{load}}{\omega C_1} + \left(1 + \frac{C_2}{C_1}\right) \cdot \frac{\omega \cdot C_2}{Y_{load}} - \left(1 + 2 \cdot \frac{C_2}{C_1}\right) \cdot \sin\varphi_{load} \right] \quad (4.33)$$

This implies that the angle β will grow at low loads and at high loads it will have a minimum defined by the ratio C_2/C_1 at average loads.

Resonant inverters

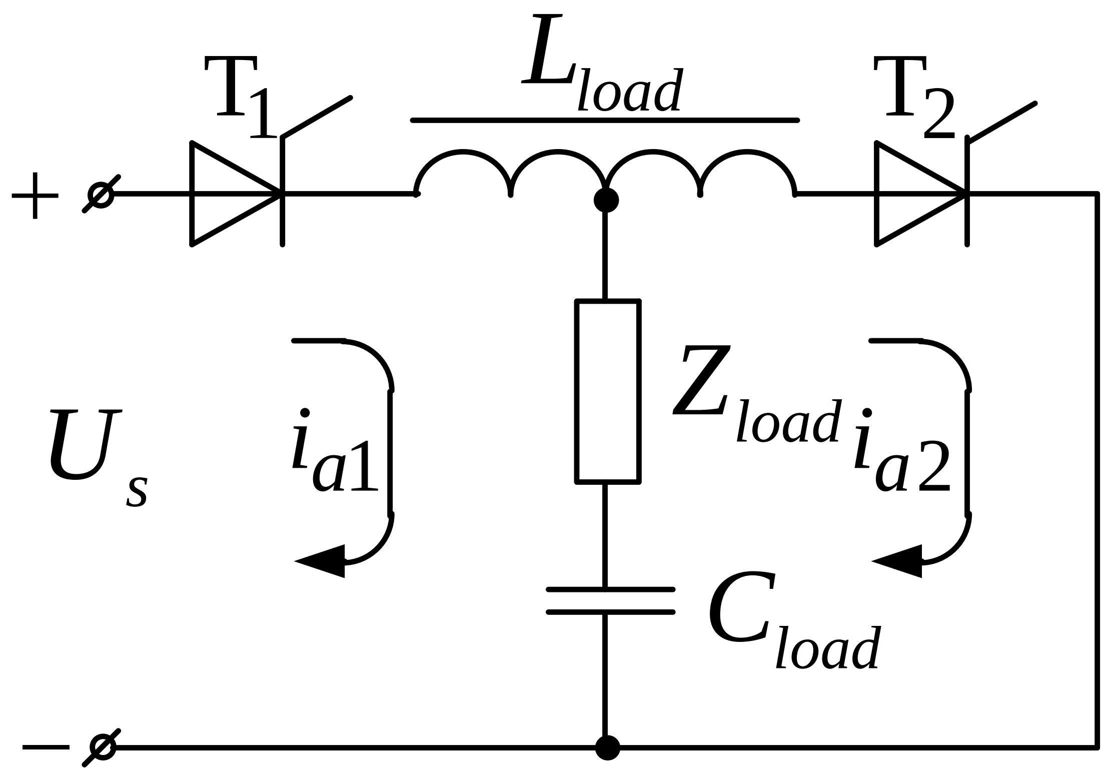

Fig. 4.26. Half-bridge resonant current inverter circuit

Depending on the frequency ω of thyristor switching there are three modes (Fig. 4.27)

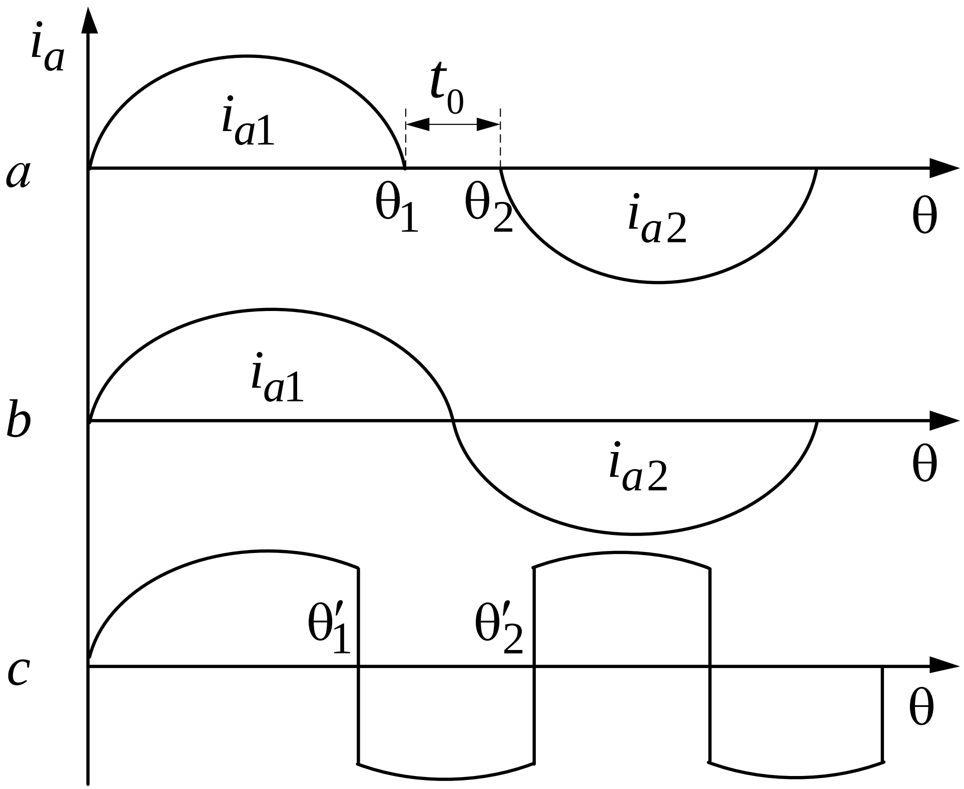

1. Discontinuous current mode, when $\omega < \omega_0$

2. Boundary-continuous mode, when $\omega = \omega_0$

3. Continuous current mode, when $\omega > \omega_0$

Fig. 4.27. Operating modes of half-bridge resonant current inverter circuit

There are many variants of the resonant inverter circuits, each of which has its own distinctive features, advantages and drawbacks. But there is one feature of the resonant inverters, providing them broad application prospects in various fields of engineering.

Voltage inverters

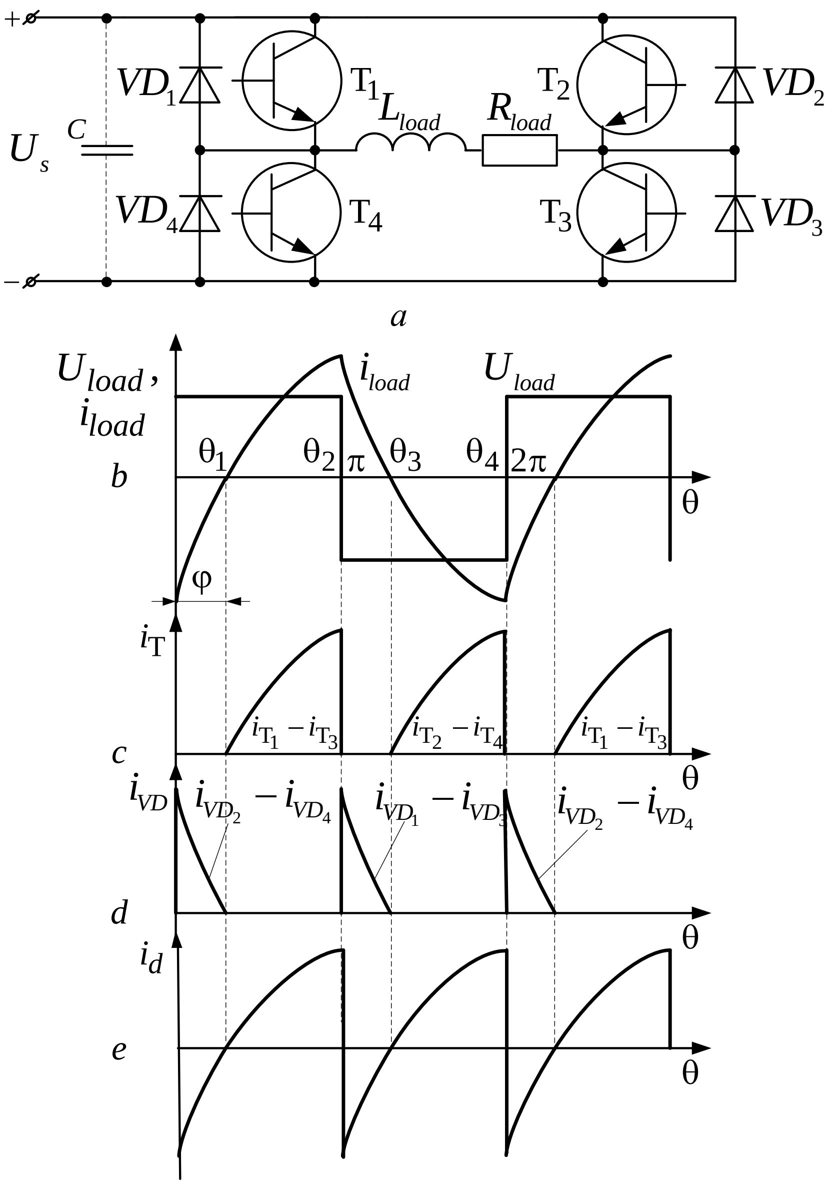

Fig. 4.28. Single-phase voltage inverter

The differential equation for the interval $\theta_1 \ldots \theta_3$ provided that all the power circuit and source components are ideal is as follows:

$$X_{load} \frac{\mathrm{d}i_{load}}{\mathrm{d}\theta} + i_{load} \cdot R_{load} = \pm U_s \qquad (4.34)$$

where $+U_s$ corresponds to the interval $\theta_1 \ldots \theta_2$, and $-U_s$ – to the interval $\theta_2 \ldots \theta_3$.

Solving the equation (4.34) with respect to the current i_{load}, taking into account that $-i_{load}\Big|_{\theta=0} = +i_{load}\Big|_{\theta=\pi}$, we obtain:

$$i_{load} = \pm\frac{U_s}{R_{load}}\left(1-\frac{2e^{\left(-\theta R_{load}/X_{load}\right)}}{1+e^{\left(-\pi R_{load}/X_{load}\right)}}\right) \qquad (4.35)$$

The maximum power valves current value:

$$i_{load\,\max} = i_{load}\Big|_{\theta=0} = \frac{U_s}{R_{load}}\left(1 - \frac{2}{1 - e^{\left(-\pi R_{load}/X_{load}\right)}}\right)$$

From the condition $i_{load}\Big|_{\theta=\varphi} = 0$ we find

φ – the moment of current i_{load} transition through zero:

$$\varphi = \ln\left(\frac{2}{1 + e^{\left(-\pi R_{load}/X_{load}\right)}}\right)\frac{X_{load}}{R_{load}} \qquad (4.36)$$

The average current for the main valves of the inverter

$$I_{\mathrm{T}} = \frac{1}{2\pi}\int_{\varphi_{\mathrm{H}}}^{\pi} i_{load}\,\mathrm{d}\theta = \frac{U_s\cdot(\pi-\varphi)}{2\pi\cdot R_{load}} + $$

$$+\frac{U_s\cdot X_{load}\cdot\left(e^{\left(-\pi R_{load}/X_{load}\right)} - e^{\left(-\varphi R_{load}/X_{load}\right)}\right)}{\pi R_{load}^2\cdot\left(1+e^{\left(-\varphi R_{load}/X_{load}\right)}\right)} \qquad (4.37)$$

For the reverse diodes:

$$I_{VD} = \frac{1}{2\pi} \int_{0}^{\varphi_{load}} i_{\text{H}} d\theta = \frac{U_s \cdot \varphi_{load}}{2\pi \cdot R_{load}} + \\ + \frac{U_s \cdot X_{load} \cdot \left(e^{\left(-\varphi R_{load} / X_{load} \right)} - 1 \right)}{\pi \cdot R_{\text{H}}^2 \cdot \left(1 + e^{\left(-\pi R_{load} / X_{load} \right)} \right)} \qquad (4.38)$$

Average current value of power supply

$$I_d = \frac{1}{\pi}\int_0^{\pi} i_{load}\,\mathrm{d}\theta = 2(I_{\mathrm{T}} + I_{VD}) =$$

$$= \frac{U_s}{R_{load}}\left[1 + \frac{2\cdot\left(e^{\left(-\pi R_{load}/X_{load}\right)} - 1\right)}{\frac{R_{load}}{X_{load}}\cdot\pi\cdot\left(1 + e^{\left(-\pi R_{load}/X_{load}\right)}\right)}\right] \qquad (4.39)$$

Active load power equals to the power consumed from the power supply:

$$P_{load} = U_s \cdot I_d = \frac{U_s^2}{R_{load}} \left[1 + \frac{2X_{load} \cdot \left(e^{\left(-\pi R_{load} / X_{load} \right)} - 1 \right)}{\pi \cdot R_{load} \left(1 + e^{\left(-\pi R_{load} / X_{load} \right)} \right)} \right] \quad (4.40)$$

Total load power is defined as

$$S_{load} = U_{load} \cdot I_{load}$$

where I_{load} – the RMS value of the load current.

RMS value of the load current:

$$I_{load} = \sqrt{\frac{1}{2\pi}\int_0^{2\pi} i_{load}^2 \mathrm{d}\theta} = \frac{U_s}{R_{load}}\sqrt{1+\frac{2X_{load}\cdot\left(e^{\left(-\pi R_{load}/X_{load}\right)}-1\right)}{\pi\cdot R_{\mathrm{H}}\left(e^{\left(-\pi R_{load}/X_{load}\right)}+1\right)}} \quad (4.41)$$

Since $U_{load} = U_s$ then

$$S_{load} = \frac{U_s^2}{R_{load}}\sqrt{1+\frac{2X_{load}\left(e^{\left(-\pi R_{load}/X_{load}\right)}-1\right)}{\pi R_{load}\left(e^{\left(-\pi R_{load}/X_{load}\right)}+1\right)}} \quad (4.42)$$

Total power factor

$$\chi = \frac{P_{load}}{S_{load}} = \sqrt{1 + \frac{2X_{load}\left(e^{\left(-\pi R_{load}/X_{load}\right)} - 1\right)}{R_{load}\pi\left(1 + e^{\left(-\pi R_{load}/X_{load}\right)}\right)}} \quad (4.43)$$

From the principle of the voltage inverter it follows that its output voltage does not depend on the load and, consequently, the external characteristic is rigid.

Pulse-width modulation (PWM)

PWM principle lies in that the output voltage is formed by pulses of variable duration within the cycle modulated at a predetermined law, for example sinusoidal. This allows to reduce the higher order harmonic components values.

The ways of PWM signal generation are divided into five kinds, two of which are widely used in the power converters: the first PWM techniques and the second one.

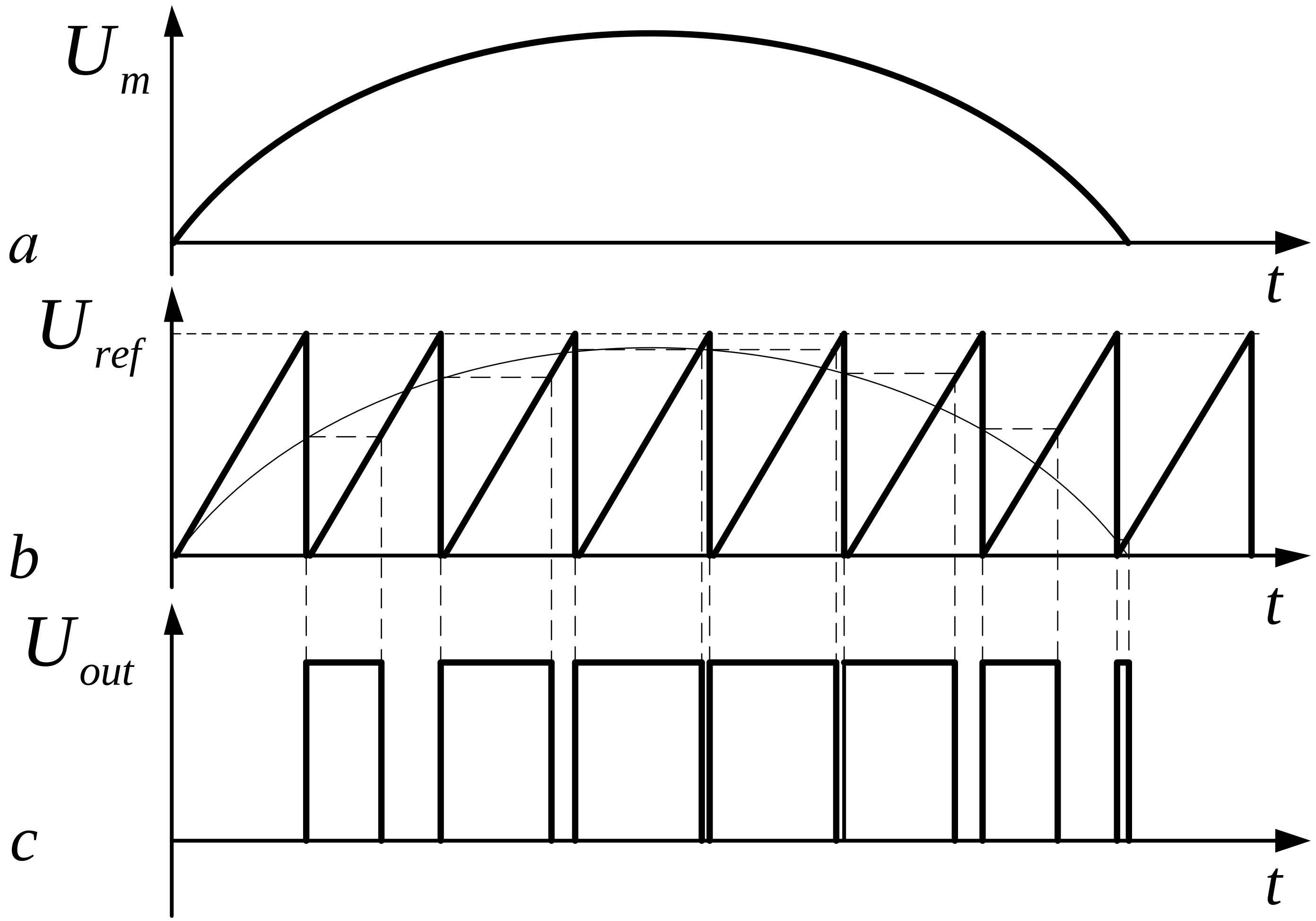

Fig. 4.29. The first techniques of PWM

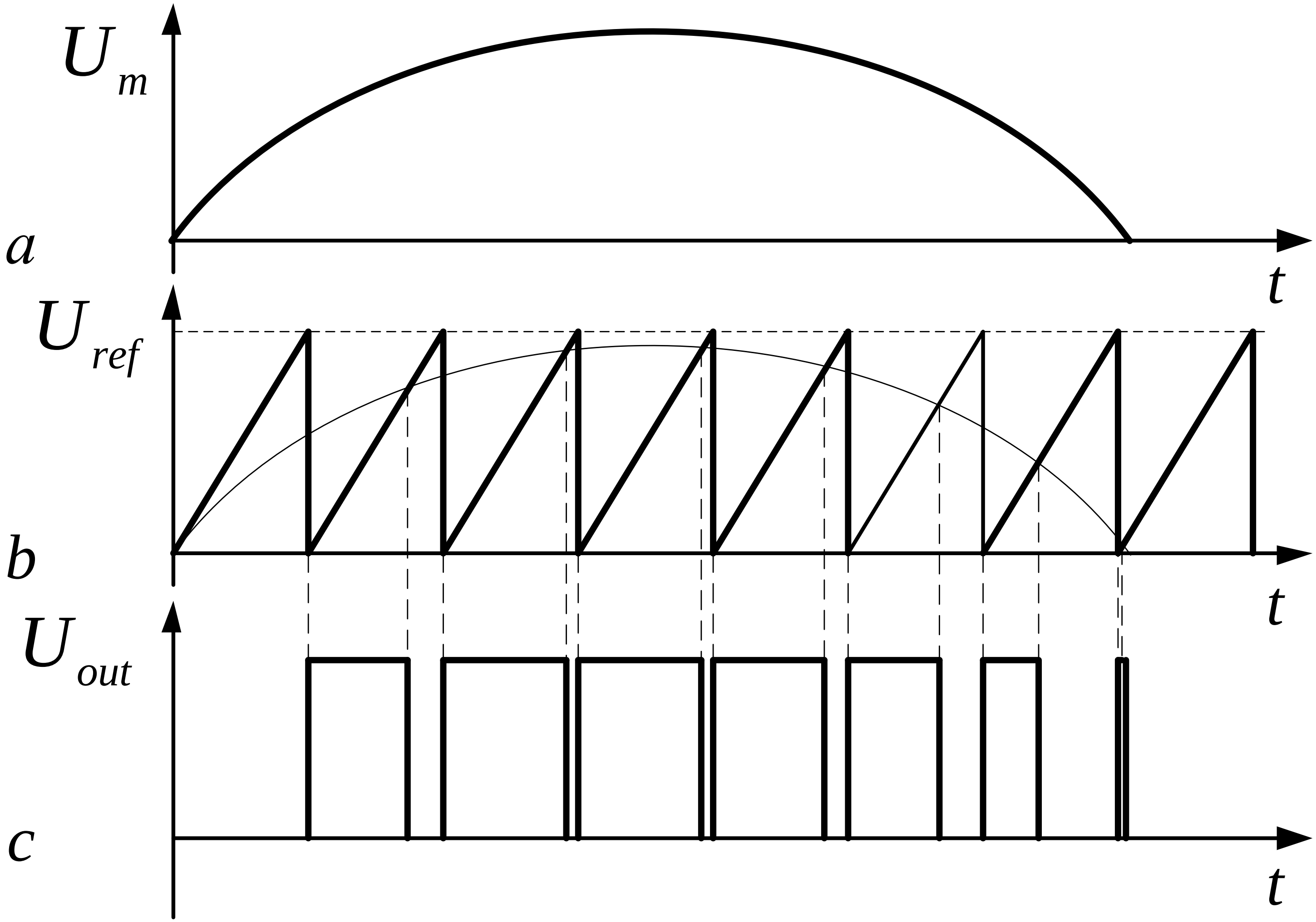

Fig. 4.30. The second techniques of PWM

When evaluating the non-sinusoidality of output voltage curves total harmonic distortion coefficient (TDH) is generally used:

$$TDH = \frac{\sqrt{\sum\limits_{k \to \infty} U_k^2}}{U_1} \qquad (4.44)$$

where U_k – the RMS value of the higher harmonic component with a sequence number k. Typically, for most electrical equipment components the requirements to TDH is set at the level of 5%.

Methods of regulating and stabilizing the autonomous inverter output voltage

There are three ways to regulate the output voltage of autonomous inverters:

1. By changing the voltage of the autonomous inverter power supply.
2. Voltage regulating based on the influence on the processes in the inverter which affect the output voltage.
3. Voltage regulation at the load by means of AC voltage stabilizers established between the load and the inverter.

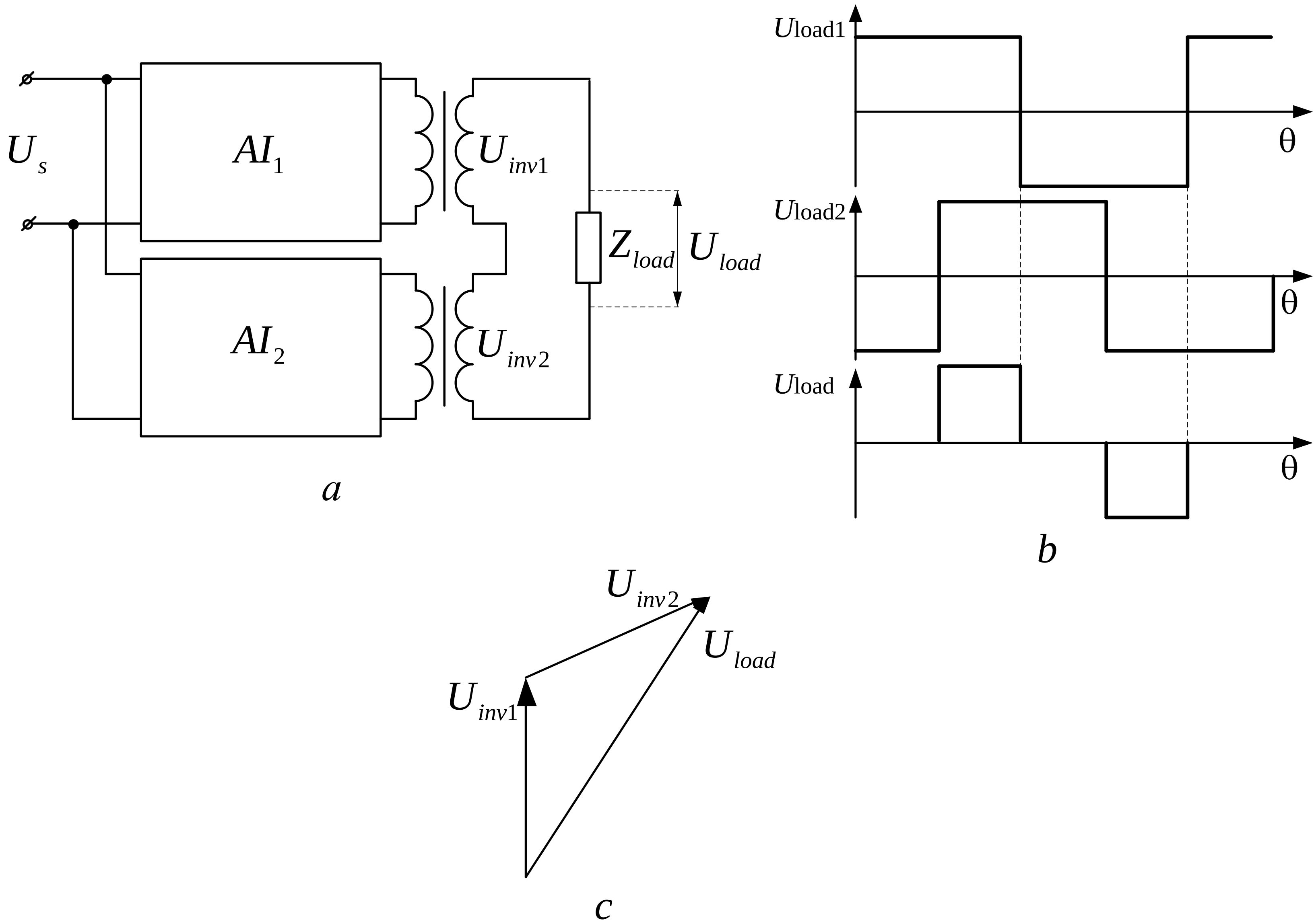

Fig. 4.31. The geometric sum of the voltages of the two inverters

FREQUENCY CONVERTERS

Frequency converters are the devices converting AC electric power of one frequency into AC electric power of another frequency.

Frequency converters are divided into two groups:

1. With DC link.
2. Without DC link or direct frequency converters.

Frequency converters with DC link

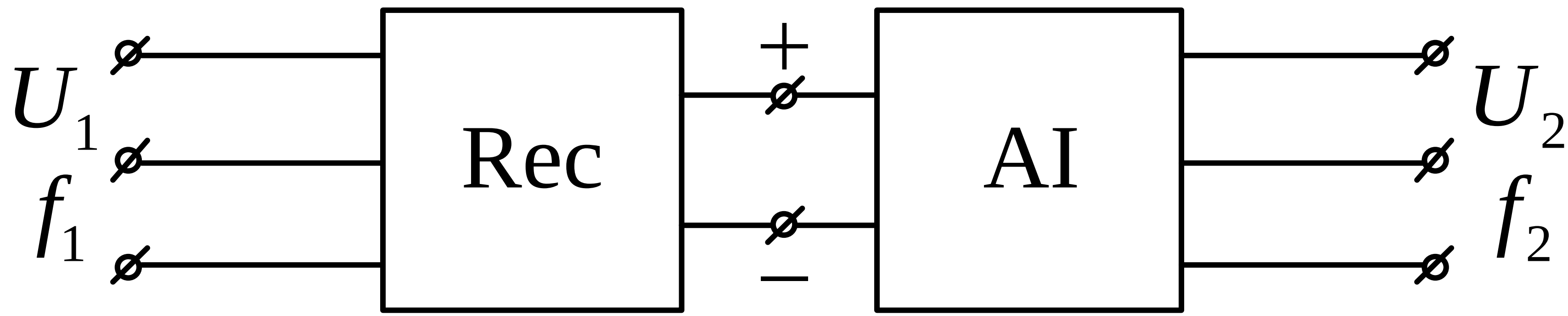

Fig. 5.1. Frequency converter with DC link

Converters of this class has all the features of autonomous inverters and rectifiers, already discussed above.

Direct frequency converters

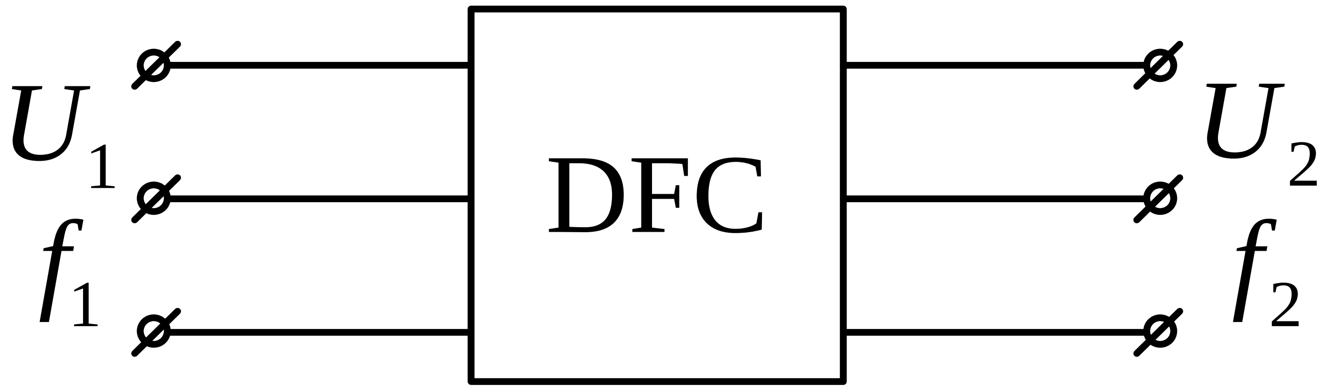

Fig. 5.2. Direct frequency converter

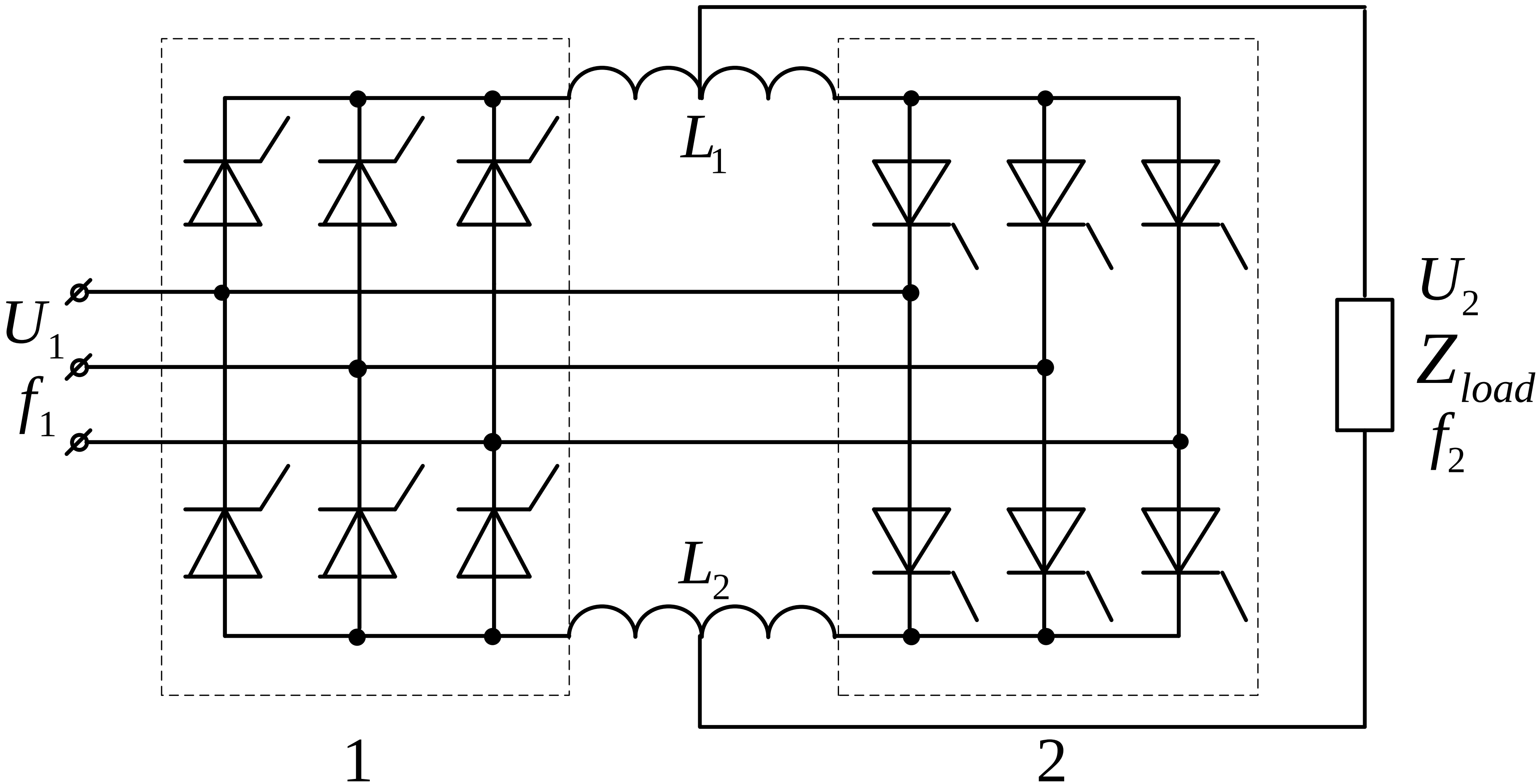

Fig. 5.3. Three-phase-single-phase direct frequency converter

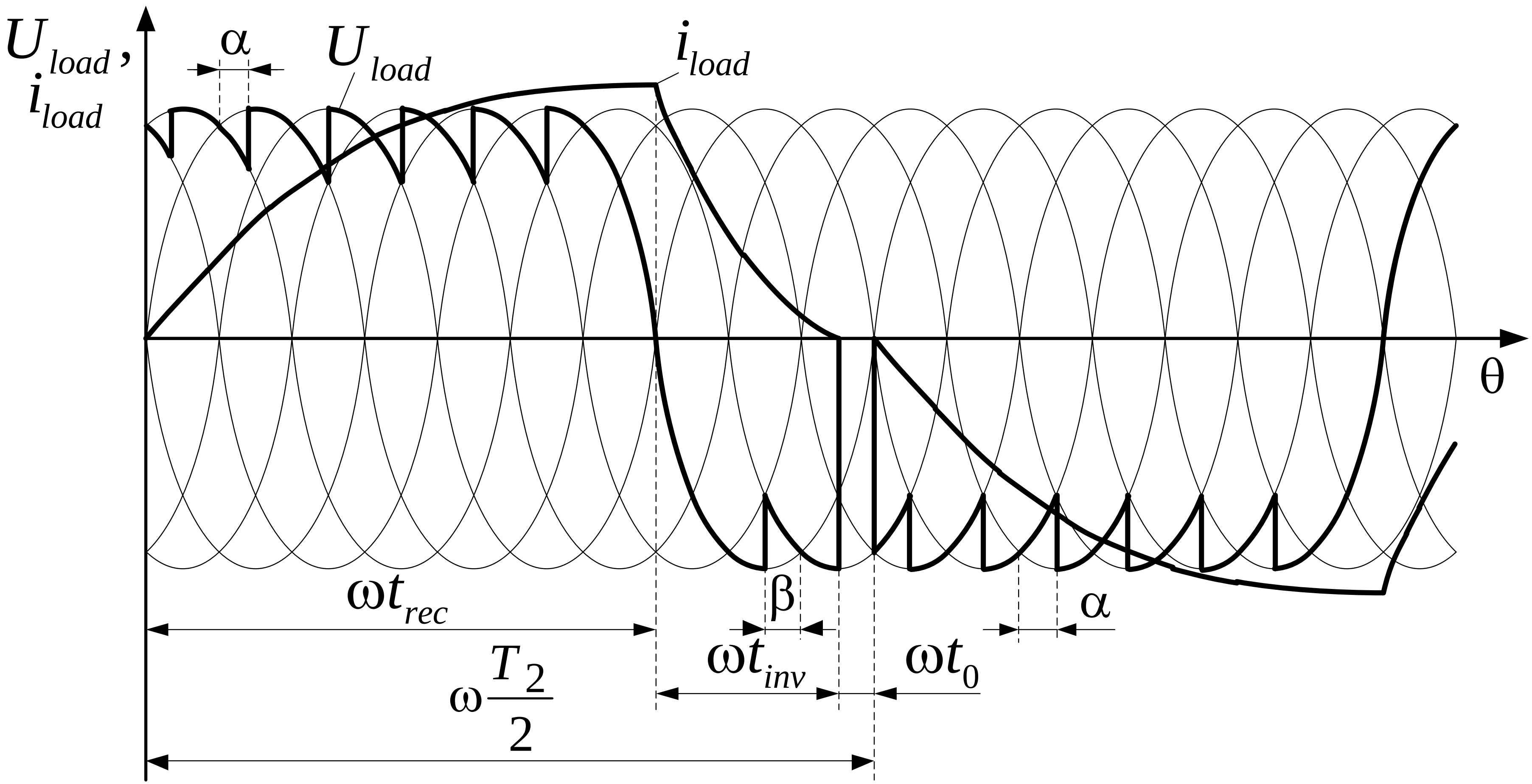

Fig. 5.4. Diagram explaining the operation of three-phase-single-phase direct frequency converter

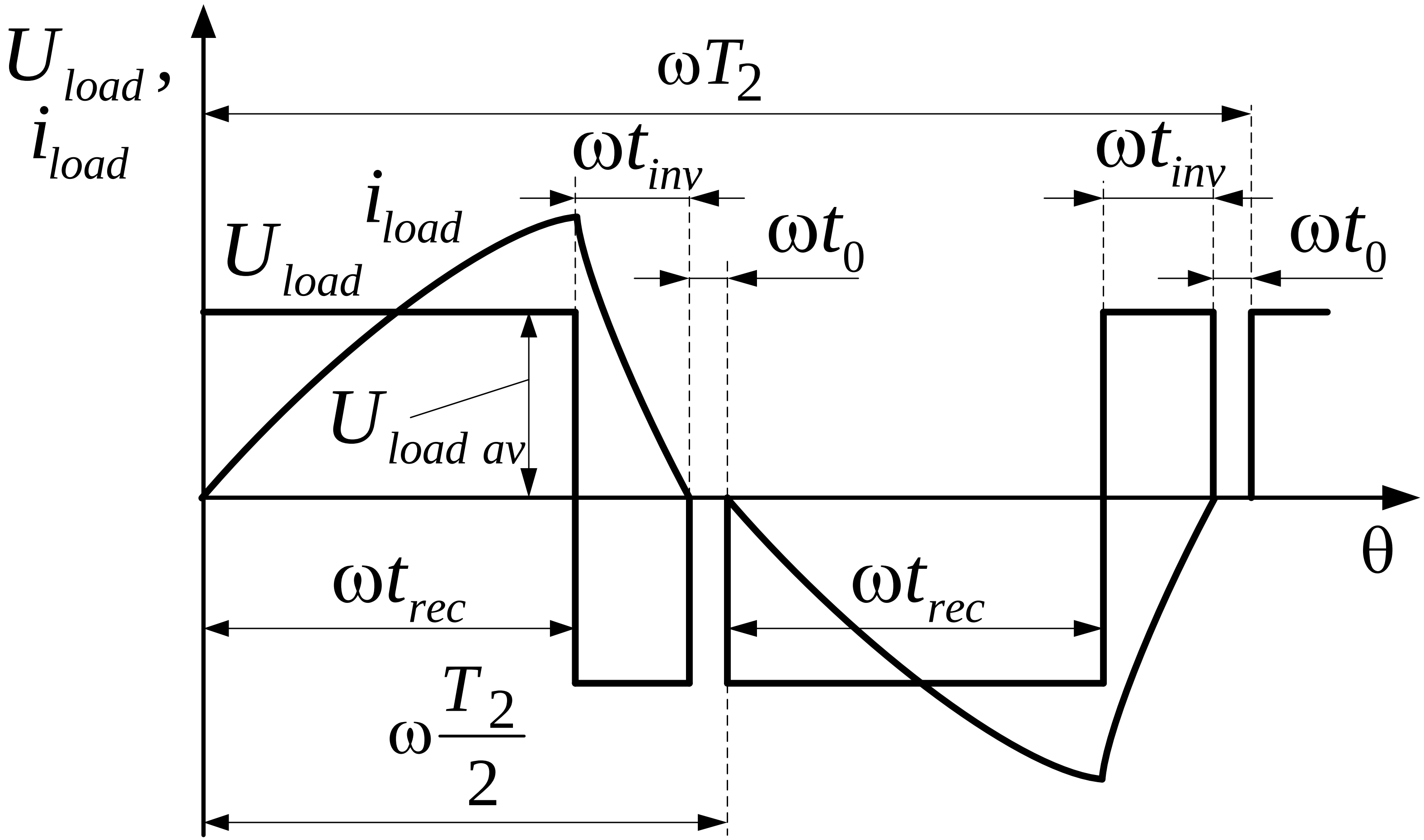

Fig. 5.5. Separate control of valve groups of the direct frequency converter

Ways of direct frequency converters control

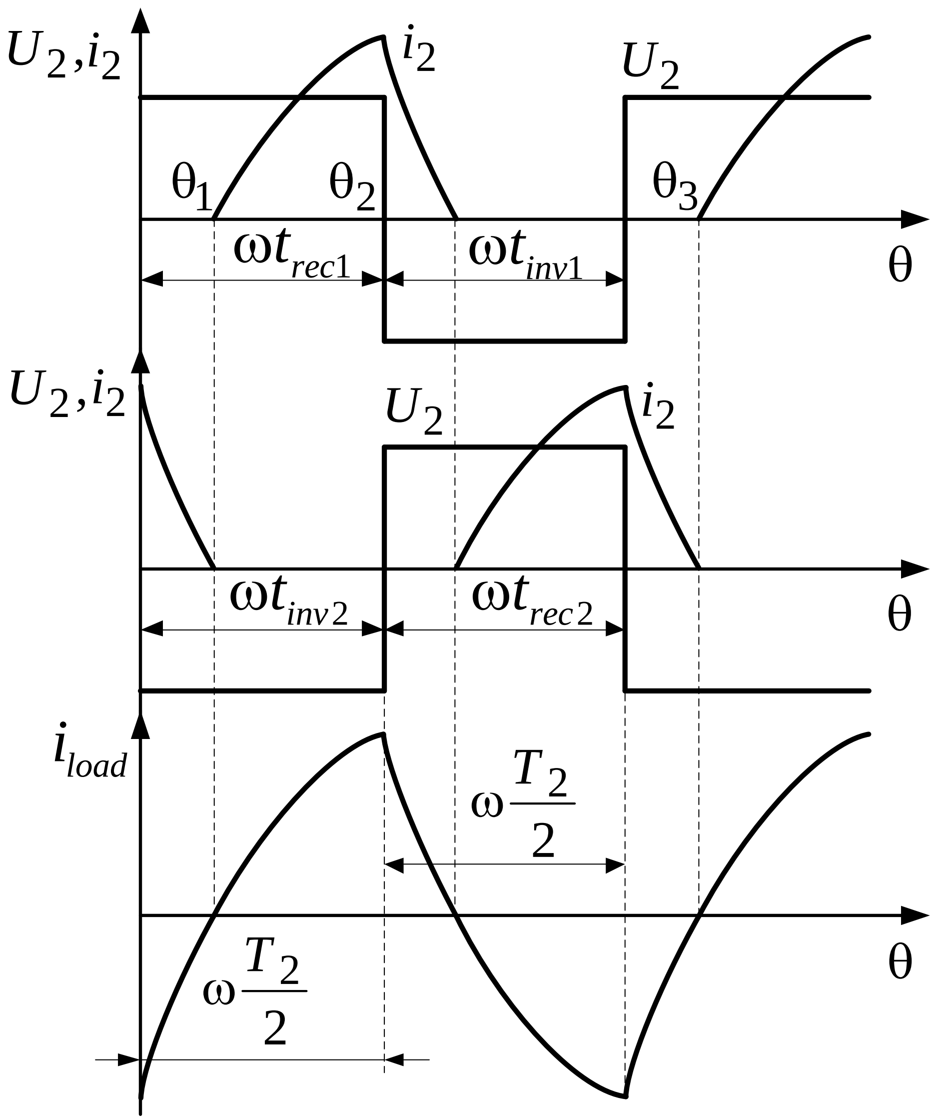

Fig. 5.6. Shared control of the valve groups of the direct frequency converter

In order to obtain a sinusoidal output voltage

$$U_{load} = U_{load\,\max} \cdot \sin\theta \quad (5.1)$$

it is necessary that the average value of the output voltage of one group, e.g. the first group

$$U_1 = 2{,}34 \cdot U_1 \cdot \cos\alpha_1 \quad (5.2)$$

is changed according to the expression (5.1):

$$2{,}34 \cdot U_1 \cdot \cos\alpha_1 = U_{load\,\max} \cdot \sin\theta$$

Hence, we find α_1

$$\alpha_1 = \arccos\left[\frac{U_{load\ \max}}{2{,}34 \cdot U_1} \cdot \sin\theta\right] = \arccos(\nu \cdot \sin\theta) \quad (5.3)$$

where $\nu = \dfrac{U_{load\ \max}}{2{,}34 \cdot U_1}$ – the depth of modulation of the output voltage. It is obvious that $\alpha_2 = -\arccos(\nu \cdot \sin\theta)$, since U_2 varies in antiphase with U_1.

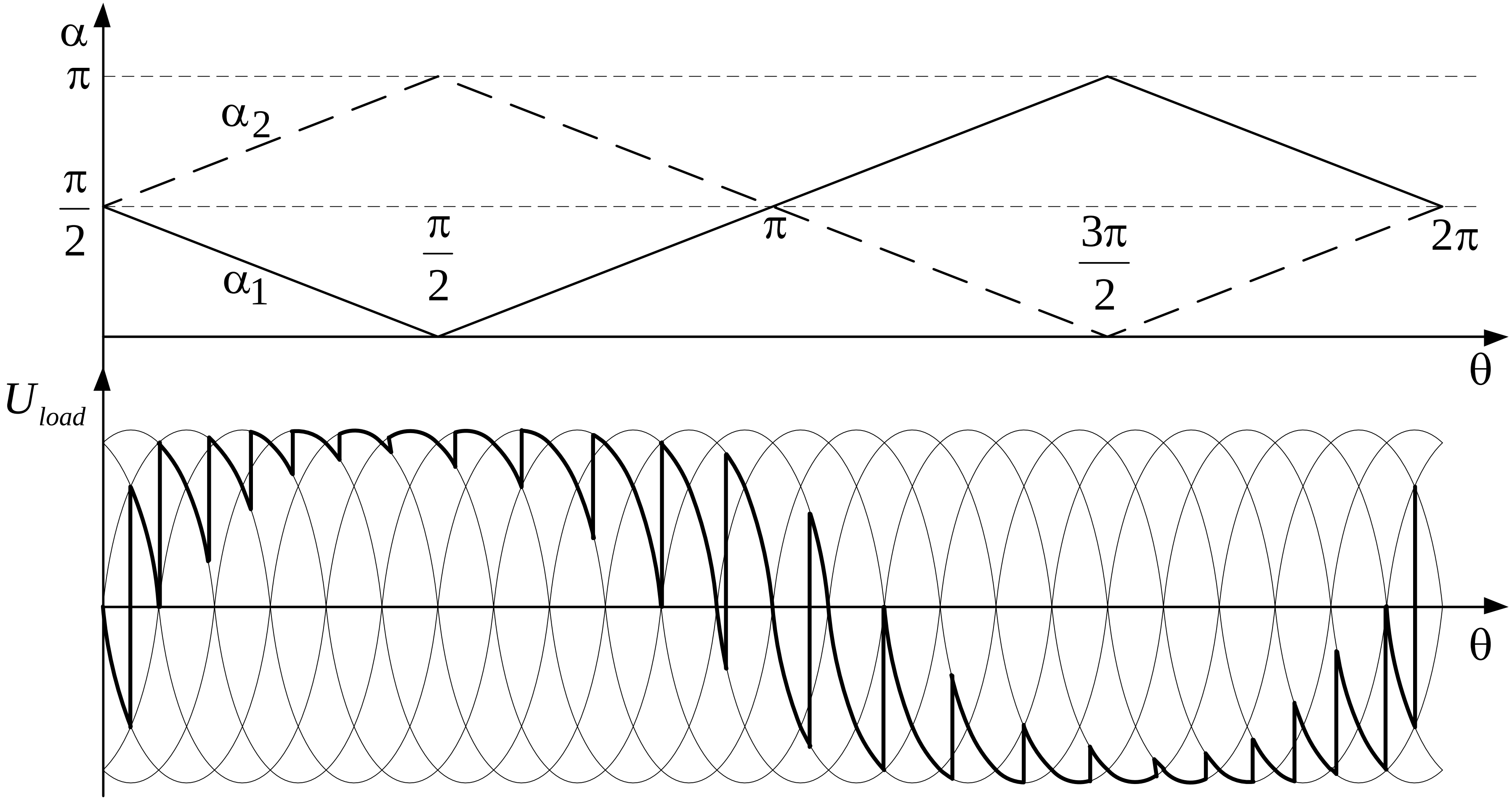

Fig. 5.7. The principle of sinusoidal output voltage forming of direct frequency converter

Main characteristics of direct frequency converter

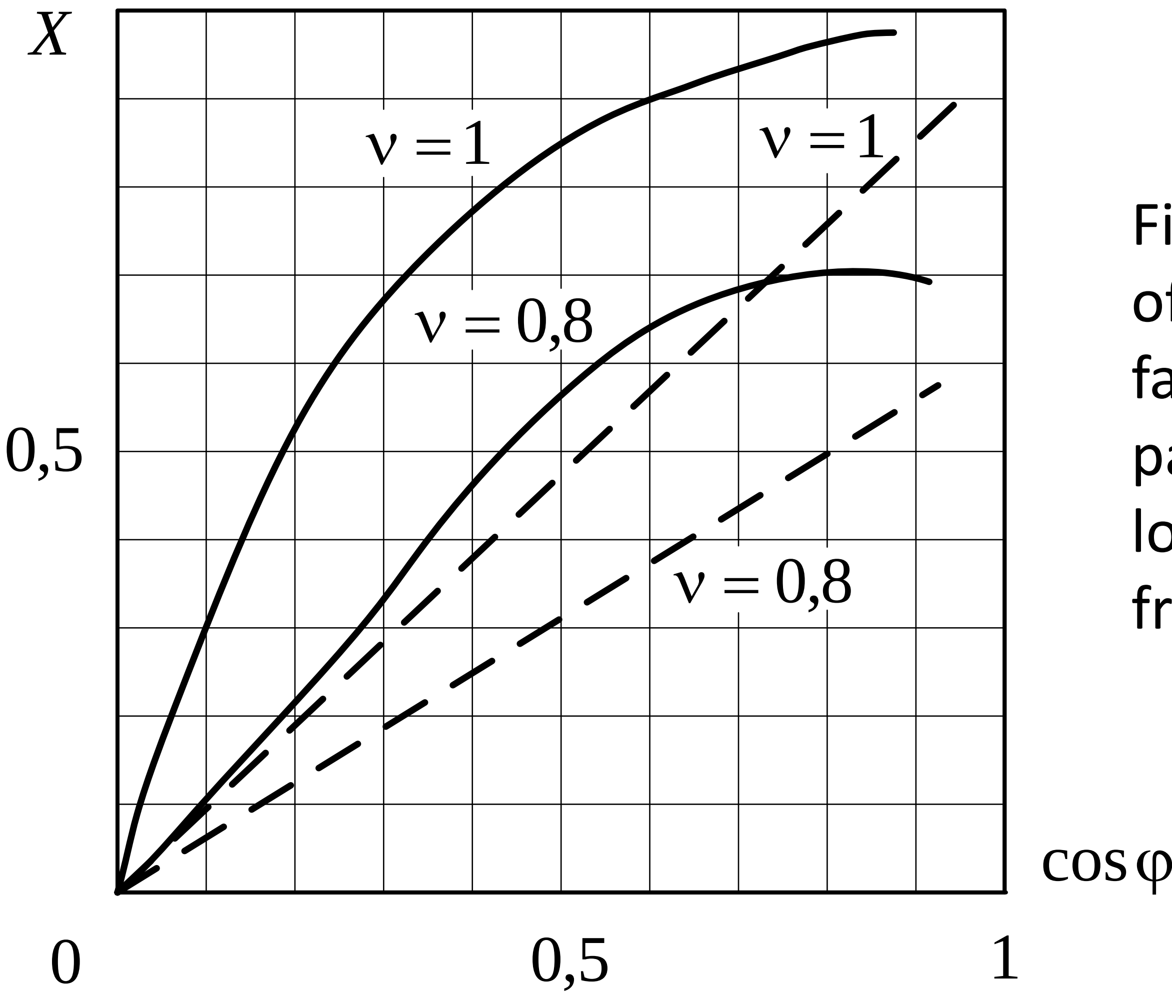

Fig. 5.8. Dependence of the total power factor from the parameters of the load for direct frequency converter

Direct frequency converters with forced valves switching

Basic drawbacks of the above circuits of the direct frequency converters are limited range of the output frequency (usually $f_2 \leq 0{,}25\, f_1$),

To eliminate these drawbacks the direct frequency converters with forced valves switching are usually used.

The most widespread way of output voltage formation is quasi single sideband modulation to generate the output voltage.

Its implementation in direct frequency converters with forced switching is provided through switching the mains phases to the load phases with cyclic regular time intervals:

$$T_m = \frac{1}{f_m m_1} = \frac{1}{(f_1 \pm f_2) m_1}, \qquad (5.4)$$

where f_m is the switching frequency of the power valves (modulation frequency),

m_1 – the number of phases of the mains supply,

f_1 and f_2 – respectively the frequency of mains supply and the frequency of the output voltage of the converter.

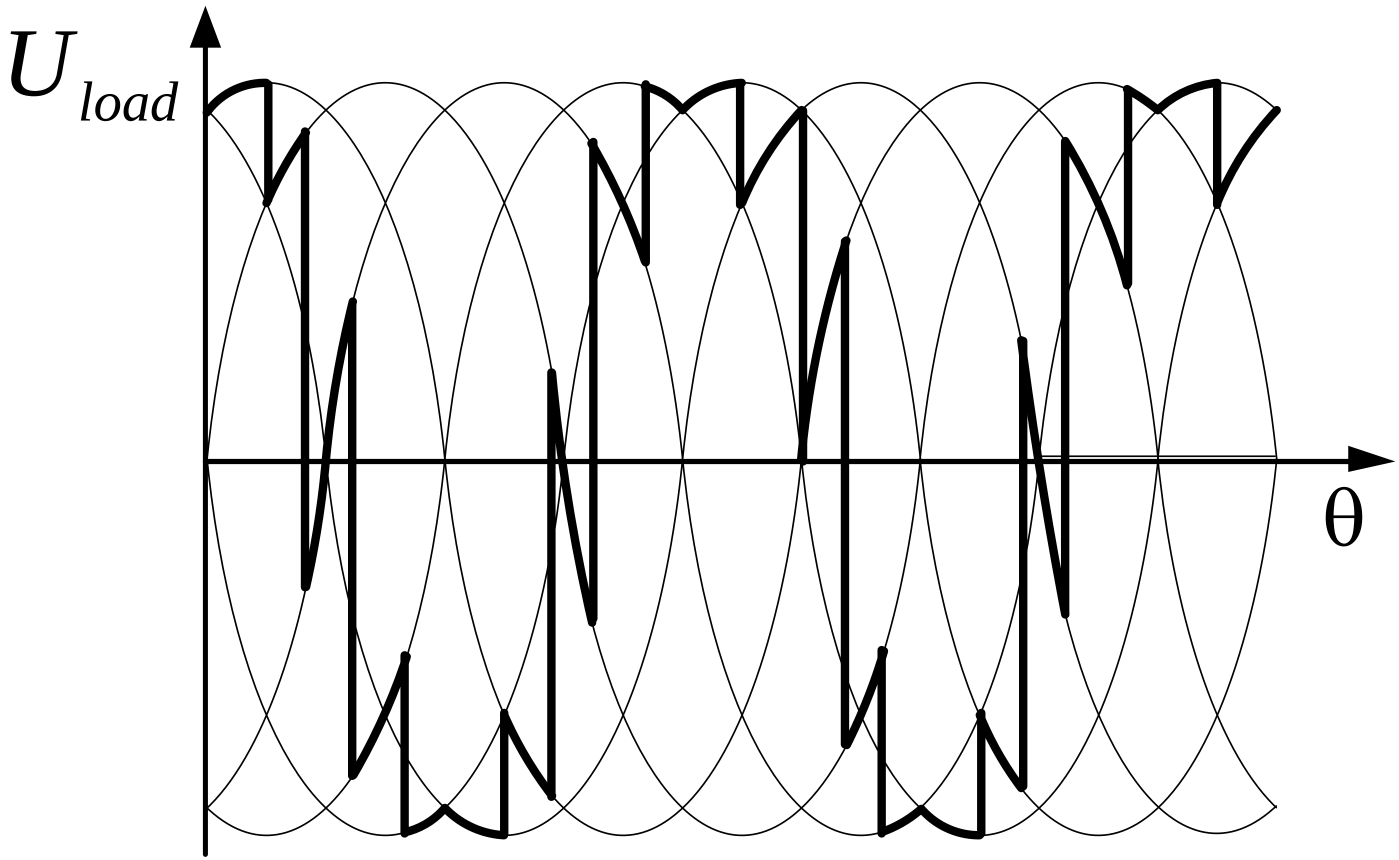

Fig. 5.9. Output voltage generation in direct frequency converter with forced valves switching

PULSE DC-DC CONVERTERS

Pulse DC-DC converter is a device converting DC power of one voltage to DC power of another voltage.

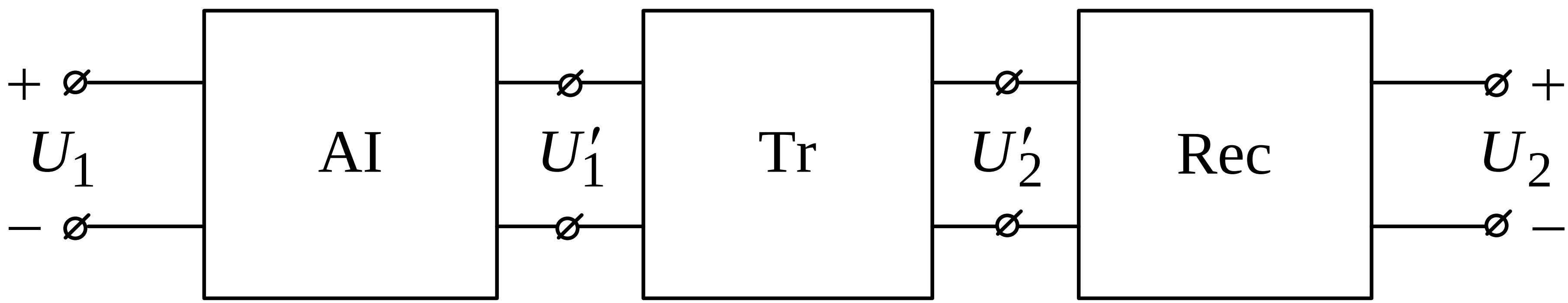

Fig. 6.1. Block diagram of DC-DC converter

Non-reversible pulse DC-DC converters

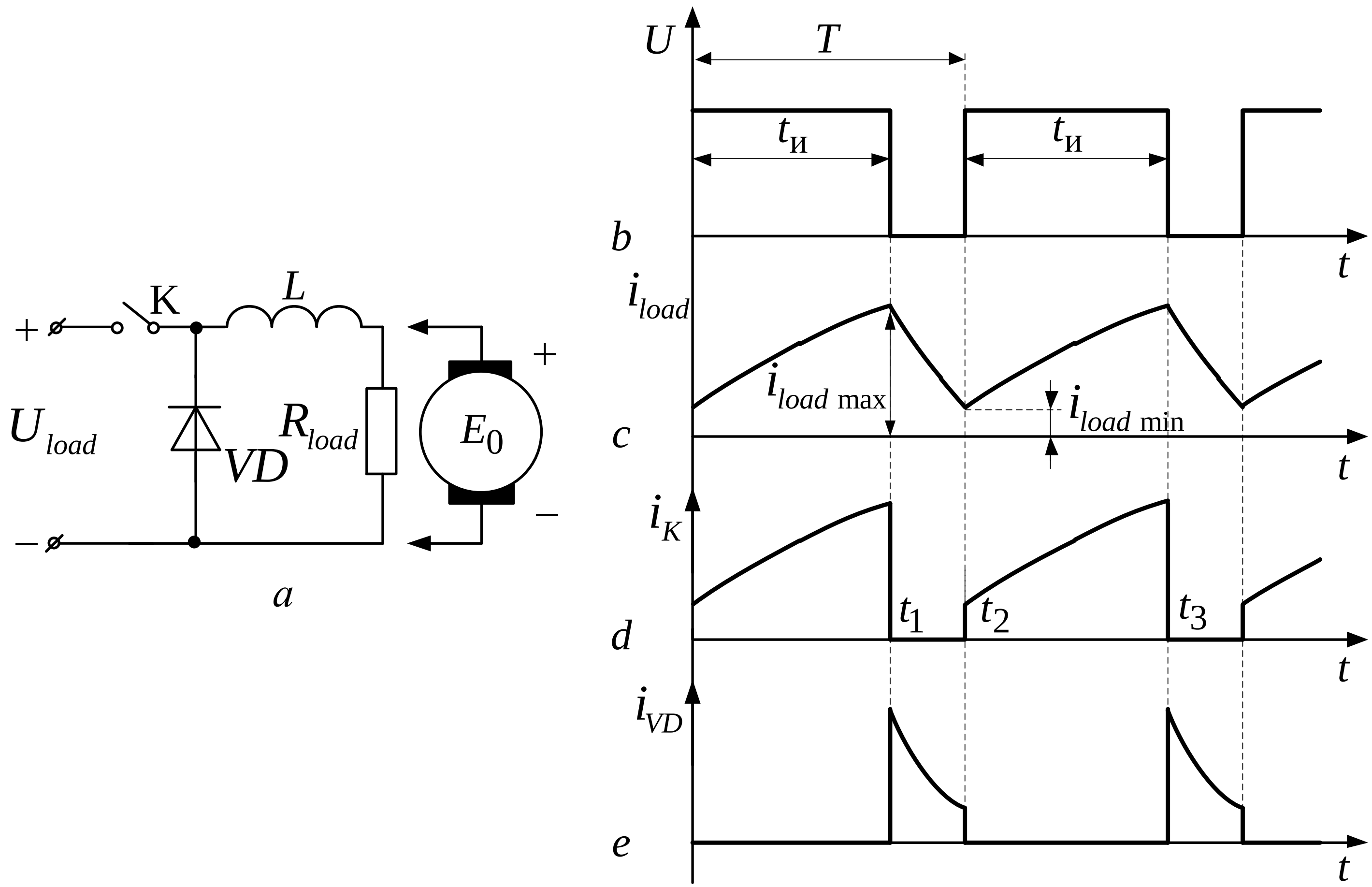

Fig. 6.2. Non-reversible pulse DC-DC converter

Closing the switch for the time t_p and opening it for the time t_0 with frequency $f = \frac{1}{T}$,

we obtain the average value of the load voltage:

$$U_{load} = \frac{1}{T}\int_0^{t_p} U_s \mathrm{d}t = \frac{U_s \cdot t_p}{T} = U_s \cdot \gamma \qquad (6.1)$$

The ratio $\frac{t_p}{T} = \gamma$ is called the duty cycle.

Voltage regulation can be carried out either by changing t_p at constant T or by changing T at constant t_p, and at the same time by changing both T and t_p

The first method at $t_p = \mathrm{var},\ T = \mathrm{const}$ is referred to as pulse-width method,

the second – $T = \mathrm{var}, t_p = \mathrm{const}$ – pulse-frequency method,

the third – $t_p = \mathrm{var},\ T = \mathrm{var}$ – time-pulse method.

Deriving the equation for the circuit shown in Fig. 6.2, in the interval from 0 to t_1 provided the switch K and the valve VD are ideal, we obtain:

$$L\frac{\mathrm{d}i_{load1}}{\mathrm{d}t}+i_{load1}R_{load}=U_s \quad (6.2)$$

and in the interval from t_1 to T

$$L\frac{\mathrm{d}i_{load2}}{\mathrm{d}t}+i_{load2}R_{load}=0 \qquad (6.3)$$

Solving these equations with respect to the current i_{load} given that

$$i_{load1}\Big|_{t=0} = i_{load2}\Big|_{t=T},$$ we get:

$$i_{load1} = \frac{U_s}{R_{load}}\left(1 - \frac{1 - e^{-\left(TR_{load}/L_{load}\right)} e^{\left(\gamma TR_{load}/L_{load}\right)}}{1 - e^{-\left(TR_{load}/L_{load}\right)}} e^{-\left(R_{load}t/L_{load}\right)}\right) \quad (6.4)$$

$$i_{load2} = \frac{U_s}{R_{load}} \frac{\left(1 - e^{-\left(\gamma TR_{load}/L_{load}\right)}\right)}{\left(1 - e^{-\left(TR_{load}/L_{load}\right)}\right)} e^{-\left(R_{load}t/L_{load}\right)} \quad (6.5)$$

$$i_{load\,\max} = i_{load1}\Big|_{t=t_p} = \frac{U_s}{R_{load}} \frac{\left(1-e^{-\left(\gamma T R_{load}/L_{load}\right)}\right)}{\left(1-e^{-\left(T R_{load}/L_{load}\right)}\right)} \quad (6.6)$$

$$i_{load\,\min} = i_{load2}\Big|_{t=T} = \frac{U_s}{R_{load}} \frac{\left(-1+e^{\left(\gamma T R_{load}/L_{load}\right)}\right)}{\left(1-e^{-\left(T R_{load}/L_{load}\right)}\right)} e^{-\left(T R_{load}/L_{load}\right)} \quad (6.7)$$

Load current ripples magnitude

$$\Delta i_{load} = i_{load\,\max} - i_{load\,\min} =$$

$$= \frac{U_s}{R_{load}} \frac{\left(1-e^{-\left(\gamma T R_{load}/L_{load}\right)}\right)}{\left(1-e^{-\left(T R_{load}/L_{load}\right)}\right)} \left(1-e^{-\left(T R_{load}/L_{load}\right)} e^{\left(\gamma T R_{load}/L_{load}\right)}\right). \quad (6.8)$$

Average switch K current

$$I_K = \frac{1}{T}\int_0^{t_p} i_{load1}\mathrm{d}t = \frac{U_s}{R_{load}} \times \qquad (6.9)$$

$$\times\left(\gamma - \frac{L_{load}\left(1-e^{-\left(\gamma T R_{load}/L_{load}\right)}\right)\left(1-e^{\left(\gamma T R_{load}/L_{load}\right)}e^{-\left(T R_{load}/L_{load}\right)}\right)}{R_{load}T\left(1-e^{-\left(T R_{load}/L_{load}\right)}\right)}\right).$$

Average value of the valve VD current:

$$I_{VD} = \frac{1}{T}\int_{0}^{t_0} i_{load\,2}\mathrm{d}t = \frac{U_s L_{load}}{R_{load}^2 T} \times \left(\frac{\left(1 - e^{-\left(\gamma T R_{load} / L_{load}\right)}\right)\left(1 - e^{\left(\gamma T R_{load} / L_{load}\right)} e^{-\left(T R_{load} / L_{load}\right)}\right)}{\left(1 - e^{-\left(T R_{load} / L_{load}\right)}\right)} \right). \qquad (6.10)$$

Average value of the load current:

$$I_{load} = I_K + I_{VD} = \frac{U_s}{R_{load}} \cdot \gamma \qquad (6.11)$$

Output voltage ripple coefficient:

$$K_r = \frac{\Delta i_{load} R_{load}}{U_s} = \tag{6.12}$$

$$= \frac{\left(1 - e^{-\left(\gamma T R_{load} / L_{load}\right)}\right)\left(1 - e^{\left(\gamma T R_{load} / L_{load}\right)} e^{-\left(T R_{load} / L_{load}\right)}\right)}{\left(1 - e^{-\left(T R_{load} / L_{load}\right)}\right)}$$

In the case of DC motor load (Fig. 6.2) the equations (6.2) – (6.3) take the form

$$i_{a1}R_a + L_a \frac{\mathrm{d}i_{a1}}{\mathrm{d}t} = U_s - E_0, \qquad \text{for } 0 < t < t_1 \quad (6.13)$$

$$i_{a2}R_a + L_a \frac{\mathrm{d}i_{a2}}{\mathrm{d}t} = E_0, \qquad \text{for } t_1 < t < t_2 \quad (6.14)$$

where i_a – the armature current of the motor;
R_a – the resistance of the armature winding;
L_a – the inductance of the armature winding;
E_0 – motor back-EMF.

There may be three modes of DC-DC converter operation:

- continuous current (Fig. 6.3, b, c, d);
- boundary-continuous mode (Fig. 6.3, d, e, f);
- discontinuous current mode (Fig. 5.3, h, i, k).

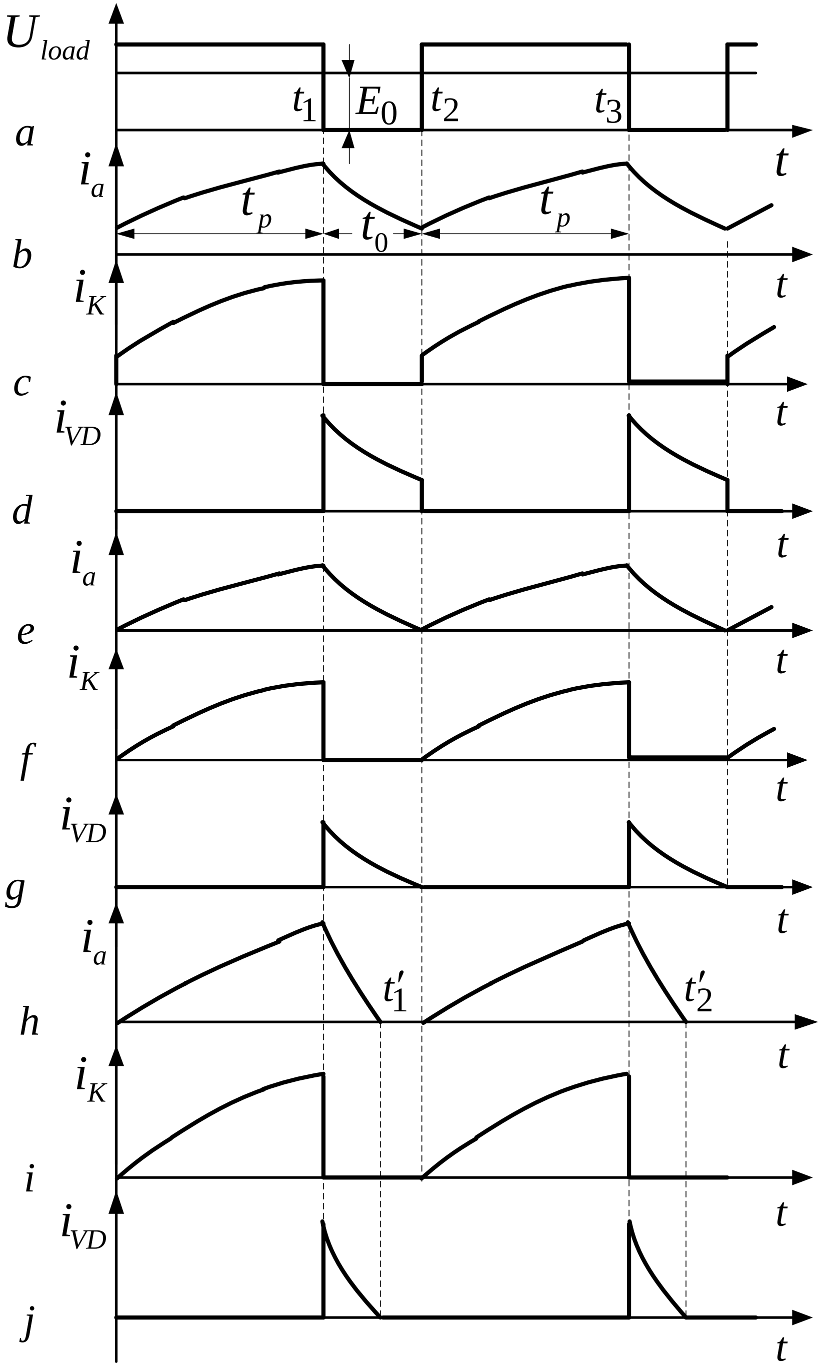

Fig. 6.3. Various operation modes of non-reversible pulse DC converter when operating on the motor load

For continuous current mode from the equations (6.13) and (6.14) we find i_a provided

$$i_{a1}\Big|_{t=0} = i_{a2}\Big|_{t=T}$$

$$i_{a1} = \frac{U_s - E_0}{R_a} - \frac{U_s}{R_a}\frac{\left(1 - e^{-\left(TR_a/L_a\right)}e^{\left(\gamma TR_a/L_a\right)}\right)}{\left(1 - e^{-\left(TR_a/L_a\right)}\right)}e^{-\left(R_a t/L_a\right)} \quad (6.15)$$

$$i_{a2} = -\frac{E_0}{R_a} + \frac{U_s}{R_a}\frac{\left(1 - e^{-\left(\gamma TR_a/L_a\right)}\right)}{\left(1 - e^{-\left(TR_a/L_a\right)}\right)}e^{-\left(R_a t/L_a\right)} \quad (6.16)$$

Maximum and minimum values of the armature current

$$i_{a\,\max} = -\frac{E_0}{R_a} + \frac{U_s}{R_a}\frac{\left(1-e^{-\left(\gamma TR_a/L_a\right)}\right)}{\left(1-e^{-\left(TR_a/L_a\right)}\right)} \qquad (6.17)$$

$$i_{a\,\min} = -\frac{E_0}{R_a} + \frac{U_s}{R_a}\frac{\left(e^{\left(\gamma TR_a/L_a\right)}-1\right)}{\left(1-e^{-\left(TR_a/L_a\right)}\right)}e^{-\left(TR_a/L_a\right)} \qquad (6.18)$$

Anchor current ripples magnitude

$$\Delta i_a = i_{a\,\max} - i_{a\,\min} = \frac{U_s}{R_a} \frac{\left(1 - e^{-\left(\gamma T R_a / L_a\right)}\right)}{\left(1 - e^{-\left(T R_a / L_a\right)}\right)} \times \qquad (6.19)$$

$$\times \left(1 - e^{\left(\gamma T R_a / L_a\right)} e^{-\left(T R_a / L_a\right)}\right). \quad (6.20)$$

Average value of the armature current

$$I_a = \frac{U_s \cdot \gamma - E_0}{R_a} \qquad (6.20)$$

In the continuous and boundary-continuous current modes the next condition is valid

$i_a\Big|_{t=0} = 0$ and the currents are defined as follows:

$$i_{a1} = \frac{U_s - E_0}{R_a}\left(1 - e^{-\left(R_a t / L_a\right)}\right) \qquad (6.21)$$

$$i_{a2} = \frac{U_s - E_0}{R_a}\left(1 - e^{-\left(\gamma T R_a / L_a\right)}\right) e^{-\left(R_a t / L_a\right)} - \frac{E_0}{R_a}\left(1 - e^{-\left(R_a t / L_a\right)}\right) \qquad (6.22)$$

Maximum value of the armature current

$$i_{a\,\mathrm{max}} = \frac{U_s - E_0}{R_a}\left(1 - e^{-\left(\gamma T R_a / L_a\right)}\right) \qquad (6.23)$$

The average value of the armature current

$$I_a = \frac{U_s \cdot \gamma}{R_a} - \frac{E_0 \cdot t_1'}{R_a} \qquad (6.24)$$

The conditions of boundary-continuous mode are found at:

$$i_{a1}\Big|_{t=0} = 0$$

$$E_{0bm} = U_s e^{-\left(TR_a/L_a\right)} \frac{e^{\left(\gamma TR_a/L_a\right)} - 1}{1 - e^{-\left(TR_a/L_a\right)}} \quad (6.25)$$

$$I_{bm} = \frac{U_s}{R_a}\left(\gamma - e^{-\left(TR_a/L_a\right)} \frac{e^{\left(\gamma TR_a/L_a\right)} - 1}{1 - e^{-\left(tR_a/L_a\right)}}\right) \quad (6.26)$$

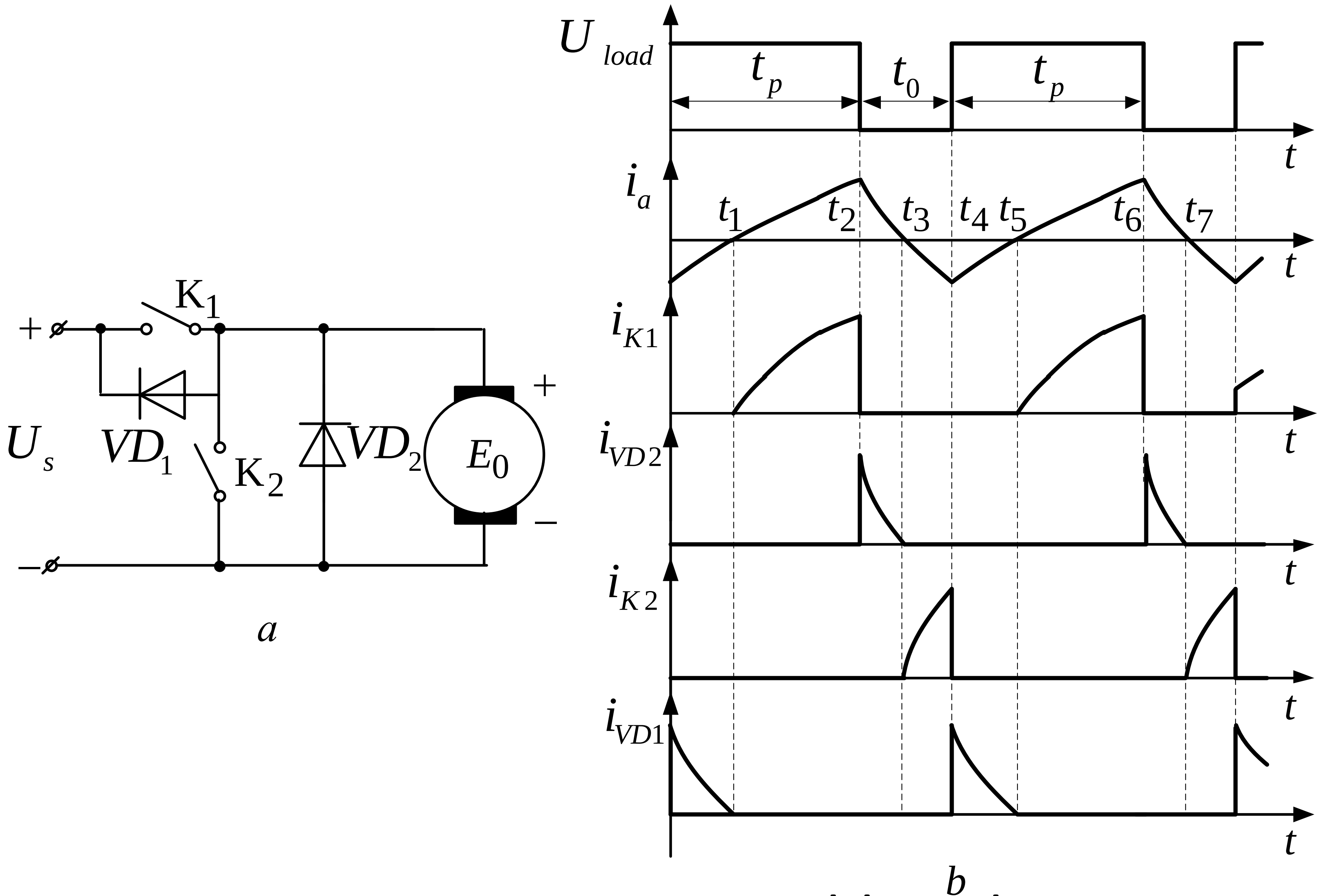

Fig. 6.4. Non-reversible pulse DC converter with energy regeneration

The equation of electromagnetic processes in the interval $0 \ldots t_1$:

$$U_s = L\frac{\mathrm{d}i_1}{\mathrm{d}t} + i_1 R_{eqv} \qquad (6.27)$$

and for the interval $t_1 \ldots t_2$:

$$U_s - U_{load} = L\frac{\mathrm{d}i_2}{\mathrm{d}t} + i_2 R_{eqv} \qquad (6.28)$$

where $R_{eqv} = r_L + r_{\mathrm{int}}$, r_L – active resistance of the inductor winding, r_{int} – internal resistance of the power supply.

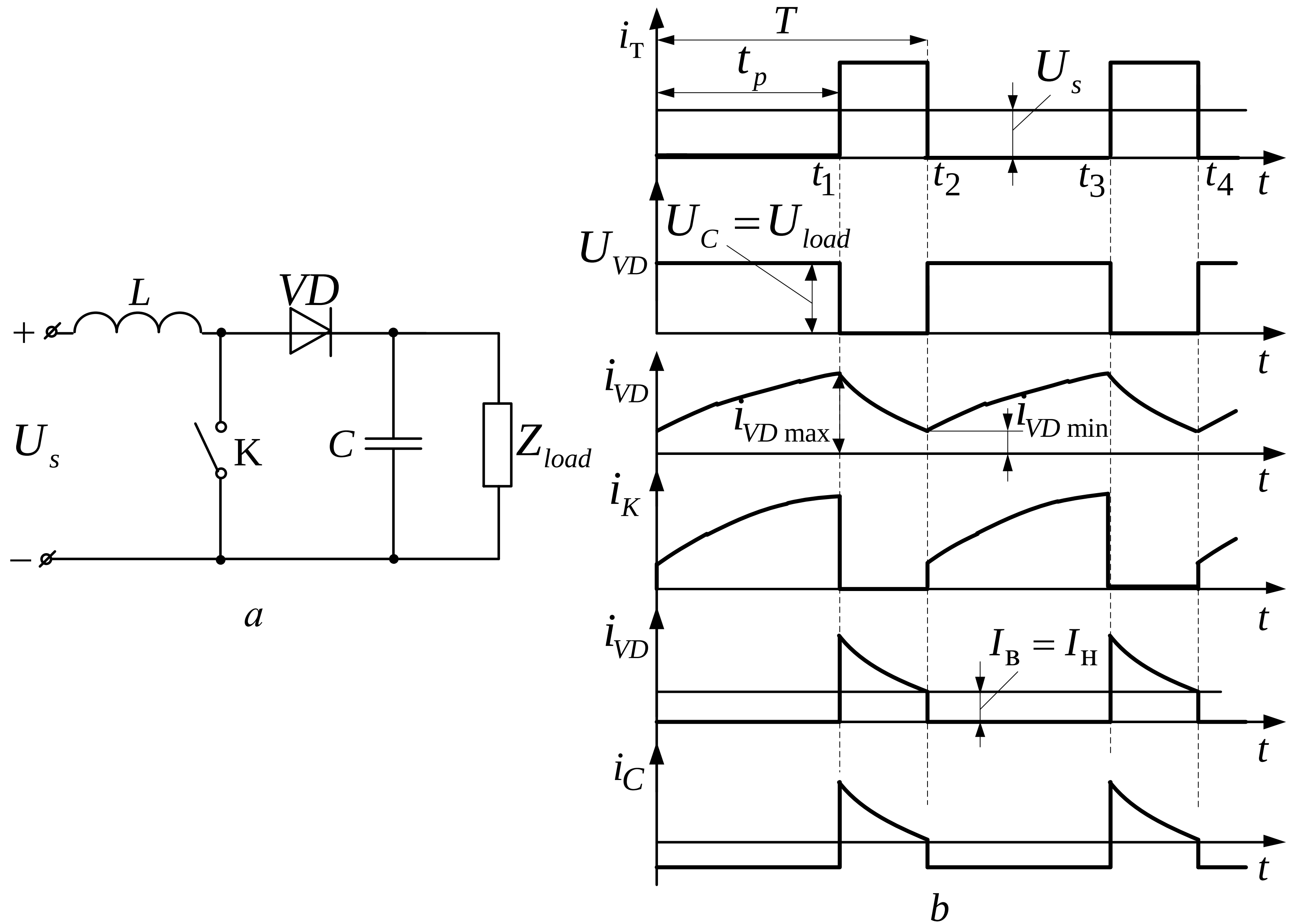

Fig. 6.5. Non-reversible pulse step-up DC-DC converter

Solving equation (6.27) – (6.28) with respect to the currents i_1 and i_2 provided

$$i_1\Big|_{t=0} = i_2\Big|_{t=T}$$

we obtain:

$$i_1 = \frac{U_s}{R_{eqv}} - \frac{U_s}{R_{eqv}} \frac{\left(1 - e^{-\left(TR_{eqv}/L\right)} e^{-\left(\gamma TR_{eqv}/L\right)}\right)}{\left(1 - e^{-\left(TR_{eqv}/L\right)}\right)} e^{-\left(tR_{eqv}/L\right)} \quad (6.29)$$

$$i_2 = \frac{U_s - U_{load}}{R_{eqv}} + \frac{U_{load}}{R_э} \frac{\left(1 - e^{-\left(\gamma T R_{eqv}/L\right)}\right)}{\left(1 - e^{-\left(T R_{eqv}/L\right)}\right)} e^{-\left(t R_{eqv}/L\right)} \tag{6.30}$$

$$i_{L\,\max} = i_{K\,\max} = i_{VD\,\max} =$$

$$= \frac{U_s}{R_{eqv}} - \frac{U_{load}}{R_{eqv}} \frac{\left(e^{-\left(\gamma T R_{eqv}/L\right)} - e^{-\left(T R_{eqv}/L\right)}\right)}{\left(1 - e^{-\left(T R_{eqv}/L\right)}\right)} \tag{6.31}$$

$$i_{L\min} = i_{K\min} = i_{VD\min} =$$

$$= \frac{U_s}{R_{eqv}} - \frac{U_{load}}{R_{eqv}} \frac{\left(1 - e^{-\left(TR_{eqv}/L\right)} e^{\left(\gamma TR_{eqv}/L\right)}\right)}{\left(1 - e^{-\left(TR_{eqv}/L\right)}\right)} \qquad (6.32)$$

Current ripples magnitude of the inductor

$$\Delta i_L = i_{L\max} - i_{L\min} =$$

$$= \frac{U_{load}}{R_{eqv}} \frac{\left(e^{-\left(TR_{eqv}/L\right)} - e^{-\left(\gamma TR_{eqv}/L\right)}\right)\left(1 - e^{-\left(\gamma TR_{eqv}/L\right)}\right)}{\left(1 - e^{-\left(TR_{eqv}/L\right)}\right)} \qquad (6.33)$$

The average value of the load current

$$I_{load} = \frac{1}{T}\int_{t_p}^{T} i_2 \mathrm{d}t = \frac{U_{load} - U_s}{R_{eqv}}\left(1-\gamma\right) + \tag{6.34}$$
$$+\frac{LU_{load}\left(e^{-\left(TR_{eqv}/L\right)} - e^{-\left(\gamma TR_{eqv}/L\right)}\right)\left(1-e^{-\left(\gamma TR_{eqv}/L\right)}\right)}{R_{eqv}^2 T\left(1-e^{-\left(TR_{eqv}/L\right)}\right)}$$

From Fig. 6.5 we find:

$$U_{load} = \frac{E_s}{1-\gamma} - \frac{r_{\mathrm{int}} I_{load}}{\left(1-\gamma\right)^2} \tag{6.35}$$

$$U_s = E_s - \frac{r_{\text{int}} I_{load}}{1-\gamma} \qquad (6.36)$$

Exploring the function (6.35) on the extremum, we find

$$U_{load\,\max} = \frac{E_s^2}{4 r_{\text{int}} I_{load}} \qquad (6.37)$$

Neglecting the fluctuations of the load current, i.e. considering that $I_{load} = I_C = \text{const}$, we find the output voltage ripple value:

$$\Delta U_{load} = \Delta U_C = \frac{1}{C}\int_0^{t_p} I_C dt = \frac{I_{load} \cdot t_p}{C} \qquad (6.38)$$

Multiplying (6.38) by $\frac{T}{T}$, we get:

$$\Delta U_{load} = \frac{I_{load} \cdot \gamma}{C \cdot f} \qquad (6.39)$$

At any condition the value voltage ripple ΔU_{load} decreases with increasing frequency *f*.

This parameter is limited by the properties of switches and other power components used in this circuit. To eliminate this drawback multi-phase converters are sometimes used (Fig. 6.6), which correspond n single-phase converters operating on one load and supplied by one power source.

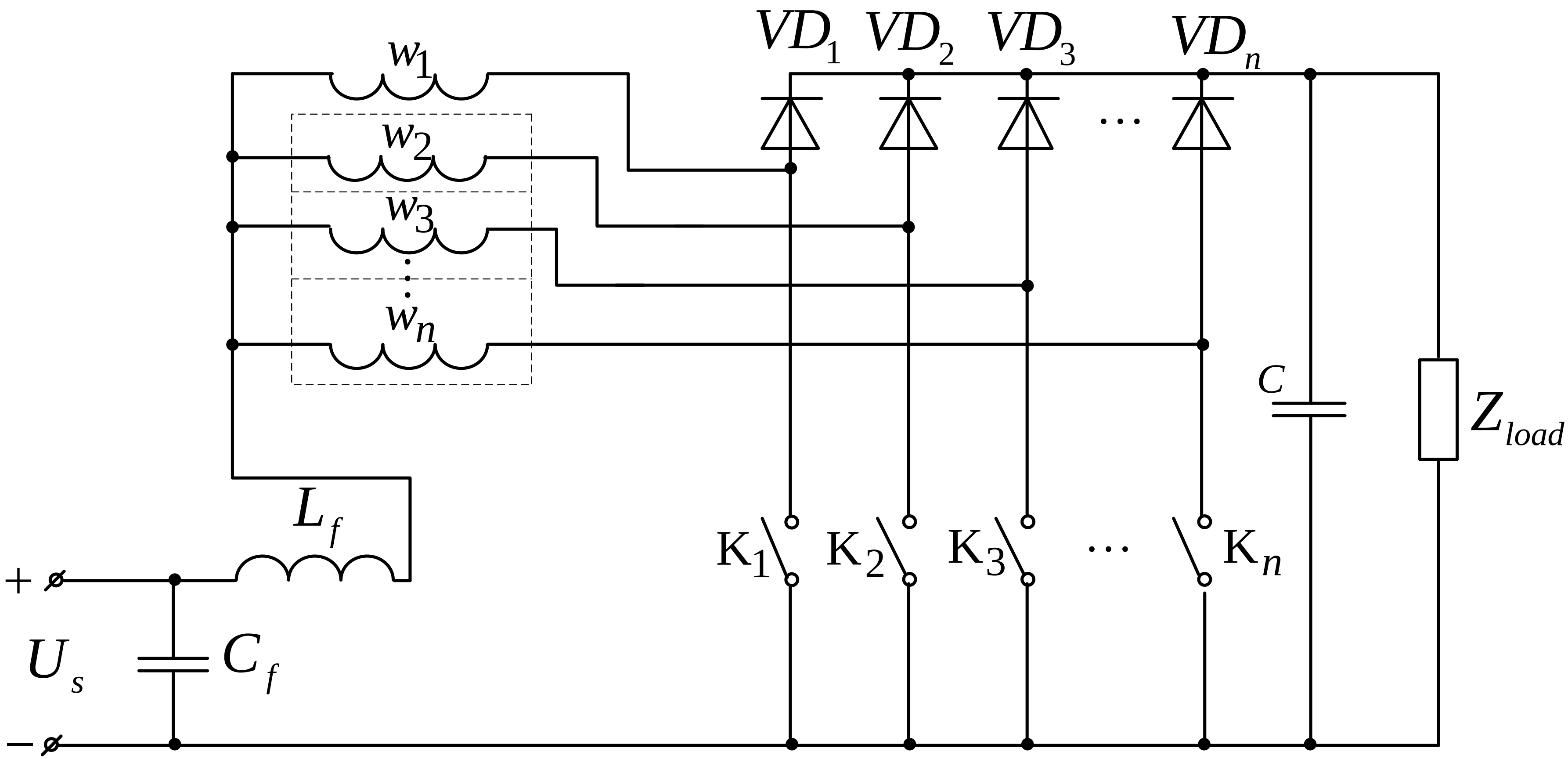

Fig. 6.6. Multiphase pulse DC-DC converter

To expand the range of output voltage in this class of converters two windings inductors with auto-transformer link are sometimes used (Fig. 6.7).

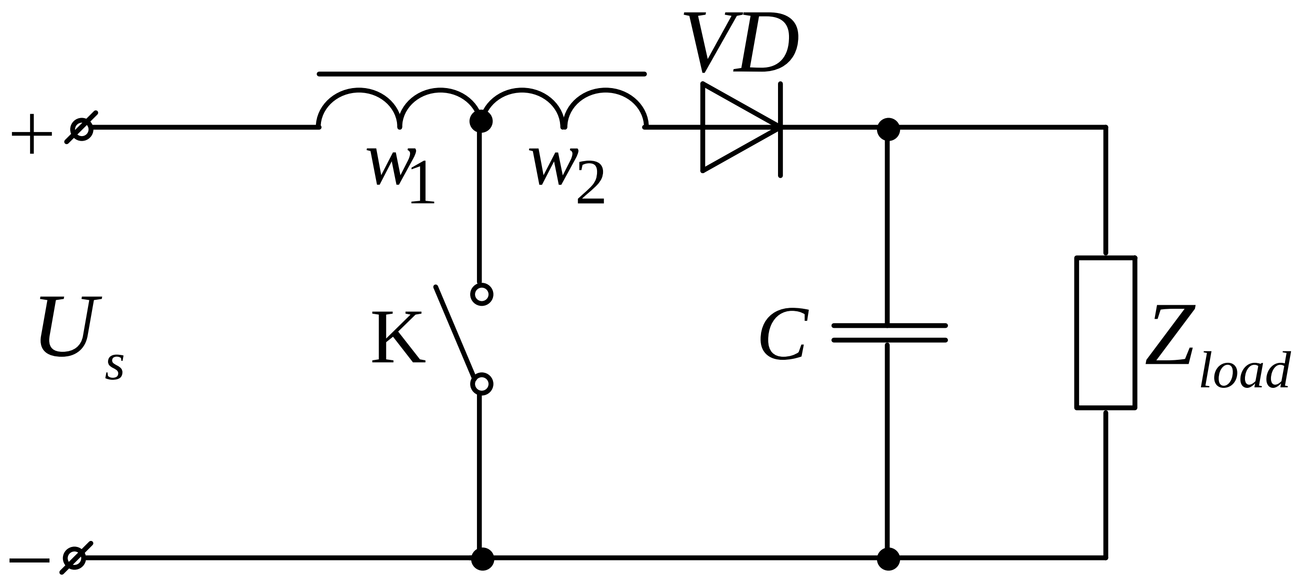

Fig. 6.7. Pulse DC-DC converter with auto-transformer link

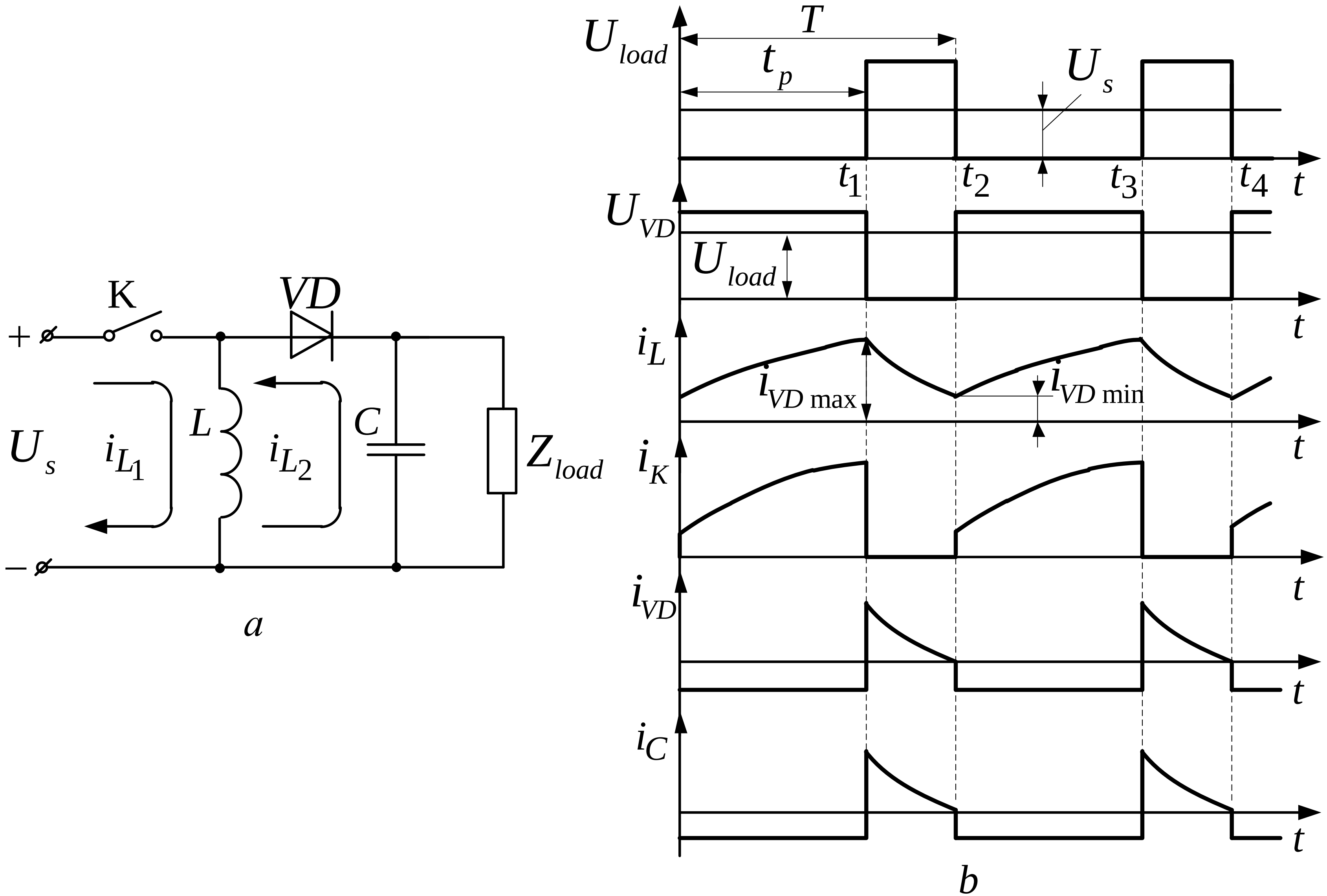

Fig. 6.8. Pulse DC-DC up-and-down converter

The equations of the electromagnetic processes are:

- for the interval $0 \ldots t_1$:

$$U_s = L\frac{\mathrm{d}i_{L_1}}{\mathrm{d}t} + i_{L_1} R_{eqv1} \qquad (6.40)$$

- for the interval $t_1 \ldots t_2$:

$$U_{load} = L\frac{\mathrm{d}i_{L_2}}{\mathrm{d}t} + i_{L_2} R_{eqv2} \qquad (6.41)$$

where $R_{eqv1} = r_L + r_{\text{int}}$, $R_{eqv2} = r_L + r_{VD}$,

r_L – active resistance of the inductor,

r_{int} – internal resistance of the power supply,

r_{VD} – resistance of the valve VD.

Given that $i_{L_1}\Big|_{t=0} = i_{L_2}\Big|_{t=T}$, and taking into account that $R_{eqv1} \approx R_{eqv2} \approx R_{eqv}$ we solve the equations (6.40), (6.41) with respect to currents i_{L_1} and i_{L_2} :

$$i_{L_1} = \frac{U_s}{R_{eqv}} - \frac{\left(U_s + U_{load}\right)\left(1 - e^{-\left({TR_{eqv}}/{L}\right)} e^{\left({\gamma TR_{eqv}}/{L}\right)}\right)}{R_{eqv}\left(1 - e^{-\left({TR_{eqv}}/{L}\right)}\right)} e^{-\left({R_{eqv}t}/{L}\right)} \tag{6.42}$$

$$i_{L_2} = \frac{\left(U_s + U_{load}\right)\left(1 - e^{-\left({\gamma TR_{eqv}}/{L}\right)}\right)}{R_{eqv}\left(1 - e^{-\left({TR_{eqv}}/{L}\right)}\right)} e^{\left({R_{eqv}t}/{L}\right)} - \frac{U_{load}}{R_{eqv}} \tag{6.43}$$

$$i_{L\min} = \frac{U_s}{R_{eqv}} - \frac{\left(U_s + U_{load}\right)\left(1 - e^{-\left({TR_{eqv}}/{L}\right)} e^{\left({\gamma TR_{eqv}}/{L}\right)}\right)}{R_{eqv}\left(1 - e^{-\left({TR_{eqv}}/{L}\right)}\right)} \tag{6.44}$$

$$i_{L\max} = \frac{U_s}{R_{eqv}} - \frac{\left(U_s + U_{load}\right)\left(e^{-\left(\gamma T R_{eqv}/L\right)} - e^{-\left(T R_{eqv}/L\right)}\right)}{R_{eqv}\left(1 - e^{-\left(T R_{eqv}/L\right)}\right)} \tag{6.45}$$

Inductor current ripples magnitude:

$$\Delta i_L = i_{L\max} - i_{L\min} = \tag{6.46}$$

$$= \frac{\left(U_s + U_{load}\right)\left(1 - e^{-\left(T R_{eqv}/L\right)} e^{\left(\gamma T R_{eqv}/L\right)}\right)\left(1 - e^{-\left(\gamma T R_{eqv}/L\right)}\right)}{R_{eqv}\left(1 - e^{-\left(T R_{eqv}/L\right)}\right)}$$

Average value of the load current

$$I_{\text{н}} = \frac{1}{T}\int_{0}^{T-t_{\text{и}}} i_{L_2}\,\mathrm{d}t =$$

$$= \frac{\left(U_{\text{пит}} + U_{\text{н}}\right) L \left(1 - e^{-\left(\gamma T R_{\text{э}} / L\right)}\right)\left(1 - e^{-\left(T R_{\text{э}} / L\right)} e^{\left(\gamma T R_{\text{э}} / L\right)}\right)}{R_{\text{э}}^{2} T \left(1 - e^{-\left(T R_{\text{э}} / L\right)}\right)} - \qquad (6.47)$$

$$-\frac{U_{\text{н}}}{R_{\text{э}}}\left(1 - \gamma\right).$$

From diagrams in Fig. 6.8 we obtain:

$$U_{load} = \frac{\gamma}{1-\gamma}\left(E_s - \frac{\gamma}{1-\gamma} r_{VD} I_{load} - \frac{1}{\gamma(1-\gamma)} r_L I_{load} \right) \quad (6.48)$$

$$U_s = E_s - \frac{\gamma}{1-\gamma} r_{\mathrm{int}} I_{load} \quad (6.49)$$

As in the previous circuit, the magnitude of the output voltage ripple:

$$\Delta U_{load} = \Delta U_C \frac{I_{load}\gamma}{Cf} \quad (6.50)$$

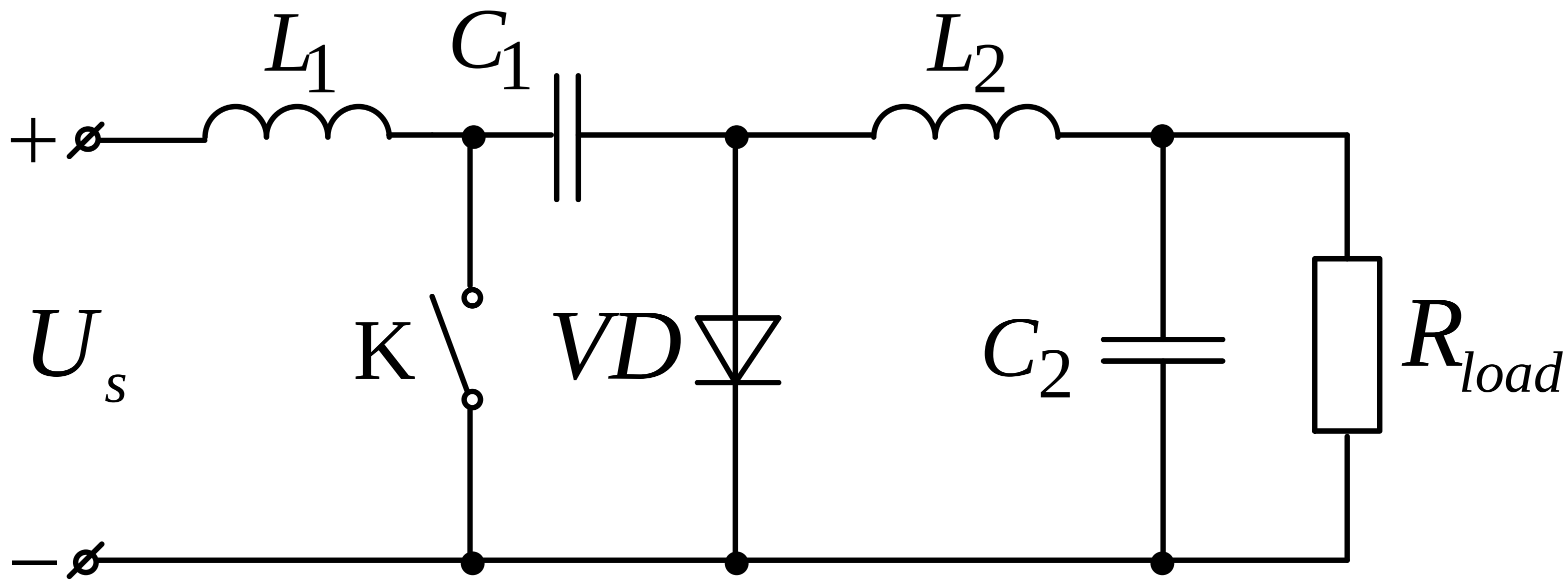

Fig. 6.9. Hook’s converter

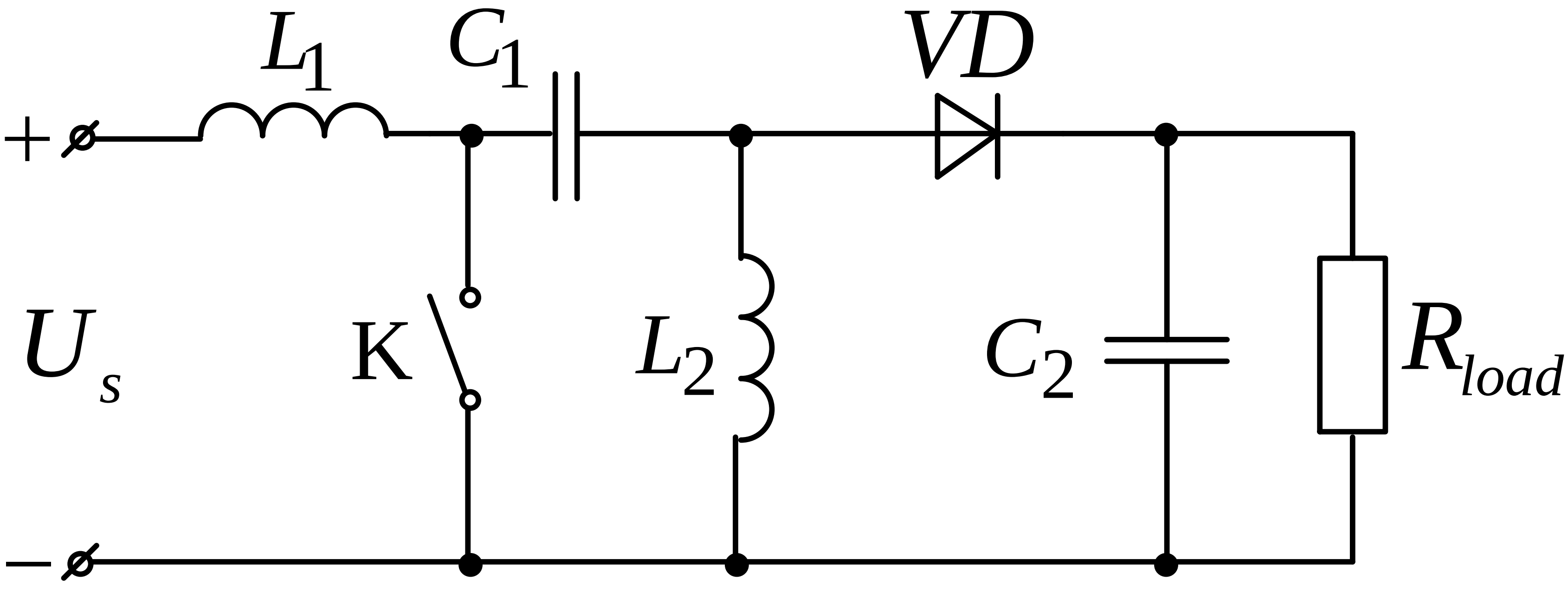

Fig. 6.10. SEPIC type converter

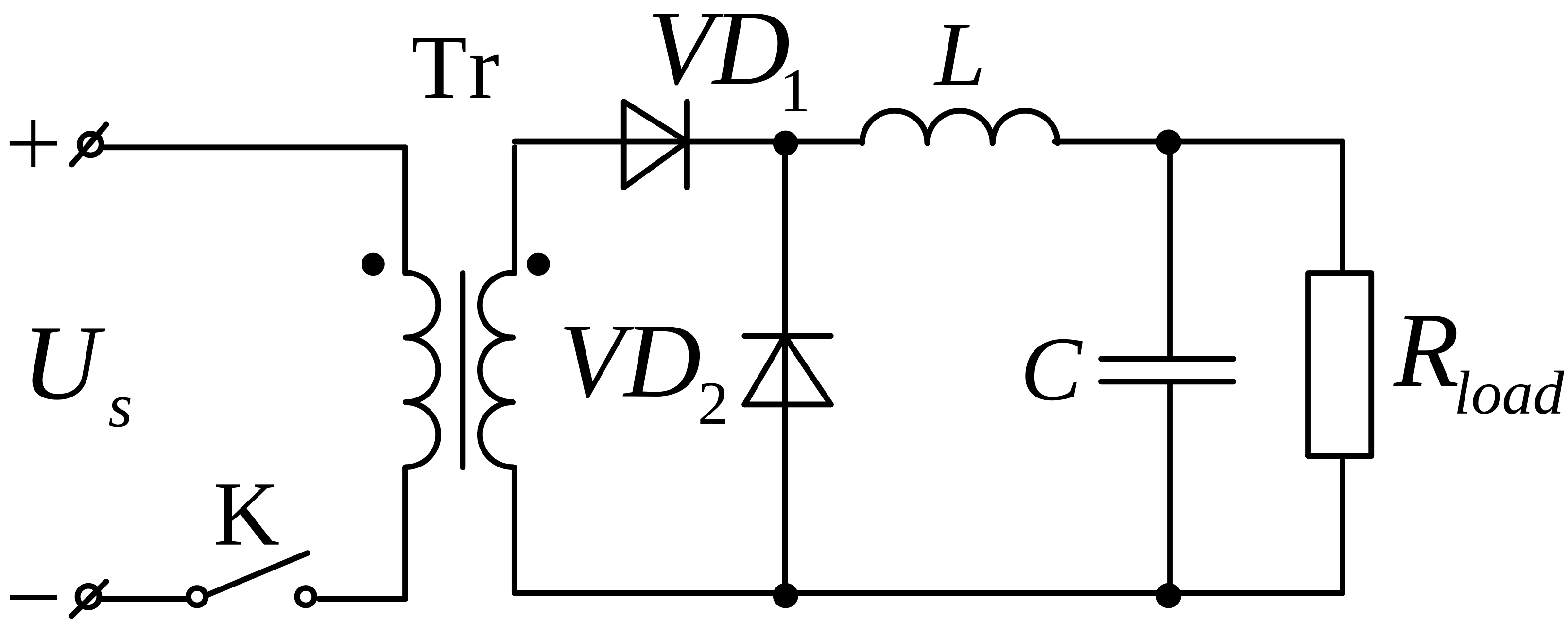

Fig. 6.11. Forward converter

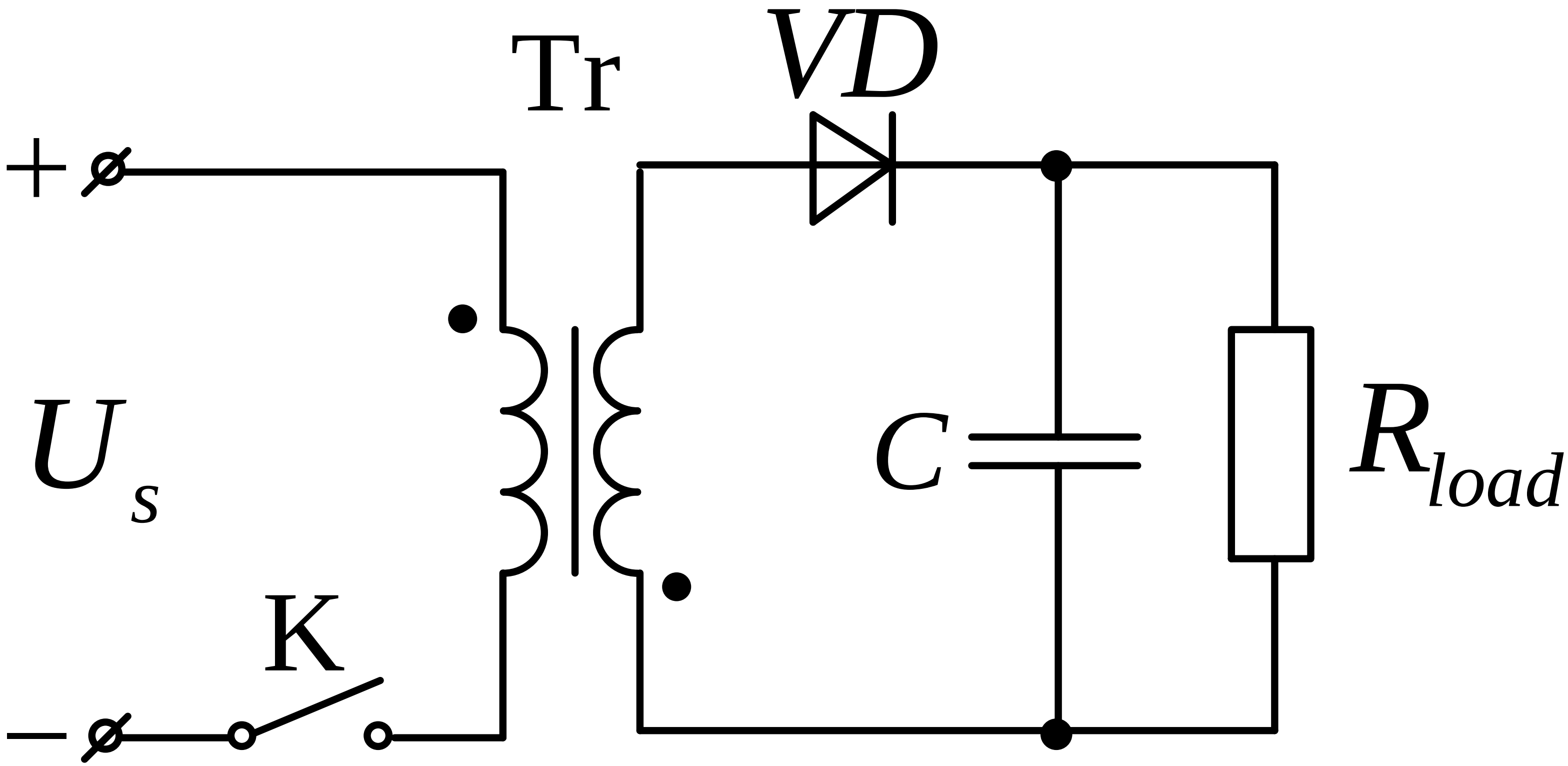

Fig. 6.12. Flyback converter

Reversible pulse DC-DC converters

To combine the regulation of the load current and reverse the reversible converters are used.

Typically they are performed on the basis of a bridge circuit (Fig. 6.13), which consists of the switches $\mathrm{K}_1 - \mathrm{K}_4$ and the reverse current valves $\mathrm{B}_1 - \mathrm{B}_4$.

The following control methods are possible:

1. Symmetric control method.
2. Asymmetric control method.
3. Alternate control method.

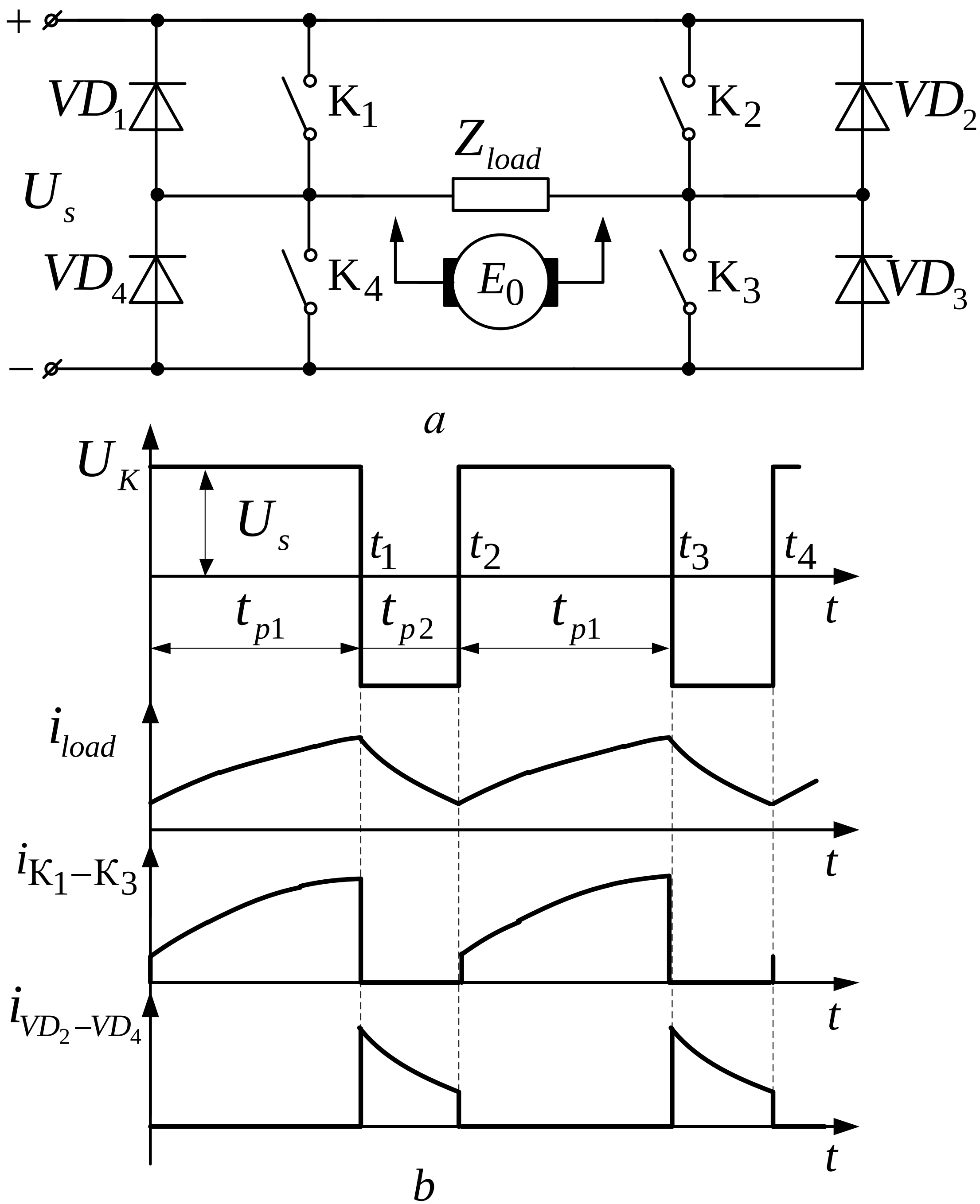

Fig. 6.13. Reversible pulse DC-DC converter (Symmetrical control method)

The average value of load voltage:

$$U_{load} = \frac{U_s t_{p1}}{T} - \frac{U_s t_{p2}}{T} = U_s\left(2\gamma - 1\right) \qquad (6.51)$$

where $\gamma = \dfrac{t_{p1}}{T}$

The equation of electromagnetic processes is as follows:

$$\pm U_s = i_{load} R_{load} + L_{load}\frac{di_{load}}{dt} \qquad (6.52)$$

where (+) corresponds to the interval $0\ldots t_1$, and (-) – to the interval $t_1\ldots t_2$.

Solving the equation (6.52) with respect to i_{load} and given that $i_{load}\Big|_{t=0} = i_{load}\Big|_{t=T}$, we get:

$$i_{load1}\Big|_{0\ldots t_1} = \frac{U_s}{R_{load}}\left[1 - \frac{2\left(1-e^{-\left(TR_{load}/L_{load}\right)}e^{\left(\gamma TR_{load}/L_{load}\right)}\right)}{\left(1-e^{-\left(TR_{load}/L_{load}\right)}\right)}e^{-\left(R_{load}t/L_{load}\right)}\right] \quad (6.53)$$

$$
i_{load\,2}\Big|_{t_1 \ldots T} = -\frac{U_s}{R_{load}}\left[1 + \frac{2\left(e^{-\left(\gamma T R_{load}/L_{load}\right)} - 1\right)}{\left(1 - e^{-\left(T R_{load}/L_{load}\right)}\right)} e^{-\left(R_{load} t/L_{load}\right)}\right] \quad (6.54)
$$

$$
i_{load\,\max} = i_{K\,\max} = i_{VD\,\max} =
$$

$$
= \frac{U_s}{R_{load}} \frac{\left(1 + e^{-\left(T R_{load}/L_{load}\right)} - 2e^{-\left(\gamma T R_{load}/L_{load}\right)}\right)}{\left(1 - e^{-\left(T R_{load}/L_{load}\right)}\right)} \quad (6.55)
$$

$$
i_{load\,\min} = i_{K\,\min} = i_{VD\,\min} =
$$

$$
= -\frac{U_s}{R_{load}} \frac{\left(1 + e^{-\left(T R_{load}/L_{load}\right)} - 2e^{-\left(T R_{load}/L_{load}\right)} e^{\left(\gamma T R_{load}/L_{load}\right)}\right)}{\left(1 - e^{-\left(T R_{load}/L_{load}\right)}\right)} \quad (6.56)
$$

The amplitude of the load current ripples:

$$\Delta i_{load} = i_{load\,\max} - i_{load\,\min} =$$

$$= \frac{2U_s}{R_{load}} \frac{\left(1 - e^{-\left(\gamma T R_{load} / L_{load}\right)}\right)\left(1 - e^{-\left(T R_{load} / L_{load}\right)} e^{-\left(\gamma T R_{load} / L_{load}\right)}\right)}{\left(1 - e^{-\left(T R_{load} / L_{load}\right)}\right)} \quad (6.57)$$

The amplitude of the output voltage ripples:

$$\Delta U_{\mathrm{H}} = \Delta i_{\mathrm{H}} R_{\mathrm{H}}$$

Ripple coefficient:

$$K_r = \frac{\Delta U_{load}}{U_s} =$$

$$= \frac{2\left(1-e^{-\left(\gamma T R_{load}/L_{load}\right)}\right)\left(1-e^{-\left(T R_{load}/L_{load}\right)}e^{\left(\gamma T R_{load}/L_{load}\right)}\right)}{\left(1-e^{-\left(T R_{load}/L_{load}\right)}\right)} \quad (6.58)$$

The average value of the load current:

$$I_{load} = \frac{U_s}{R_{load}}\left(2\gamma - 1\right).$$

When operating with DC motor load with back-EMF E_0 the initial equations take the form:

$$\pm\left(U_s - E_0\right) = i_a R_a + L_a \frac{\mathrm{d}i_a}{\mathrm{d}t} \qquad (6.59)$$

where $R_a,\ L_a$ – the resistance and the inductance of the armature winding accordingly.

From (6.59) we obtain:

$$\left. i_{a1} \right|_{0 \ldots t_1} = \frac{U_s - E_0}{R_a} \left[1 - \frac{2\left(1 - e^{-\left(TR_a / L_a \right)} e^{\left(\gamma TR_a / L_a \right)}\right)}{\left(1 - e^{-\left(TR_a / L_a \right)}\right)} e^{-\left(R_a t / L_a \right)} \right] \quad (6.60)$$

$$\left. i_{a2} \right|_{t_1 \ldots T} = -\frac{U_s}{R_a} \left[\left(1 - \frac{E_0}{U_s}\right) + \frac{2\left(e^{-\left(\gamma TR_a / L_a \right)} - 1\right)}{\left(1 - e^{-\left(TR_a / L_a \right)}\right)} e^{-\left(R_a t / L_a \right)} \right] \quad (6.61)$$

$$i_{a\,\max} = \frac{U_s}{R_a}\frac{\left(1 + e^{-\left(TR_a/L_a\right)} - 2e^{-\left(\gamma TR_a/L_a\right)}\right)}{\left(1 - e^{-\left(TR_a/L_a\right)}\right)} - \frac{E_0}{R_a} \qquad (6.62)$$

$$i_{a\,\min} = -\frac{U_s}{R_a}\frac{\left(1 - e^{-\left(TR_a/L_a\right)} - 2e^{-\left(TR_a/L_a\right)}e^{\left(\gamma TR_a/L_a\right)}\right)}{\left(1 - e^{-\left(TR_a/L_a\right)}\right)} - \frac{E_0}{R_a}$$

$$(6.63)$$

The amplitude of the anchor current ripples:

$$\Delta i_a = i_{a\,\max} - i_{a\,\min} =$$

$$= \frac{2U_s}{R_a} \frac{\left(1 - e^{-\left(\gamma T R_a / L_a\right)}\right)\left(1 - e^{-\left(T R_a / L_a\right)} e^{\left(\gamma T R_a / L_a\right)}\right)}{\left(1 - e^{-\left(T R_a / L_a\right)}\right)} \quad (6.64)$$

The average value of the armature current:

$$I_a = \frac{U_s}{R_a}\left(2\gamma - 1 - \frac{E_0}{U_s}\right) \quad (6.65)$$

Output voltage ripple coefficient:

$$k_r = \frac{\Delta U_{load}}{U_s} = \frac{\Delta i_a R_a}{U_s} = \\ = \frac{2\left(1 - e^{-\left(\gamma T R_a / L_a\right)}\right)\left(1 - e^{-\left(T R_a / L_a\right)} e^{\left(\gamma T R_a / L_a\right)}\right)}{\left(1 - e^{-\left(T R_a / L_a\right)}\right)} \qquad (6.66)$$

Disadvantage of the symmetric control method is change of the output voltage polarity and high ripple coefficient. That requires increased installed power of the output filters.

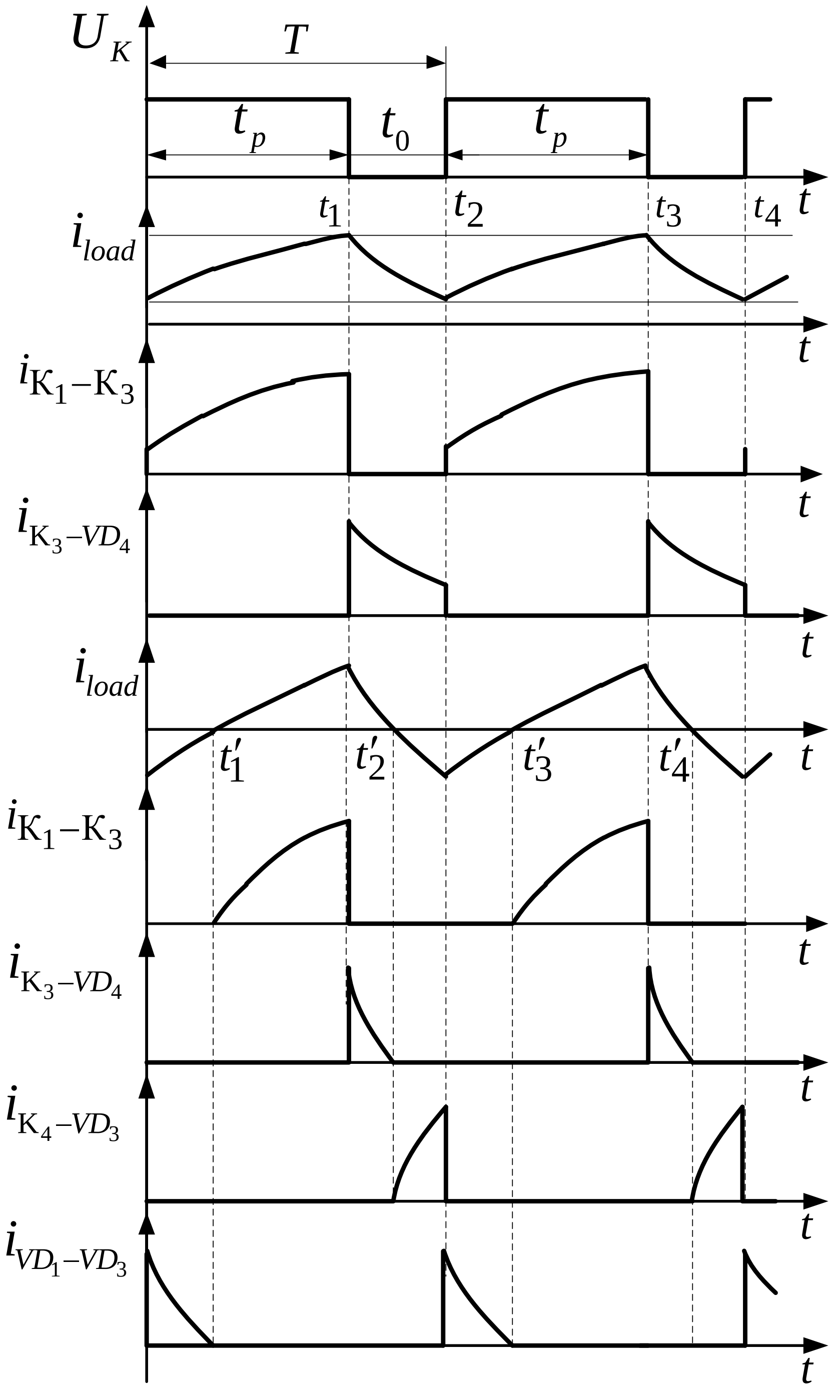

Fig. 6.14. Asymmetrical control method of pulse DC-DC converter

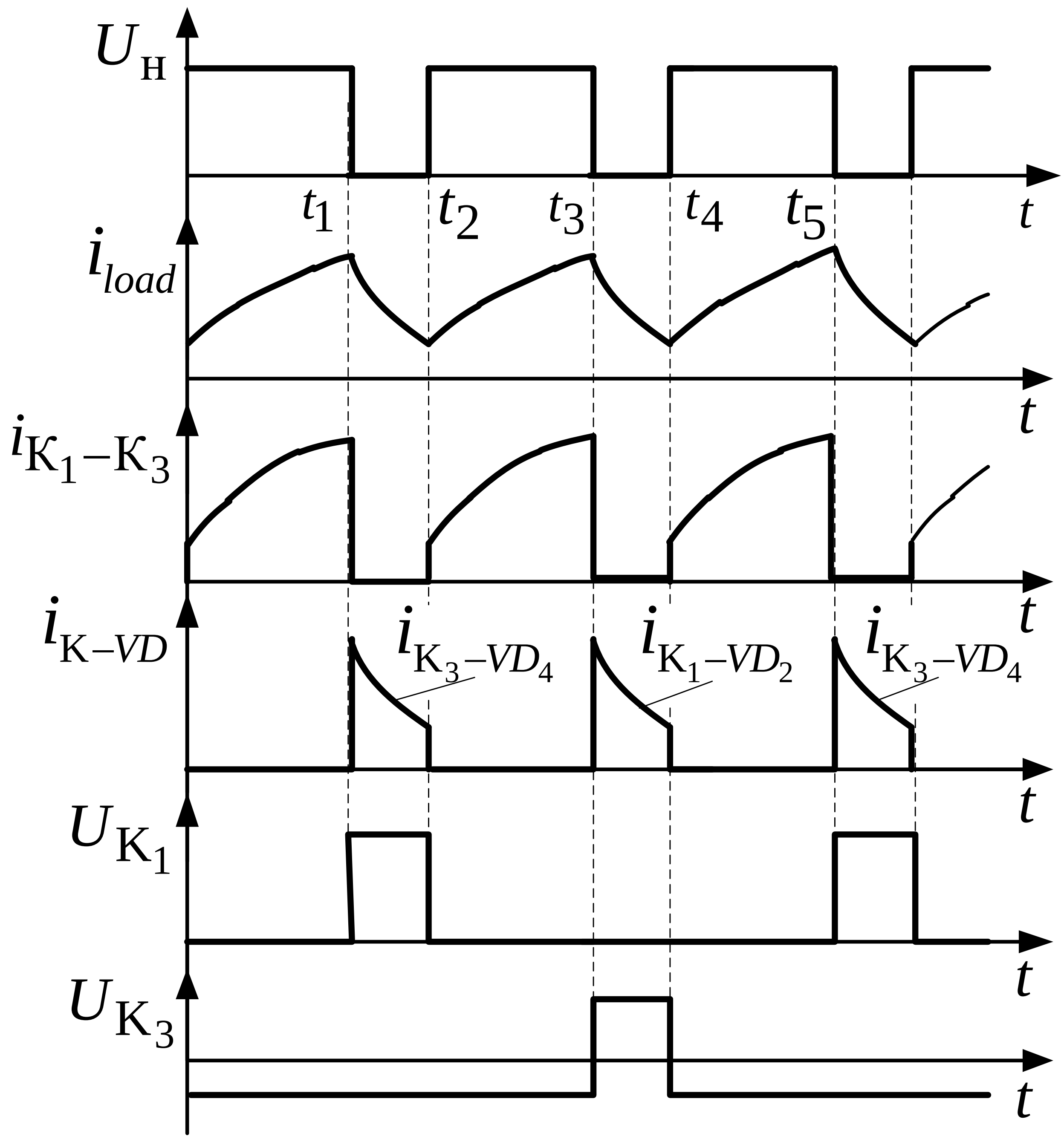

Fig. 6.15. Alternate control method of the reversible pulse DC-DC converter

PULSE AC REGULATORS

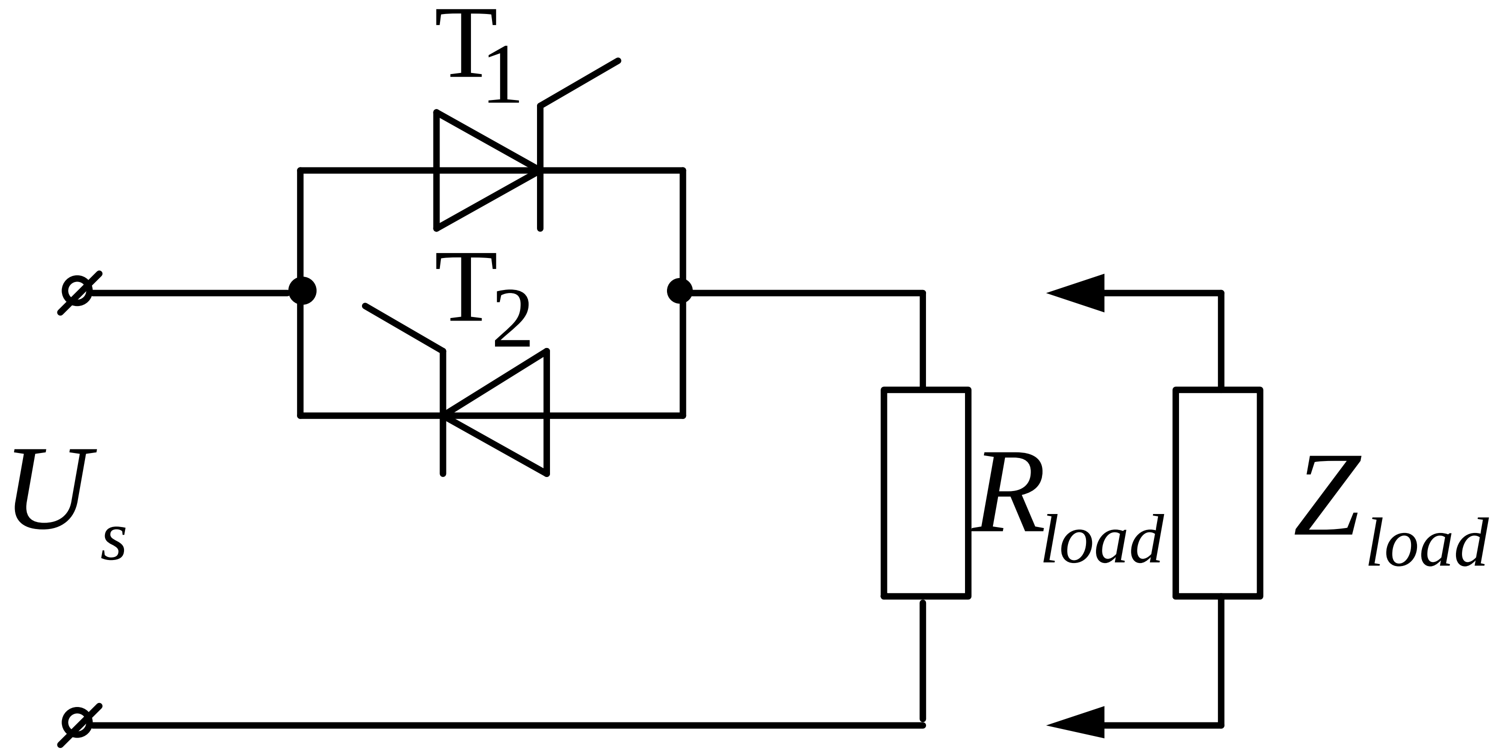

Fig. 7.1. AC regulator based on antiparallel back-to-back thyristors

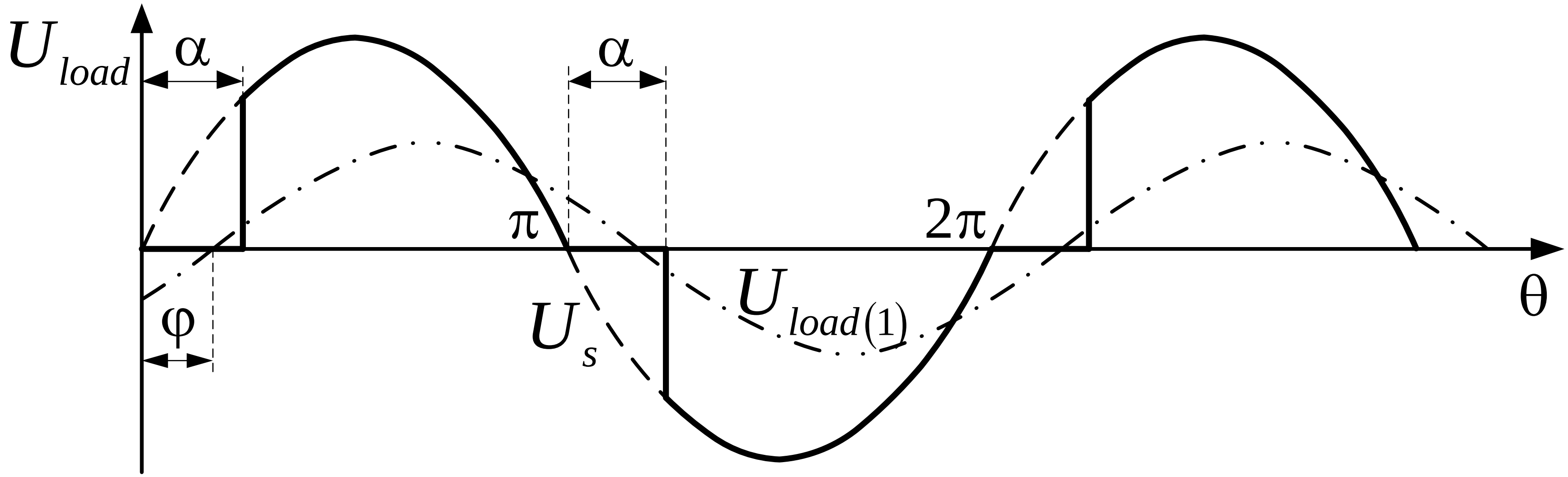

Fig. 7.2. The diagram of the AC regulator with resistive load

The regulation is possible under the condition

$\varphi < \alpha < \pi$ where $\varphi = \mathrm{arctg}\left(\dfrac{\omega L_{load}}{R_{load}}\right)$

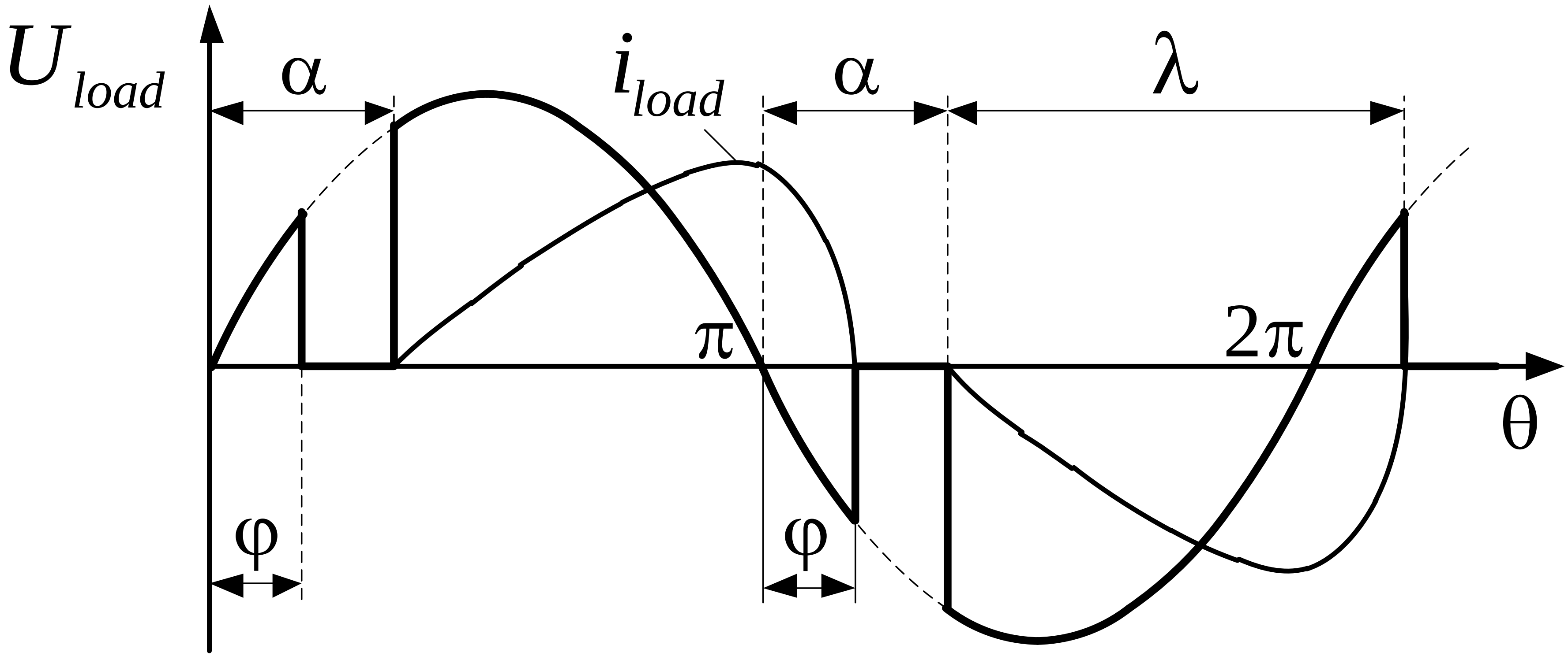

Fig. 7.3. The diagram of the AC regulator operation with the active-inductive load

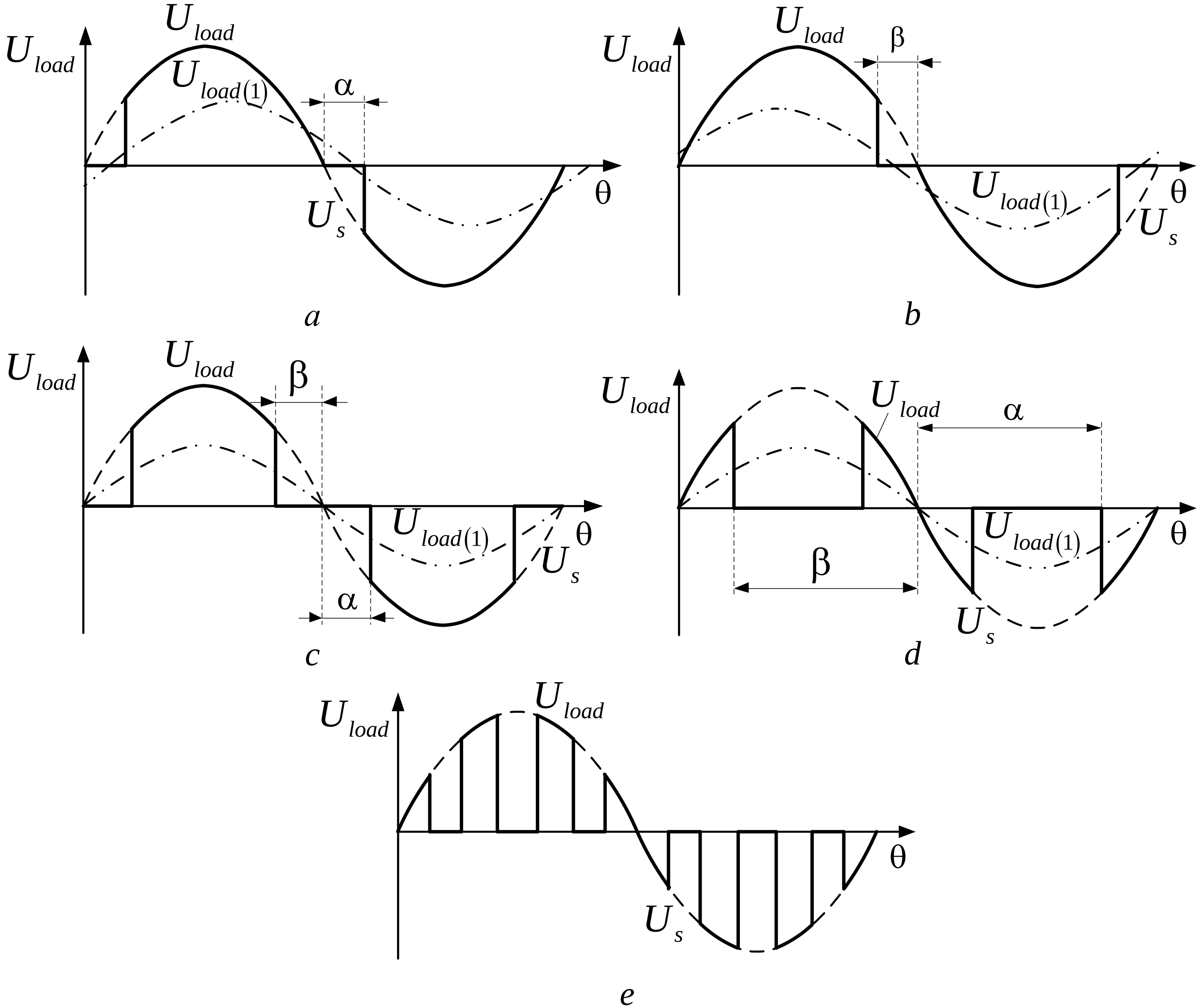

Fig. 7.4. Various methods for AC voltage regulation using fully controlled switches

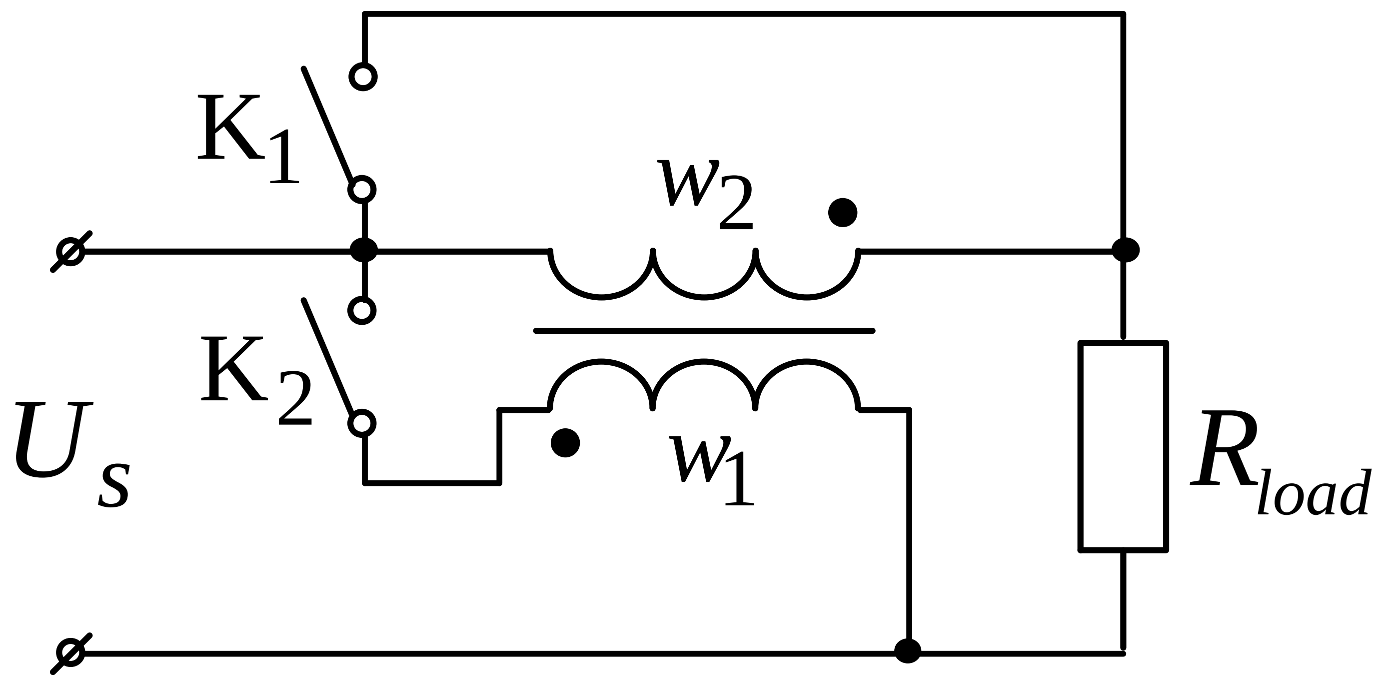

Fig. 7.5. Basic AC voltage regulator circuit with voltage boosting

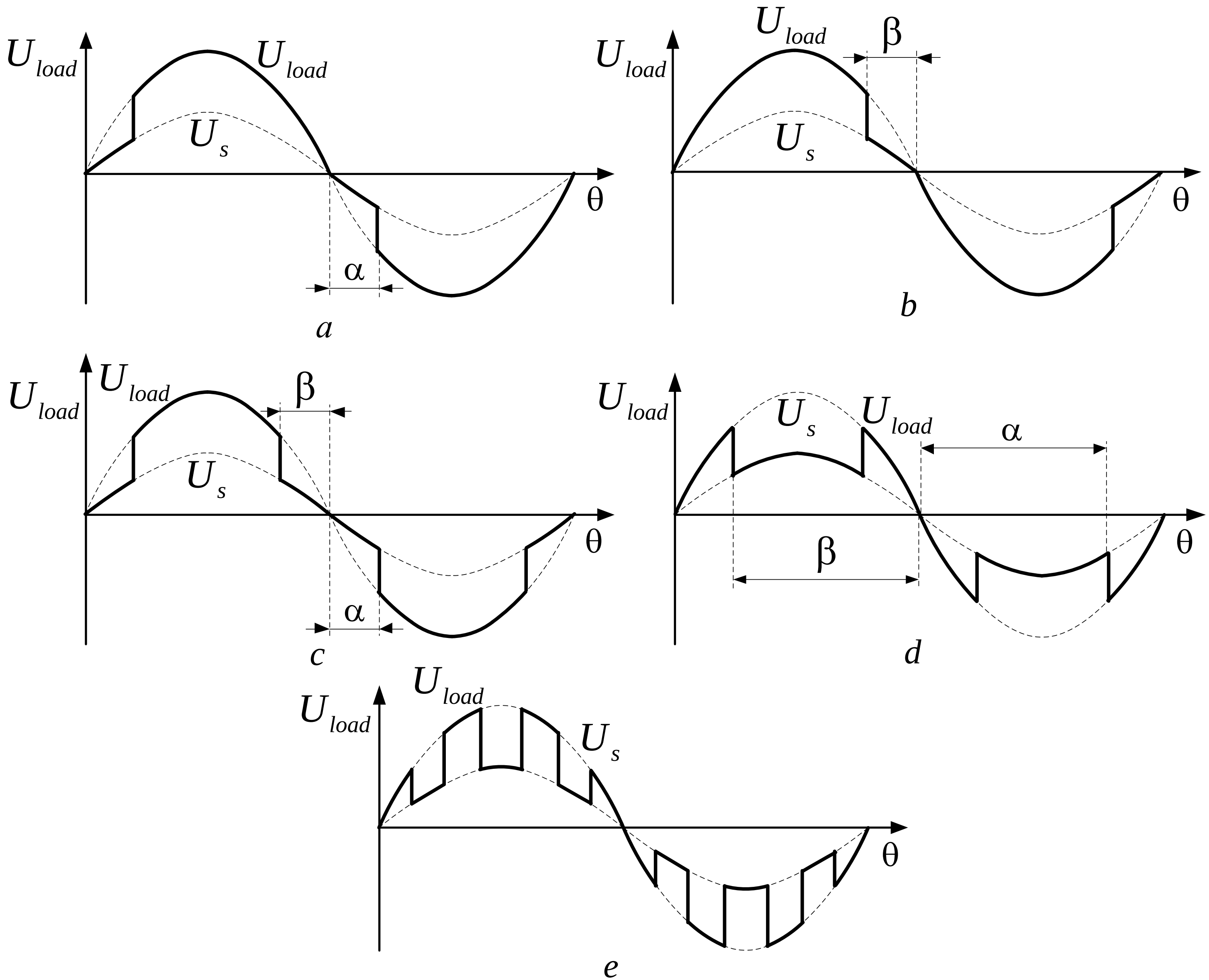

Fig. 7.6. Different ways of AC voltage regulating using voltage boosting

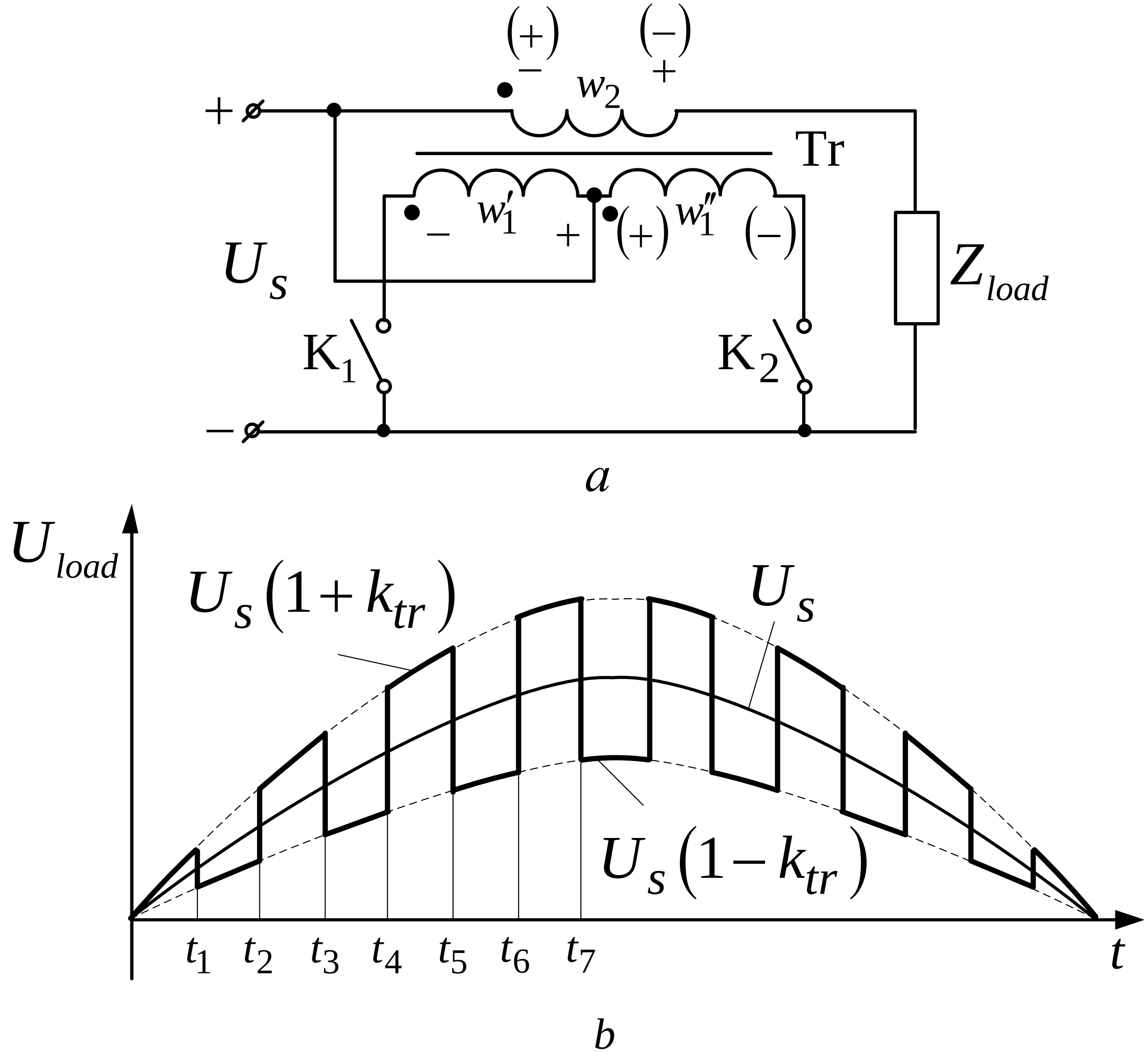

Fig. 7.7. AC voltage regulator using high-frequency transformer

Thank you